DRYING OF GRANULATED PRODUCTS BY CONVENTIONAL HEAT TRANSFER AND HIGH FREQUENCY TECHNIQUES

by

Fernando Pinto Caldas

A Doctoral Thesis

Submitted in partial fulfilment of the requirements for the award of Ph.D. of the Loughborough University of Technology

August 1988

To my father-in-law,
Luis Donato, who sadly
passed away while this
report was being finished.

TABLE OF CONTENTS

ACKNOWLEDGEMENTS

My deepest gratitude is expressed to Brazil´s "Conselho Nacional de Desenvolvimento Cientifico e Tecnologico" (CNPq) which financed my studies in Britain. My sincere thanks to Loughborough University of Technology, particularly my supervisor, Mr. H. Barber, for his personal interest and careful guidance, and the staff of the Department of Electronic and Electrical Engineering. I appreciate the special contibutions of Mr. P. Barrington, Mr. D. Hackett and Mr. J. Rippon, and also those of of Dr. P. Finlay, Dr. M. King, Prof. J. Saunders from Management Studies Department and Dr. A. Foord from Chemical Engineering Department for their extra-departamental courses I attended.

I express my love and appreciation to my wife Elsie and children for their continuous support, as I do to my father for his, from the start of this research programme to the final edition of the thesis. I want to thank Pastor K. D. Shaw and the congregation of Packe Street Church for their warm welcome and fellowship during our stay. My thanks to Mr. D. Kennedy for checking the English of the final draft and to Mr. J. Salazar, Mr. J. Vindas and Mr. P. Atkinson for their fine work with the figures, graphs and photographs.

ABSTRACT

In this study the contribution of the different heat transfer methods in the drying of granulated materials is analysed from the viewpoint of the available electroheat technology. Although the work has been directed to present day commercial applications and proposes definite drying schemes the research has been focussed on high frequency heating techniques, which appear to be the most promising alternatives as far as medium and large throughput continuous processes are concerned. An experimental rig has been designed and built, this unit has been used to obtain a preliminary set of data on the performance of the high frequency drying process under different operating conditions.

LIST OF SYMBOLS

A, A′, A″, A‴	Surface area, m^2
a, b, c, d	Microwave applicator dimensions, m
c	Speed of light, m/s
C, C_e, C_i	Moisture concentration: general, equilibrium, initial, kg/m^3
CR	Concentration ratio, per-unit
ΔCap	Capacity increase in crossflow column volume, m^3
C_L	Load capacitance, F
C_T	Tank circuit capacitance, F
C_0	Unloaded applicator capacitance, F
C_c	Unit energ costs for crossflow dryer, US$/kWh
C_{ir}	Unit energy costs for infrared dryer, US$/kWh
C_{die}	Unit energy costs for dielectric dryer US$/kWh
Cp, Cp_{air}, Cp_w, Cp_d	Specific heat: general, air, water and dry material, Wh/kg/ C
D	Diffusivity, m^2/h
d	Dielectric power penetration depth, m

D_o	Geometric dimension, m
D'	Diameter, m
d'	Separation between electrodes, m
d''	Dielectric load thickness, m
d_{ag}	Air gap thickness, m
E	Electric field strength, V/m and kV/m RMS
E_{air}	Electric field strength in air, kV/m RMS
E_i	Electric field strength in an insect, V/m RMS
Ep	Electric field strength, V/m and kV/m peak
Ep_{air}	Electric field strength in air, kV/m peak
E_{ext}	Energy from external heat sources, Wh
E_{int}	Energy produced internally, Wh
E_o	Energy required to dry $v\,m^3$ of product in crossflow dryer, kWh
E_{ir}	Energy required to dry $v\,m^3$ of product in an infrared dryer, kWh
E_{sl}	Energy required to provide the sensible and latent heat per unit volume of dried product, Wh/m^3 and kWh/m^3
E_w	Energy required to heat up water, Wh
e	Magnitude of the complex relative permittivity
e_o	Permittivity of free space, F/m

e^*	Complex permittivity
e'	Dielectric constant (relative)
e''	Loss factor
F	View factor, per-unit
f	Frequency of the electric field, Hz or MHz
FF	Filling factor, per-unit
F'	Geometrical factor, per-unit
F_{ta}	Annual cash flow of project A, US$
Fo	Fourier Number for mass transfer
G	Mass velocity of air, $kg/s/m^2$
g	Gravitational acceleration, m/s^2
H	Magnetic field strength, A/m
h	Height, m
HR	Annual hours of plant operation, h
h_c	Coefficient of convective heat transfer, $W/m^2/C$
h_m	Coefficient of mass transfer, 1/h
h_v	Latent heat of evaporation of water, Wh/kg
I	Electric current, A RMS
i	Minimum annual return on investment, per-unit
I^2	Square of the coefficient of correlation, per-unit
I_c	Capacitive component of current I, A RMS

I_r	Resistive component of current I, A RMS
Inv, Inv_c, Inv_{die}	Unit investment cost of plant: general, crossflow, dielectric, US$/kW
K	Factor accounting for the relative price of fuels
k, k_{air}	Thermal conductivity: general, air, W/h/C
k′	Air drying constant, 1/h
$K_{a.m.}$	Amplitude modulation factor, per-unit
k_c	Cut-off constant, $1/m^2$
k_d	Dielectric drying constant, 1/min
k_p	Propagation constant, $1/m^2$
k_q	Dielectric drying constant
L	Inductance, H
L_T	Tank circuit inductance, H
l	Permissible thickness, m
l, l_1, l_2, l_3, etc	Lengths, m
M	Moisture content, per-unit or %; on wet or dry basis (w.b., d.b.)
m	Weight of contained moisture, kg
m, n, p	Integers
m′	Weight of evaporated water, kg
M_e	Equilibrium moisture content, as M
M_f	Final moisture content, ibid
M_i	Initial moisture content, ibid

M_t	Target moisture content, ibid
$\dot{m}$	Throughput of wet material, kg/h
m_d	Weight of dry material, kg
MR	Moisture ratio, per-unit
n	Lifetime of plant, years
NPV(a,i,n)	Net present value of cash flow of project A over n years discounted at an annual rate of i, US$
N_u	Nusselt Number, per-unit
P	Internal Pressure, kg/m^2
P	Vapour pressure of air, kg/m^2
P_b	Vapour pressure of surface water, kg/m^2
PBP	Compounded payback period, years
P_c	Installed heating capacity in crossflow plant, kW
P_{die}	Installed heating capacity in dielectric plant, kW
Pd	Rate of radiated energy per unit time per unit surface at a given absolute temperature, W/m^2
Pd_g	Grey body rate of radiated energy per unit time per unit surface at a given absolute temperature, W/m^2
P_i	Input power, kW

P_{ir}	Installed heating capacity in infrared plant per unit of floor area, kW/m^2
P_o	Output power, kW
P_r	Prandtl Number
P.V.	Variac setting, %
$\mathbf{P}$	Magnitude of the Poynting vector, W/m^2
Q	Rate of energy transferred in unit time, W
q	Rate of energy transferred in unit time per unit surface area, W/m^2
$\dot{Q}$	Air flow, m^3/h
Q_d	Rate of energy dissipation in a dielectric in unit time, W
q_d	Rate of energy dissipation in a dielectric per unit volume in unit time, W/m^3 and kW/m^3
Q_g	Net exchange of grey body radiation per unit time, W
Q_L	Loaded applicator Q-factor
Q_O	Unloaded applicator Q-factor
R	Electric resistance,
r	Radial coordinate, m
R_d	Coaxial applicator external radius, m
$R_{heating}$	Temperature rise ratio

Re	Reynolds Number
r.h.	Relative humidity of air, per-unit
R_L	Load electric resistance, Ω
R_o	Resistance of unloaded applicator, Ω
r_o	Radius of a sphere, m
R_s	Applicator wall surface resistivity, Ωm
R_w	Coaxial applicator internal radius, m
S	Factor accounting for the reduction in average solar radiation due to atmospheric and geographical conditions, per-unit
S_e	Standard deviation
T, T_a, T_b, T_f, T_h, T_i, T_s, T_m	Temperature: general, air (dry bulb), air (wet bulb), final, heater surface, initial, heat source, material, C
t	Time, h or min
t_d	Drying time, min
t_{dv}	Time to dry a given volume of material, h
$\mathcal{T}$	Throughput, m^3/h; defined in terms of volume of finally processed material
V	Voltage, V and kV RMS
V_i	Input mains voltage, V RMS
V_o	Applied voltage, V
V_p	Voltage, V and kV peak

V_{pr}	RF field probe voltage, V peak
V_R	RF voltage at oscillator terminals, V RMS
V_x	Terminal voltage, V
v	Volume, m^3
X	Reactance, Ω
x_Q	Length of heat conduction path, m
x, y, z	Cartesian coordinates, m
W	Weight, g
w	Angular frequency, rad/s
w_c	Cut-off frequency, rad/s
w_R	Resonant frequency, rad/s
α	Absorptivity, per-unit
α_a	Attenuation constant, neper/m
α_v	Absorptivity of water vapor, per-unit
β	Phase constant, 1/m
δ	Loss angle, rad
δ_s	Skin depth in applicator walls, m
δ_t	Thermal gradient coefficient, 1/C
ε	Emissivity, per-unit
ε_s	Emissivity of heat source, per-unit
ε_m	Emissivity of material, per-unit
λ	Wavelength, m or μm (1E-6 m)
λ_g	Waveguide wavelength, m

λ_o	Free space wavelength, m
λ_R	Resonant wavelength, m
μ	Permeability, H/m
μ_{air}	Viscosity of air, kg/m/s
μ_o	Free space permeability, H/m
η, η_c, η_e, η_d, η_s, η_R, η_t	Energy efficiency: general, microwave coupling, instantaneous drying, drying run, microwave source, radiation, waveguide; per-unit
ρ	Bulk density of wet material, kg/m^3
ρ_r	Reflectivity, per-unit
ρ_s	Bulk density of dry material, kg/m^3
ρ_w	Bulk density of water, kg/m^3
σ	Stefan-Boltzman constant, $W/m^2/k^4$
τ	Transmissivity, per-unit
ϕ,θ	Angular coordinates, rad

1. INTRODUCTION

1.1 Objectives and Scope of the Study

Drying can be classed as a separation process the speed of which is affected by the characteristics and state of the components which form the mixture to be dried, the amount of thermal energy which is supplied to these materials and also,although seldom recognised, by the type of heat transfer technique used. Mechanical methods, i.e. draining, compression and centrifugeks are not effective in removing internal moisture from a capillary-porous material as will be noted below. Hence the product is usually heated since in most applications this is the most effective method to produce the internal moisture migration, which is ultimately caused by moisture, temperature and pressure gradients. Moreover by heating the product surface and the drying medium it is possible to mantain maximal evaporation rates. If a particular industry is concerned with drying operations it needs to schedule its operations to take into account the required drying time, this usually presents a classical 'bottle-neck' problem and allowances must be made for the fact that increased amounts of energy supplied will produce progressively lower increases in throughput. The thermal efficiency of the equipment may be reduced,the product quality adversely affected and, in some instances, the reliability of the plant jeopardised. Most current dryers are based on convective heat transfer mechanisms aided by some conduction and, in special cases, by radiation. High frequency techniques, involving phenomena similar to those occuring in a conventional domestic microwave oven, are not commonly used although they could bring significant improvements to an existing drying plant.

This study is concerned with electroheat techniques which might be employed as a substitute for part of the petroleum used in those applications involving temperatures lower than 200^{0}C (Figure 1.1), in particular the drying of granulated materials in primary agro-industrial processes. Several options have been considered with most attention being paid to those most promising where the present practice is to use fuel-fired, medium and large throughput dryers. Most equipment used for drying purposes in other sectors of agro-industry is similar in the technology used despite differences in scale and hence it was considered desirable to concentrate this study on the most common types. Any electrical technique finally adopted should be flexible enough to allow the design to be extended to higher throughputs and larger installed capacities as might be required in those regions, e.g. Brazil, where the required outputs are

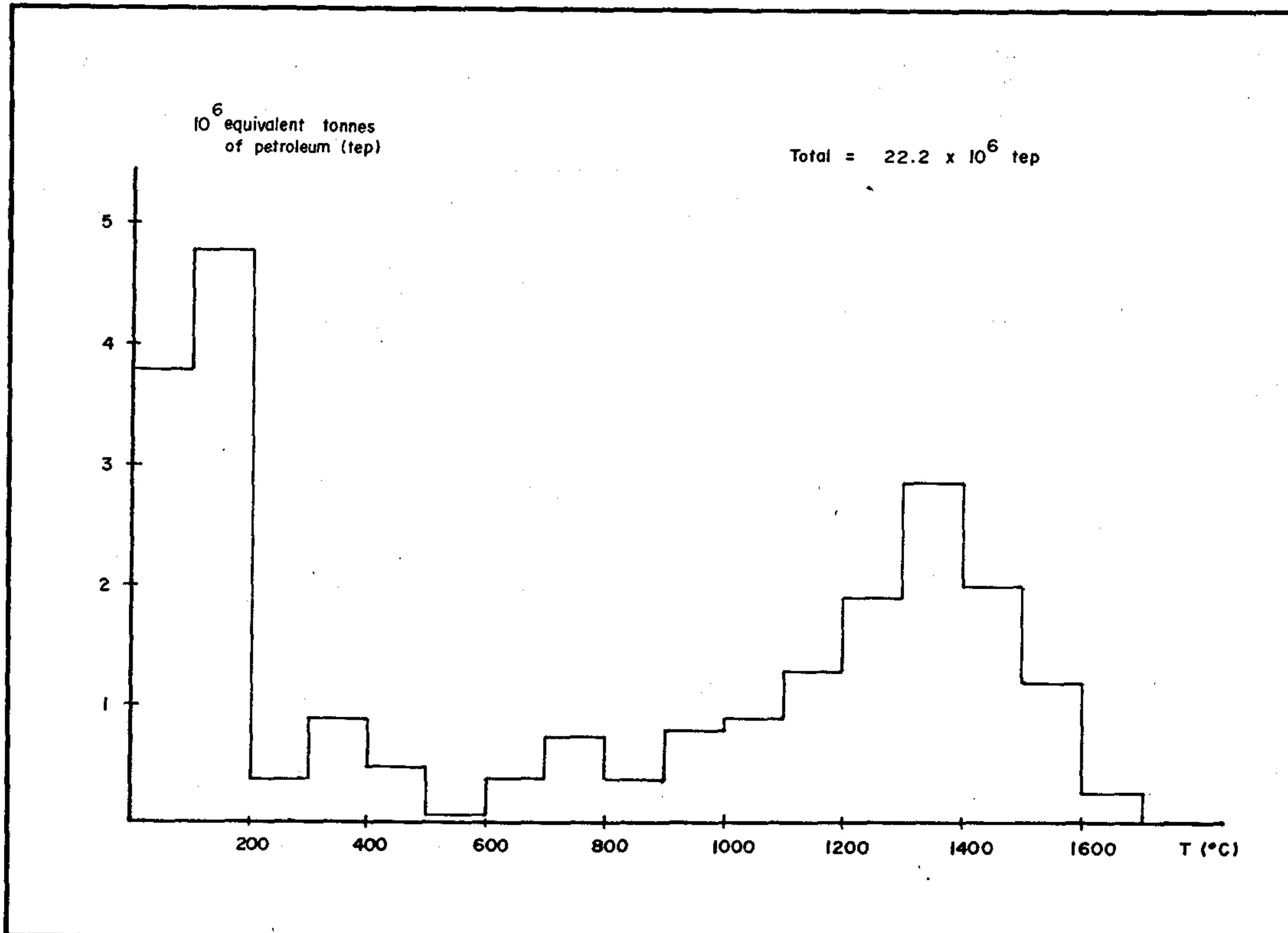

Figure 1.1 Distribution of Process Temperatures and Energy Consumption in Brazilian Industry [95].

greater.

It is appreciated that the high temperature region in Figure 1.1 (mainly between 1000 and 1600^{0}C) also presents an opportunity for the replacement of combustion systems by electrothermal processes. This is the case, for example, in metallurgical plants where metal melting, refining and heat treatment can be carried out by electric arc and induction heating techniques. Ultra-high temperature discharges obtained from plasma torches can activate chemical reactions which have not hitherto been feasible. These latter are outside the scope of Figure 1.1 although they may constitute important factors in the development of metallurgy in many regions, for example the production of high value alloys from the large mineral reserves of the Amazonas region. The development of more efficient drying techniques will also contribute to the progress of industry in general and, in particular, such applications as the drying of food products, textiles, paper, board and leather and to the heating and drying of polymers, chemicals and mineral products so bringing multiple benefits to the economy as a whole.

When proposing an alternative drying technique it is necessary to be aware of the physical, optical, thermal and electrical properties of the material. The economic and management aspects involved in the introduction of a new technology into a well established industry need to be taken into account. It is also essential that the designer be aware of the physics of heat and mass transfer and of the properties of electromagnetic fields. There are many design possibilities, the more significant of these have been investigated and the most promising selected, these are discussed in the remainder of this report. The major criteria adopted are that the result should be capable of retrofitting into an existng drying plant and the resulting throughput must be at least equal to that of the existing plant (ideally much greater), the equipment must be as compact as possible and the capital and operating costs should be kept to a minimum.

Although high frequency heating techniques have been used in industry for a long time they have captured only a limited fraction of the potential market, chiefly in those instances where increased throughputs and better product quality outweigh the energy cost considerations. Thus high frequency heating has found its major market in processes where the rapid through-heating of non-conductive materials is required. In these cases the conventional heating techniques of convection, conduction and infra-red radiation are not favourable, first because in most instances the warm-up and standby losses of the plant are considerable and, secondly, the energy supplied needs to pass through the surface of the material and internal conduction is the only process by which the bulk can be heated. This can take a considerable time when materials of poor thermal conductivity are being processed thus slowing down the whole operation considerably. In drying applications high frequency methods can greatly increase the throughput of a plant since water is much more receptive to the electric field applied than the dry material and also due to the fact that since heat is produced internally there is an effective temperature and vapor pressure gradient from the inside to the surface which aids the drying process.

The main obstacle to the introduction of high frequency heating in industry is the lack of practical experience of the method together with the limited amount of research and development of new applications which has been undertaken so far, due to the generally small size of the corresponding equipment manufacturing industry. The latter has induced only a limited demand from industrial customers which has caused the corresponding investment costs to remain at high levels. Some advances have been made and some fundamental and theoretical work has been undertaken but this is only slowly being transformed into applied knowledge. High frequency heating methods involve concepts which are still not widely available for use (see, for example, Chemical Engineers Handbook (50th Ed.) McGraw-Hill, 1984). The technical terms are still not completelly understood and the physicist finds it difficult to transmit effective and useful information to chemical, mechanical and electrical engineers, and vice-versa.

The present situation may change when more resources are dedicated to the study of the technique and its applications and when the size of the industry increases. The objective of this Report is an attempt to contribute to the store of applied knowledge, incorporating the fundamental technical and economic factors to be considered upon tackling a particular electrothermal application. The particular case studied is that of granular agricultural crops. The methods and procedures considered, however, can be adapted and transferred to the processing of other granular products. The following questions were taken as the starting point of the research:

What type of equipment is to be used ?
What are the main features and limitations (throughput, dimensions, input parameters, heating requirements, etc.) ?
How long will it take to process the material ?

How can the equipment be designed?

What are the main variables which affect the performance of the equipment and how can the information be obtained ?

What are the factors which most affect the economics of the technique and what is the extent of these effects ?

1.2 The Agro-industrial Sector

It has been reported recently that nearly 14% of the industrial output of developing countries is represented by food products arising from the agro-industrial sector of the economy which contributes 16% of the total manufacturing value added in 1980. Latin America was the fastest growing food producer in the World during the period 1970-1981, 85% of this production came from large size industries with 50% of the total output generated in Brazil, Argentina and Mexico [163]. The same source identifies the Latin American agro-industrial business as a unique opportunity to jointly develop the industrial and rural sectors in their present status. The food potential of Latin America has been recognised by many multinationals which have more than doubled the number of plants in that region as compared with, say, Asia, the Pacific or Africa.

Amongst the many granular food commodities are animal feeds, cocoa, sugar, meat, shrimp, fish, fruit and vegetable preparations, flour and cereal products. All these come from the primary processing of sugar-cane, several types of meat and products such as cocoa, coffee, soya, cereals (maize, rice, wheat), banana, cassava and other roots, beans, nuts, spices and fruits.

This report is focussed on the primary processing of granulated materials, specifically with the products shown in Figure 1.2. A general view of the agro-industrial sector and its internal relationships is given in Figure 1.3.

Wheat, maize and rice are the leading products of interest to the world milling industry [164] providing a major food source for both humans and animals. In production terms wheat is the leading cereal although rice plays an important part in the diet of most Asian countries [20], these grains have been cultivated since the beginnings of civilisation, they were amongst the first commodities used by man. Other crops such as cocoa, peanuts, soya and coffee are important cash products in developing countries and different types of pea and bean are part of the normal diet in most regions of the world. In addition to being used for food, soya and peanuts are a raw

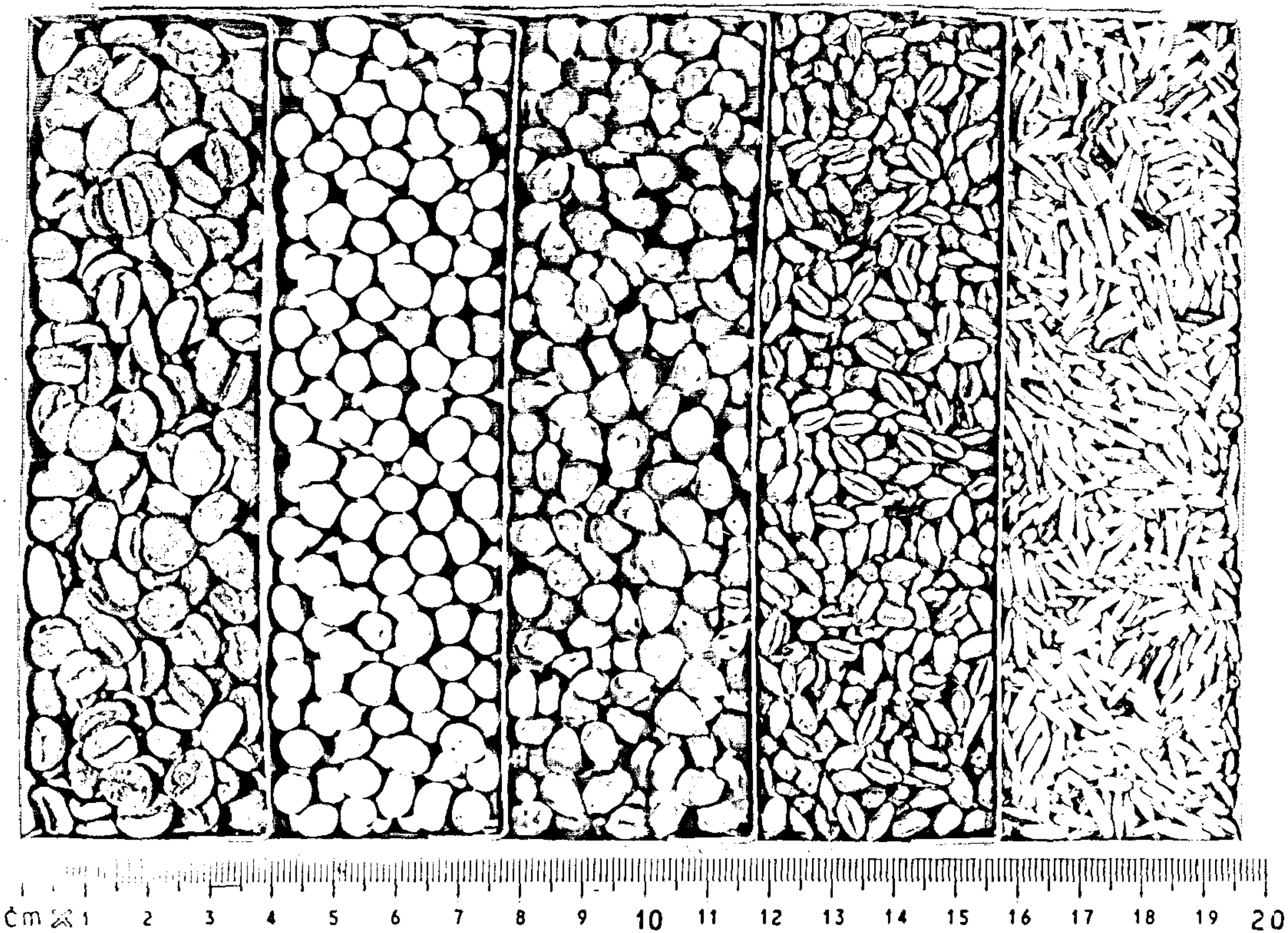

Figure 1.2 Major Agricultural Commodities.

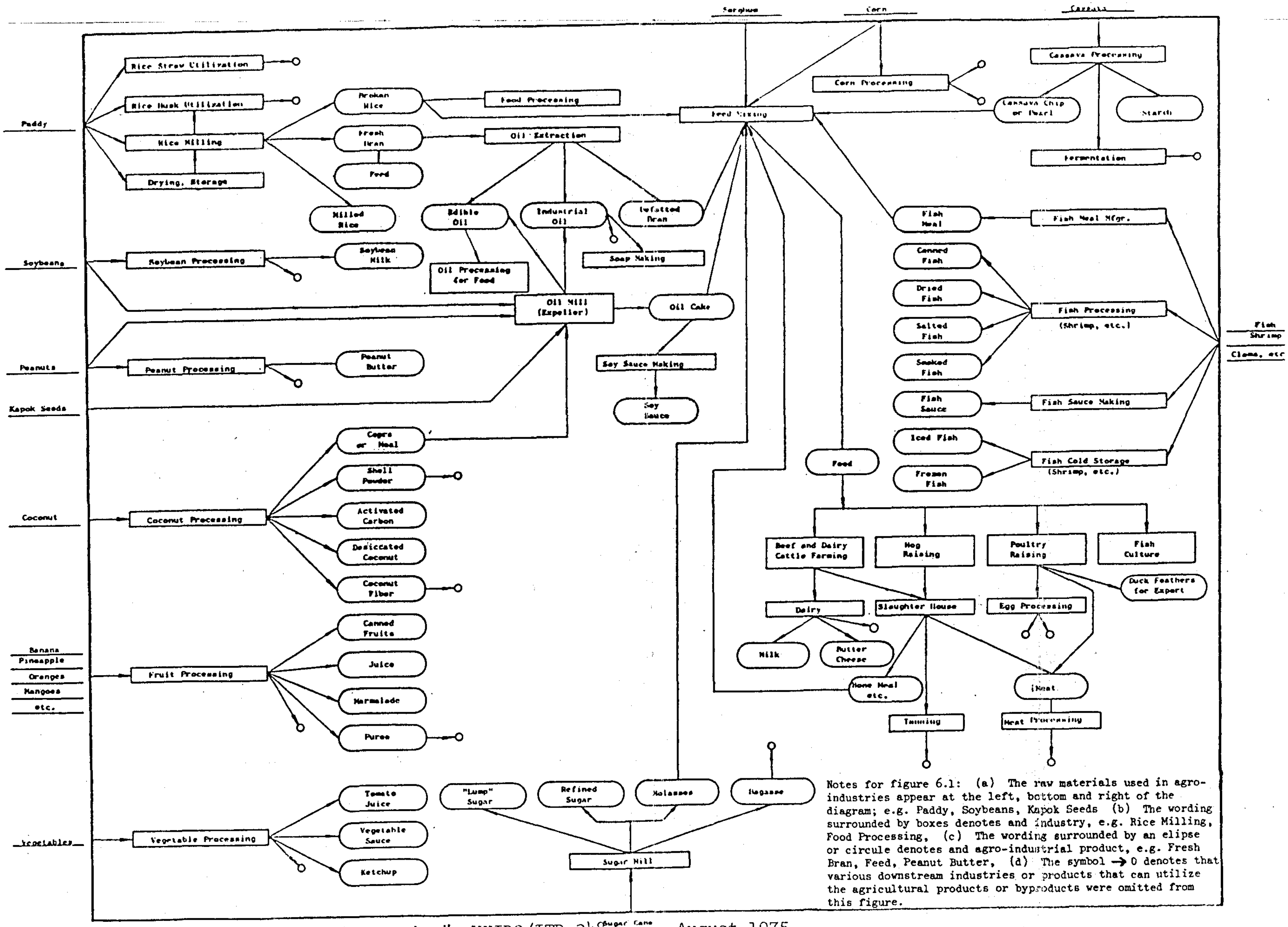

Notes for figure 6.1: (a) The raw materials used in agro-industries appear at the left, bottom and right of the diagram; e.g. Paddy, Soybeans, Kapok Seeds (b) The wording surrounded by boxes denotes and industry, e.g. Rice Milling, Food Processing, (c) The wording surrounded by an elipse or circule denotes and agro-industrial product, e.g. Fresh Bran, Feed, Peanut Butter, (d) The symbol $\rightarrow$0 denotes that various downstream industries or products that can utilize the agricultural products or byproducts were omitted from this figure.

Source: "Types of agro-industries", UNIDO/ITD.348, August 1975

Figure 1.3 Inter-relationship of Agro-industries.

material for many industrial processes.

This Report focusses on two particular Latin American countries, Brazil, which is one of the largest food exporters in the world, and Costa Rica. The latter is representative of the present situation and trends observed in Central American countries and in Colombia although, in relative terms it may be that, at present, the Costa Rica agroindustry is more advanced than in most developing countries. It is worth noting that Brazil, in spite of unfavourable circumstances, in 1980 moved ahead of France in the quantity and variety of agricultural products exported being just behind the USA [176]. Although the potential of the Brazilian agroindustry has been evident for some time the exploitation of this resource is still limited due to the difficult socio-economic conditions in the rural areas where small, inefficient plantations co-exist with large, well managed businesses. Cooperative enterprises, which have been so successful elsewhere, have been developed in only a limited form.

In the primary agro-industrial sector of Brazil the most important commodities in terms of the total amount processed are maize, soya and rice [2] although coffee also plays a major role in the economy. In Costa Rica the most important crop (and the largest export) is coffee followed by rice and maize. The relative importance of coffee exports in the economy of Central American countries and Columbia has increased over the past two decades although it is declining in Brazil [42]. In Brazil the value of soya exports in 1980-82 exceeded those of coffee although both together still account for one fifth of the total for the country [35]. Peanuts are used in snack and cereal products and in the manufacture of butter, bakery and dessert products or food additives. The oil is the raw material for producing margarine, mayonnaise, fats, cosmetics and soap, as a cooking or salad oil and as a lubricant or even a substitute for diesel oil.

All crops contain moisture when harvested and some, such as coffee, may require the addition of water during the post-harvest treatment to improve the product quality. In contrast to other crops, there are two alternative methods of coffee production, one is the washed (or wet) process and the other the natural (or dry) process. Cereals, grain and oil-seeds (legumes) such as soya and peanuts normally contain 30-40% moisture content on a wet basis (w.b.) when harvested [113]. This may be reduced to 15-25% w.b. at entry to the drying plant [2, 64, 175] which it leaves near its equilibrium value of 10-13% w.b.Coffee, however, may need to be dried from above 50% w.b. [25, 27, 42].

If the crops were used within a short time of harvesting then drying would probably not be necessary. If the product is to be stored for more than a few days or if the material is to be ~~material is to be~~ subjected to additional processing then drying is required in order to maintain the quality, and therefore the economic value, of the final product. This is a consequence of the biological nature of the material in which the presence of moisture may lead to the growth of damaging organisims, the proliferation of pests, etc., these factors will decrease both the final yield and the quality. A further cause of material loss during storage is the germination of the product itself. Many of these products are the raw materials for another industry in which they are reprocessed, they are delivered, sometimes after a considerable period of time, in a state which conforms to specified standards. Some products, such as soya and peanuts need to be dried to eliminate toxins which may be harmful to humans and animals, others need to be dried to allow the external shell which encloses the kernel to be cracked for removal [98].

Following drying, the soya beans are passed through cracking mills and dehulling machines where the hulls are removed from the oil-bearing material [164], peanuts are shelled and then usually either roasted or crushed for oil extraction. Coffee presents a different problem. In the wet process the product, the cherry, is first separated from waste material using a water flotation process and is then pulped where much of the material covering the kernels is extracted. After this stage the product is covered with a thin slippery layer, the mucilage, which is insoluble in water. This layer is removed by a digestion technique involving natural fermentation or chemical treatment. After dissolving the mucilage the kernels are washed in water and the material is either pre-dried by solar radiation or passed directly to a mechanical drying stage. In natural processing the whole cherry is dried after which the material covering the kernels is removed by mechanical methods. This latter method is much cheaper but it can only produce a good quality product in special circumstances whereas the wet method is a more controlled route. If there is a large quantity of coffee available in the market the buyer naturally presses for higher quality, more washed coffee can be sold and the additional costs are covered by a higher price. About half the world production of coffee is processed naturally although Columbia and Central America rely almost entirely on washing.

Brazil, the major coffee producer, uses mainly natural processing. The reasons for choosing one or the other are related to weather conditions, economic factors (price of coffee, land, labour, machinery and infrastructure) and tradition. Weather is important since the mucilage is not present until the cherry is almost ripe, when it is over-ripe the mucilage is digested by the product. When the harvest season coincides with a period of dry weather more over-ripe cherries are produced in the plantations over a short time period, these fruits are already partially dried on the tree. In these circumstances there is a large variation in ripeness and moisture content resulting in a "quality unknown" harvest. If rainy weather occurs during the harvesting period then a longer and more uniform maturation of the cherry is obtained. However in wet conditions it is important to pick the cherries as soon as they are ripe and to process them immediately. The labour input required in the "wet" case is much greater than that in the "dry". In Brazil less than 14% of the total production costs are due to harvesting labour, the figure may be higher than 50% in Colombia and Central America [42]. Hence, as might be expected, the wet process has a greater appeal in those regions where the cherry is picked with the mucilage intact and enough water is available for washing as opposed to the places where the harvest includes a significant amount of both over-and under-ripe cherries due to climatic conditions.

1.3 Agro-industrial Drying Plants

In the last few years the drying of agricultural products in Latin America and other developing regions has changed from what was entirely a farm-based operation using large amounts of labour and the sun as a heat source. It is now often carried out in large plants using fuel combustion to provide the energy. There is no relying on suitable weather conditions for drying in the quantities required in a reasonable time. Some of these plants are attached to large farms and others are owned by tenant farmers on a cooperative basis. However in some countries these large plants co-exist with traditional methods.

Natural methods of drying are still very common, with the crop being spread on tables or "patios", sometimes with the help of solar heat traps which increase the effectiveness of the radiative heat process. Forced air convection, either at ambient or elevated temperature, is also employed. The drawback with solar energy is that, although "free", it requires a large area and this, together with progressively increasing labour costs, renders it uneconomical if the production requirement is large. Thus, particularly in the more developed countries, there has been an ever-increasing use of mechanical drying equipment. The increased production obtainable by the use of capital intensive technology justifies the additional investment with the added benefit of independence from unfavourable weather conditions and a reduction in product losses caused by attack by moulds and pests. This situation is evident even in the case of a relatively poor country such as Costa Rica where almost the whole coffee and cereal grain crop is mechanically dried. In Brazil much of the crops are produced in regions where electricity is not yet available and sun drying still plays an important role in the operation of medium and small farms. In this case the choice of the natural method is mainly determined by the lack of a proper infrastructure and, perhaps, the inavailability of finance and technical assistance.

McDonald and Freire [116] have reported that traditional techniques are used for almost all the artificial drying of cocoa in Brazil. The method basically consists of a drying house in which a relatively thin layer of the product is spread on a perforated drying platform under which hot air is produced by the combustion of wood and other biomass products. It is estimated that 25,000 such plants exist in the Bahia region alone with a throughput of almost 80 kg/h per 100 m^2 of drying floor. Similar methods are also used for drying coffee and peanuts in other developing regions although a trend towards mechanisation and large throughput plants is expected as the infrastructure is improved and financial resources become available. Some agricultural products are dried in deep bed stationary systems, e.g. in bins and large columns. This is the case, for example, with nuts [98, 172] as well as coffee and some cereal grain [20, 27]. However the most popular types of dryer at the present time in the applications of interest here are (see, for example, [64], [20], [7] and [42]) of the following types

i) Crossflow
ii) Rotary.

The crossflow dryer, originally designed for cereal products, is used in the first stage of coffee drying. According to Desrosier & Sivetz [42] the typical capacities of this unit when used for coffee range from 900 to 14,000 kg (12% w.b.) per day which corresponds to 2-36 m^3 of dry material. Caldas [27] reported on a sample of more than 40 crossflow dryers from which it can be concluded that the total drying time in this type of plant ranges between 2 and 10 h, being this plant commonly used for the first, or pre-drying as it is called, stage of the operation. A more recent assessment of this industry gives that the wet coffee enters the crossflow dryer with 51% w.b. and leaves at approximately 40%, from which it is transported to the final phase of the process, carried out in a rotary dryer [25].

In principle the crossflow dryer is a continuous system but product recirculation is usally necessary before an acceptable output is obtained. In principle the operator can alter the quantity and temperature of the drying air in order to vary the throughput of the plant but in practice this is seldom done. Instead the output moisture content is checked and the flow of product controlled manually until the output moisture content is satisfactory.

It is noted from figure 1.4 that in the crossflow dryer the material is circulated in drying columns through which the heated air is passed. The product is recirculated as many times as necessary to achieve a final moisture content, this is done by the operation of the screw conveyor at the bottom and the attached elevator. Note that the drying air interacts with a moving layer of product, the thickness of which is generally in the range 0.1-0.4 m. For more details on the typical crossflow

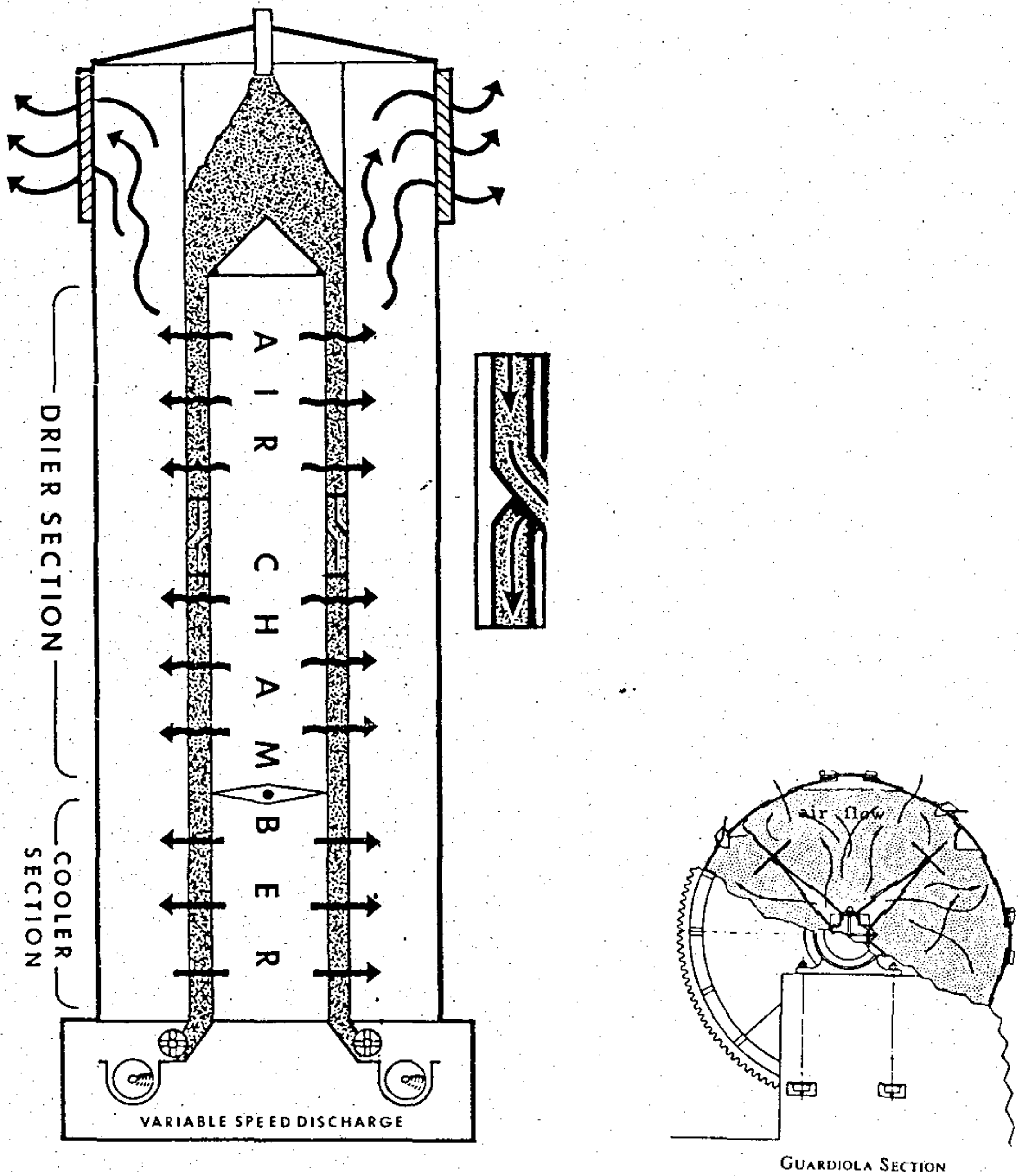

(a) (b)

Figure 1.4 Typical agro-industrial dryers.
(a) Crossflow Dryer (after Berico, USA);
(b) Guardiola (rotary) Coffee Dryer [42]

plant see Appendix II.

In the case of the rotary, or guardiola tumble dryer the material is loaded in batch in the system and the heated air interacts with single particles although conduction is also used to transfer heat from the internal metal surfaces to the material itself. This unit (figure 1.4) is one of the most used dryers in the coffee industry [42], being mostly used after the pre-drying phase as exposed above. The size of a Guardiola unit capable of processing a 2,300 kg batch of coffee is, typically, 5 m long and 1.8 m in diameter. These two types of dryer are capable of producing at least ten times the output which could be obtained from the type of unit reported by McDonald & Freire occupying the same floor space. Photographs of typical dryers are shown in figs. 1.5-1.10.

The size of the drying plant is governed by such factors as the size and geographic distribution of the farms, the duration of the harvest, the type of management of the plants, the infrastructure, the size and location of internal markets and the location of exporting ports. Taking as an example the case of coffee, in some Central American countries where the size of privately owned plantations is relatively large there is a greater number of large plants than in those countries where

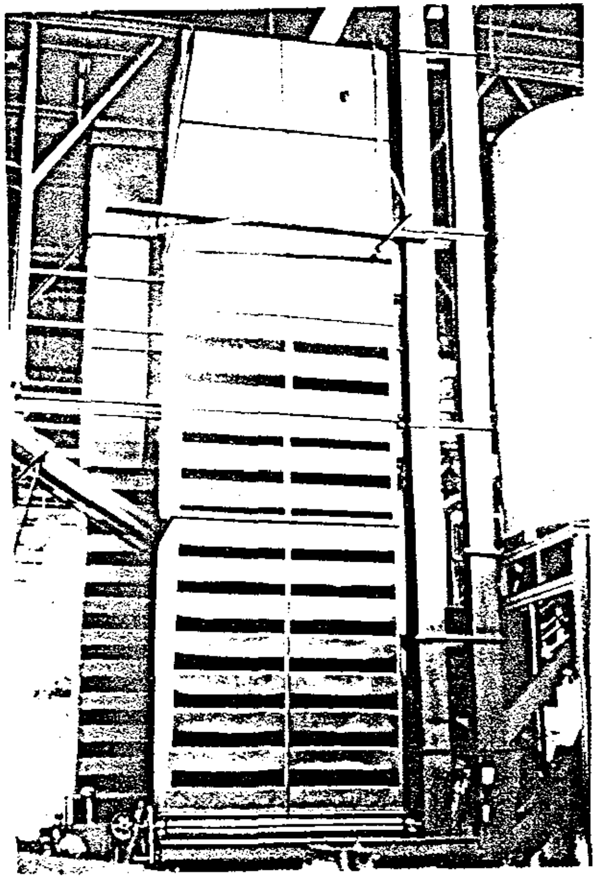

Figure 1.5 Twin system of crossflow dryers and bucket elevators.

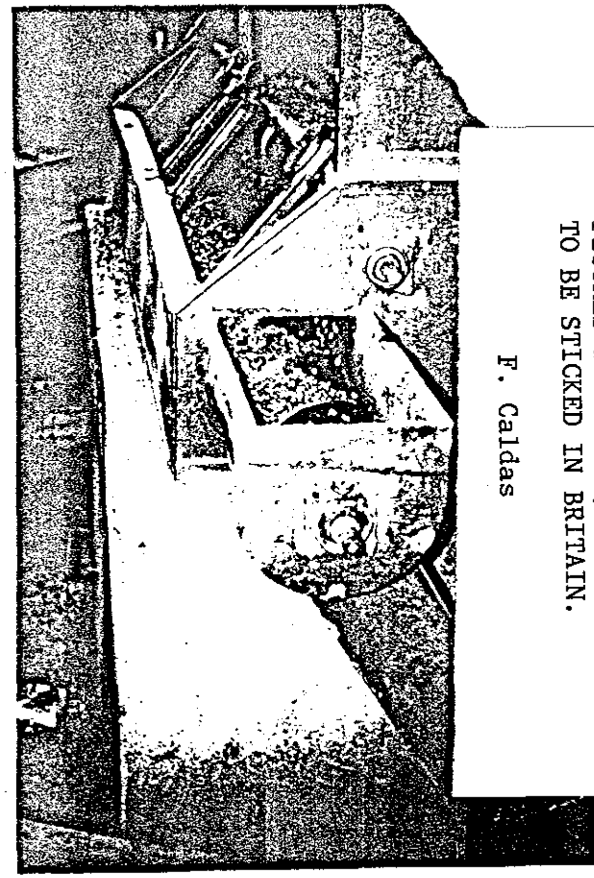

Figure 1.6 Screw conveyor at bottom of crossflow dryer.

NOTE:
FIGURES 1.5-1.10 (PHOTOGRAPHS) TO BE STICKED IN BRITAIN.
F. Caldas

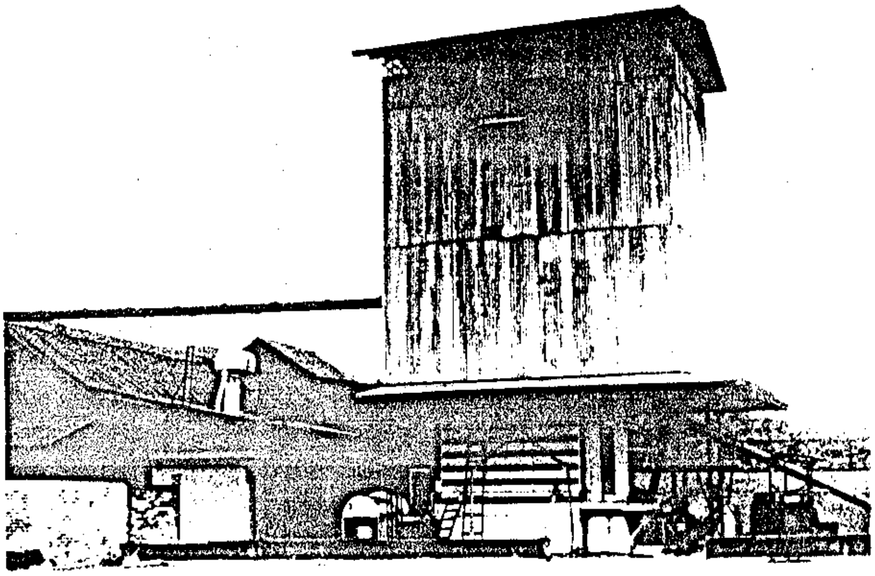

Figure 1.7 Crossflow dryer in agro-industrial (coffee processing) plant.

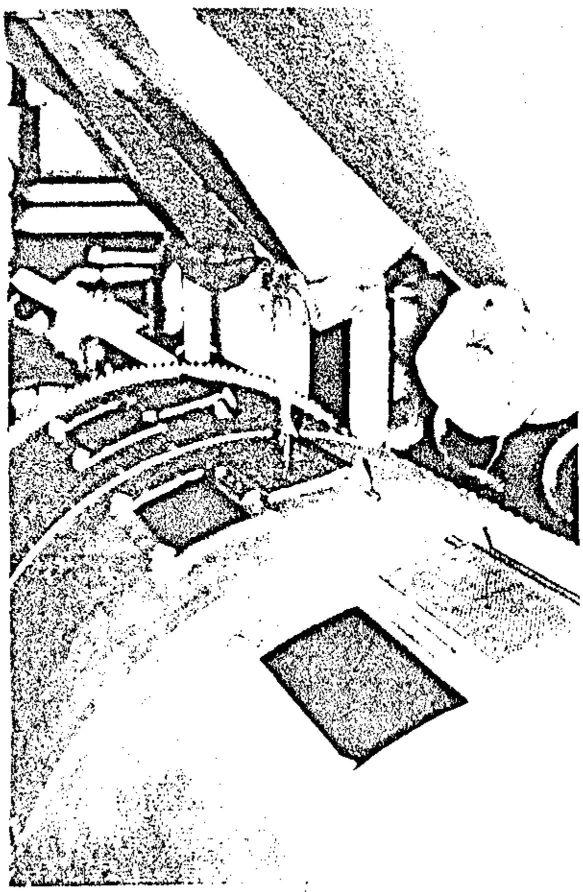

Figure 1.8
Feeding a guardiola rotary dryer from hoppers.

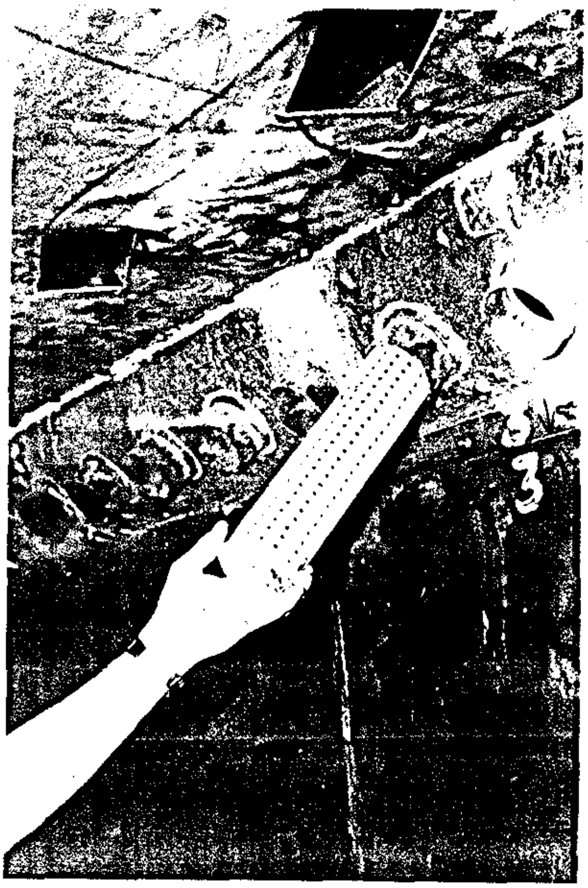

Figure 1.9
Dismantled guardiola coffee dryer; note the position of the heat exchangers on the central hot air tube.

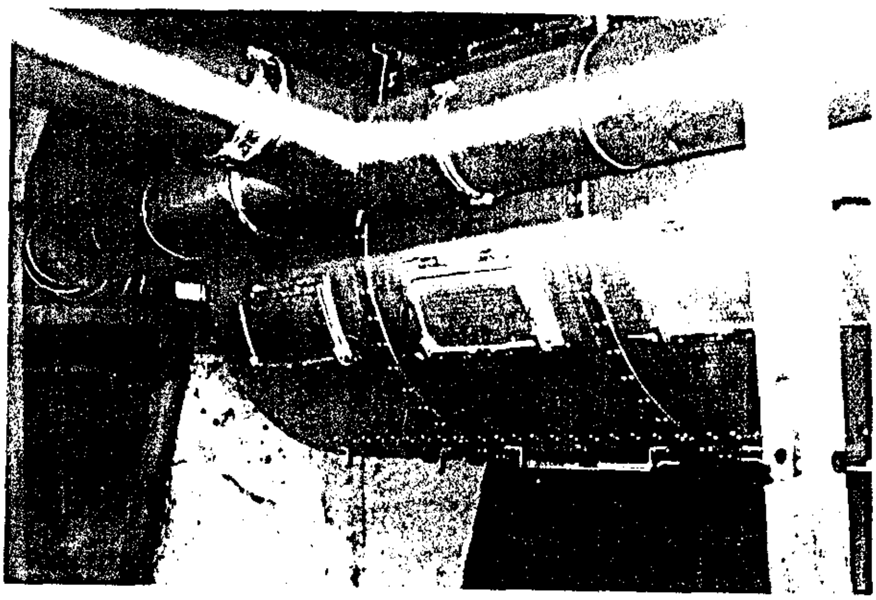

Figure 1.10 When the coffee is finally dried the compartments of the guardiola are opened, the product is taken out and placed on the floor below the dryer.

co-operatives are responsible for a major part of the production. To illustrate the variations in scale, one Brazilian company which is responsible for processing most of the cereal grain output of the state of Sao Paulo has an output, in volume terms, almost three times as great as all the coffee plants in Costa Rica [2, 27]. In Costa Rica approximately 74,000 tonnes of water need to be removed from the coffee crop every year, thus about 48 GWh are needed to supply the latent heat with an additional 5 GWh for the sensible heat of the water and base material.

It might be thought that, as the levels of technology in the plant are increased, the less important drying costs become in terms of the overall production economics. In the washed coffee process, for example, the capital equipment investment is likely to be greater than that in the natural process or in cereal drying plant, the recent studies of Marin et al [104], Rojas and Moya [139] and Rojas [138] estimate that drying accounts for no more than 13% of the total production costs of washed coffee (excluding labour and administrative costs). Cereals must be dried and hulled and in natural coffee and peanut production the sorting operations add a little more complexity to what is essentially a basic process. It might be concluded that, as the proportion of drying as compared with the total costs is reduced then less importance will be placed on relative fuel prices, this is particularly true of high value products, in general the reverse applies for low value products. This potential for energy substitution is of great importance for many countries as discussed in Appendix I but although the energy factor is important it is a macroeconomic effect and, as such, is not of primary concern to the industrialist. It is, however an incentive to Government to invest in new technology and to adopt policies, e.g. favourable tax conditions and grants for capital investment in energy saving equipment, which will eventually benefit the country as a whole. Nevertheless, the key factor which will persuade the industrialist to invest in electrical heating processes is likely to be related to a perceived enhancement in terms of better products and higher throughputs.

2. THE DRYING PROCESS

2.1 Introduction

Drying as considered here is a process by which a liquid, normally water, is evaporated from a solid using thermal energy, i.e. by conduction, convection, radiation or internal heating (high frequency) techniques. Mechanical methods such as draining, compression and centrifuges are not considered here although, wherever possible, they should be used in preference to thermal methods since the latter are usually more expensive (see for example [30] and [44]). The reason is that if the product is very wet the quantity of heat required to heat up the material (solid plus water) to a given temperature and then change the water from liquid to vapor is far greater than the energy needed to extract the liquid by mechanical methods. However, if the water is contained in the interior of a capillary-porous body it is restrained by forces which cannot be completelly overcome by means of external effects such as those produced by gravity (draining, centrifugion) or compression. Most biological materials, particullarly agricultural products, are such bodies according to Luikov [100] who defined a capillary-porous body as one in which the potential created by the internal forces is much greater than the potential due to gravity.

Thus thermal methods of drying are usually required, these normally involve air as the transport medium, i.e. air transfers heat to the material and also carries away moisture. In some cases however it may be convenient to use the air just as a moisture extraction agent (e.g. in conductive, radiative and internal heating methods) and in some circumstances (e.g. vacuum drying) it may not be used at all.

A brief treatment of the drying process is presented below, the material is intended to provide a background from which the work described in this Report was developed and is concerned with the main external and internal factors which may be measured or controlled, therefore it is inherently practical. A more fundamental approach can be found in the works of Luikov [100, 101] and Whitaker [167]. The latter examines the theory and phenomena of drying from the point of view of physics whilst Luikov presents a simplified formulation of the heat and mass transfer mechanisms used in the present Report. He also comments on important properties of materials which are relevant to the present application.

2.2 Theory of Drying: Heat Supplied from External Sources

When the heat is applied to the surface of the material the drying mechanism is controlled by the following factors:

i) Environmental conditions, i.e. temperature, relative humidity and flow of air, and also ambient pressure;

ii) Physical properties of the material, i.e. dimensions, thermal (e.g. specific heat, thermal conductivity, thermal gradient coefficient) properties, physical (e.g. diffusivity, density) properties and, in some cases, optical (e.g. absorptivity and reflectivity) properties of the material being dried;

iii) Other intrinsic properties of the material related to the resistance that it poses to mass flow within the structure;

iv) Temperatures of the material and heat source;

v) Relative position of heat source and the material.

Although a knowledge of the above characteristics of the material and external conditions is useful for understanding, up to a point, the phenomena involved, in practice the design of the plant is based on an experimental assessment of the performance of the drying process. Even the most simplified theoretical modelling of the latter is extremely complex and the results can only be approximate due to the large variations in the properties of most materials, particularly biological products, and also because of the difficulty involved in actually defining and measuring some of the parameters required for the mass and heat transfer equations.

Initially, when heat is applied to the surface of the material, both the water and the dry material approach a temperature equilibrium. Provided that the surface of the material is wet, i.e. the internal water is constantly migrating due to internal mechanisms discussed later, all additional energy supplied is used to maintain this equilibrium and to evaporate the surface water. This creates a constant temperature/evaporation phase, which remains until there is insufficient water migration to the surface to keep it covered by a layer of water. At this point the temperature of the wet material starts to increase since not all the energy supplied to the material can be used to evaporate water, the surplus energy is absorbed by the material itself. These two different drying phases after the initial temperature equilisation period, are commonly refered to as the constant and falling rate drying periods.

2.2.1 Constant and Falling Rate Drying Periods

In theory the steady state characteristics of air drying (i.e. those corresponding to constant rates of evaporation) can be defined by psychrometry and conventional mass and convective heat transfer equations and the internal mechanisms of mass and heat transfer within the material do not need to be taken into account. Psychrometry is concerned with the characteristics of gas-vapor mixtures which, in the case of interest here, is moist air, i.e. dry air plus water vapour. The properties of this mixture are determined by thermodynamic relationships considering perfect gas laws, i.e the mixture of dry air and water vapor is assumed to follow the characteristics of the individual components. Hence theoretical relationships can be derived and depicted in graphs called psychrometric charts (see for example the termodynamic relationships presented by Chilton & Perry [30] and Brooker et al [20]).

If sufficient heat is applied to the surface of the material then, provided internal mechanisms have forced moisture from the interior to the surface through the internal layers of the material, the molecules on the surface will acquire sufficient energy to overcome the molecular forces which bind them together. Then, due to the moisture concentration gradient between the saturated surface and the surrounding air, they will leave the surface and mix with the medium. This process is called evaporation and depends on the temperature of the surface, which governs the amount of kinetic energy attained by the molecules and which enables them to escape, the relative humidity of the air and the air velocity.

The use of psychrometrical estimations is based in the fact that if a material is air-dried then, as long as the surfaces in contact with air are moist, their temperature will be approximately equal to that measured by a thermometer placed in contact with the same air flow if the bulb of that thermometer is covered with a wet wick, a so called wet bulb thermometer. This is due to the fact that similar surface evaporation conditions will be experienced by the soaked wick and the surface of the material. The practical significance of this is that, as long as the surface of the product is wet, its temperature can be read from a psychrometric chart if at least two characteristics of the drying medium are known, e.g. dry bulb temperature T_a (the temperature measured by an ordinary thermometer) and the relative humidity r.h.

Hence, in order to find a relationship for the rate of evaporation of water when the material is air dried and is covered by a layer of liquid, the heat transferred to the material can be equated to the heat required to evaporate the water. this assumes that there is a continuous flow of moisture to the surface and that the material has reached a constant temperature, all heat received being used for evaporation. Taking dm'/dt as the rate of evaporation in kg/h, and h_v as the latent heat of evaporation (Wh/kg), we have

$$Q_{convection} = h_v \, dm'/dt$$

Convection occurs at the surface and conduction within the internal layers of the body. In so far as this study is concerned it should be noted that conduction will also take place between the individual particles and between them and the walls of the dryer. There will also be radiation from heat sources to the surface of the body. However, in most cases, convection is the major mechanism involved in the transfer of heat to the body when using heated air drying systems and, to a good approximation, it may be said that it is the only significant method in conventional crossflow dryers. Conduction between particles and between the latter and the walls of the dryer is usually neglected in very complex drying simulations of commercial drying techniques as will be discussed later in this Chapter.

The moisture concentration gradient between the wet surface and air is the driving mechanism for evaporation, this potential is usually expressed in terms of the difference between the vapor pressure of the body and that of air at the particular value of relative humidity. The vapor pressure of water is an exponential function of temperature as shown in figure 2.1 and that of a saturated moist (or liquid) surface will correspond to the value for pure water. The vapor pressure of moist air at a relative humidity of r.h. (per-unit) is equal to that of water multiplied by the factor r.h. Hence, for the evaporation potential to be a maximum, the vapor pressure of the body should be as high as possible relative to that of air. This can be achieved by maintaining a permanent layer of moisture on the surface of the body and using drying air whose relative humidity is as low as possible. The evaporation potential also increases with an increase in the dry bulb temperature of air (which also increases the wet bulb temperature), this is due to the resultant decrease in relative humidity of air and the increase in water vapor pressure of the layer (due to the increase in its temperature).

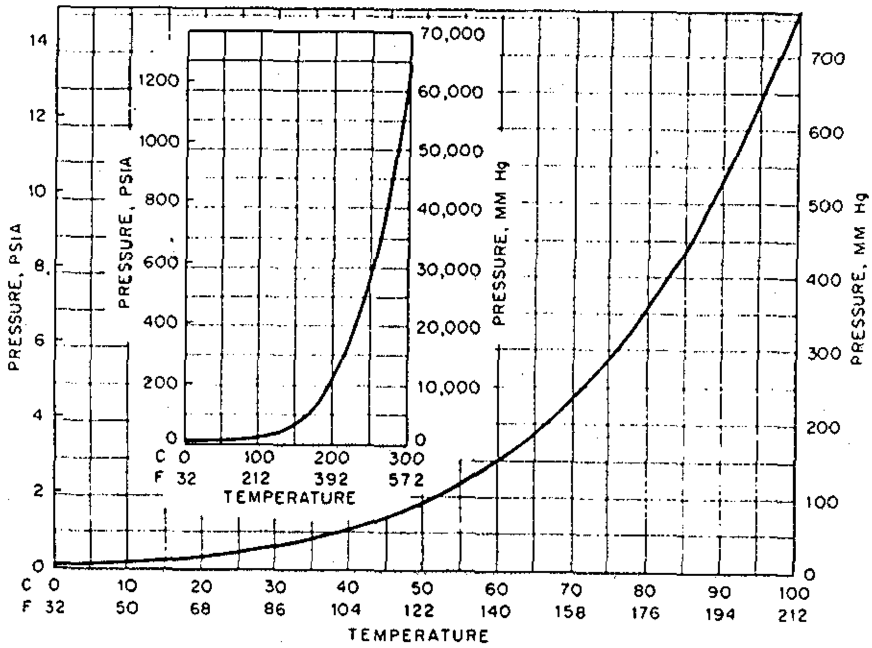

Figure 2.1
Vapor Pressure
of Water[42].

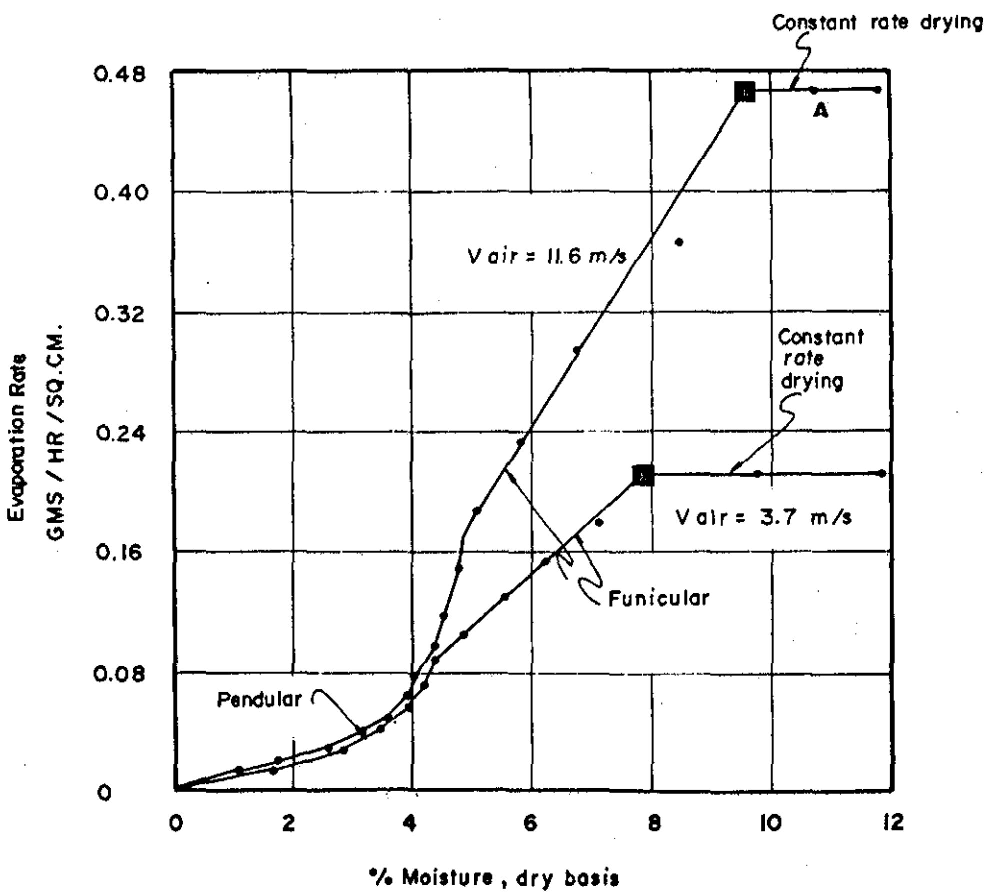

Figure 2.2 Typical Evaporation Curves for a Porous Material, Air Temperature 53°C[144].

If high rates of moisture evaporation from the surface are required, the heat transfer resistance of the air-water/surface interface layer (where the bulk of convection occurs) should be as low as possible. An increase in the air flow rate at the surface will assist in heat transfer across the interface layer by reducing its thickness. Alternatively, other mechanisms of heat transfer can be used to increase the total heat supplied to the surface of the material although, as will be noted later, increasing the external energy supply to the material may actually hinder the internal drying mechanism. Considering both conduction and radiation in addition to convection, the rate of heat transferred, i.e. the amount of heat (Wh) supplied in unit time is given by:

$$Q_{convection} + Q_{conduction} + Q_{radiation} = h_v \, dm'/dt \quad W \qquad (2.1)$$

Alternatively the rate of evaporation is proportional to the difference between the vapor pressure of water on the surface of the body, P_b and the vapor pressure of air in the surrounding drying medium, P, i.e. [30, 64]

$$dm'/dt = h_m A(P_b - P) \qquad kg/h \qquad (2.2)$$

where P_b and P are given in kg/m^2 and h_m is the coefficient of mass transfer (1/h). A is the surface area of the material available for evaporation (m^2).

The Q terms of equation (2.1) are developed in the following Chapters, they are the rates of heat transferred in unit time when each of the heating techniques is employed;

$$Q_{convection} = h_c A'(T_a - T_b) \quad W \qquad (2.3a)$$

$$Q_{conduction} = [k A''(T_s - T_b)]/x_Q \quad W \qquad (2.3b)$$

$$Q_{radiation} = A'''\sigma F(T_s^4 - T_b^4) \quad W \qquad (2.3c)$$

where h_c is the convective heat transfer coefficient in W/m²/ C, k is the thermal conductivity of the material in W/m/C, x_Q is the length of the heat conduction path in m, between the two points at which the temperatures T_s and T_b are measured, F is the generalized view factor between the heat source and the material, σ is the Stefan-Boltzman constant, 5.67E-8 W/m²/K⁴, A′, A′′ and A′′′ are, respectively, the total area for convective heat transfer, the area of the material in contact with the heat source and the area of the source. T_a, T_s and T_b are, respectively, the temperatures of air, heat source and material.

In the above equations the conduction and radiation sources have been assumed to operate at the same temperature. If this is not the case then the two different heat source temperatures need to be used in the appropriate equations. It is also assumed that, since the individual particles are almost at the same temperature (tumbled particles in a rotary dryer, moving grain in the columns of a crossflow dryer) conduction between them is negligible. Constant movement of the particles is recommended to avoid non-uniform and excessive heating within the bulk of product.

Combining equations (2.1)-(2.3) we have;

$$dm'/dt = [h_c\ A'(T_a - T_b)]/h_v + [k\ A''(T_s -$$

$$T_b)]/x_Q h_v + F\sigma\ A'''\ (T_s^4 - T_b^4)/h_v \qquad (2.4a)$$

$$dm'/dt = h_m\ A'\ [P_b - P] \qquad (2.4b)$$

where P_b, the water vapor pressure of the surface water (see figure 2.1), is evaluated at T_b, and P, the water vapor pressure of the moist air, at temperature T_a.

At saturation the latter is obtained from figure 2.1, however in general P is given by the product of the relative humidity of air and the vapor pressure of water evaluated at T_a. In theory, knowing the temperatures of air and source and all the coefficients and dimensions involved, the evaporation rate dm'/dt and the wet bulb temperature of the material T_b can be found. The evaporation can therefore be estimated from the air flow conditions, i.e velocity (which affects h_c), temperature and humidity, in addition to the thermal conductivity of the material, the heat source temperature and the relative positions of the heat source and the material.

In this phase the air and source temperatures can be maintained as high as possible so long as the temperature of the layer of water covering the material is not greater than the temperature limits for the product. Hence, if the contribution of radiation and conduction is negligible, e.g. in crossflow dryers, the dry bulb temperature of air can be increased up to the point where the corresponding wet bulb temperature (read from the psychrometric chart) approaches the limits for the particular product. If radiation and conduction are taken into account then the system of equations needs to be solved for T_b and, since in this case the temperature will exceed the wet bulb level, it is important to prevent this from exceeding the temperature limit of the product.

The evaporation rate, dm'/dt, can be related to a drying rate since an amount of evaporated water dm' corresponds to a reduction dm in the water contained in the material, i.e. $dm' = -dm$. Moreover, if the contained water is expressed in terms of moisture content dry basis (d.b.), M, we have

$$dM = dm/(\text{mass of dry solid}) \qquad (2.5a)$$

and,

$$dM = dm/(\rho_s V) \qquad (2.5b)$$

this is a per unit quantity where ρ_s is the bulk density of the dry material in kg/m^3 and V is the volume of material in the drying zone in m^3. Substituting eq (2.5b) in eq (2.4a) and assuming that conduction and radiation are not present gives

$$dM/dt = -[h_c A'(T_a - T_b)]/(h_v \rho_s V) \qquad (2.6)$$

which is the rate of variation of the moisture content of the material in a dry weight basis (i.e. kg water/h/kg dry material) when air-drying in the constant rate period.

From the above it will be realised that a limited amount of information can be obtained from the psychrometric chart and the equations quoted. If the relative humidity and temperatures (dry and wet bulb) are known the maximum drying capacity of the air can be estimated from the psychrometric chart, i.e. the weight of water which a given amount of air (m^3, kg) can absorb before it is completelly saturated. The theoretical air flow required is then the ratio between the evaporation rate, dm'/dt, and the drying capacity of air under the specified ambient conditions. In practice more flow may be required since the air saturates only in a, relatively thick, layer of material. The energy required in unit time to raise the temperature of ambient air to the dry bulb temperature is then given by the product of the specific heat, temperature increase and flow of air.

Note that, as long as the operating conditions of the system do not change, a so-called constant rate drying will continue provided that the surface of the material is saturated with moisture. The vapor pressures of the surface and the air under these conditions are such as to result in a constant evaporation potential. The constant rate drying period ends when, at a point which is refered as the critical moisture content of the material, the internal moisture migration is reduced below that necessary to maintain an evaporative water layer on the surface of the material. This reduction in available moisture will reduce the evaporation rate from the surface and the temperature of the product will rise until it reaches that of the air, if convection only is used in the process, or a higher level if the contribution of radiation and conduction is considerable. Nearly all drying of crops occurs in the falling rate period [64] therefore the relationships derived for constant rate drying have only limited relevance in such applications. Some agricultural products are dried from high initial moisture levels, e.g. coffee in which case the constant rate period may be important, this also appears to be the case in drying sugar beet. Other granular products may be partially dried in this phase, and if high frequency techniques are used it is likely that the constant rate stage is enlarged.

In general the total drying time cannot be calculated using only the above theory. It is not simply the ratio between the weight of water to be extracted and the evaporation rate obtained from the above since the latter is only applicable to the constant rate period. When the falling rate period commences the variables which control the drying rate cannot be defined only by the external conditions which have been described, they also depend on the internal characteristics of the material being dried. When this second phase is established the temperature of the product is very close to that of the air and therefore convection becomes less effective. Moreover most of the energy supplied in heating up the air may well be wasted unless the air flow is considerably reduced. Drying continues as long as the vapor pressure of the moisture in the product is higher than that of air provided that the internal structure of the material allows the diffusion of water to the surface.

Sherwood [144] was one of the first to develop the concept of different phases, or periods, of drying. It is important to note that these periods are not identical for all circumstaces but are dependent on the particular material being dried, and more important, they change with the conditions under which the process is carried out. Thus there is no such thing as a constant value for the so called critical moisture content, it can be affected by variation in the air flow as shown in figure 2.2 which describes a typical evaporation curve for a porous ceramic material.

McCabe [115] separates the drying phases into constant rate, funicular and pendular, the latter two are included in the falling rate period since the rate of evaporation continuously decreses. Chilton & Perry [30] divide the falling rate period into two phases, unsaturated surface drying and internal moisture movement, these are equivalent to the second and third terms used by McCabe.

The funicular, or unsaturated surface phase, starts when the surface of the material is not completely wet, hence the effective area of evaporation is reduced. The evaporation rate per unit wetted area may still remain constant and therefore the velocity of air still plays a significant role as seen from figure 2.2. This phase is equivalent to constant rate drying on a continuously reducing evaporating area. The pendular phase starts when all the moisture is contained within the capillary network of the material, this stage constitutes the main case of interest of the present Report, and in what follows it will be referred to simply as the falling rate drying period. It is worth noting that, once this stage is reached, the air velocity plays no significant part in the drying process (fig 2.2). Therefore, if conduction and radiation are present in additon to convection, the following is obtained:

$$h_c\, A'(T_a - T_m) + [k\, A''(T_s - T_m)]/x_Q +$$

$$+ F\sigma A'''(T_s^4 - T_m^4) = h_v\, dm'/dt + \dot{m}\,(T_m - T_i)Cp$$

$$= -h_v dm/dt + dm/dt(T_m - T_i)Cp_w + dm_d/dt(T_m - T_i)Cp_d \qquad (2.7a)$$

where T_s, T_m, T_i and T_a are, respectively, the temperatures of the heat source, the material at time t, the material when the falling rate period commences and the air. Cp, Cp_w and Cp_d are the specific heats of wet material, water and dry solid respectively.

$\dot{m}$ is the throughput of wet material in weight terms, it can be divided into water and solid, i.e.

$$\dot{m} = dm/dt + dm_d/dt$$

The flow rate of the dry solid can be approximated to

$$dm_d/dt = \rho_s \tau$$

where τ is the drying throughput expressed in terms of the volume of processed material per unit time, i.e. m^3/h.

Then,

$$h_cA'(T_a-T_m) + [kA''(T_s-T_m)]/x_Q +$$

$$+ F\sigma A'''(T_s^4-T_m^4) = -h_v dm/dt + dm/dt(T_m-T_i)Cp_w$$

$$+ \tau\rho_s(T_m-T_i)Cp_d \qquad (2.7b)$$

Eq (2.7b) relates the temperature (T_m) to moisture (m) contained in the product at a given time after the (falling rate) drying period begins. There are two unknowns in the one equation. The drying rate (and consequently the moisture contained in the product at a given time) is not determined only by the external forces acting on the material, i.e. the levels of applied energy shown in eq (2.7b), it is also affected by the different barriers which the moisture finds on its paths within the material. The latter vary with the internal structure of the body and by the way in which the fluid responds to different stimulae, e.g. internal temperature, moisture and pressure gradients in the medium. Different responses can be expected if the internal moisture is in the liquid, vapor or mixed state.

Hence even if all the coefficients, dimensions and properties referred to in eq (2.7b) are known, the temperature of the material, T_m, cannot be estimated for particular values of T_a, T_s and T_i, since the drying rate dm/dt cannot be determined from eq (2.4b) and figure 2.1. In this case the surface of the product is no longer covered by a layer of water and the vapor pressure within the material is not equal to that of a free water (saturated) surface, it is continuously decreasing in accordance with the fall in the interior moisture content.

Using eqs (2.7b) and (2.5b) and considering the air-drying mechanism alone,

$$h_cA'(T_a-T_m) = -h_v\rho_s V dM/dt + v\rho_s dM/dt(T_m-T_i)Cp_w$$

$$+ \tau\rho_s(T_m-T_i)Cp_d$$

$$T_m = [v\rho_s(h_v + T_iCp_w)dM/dt +$$

$$+ \tau\rho_sT_iCp_d + h_cA'T_a]/[\rho_s(v dM/dt Cp_w + \tau Cp_d) + h_cA'] \qquad (2.8)$$

In order to estimate T_m the drying rate dM/dt needs to be known, in this phase this can only be obtained by considering the heat and mass transfer mechanisms within the material, these will be examined below.

2.2.2 Equilibrium Moisture Content

For particular set of ambient conditions the material will tend assymptotically towards an equilibrium moisture content, it will remain at this value provided that the ambient conditions are not modified and that the product is not subjected to any external influences other than that of the air surrounding it, i.e. radiation, conduction or internal heating are absent. The conditions refered to above are the pressure, temperature and relative humidity of the air. Hence for a mass of product surrounded by air at a particular temperature and pressure there is a particular relationship between the moisture content at equilibrium and the relative humidity of the air. If the material is to be stored in a controlled environment (constant pressure, temperature and relative humidity) for a long period then there is no point in drying it below the corresponding equilibrium moisture content since, in such a case, it would regain moisture from the air until the moisture content reached the equilibrium value.

Many relationships connecting relative humidity, ambient temperature and equilibrium moisture content are available for different products, they are usually presented in the form of graphs or tables, see for example figure 2.3 for ambient temperature. The temperature and relative humidity must both be considered when computating dynamic conditions, e.g during drying simulations.

Chung and his colleagues [33] examined the precision of several equilibrium moisture models and derived constants which describe these relationships for several products of interest. The paper referred to presents five models, among which Henderson's equation is one of the most widely used. This can be expressed as

$$r.h. = \{1 - \exp\left[-a\,(T_a+b)M_e{}^c\right]\} \qquad (2.9)$$

where M_e (per-unit d.b.) is the equilibrium moisture content of the material and (a,b,c) are positive constants which take into account the nature of the product being dried.

Safe storage of crops is of utmost importance, the major factors needing to be controlled are those responsible for the biological effects which cause infestation and deterioration of the product. The limits for safe storage can be expressed in terms of boundary constraints which take into account the germination characteristics, insect and fungal action, etc as

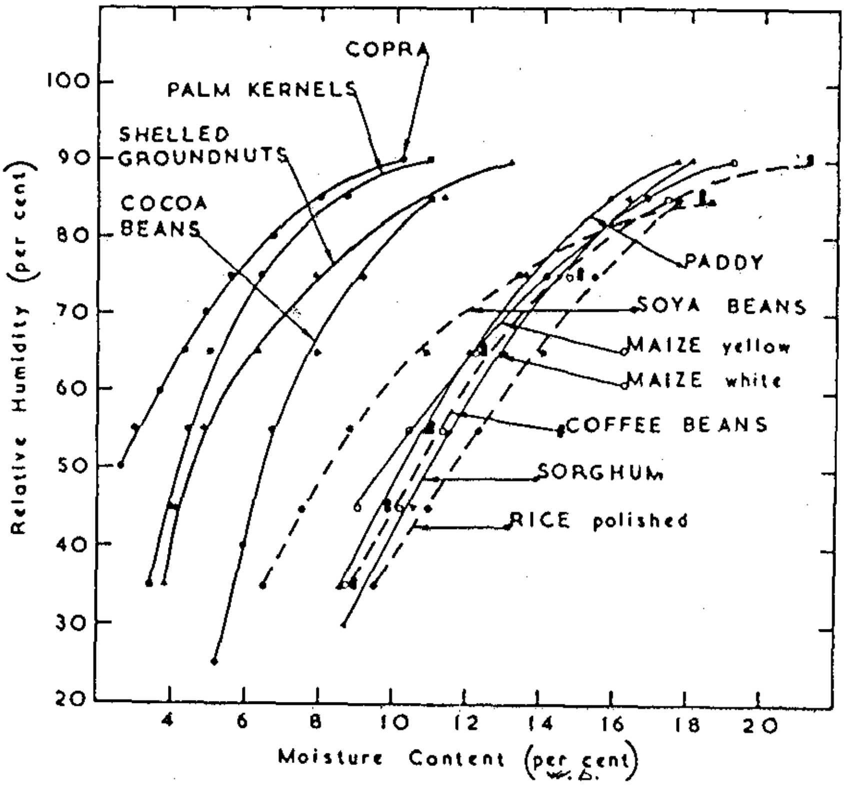

Figure 2.3 Equilibrium Moisture Content as a Function of Relative Humidity of Air[113].

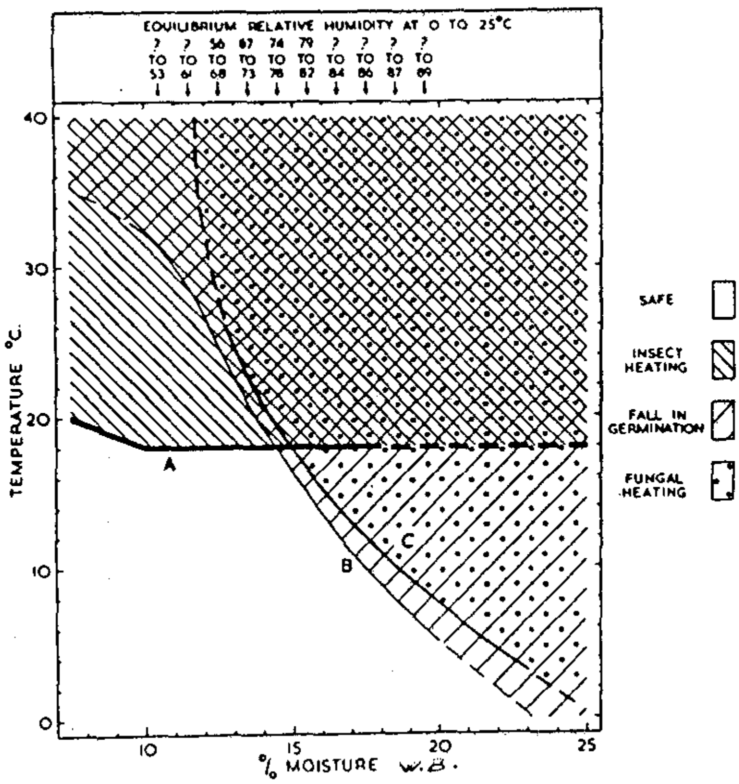

Figure 2.4 Relationship of storage temperature and grain moisture content to insect heating, fall in germination, and fungal heating in cereals. (A=lower limit for insect heating, B=lower limit for germination, C=lower limit for fungal heating)[113].

shown in figure 2.4. This graph can be used as follows: given certain ambient conditions a definite equilibrium moisture content is established by eq (2.9), the material then has attained a given temperature which can be measured by a thermometer, neither this temperature nor M_e should be outside the limits depicted in figure 2.4, they can be controlled if necessary by an air conditioning systems, i.e. by storing the product in a controlled environment.

2.2.3 Falling Rate Air Drying Models for Particles with Fully Exposed Surfaces

2.2.3.1 Lewis Model

Lewis [97] observed that, in the falling rate drying period, the moisture content of the material shows an initial rapid drying phase followed by a characteristic falling curve, the latter being assymptotic to the equilibrium moisture content. The simplest assumption is to consider the drying rate as being directly proportional to the free moisture content, i.e. that amount of water which is left in excess of the equilibrium moisture content. Then,

$$dM/dt = -k'(M-M_e) \qquad (2.10$$

where k′ is a constant.

Integration of eq (2.10) yields,

$$\ln(M - M_e) - \ln(M_i - M_e) = -k't$$

$$MR = (M-M_e)/(M_i-M_e) = \exp(-k't) \qquad (2.11)$$

MR is the moisture ratio and M_i is the initial moisture content of the product when the falling rate period commences.

This approach has been adopted by other workers to describe the drying rates of different products, it is sometimes referred to as the logarithmic drying model. The aim is to fit an experimentally obtained falling rate drying curve to the above equation. k′ is known as the drying constant, its units are 1/h.

Simmonds et el [146] examined the drying of wheat from initial moisture contents as high as 38 % w.b. under different air velocities in the range 0.16 - 0.82 m/s, temperatures (21-77 C) and absolute humidities 0.0078 - 0.033 kg of water/kg of dry air. They found that a fourfold variation in air velocity produced a negligible effect in the drying rate when ambient conditions where not altered, the estimated value of k′ and the observed M_e were constant. It is worth noting that these authors introduced a new concept, the dynamic equilibrium moisture content, which is the corresponding value to that which fits the experimental data into eq (2.11) if a time independent value of k′ is assumed. This equilibrium value has been interpreted as a "premature equilibrium" which is somewhat higher than the "static equilibrium" given by eq (2.9), which by definition is only attained over a long period of time.

When the effect of air temperature was examined by Simmonds et al at constant velocity and relative humidity, the evaporation rate was found to increase with temperature. The dynamic equilibrium moisture content decreased considerably and the drying constant experienced a sharp increase. The effect of air humidity was studied at two air temperatures, 49 and 66 C. The variation in relative humidity at 49 C was between 0.1 and 0.4, the corresponding range at 66 C was 0.04 to 0.20. It was found that the rate of evaporation slightly decreased when the relative humidity increased, the drying constant decreased by 22% when the relative humidity was increased from 0.1 to 0.4 at 49 C, M_e was not significantly affected.

Allen [5], using maize, investigated further the phenomena studied by Simmonds et al, the results are similar, i.e. the drying constant shows a significant increase with air temperature, with M_e (dynamic) being substantially reduced over the same range of temperatures. A variation in relative humidity from 0.2 to 0.8 gave rise to minor effects in both drying constant and M_e.

Henderson and Pabis [74, 75] concentrated on an analysis of the effects caused by variations in air temperature and velocity, they concluded that the drying constant can be expressed as

$$k' = 6/\pi^2 a \exp(-b/T_a) \qquad (2.12)$$

where a and b are constants and T_a is the absolute temperature of air. They fitted the data presented by Simmonds et al and Allen to eq (2.12), the results are shown in figure 2.5. It was found that a variation in the air flow from 0.02 to 0.68 m/s produced an insignificant effect on the drying rate.

2.2.3.2 <u>Empirical Models</u>

It has been said that empirical drying models usually give

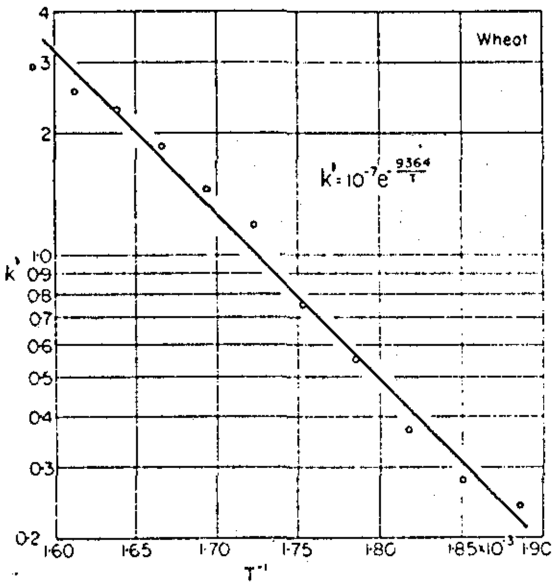

Figure 2.5 (a) Relationship between the Drying Constant and the Reciprocal of Temperature for Wheat from data by Simmonds et al [146]. Correlation coefficient = 0.949[75].

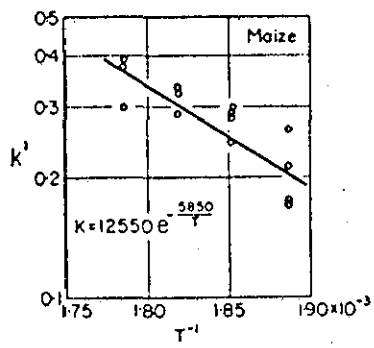

Figure 2.5 (b) Relationship between the Drying Constant and the Reciprocal of Temperature for Rice and Shelled Maize from data by Allen[5]. Correlation coefficient for Maize = 0.832[75].

the best description of the drying rate of agricultural products although, until recently, satisfactory models were only available for maize [20]. More recently many empirical equations have been proposed for predicting the air drying of agricultural products in the falling rate drying period.

Singh and Agrawal [150] carried out drying experiments, using rough rice, at a relative humidity of air of 0.26 and temperatures from 32 to 51 C, and at a constant air temperature of 51 C and relative humidities from 0.19 to 0.85. The moisture ratio MR was computed by substituting M_e using the so-called Pfost equation which has the same form of eq (2.9), the values of M(t) can be obtained from the experimental data and a formula similar to eq (2.11) used. In this case an empirical drying exponent n is included, i.e.

$$MR = [M(t) - M_e]/[M_i - M_e] = \exp(-k't^n) \qquad (2.13$$

Then, using regression analysis, the coefficients k′ and n can be expressed in terms of the temperature and relative humidity of air.

Singh and Wang [147] continued the previous experiments with rice using various air temperatures (30 - 55 C) and relative humidities (0.15 - 0.85), they compared the following empirical models

$$MR = \exp(-k' t^{n}) \tag{2.14a}$$

$$MR = 1 + A\,t + B\,t^{2} \tag{2.14b}$$

$$t = A \ln MR + B(\ln MR)^{2} \tag{2.14c}$$

Equation (2.14b) was found to be preferable whenever drying is not too long, equation (2.14a) is more appropriate over long drying periods, e.g. when drying under ambient conditions with a very limited energy input. Similar studies were carried out with soya by White et al [168], who adopted the model described by eq (2.14a).

2.2.3.3 Simplified Theoretical Approach : Diffusion Models

2.2.3.3.1 Background

Several concepts have been employed to explain the internal moisture movement in capillary porous materials, for a detailed discussion of these mechanisms see, for example, Allen [5], Chilton & Perry [30], Husain et al [82], Luikov [100] pgs 233-48. Amongst these mechanisms diffusion has received most attention, particularly when describing the drying characteristics of agricultural products.

Luikov and others (see references given by Husain et al) have used fundamental thermodynamic relationships to derive transient equations which describe the variation of moisture (M), temperature (T) and pressure (P) within a body, these are

$$\partial M/\partial t = K_{11}\nabla^2 M + K_{12}\nabla^2 T + K_{13}\nabla^2 P \qquad (2.15a)$$

$$\partial T/\partial t = K_{21}\nabla^2 M + K_{22}\nabla^2 T + K_{23}\nabla^2 P \qquad (2.15b)$$

$$\partial P/\partial t = K_{31}\nabla^2 M + K_{32}\nabla^2 T + K_{33}\nabla^2 P \qquad (2.15c)$$

where $\nabla^2 X = \mathrm{div}\,(\vec{\mathrm{grad}}\; X) = \nabla\cdot(\vec{\nabla} X)$, in spherical coordinates i.e.

$$\nabla^2 X = \frac{1}{r^2}\frac{\partial}{\partial r}\left(r^2\frac{\partial X}{\partial r}\right) + \frac{1}{r^2\sin^2\theta}\frac{\partial^2 X}{\partial\phi^2} + \frac{1}{r^2\sin\theta}\frac{\partial}{\partial\theta}\left(\sin\theta\frac{\partial X}{\partial\theta}\right)$$

The above coupled system of partial differential equations can, in theory, describe the heat and mass transfer within individual spherical granules when different moisture migration mechanisms are taken into account provided that the coefficients of eqs (2.15) are constant. These coefficients however vary with moisture content, temperature, and pressure, these variations have not been taken into account in the above simplified model. The coefficients for which $i = j$ relate the transient behaviour of a variable given a particular state of the same variable, those for which $i \neq j$ account for the contribution of the state of different variables in the transient behaviour of a particular variable.

Even if the above simplification is justifiable in some cases, the major problem in using eqs (2.15) to analyse the internal drying phenomena is the lack of data concerning the coefficients. Hence several simplifications are usually made when studying the air drying of agricultural products, these are:

i) The size of the particle does not change during drying, this argument rests on the fact that the variation in volume of most materials may not be significant within the range of moisture content of interest. It will be shown in Chapter 8 that in practice this assumption limits the initial moisture content to a very low value indeed.

ii) The effect of changes in pressure on the drying rate is neglected since atmospheric conditions prevail and the temperatures involved will not cause boiling of water. Therefore eq (2.15c) and all pressure terms are not taken into account.

iii) The effect of temperature gradients is neglected, it is assumed that the particle attains a fast thermal equalization, see for example Brooker et al [20], Pabis [129]. This assumption is further dicussed below, it results in the elimination of all terms containing thermal gradients and leads to a coupled system of two differential equations in which the moisture gradients are related to the variation of moisture content and temperature with time.

iv) The coupling effect between temperature variation and moisture gradient is not considered to be important [20].

Hence a simplified formula is obtained whereby the moisture variation can be expressed in terms of internal moisture gradients. The drying rate equation becomes

$$\partial M/\partial t = K_{11}\nabla^2 M \qquad (2.16)$$

where K_{11} is known as the diffusivity, the units are m^2/h or cm^2/h.

2.2.3.3.2 The Diffusion Models

Mass diffusion refers to the transport of matter from regions of higher to lower concentration and is produced by random molecular motion [39]. It has been observed that this phenomenon is analogous to heat conduction (ibid), thus the rate of diffusion per unit of perpendicular area from one region to another is proportional to the concentration gradient in the direction of flow of matter, the proportionality factor being the diffusivity D. This parameter may be interpreted as a measure of the opposition which the water molecules face in diffusing through the medium, i.e. a low value of D reflects a difficult difusion process. This opposition may come from the medium itself and/or from the diffusing substance, e.g. a more viscous substance will have very low diffusivities as compared to those of gases. In the general case D may also be affected by the position in the medium, i.e. diffusion may be easier in some areas within the material than in others.

The utilization of most diffusion models in crop drying analysis so far has been based in the assumption that the diffusivity is independent of moisture content. If the diffusion is limited to one direction, x,

$$\partial C/\partial t = D\ \partial^2 C/\partial x^2 = D\ \nabla^2 C \qquad (2.17)$$

where C is the mass of the diffusing substance per unit volume of dry medium, in this case the material to be dried. Considering the case of a sphere of radius r_o and volume v in which C changes only with r,

$$\partial C/\partial t = D/r^2\ \partial/\partial r(r^2\ \partial C/\partial r) = 2\ D/r\ \partial C/\partial r + D\ \partial^2 C/\partial r^2 \qquad (2.18)$$

The boundary conditions for eq (2.18) are

$$C(r,\ t=0) = C_i$$

$$C(r=r_o,\ t) = C_e(r.h.,T) \qquad (2.18a)$$

where C_i is the initial concentration and C_e the concentration at the surface of the sphere (C_e is affected by the relative humidity and temperature of the air). The solution to eq (2.18) is (see for example [128])

$$[C(t,r)-C_e(r.h.,T)]/[C_i-C_e(r.h.,T)]=(2r_o/\pi r)\{\sin(\pi r/r_o)$$

$$\exp[-Dt(\pi/r_o)^2]-1/2\sin(2\pi r/r_o)\exp[-4Dt(\pi/r_o)^2] + \ldots\} \qquad (2.19)$$

Taking $\overline{C}(t)$ as the average moisture concentration , i.e.

$$\overline{C}(t) = 1/v \int_V C(t,r)\, dr \qquad (2.20)$$

a concentration ratio can be defined as

$$CR = [\overline{C}(t) - C_e(r.h.,T)]/[C_i - C_e(r.h.,T)] \qquad (2.21)$$

The free liquid content at any time t can be defined as

$[\overline{C}(t) - C_e(r.h.,T)]$(volume of particle), i.e.

$$[\bar{C}(t)-C_e(r.h.,T)](4\pi r_o^3/3) = \int_0^{r_o} 4\pi r^2 dr[C(t,r)-C_e(r.h.,T)]$$

Dividing the above expression by $C_i-C_e(r.h.,T)$ yields

$$CR r_o^3/3 = \int_0^{r_o} r^2 dr[C(t,r)-C_e(r.h.,T)]/[C_i-C_e(r.h.,T)],$$

hence, considering eq (2.19), $CR = 6/\pi r_o^2 \int_0^{r_o} r\{\ \ldots\ \}\, dr$

Which, when evaluated term by term gives [128]

$$CR=6/\pi^2\{\exp[-(Dt/r_o^2\pi^2)]+1/4\exp[-(4Dt/r_o^2\pi^2)]+\ldots\} \qquad (2.22)$$

The a-dimensional term Dt/r_o^2 is the Fourier number for mass transfer F_o (see for example [64, 129]).

The values of $\bar{C}$, C_e and C_i are given in terms of kg of moisture per m^3 of dry material, i.e. if the former are to be expressed as moisture content dry basis, i.e. kg of moisture per kg of dry solid, they merely need to be multiplied by the density of the solid;

$$[M(t)-M_e(r.h.,T)]/[M_i-M_e(r.h.,T)] =$$

$$= [\rho_s\overline{C}(t)-\rho_s C_e(r.h.,T)]/[\rho_s C_i-\rho_s C_e(r.h.,T)]$$

which gives $MR = CR = 6/\pi^2 \sum_1^\infty 1/n^2 \exp(-n^2\pi^2 Dt/r_o^2)$ (2.23)

Differentiating eq (2.23) yields

$$dM/dt = -(M_i-M_e)6D/r_o \sum_1^\infty \exp(-n^2\pi^2 Dt/r_o^2) \qquad (2.24)$$

Equations (2.23) and (2.24) are only applicable when D is independent of M and the boundary conditions (2.18a) are satisfied.

The series in eq (2.23) has been evaluated (see, for example, [128, 129], to produce tables and curves which give MR or CR as a function of the Fourier number. Using a single measurement and this curve it is possible to construct a drying curve. Consider for example a given set of values for M_e and M_i; if one experimental point $M(t_o)$ is available then a drying ratio can be defined;

$$MR_o = [M(t_o)-M_e]/[M_i-M_e]$$

This enables the Fourier number to be obtained from a curve or table. The diffusivity is then estimated as;

$$D = F_o r_o^2 / t_o$$

Once D is obtained the rest of the drying curve can be constructed by consulting the tabulated values of MR vs F_o, i.e. for any t a new value of F_o is defined when D and r_o are known, and so on.

It is important to note that, in general, M can vary with r, as noted in eqs (2.15) and (2.16). This is, however, only of theoretical interest since, in practice, we are concerned with, and can only measure, the average moisture content of the particles.

The general diffusion equation has also been solved using numerical methods;

$$\partial M/\partial t = \text{div}\,(D\,\vec{\text{grad}}\,M) = \nabla\cdot(D\,\vec{\nabla} M\,),\ \text{where } D = f(M) \qquad (2.25)$$

assuming an exponential moisture dependence for the diffusivity (see [83] for maize, [81] for rice and [82] for high moisture food). It is suggested that the results are satisfactory if it is assumed that D is independent of moisture within a given range (e.g. [16] for wheat, [84] and [143] for maize, [149] and [154] for rice and [156] for soya), it is sufficient to represent the latter as an Arrhenius type function of temperature, i.e.

$$D = D_o \exp(-a/T_a) \qquad (2.26)$$

where T_a is the absolute temperature of air. It has also been shown that the diffusivity decreases with the oil content of the product [156].

More recently the moisture and temperature dependence of the diffusivity has been considered in a number of technical papers although it has been observed that the diffusion models do not adequately predict the drying process if the variation in moisture content is large. Moreover, even when relatively complex models are used, the results are not satisfactory if the diffusivity data is not generated in the particular experiment. Sokhansanj & Gustafson [153] solved a bidimensional coupled mass and heat transfer system of equations for maize and rice, using finite element techniques applied to individual kernels. The values of diffusivities and thermal conductivities used were those of the different constituents of the kernel, i.e. endosperm, germ and husk. The results obtained from the simulation were found to depart from the experimental drying curve after a short period of time and were very simmilar to those obtained for the case when the material was considered to be homogeneous. Husain et al [82] were unable to find a single function which described the diffusivity and which predicted the drying curve within the entire range of moisture of interest. In a recent Ph.D. thesis Syarief measured the diffusivity of maize components, in this work an empirical model for the diffusivity, based in the formula of Hustrulid & Chu [83], was obtained. In this work the diffusivity was expressed in terms of the moisture content at constant temperature (40 C) (see [158]).

Recently the so called theoretical drying equations based on diffusion have become very popular. In this approach the diffusivity is estimated from experimental data fitted to either the complete series of eq (2.23) or to a few terms of the latter (see for example a two-term diffusion equation for rice given by [174]). Alternatively the data can be fitted to empirical equations for the diffusivity such as those developed by Hustrulid & Chu [83] and Syarief et al [158], which are used in the numerical solution of a simultaneous system of mass and heat transfer equations. It must be realised, however, that the models finally obtained have the same limitation as the purely empirical models, i.e. they are only applicable under the specific conditions of the experiment (temperature, moisture content, etc). This is as to be expected if one considers that the diffusion model is obtained by making simplifying assumptions regarding the complex mass and heat transport phenomena within a biological material which in most cases is neither homogeneous nor uniformly shaped and which, in practice, can experience a considerable variation in volume during the drying process.

2.2.4 Air Drying in a Deep Bed

Up to this point the case considered has been that in which all the surfaces of the granular material experience the same air conditions, in reality this is only achieved in single grain layers of product or in shallow beds when large air flows are used. In practical air drying systems the temperature and humidity of air vary since the air picks up moisture from the bed of material and transfers heat to the latter. In the limit it is clear that if the air has a high relative humidity and low velocity it will saturate in the bed and therefore different air and drying conditions will be established at different depths. The simulation of these external phenomena involves the solution of a very complex system of equations which can only be carried out by numerical techniques. The solution is affected by the air and product temperatures, the relative humidity of the air and the moisture content of the material.

One of the most common approaches to modelling the system is to consider mass and heat balances on individual layers of the deep bed taking the outlet conditions of the previous layer as the input for the next. In each case it is assumed that the drying factors are not changed in a given interval of time, the computations are then carried out layer by layer. The drying models described in the above paragraphs are applied consecutively many times in the running of the deep bed simulation, the drying equation being one of the differential equations incorporated in the complete drying model. Different air drying techniques, i.e. stationary and moving bed are described by similar sets of equations in which factors such as the convective heat transfer coefficient, flow of air and product, specific heats of dry air, water vapor, liquid water and dry product, heat of evaporation, specific heat transfer area (particle surface area per unit bed volume) and bulk density of dry product are taken into account. In addition to these factors the models for the equilibrium moisture content and for the psychrometric chart need to be incorporated in the program. Conduction between particles is not included in the programs. The simulation packages so defined are claimed to predict the performance of dryers within 10 % of the experimental data, they are already available for many cereal products such as maize, wheat and rice.

Parry [130, 131] proposed methods and mathematical models to simulate the heat and mass transfer phenomena in deep bed drying applications which are said to require less computing time than the packages which perform mass and energy balances layer by layer.

Consider the basic stationary bed configuration shown in figure 2.6, Brooker et al [20] simulated this system from which the following conclusions are obtained. When drying begins the temperature of the product in the top layers (x=1) is well below that of the air although it is still much higher than that of the material at the bottom (x=0). The external moisture gradient between x=0 and x=1 is initially small and the relative humidity of air reaches unity as soon as it enters the bulk of product. As the process advances the temperature of the top layers gets closer to that of the air and the moisture content of the product in this region is continously reduced. At the same time the temperatures of the inner layers continue to increase and

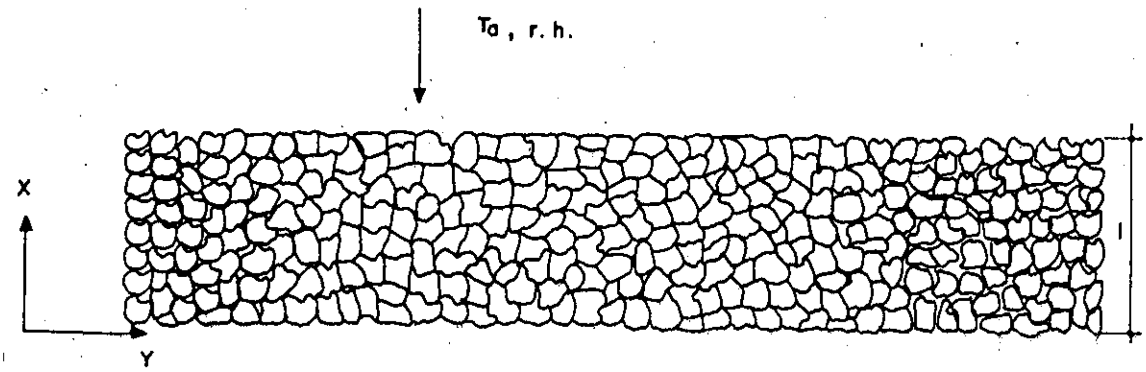

Figure 2.6 Air Drying of Grain in a Deep Bed (fixed).

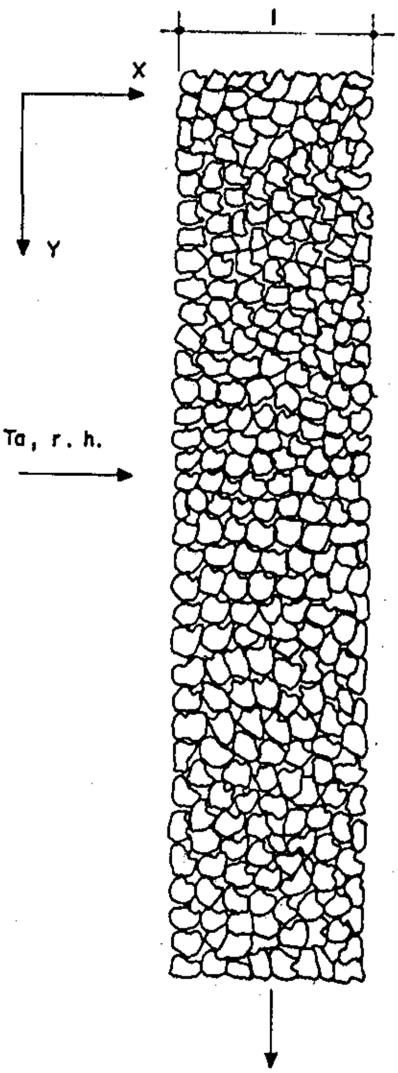

Figure 2.7 Air Drying of Grain in a Deep Bed (moving).

their moisture contents to reduce, the air becomes saturated at deeper layers and the external moisture gradient between the top and bottom layers is considerable. At the end of the drying process an average moisture content is obtained between the top and the bottom, a temperature difference is also observed. The humidity of the air at the bottom (x=0) is continuously decreased as drying advances. Moreover, if the initial moisture content of the product and the inlet temperature of the air are reduced or the air flow increased, the difference in moisture content between the bottom and top is also reduced.

The results obtained for the crossflow configuration (figure 2.7) are similar to those described above as far as the "x" coordinate is concerned. However,since the material is falling down the length of the dryer, it will become progressively drier in the direction of increasing "y". The moisture profile of the system will be constant in time as long as the operating conditions are unaltered. The outlet air temperature will increase as y is increased and the relative humidity will decrease in the same direction. These results are confirmed if an apprpriate simulation program for the crossflow dryer is used, such a program has been used by Centreinar (Brazil) [136] for maize and wheat with good results. Other simulation packages are described by [148].

Consider, for example, the case in which the initial moisture content and temperature of maize are, respectively, 18% w.b. and 20 C (ambient), the inlet drying air is at 80 C and 0.01 absolute humidity. The flow of air and product are, respectively, 1,200 m^3/h per m^2 of area of drying column perpendicular to the air flow (see figure 2.7) and 2,000 kg/h of wet maize per m^2 of cross sectional area perpendicular to the flow of material. If, in addition to this, the height and thickness of the drying bed or column are 3 and 0.3 m respectively, which corresponds in figure 2.7 to $y_{max}=3m$ and $x_{max}=l=0.3m$, the simulation indicates that the outlet temperature of air varies from 20 C at y = 0.15 m to 64 C at y = 3 m and the relative humidity goes from 0.90 (at y = 0.15 m) to 0.10 (at y=3 m).

2.2.5 <u>Drying of a Particle under Intensive Heating</u>

Converting the temperature and mass terms of eqs (2.15) into spherical coordinates,the drying equation below can be obtained using the concept of the thermal gradient coefficient ($\delta_t(M,T)$), which is a measure of the moisture diffusion produced by the variation of the internal thermal gradients (see for example [100, 101]). The case considered here is that in which diffusion occurs only in the radial direction of the particle. The diffusivity and the thermal gradient coefficient are taken as general functions of the moisture content and temperature of the material, following the rigorous approach given by eq (2.25).

$$\partial M/\partial t=1/r^2\partial/\partial r[D(M,T)r^2\partial M/\partial r]+1/r^2\partial/\partial r[\delta_t(M,T)D(M,T)r^2\partial T/\partial r] \quad (2.27)$$

Luikov [100], pp 282-7 gives information on the variation of $D(M,T)$ and $\delta_t(M,T)$ for some capillary porous bodies. He points out that, at a given temperature (T) of the material, the diffusivity increases with moisture content to a point where it reaches a constant value. This variation is affected by the state in which the moisture is transported, i.e. vapor or liquid, and also by the physical structure of the capillar system. For pine wood the diffusivity increases almost linearly to a point where it starts to fall, also linearly, after which it increases again, this time exponentially. The thermal gradient coefficient shows a rapid increase from a particular value of M, but before this point is reached the parameter is practically nil. For some materials the coefficient is constant after a particular value of moisture content is reached, for others, especially some porous materials, it reaches a maximum and then decreases. $D(T,M)$ and $\delta_t(M,T)$

vary for different materials and also, as reported by Luikov, they may vary with the drying methods used. It is therefore necessary to measure both properties for each material and each drying technique under consideration. It is possible that, if drying takes place in conditions in which the thermal gradient coefficient is very small, the second term on the right of eq (2.27) may be neglected without invalidating the result.

Examining the first term on the right of eq (2.27), i.e.

$$\mathrm{div}\ [D(M,T)\mathrm{grad}\vec{M}] \tag{2.28a}$$

This is negative provided that so also is the magnitude of $\mathrm{grad}\vec{M}$, i.e the moisture content profile within the particle decreases with increasing r (less water is found as the surface is approached). In other words the evaporation rate becomes greater if both the moisture gradient and the diffusivity remain high. Unfortunately the latter is not likely since the diffusivity will tend to a small value as the moisture content reduces. Nevertheless, considering the second term on the right of eq (2.27), it is seen that a temperature gradient in the direction of increasing r will make the drying rate more positive, i.e. it will reduce the evaporation rate. On the other hand a temperature gradient in the opposite direction will increase the evaporation rate, this can be demonstrated if the term is expressed in vectorial notation and is illustrated in figure 2.8;

$$\mathrm{div}\ [\delta_t(M,T)D(M,T)\mathrm{grad}\vec{T}] \qquad (2.28b)$$

where $\mathrm{grad}\vec{T}$ is a vector and consequently so is the term in rectangular brackets. It should be noted that div $(\mathrm{grad}\vec{T})$ is positive if the magnitude of $\mathrm{grad}\vec{T}$ is positive.

When heat is supplied from outside the initial surface temperature can be much higher than that at the centre, therefore if the contribution of the term on (2.28b) is considerable, i.e. if the thermal gradient coefficient, diffusivity and thermal gradients are high enough, the absolute value of the drying rate can actually be reduced, i.e. the evaporation rate is reduced. This aspect is usually neglected in air drying studies since it is argued that the temperature gradients are small. Nevertheless when conductive or radiative heat transfer techniques are used to produce heat at the surface of the material then, although the temperature and diffusivity may be increased, (so increasing the contribution of the first term in eq (2.28a)), the surface temperature of the material might well increase considerably.

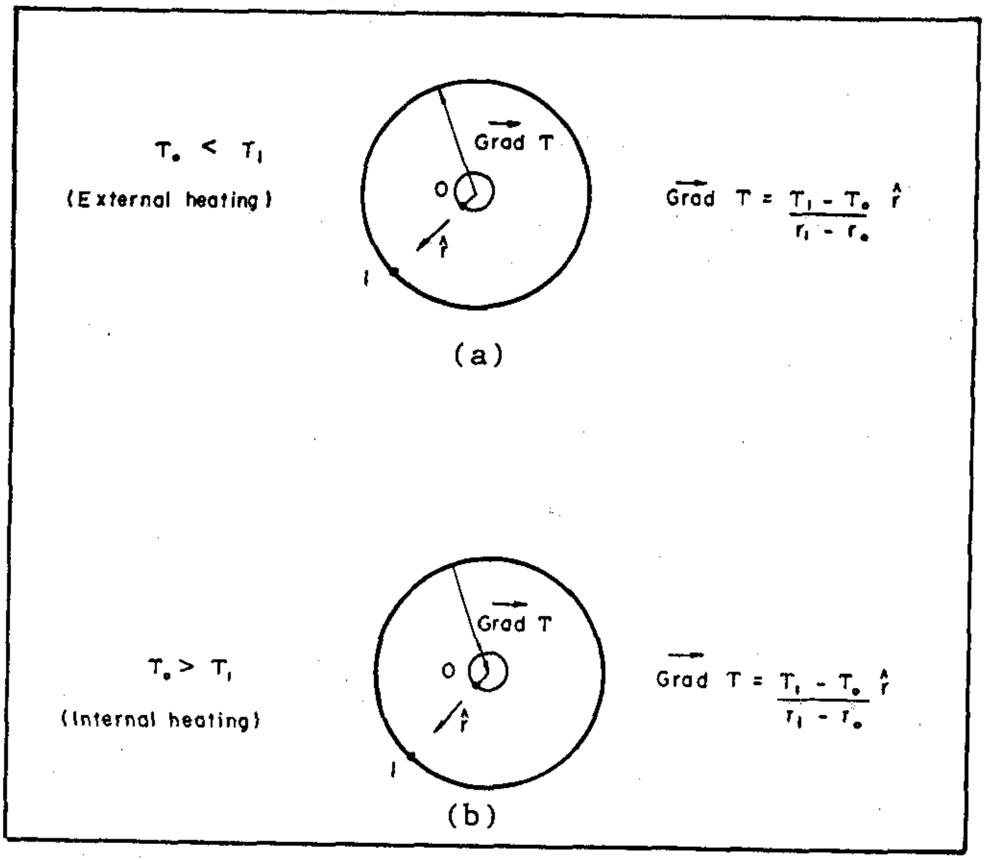

Figure 2.8 Thermal gradients in the particle when heat is applied:
a) Externally
b) Internally.

In this case the positive temperature gradient may be sufficient to hinder drying and produce product damage.

Ginzburg [54] comments on experimental observations of this effect when infrared drying methods are applied, he concludes that in this case intermittent drying should be used, although this decreases considerably the throughput of the product. The increased rate of heat transfer to the surface of the material does not help to enhance the drying process due to the internal constraints established within the body. The final outcome of an intensive heating from outside the body (e.g. infrared) is therefore related to the thermo-physical properties of the material and the resulting balance between the two terms on the right of eq (2.27). For example, if the thermal gradient coefficient remains very small and the increased rates of heat transfer from outside increases the diffusivity sufficiently this can overcome the opposition presented by (2.28b) and result in an effective increase in the evaporation rate.

If the heat is generated internally in the material the diffusivity is increased and there is also an effective negative temperature gradient, i.e. from inside to outside, This increases further the evaporation rate and hence the speed of the process. This method is discussed in the following section.

2.3 Theory of Drying: The Contribution of Internal Heating

2.3.1. Background

It has been shown above that, in air drying processes the air has two basic functions: it receives humidity and it transfers heat. The increases in the temperatures of the material and medium initiate the internal transport mechanisms (e.g. moisture difusion from wet regions to the surface of the body) and maintain the appropriate ambient conditions for water diffusion in the drying medium. The internal movement of moisture is limited by the intrinsic properties of the material such as the diffusivity which, although increasing with the temperature of the product, is continuously decreasing with the reduction in moisture content as drying proceeds. Thus the air drying process is inherently constrained even though the temperature of the air and material are held at relatively high levels. An alternative is to use conduction and radiation since the latter do not require considerable volumes of air to produce heat on the surface of the material and therefore the energy applied in heating the material is more usefully employed.

Also if a favorable combination of values of $D(M,T)$ and $\delta_t(M,T)$ throughout the drying process exists then the increase of the temperature of the product by radiation and conduction can increase the evaporation rate. Nevertheless this may not occur in all cases, hence these techniques need to be carefully controlled in order to avoid damaging the product and to maintain adequate drying conditions.

If it were possible to generate heat within the product the drying process would be enhanced since the increases in the diffusivity and temperature differences inside the product would not act in oppositions. Energy can be dissipated internally in a body if it is receptive to either the electric or magnetic part of an electromagnetic field. This is convenient for heating non-conducting materials, i.e. dielectrics, which respond to the electric component of the field. The material is directly heated by the energy drawn from the electric field, and any part of this energy which is absorbed by the product and is not used in evaporation of water is transformed into sensible heat. The air is used to carry away the water on the surface of the material, although in the case of temperature sensitive materials it could also be used to force-cool the product as will be noted in Chapter 8.

When internal heating is employed the pressure terms will play a significant role in the mass transfer phenomena since the water contained in the capillary system will begin to evaporate and, due to the pressure created by the generation of steam, the liquid water will be forced to the surface. It will be noted from the last term on the right of eq (2.15a) that a negative pressure gradient, i.e. a higher pressure in the center of the particle, will further increase the absolute value of the drying rate. McCabe [115] and Perkin [133] relate the pressure contribution to the diameter of the capillary system, Perkin [134] presents an analysis of pressure-controlled drying at the boiling temperature of water. Although it is normally accepted that when internal heating techniques are used the transport of water occurs partially as liquid and partially as vapor (see for example [100]), some authors (e.g. Lefeuvre et al [94]) state that if drying is carried out below the boiling temperature of water the flow of moisture may be assumed to occur mainly in the liquid state.

2.3.2 The Heat and Mass Transfer Model

The drying rate can be obtained from eq (2.27). A heat transfer equation in which the internal heating effect is included can be derived by considering an energy and mass balance within a small rectangular control volume in which an individual particle is contained. It is assumed that the volume so defined can gain energy from external sources (convection, radiation, conduction), ∂E_{ext}, and by internal heating, ∂E_{int}. The absorbed energy is used in heating up the material and in evaporating the water, i.e.

$$\partial E_{ext}/\partial t + \partial E_{int}/\partial t = v\,\rho C_p \partial T/\partial t + h_v\, \partial m'/\partial t \qquad (2.29)$$

where v is the control volume (dxdydz), C_p and ρ are, respectively, the specific heat and density of the moist particle.

The term $\partial E_{ext}/\partial t$ is the difference between the rate of heat flow into the infinitesimal volume v and the rate of heat flow out of it. It has been derived in several treatises in conduction heat transfer using Taylor series (see for example [36]). It can be written as

$$\partial E_{ext}/\partial t = \partial/\partial x\,(k\,dydz\,\partial T/\partial x)dx + \partial/\partial y(k\,dxdz\,\partial T/\partial y)dy$$

$$+ \partial/\partial z\,(k\,dxdy\,\partial T/\partial z)dz \qquad (2.30)$$

where k is the thermal conductivity of the particle.

The term $\partial E_{int}/\partial t$ is obtained by integrating the Poynting vector $\vec{E} \times \vec{H}$ where E and H are the strengths of, respectively, the electric and magnetic components of the applied field. This term is affected by the magnitude and direction of the field and by the dielectric properties of the material. At a given field frequency these properties are mainly influenced by the moisture content of the material. The following expression holds;

$$\partial E_{int}/\partial t = f(\vec{E},M)dxdydz \qquad (2.31)$$

i.e. the rate of internal energy dissipation is proportional to a definite function of the magnitude and direction of the electric field and the moisture content of the product.

Taking into account eqs (2.29),(2.30),(2.31) and (2.5b) we obtain:

$$\partial/\partial x(kdydz\partial T/\partial x)dx + \partial/\partial y(kdxdz\partial T/\partial y)dy + \partial/\partial z(kdxdy\partial T/\partial z)dz +$$

$$f(\vec{E},M)dxdydz = dxdydz\ \rho Cp\ \partial T/\partial t - \partial M/\partial t\ h_v\ \rho_s dxdydz$$

hence,

$$h_v \rho_m \ \partial M/\partial t + \mathrm{div}(k\,\mathrm{gr\vec{a}d}T) + f(\vec{E},M) = \rho C_p \ \partial T/\partial t \qquad (2.32)$$

Considering a spherical particle and neglecting the difference between ρ and ρ_m (from Mohsenin [111], it is found that the ratio ρ_m/ρ may vary between approximately 1.0 and 0.85, this having been observed in the results from Chapter 8). Thus:

$$\partial T/\partial t = f(\vec{E},M)/(\rho C_p) + h_v/C_p \partial M/\partial t + k/(\rho C_p)(\partial^2 T/\partial r^2 + 2/r \, \partial T/\partial r) \qquad (2.33)$$

which, together with eq (2.27), forms the complete mass and heat transfer model when internal heating exists within the particle. The boundary conditions for these equations are the initial moisture and temperature profiles in the particle and eq (2.7b) (when all external energy sources are considered) or eq (2.8) (if only convection takes place). In the latter case the temperature of air, T_a, may be lower than the temperature of the surface of the material T_m, if air is used to cool the material. Note that T_m is equivalent to the temperature of the product, T, of eq (2.33), when $r = r_o$.

The set of equations given above cannot be further simplified if it is intended to represent the process in the general case, they form a very complex model. The critical parameters for solving these equations are the diffusivity and thermal gradient coefficient of the material, these vary in a complex way and can change with the heating process involved. The thermal gradient coefficient does not appear to be known for most materials of interest, although there is limited information concerning the diffusivity as explained earlier in this Chapter.

The problem of coupled heat and mass transfer in capillary porous bodies when internal heat is present has previously been approached on only a simplified theoretical basis due to the complexity involved and the non-availability of the relevant properties of the material. Whitney and Porterfield [169] began with the simultaneous heat and mass transfer equations given by Henry and explained in detail by Crank [39], Chapter XIII. The resulting system of equations is different from that presented here since the approach adopted by those authors was to relate the concentration of water vapor in the capillary system to the moisture content of the body through a linear relationship. In this formulation of the problem the following simplifications are also implicit:

i) The rate of internal heating produced is maintained constant. In practice this would require an adequate control action to be undertaken, e.g. the electric field $\vec{E}$ would need to be adjusted to follow the variation in the properties of the material when M changes.

ii) The effect of temperature gradients on the drying rate is neglected.

iii) D(M,T) is constant for all values of T and M experienced by the product.

iV) Several characteristics which are difficult to measure are included in the model, e.g. the fraction of the total volume occupied by the solid skeleton of the product.

Young [177] pursued the above analysis, a spherical shape was assumed for the product (the earlier work assumed an infinite slab) and the values of thermal conductivity and mass diffusivity were varied in order to analyse the effect on the drying rate of the hypothetical material. The simplifications listed above were adopted with the exception of (iii). The modelling of the diffusivity is arbitrary, the aim of the study being merely to vary it over a considerable range.

Bories and Pourhiet [19] also worked on the theoretical analysis of the drying process when internal heating is used. In this case the heating source is expressed in terms of position within a porous slab. The diffusivity and thermal gradient coefficient for sand are used and the authors point out that, even with such a basic porous material, the parameters exhibit a nonlinear variation with moisture content and temperature. Even though an experimental verification of the model is not presented this approach is one of the most important contributions made recently to the theoretical analysis of internal heating mechanisms for drying applications.

2.4 Summary

It has been shown in this Chapter that a purely theoretical formulation of the internal mass and heat transfer phenomena involved in drying is difficult to obtain. The solutions in themselves are difficult to interpret in practical cases due to the assumptions and to uncertainties concerned with the nature of the products. This is the case even if a simplified model of the particle and its interaction with the external media and energy sources is adopted. The critical unkowns in the problem are the diffusivity and thermal gradient coefficient. The former is generally estimated by considering an oversimplified system for the air drying of materials. The thermal gradient coefficient is not taken into account in convective drying studies since it is normally assumed that either it or the internal temperature gradients are negligible. Many simplifications have been made in order to obtain a manageable system of equations, several of these assumptions are clearly not valid, e.g. the neglect of the contribution of the pressure terms, simplified initial profiles of temperature and moisture content within the product, simple and stable geometry of the particle, etc. All these make the theoretical approach quite difficult in all but the most trivial cases. When internal heating is used, both the thermal gradient coefficient, and the mass diffusivity may acquire an increased importance in the drying process. This is due to the direction of the internal temperature gradients and also to the fact that the pressure terms are reinforced.

Although the basic data concerning the materials of interest are generally not available some authors have pursued the theoretical model under simplified conditions and for basic porous materials. It is considered that this route should be explored further when the diffusivity and the thermal gradient coefficient have been satisfactorily determined for the particular heating method and product chosen. It is evident that, for the present, it would be a formidable if not impossible task to carry out an analysis of the best drying method to be used in the applications of interest on a theoretical basis using the sparse data available. Hence an experimental approach has been pursued. This route has its advantages, e.g. the changing and non-linear characteristics of the materials concerned are not required in order to obtain the drying models, although those properties can be used to assess the performance of the proposed system as noted below.

Moreover it is important to fully understand the practical limits imposed when using the several heating sources that are available, in this context the internal heating effect can only be achieved in practice with electrothermal techniques. If it is not controlled the term $f(\vec{E},M)$ would vary with the properties of the material during drying, being also affected by the relative position of the material in the drying zone, the distribution of the electromagnetic field and the shape of the dryer in which the product is contained. When radiation or conduction techniques are considered the relative position betweeen the energy source and the material is also important, as are the temperature levels which can be achieved. Apart from this, if a dielectric dryer is to be operated within safe limits the magnitude of $\vec{E}$ needs to be mantained below specific levels. Constructional and dimensional considerations have to be taken into account when choosing a given drying technique and heating source, these have a major impact in the final distribution of the electromagnetic field if internal heating techniques are considered.

The next four Chapters (3-6) consider various possible alternatives for drying granular products. The methods considered are convective, radiative, conductive and dielectric heating techniques. The first three methods involve heating systems in which energy is applied from outside the product, and these are dealt with in the following three chapters of this report. Chapter 6 analyses the systems, or applicators, as they are normally called, in which energy is dissipated within the product. Chapters 7 and 8 deal with the choice of best drying alternatives and with the experimental methods, measurements and apparatus used in this research. Finally the conclusions are drawn in Chapter 9.

3. CONVECTIVE HEATING SYSTEMS

3.1 Introduction

Convective electric heating equipment has been used for many years. The energy is transferred to the material from the heat generated in electrical resistances, it is classified as an indirect resistance heating process. The temperature of the heater is increased when an electric current flows through a resistive element and dissipates energy by the Joule effect, hence radiative, conductive and convective heat transfer mechanisms develop in proportion to the temperature difference between the heater and the surrounding medium. In this section convection techniques are analysed for the practical devices which might be utilized in drying by means of hot air. A comprehensive study of convective heat transfer is outside the scope of the present Report.

3.2 Heat Transfer in Convective Electric Heating Systems

Convection is the energy transfer which occurs by a combination of direct transfer of momentum (conduction) and an additional gain in kinetic energy of the molecules when they are mixed and agitated. These phenomena can be produced naturally, i.e. by the relative motion of molecules in a fluid when a temperature gradient is created, or artificially when the movement is produced by an external agent, e.g. a fan or a pump. The latter is called forced convection and this is responsible for the heating effect produced in the applications of interest.

The rate of convective heat transfer from the heater to the air is given by the Newton equation which can be found in most treatises on heat transfer

$$q = h_c (T_h - T_a) \quad W/m^2 \qquad (3.1)$$

where, in this case, T_h and T_a are, respectively, the average temperature on the surface of the heater and the temperature of the air. The convective heat transfer coefficient h_c varies in a complex way with the characteristics of the air flow and geometry of the system. The simplified formula in eq (3.1) includes in h_c complex fluid mechanics phenomena which are so involved that an analytic solution is not usually attempted even when considerable simplifications can be made. Therefore experimentation is the only way to obtain a meaningful estimate of h_c, data is available for a wide range of heat exchange arrangements, temperature, pressure and velocity of air. The condition under which experimentally based correlations can be applied is that similar state of the air and a similar system geometry must exist in the real case and the idealized situation in which the experiments are carried out. It can be shown that this is the case when both the experimental model and the real system have the same Reynolds number Re (see for example [29]).

In practice correlations are usually expressed as functions, i.e.;

$$Nu = f(Re, Pr) \tag{3.2a}$$

These relationships are only valid between a given range of the Reynolds number Re. The term Nu, the Nusselt number, is given by:

$$Nu = (h_o\ D_o)/k_{air} \tag{3.2b}$$

Pr is the Prandtl number,

$$Pr = (Cp_{air}\mu_{air})/k_{air} \tag{3.3}$$

where Do is a geometrical characteristic of the system, e.g. diameter of a sphere, cylinder, etc; k_{air}, Cp_{air} and μ_{air} are the thermal conductivity, specific heat and viscosity of air, respectively. Re, Nu and Pr are dimensionless numbers.

It will be shown later that h_o is related to the characteristics of the fluid, basically its velocity and temperature, and to the dimensions of the heat transfer areas. The intrinsic properties of the fluid such as the viscosity, thermal conductivity and specific heat are usually estimated at the average film temperature, which is defined as the arithmetic mean of the temperature of air and the temperature on the surface of the heated or heating surface.

As far as this study is concerned two convective heat transfer mechanisms are important, i.e. the transfer of heat from the surface of the heater to air and the transfer of heat from the air to the surface of the product. The latter is important to simulate the drying process, e.g. in the crossflow plant, in which case the heat transfer coefficient between air and grain is taken into account in the model equations. The heat transfer between the heater and air (eq(3.1)) is fundamental for designing the heater in a particular application.

Considering the first heat transfer stage, i.e. from the heater surface to the air, we can refer to the correlation between the Nusselt and Reynolds numbers for air heating or cooling when the flow is normal to a cylinder as shown in Fig. 3.1. The variations in the Prandtl number have not been taken into account as is usual since this parameter is found to be constant over the range of air conditions of interest. Brooker et al [20] reports on Pr for air temperatures in the range (-3, 100 C) from which it is noted that the value of this parameter is 0.7. The correlation shown in figure 3.1 is said to be applicable within the following range of variables [115].

Variable	Range
Diameter of cylinder, cms	0.001 - 15.0
Air velocity, m/sec	0.0 - 18.9
Air temperature, C	15.6 - 260
Cylinder temperature, C	21.1 - 1,004.4
Absolute pressure, atm	0.4 - 4.0
Re	0.2 - 235,000
Nu	0.5 - 500

In practical situations however the heater is neither a single tube nor a cylinder but a group of finned tubes which can

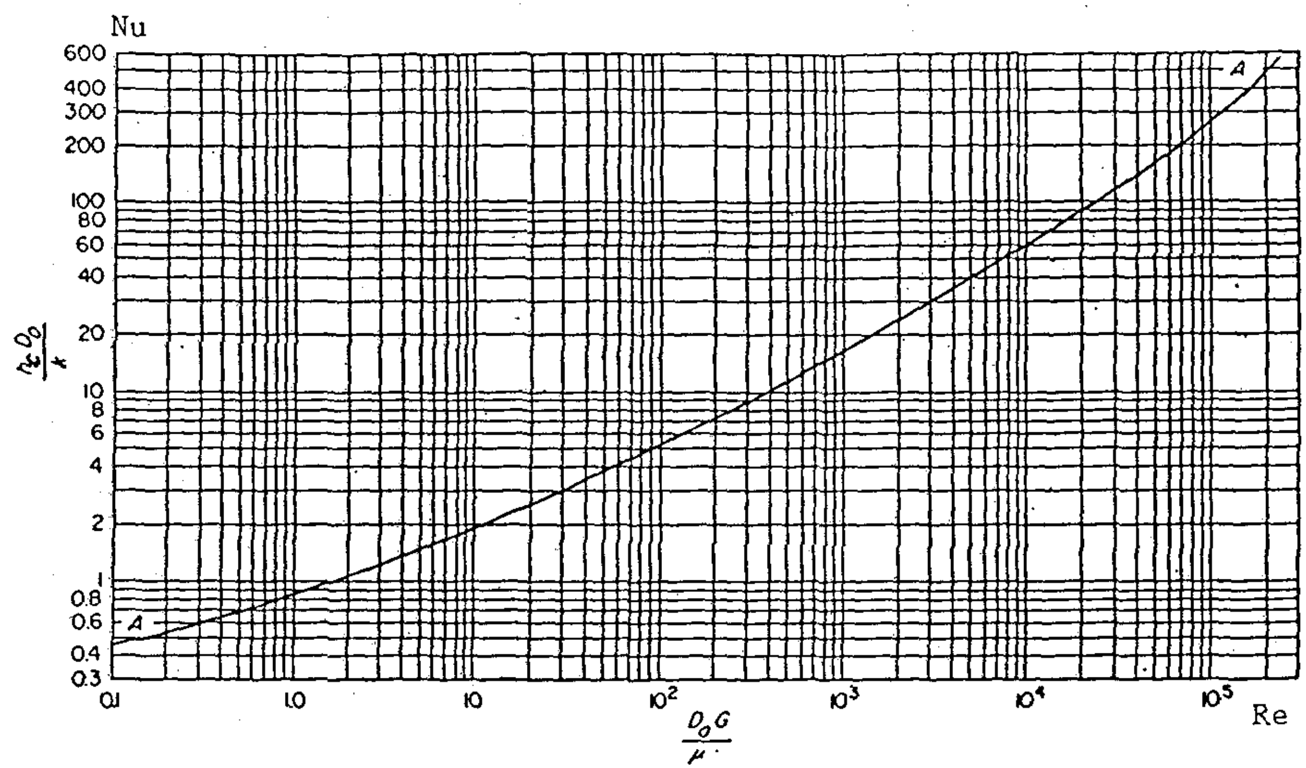

Figure 3.1 Heating and Cooling Air Flowing Normal to a Cylinder[115].

have a variety of shapes. In this case the value of h_o is dependent on the shape, arrangement and spacing of the tubes. An additional effect can also be expected from the extended surface of the finned elements.

When there are several tubes in the path of the air flow h_o can be considered to attain the same value on each row of tubes perpendicular to the air flow. Nevertheless for the inner rows of tubes h_o is varied since more turbulence is experienced by each consecutive row and hence the value can be expected to increase over the first three or four rows (ibid), although Hutchinson states that the effect is only significant when the tubes have a staggered arrangement [85]. In practice an average value should be taken, Hutchinson says that an increase of 30% above the estimate for a single cylinder should be made for staggered tubes.

In general the following correlation can be expected for any configuration of tube banks [115]:

$$(h_o\,D_o)/k_{air} = [(bD_oG)/\mu_{air}]^n \qquad (3.4)$$

where G is the mass velocity of air in kg/sec per m² of perpendicular air flow area. In reality G is not a velocity but the product of the density and velocity of the fluid. The constants b and n are affected by the arrangement of the tubes, number of rows of tubes and finned elements used. G is always evaluated for the minimum available area of air flow (where the velocity is at a maximum) and therefore both this variable and the Reynolds number attain their maximum values under a particular set of conditions. The Reynolds number is defined as

$$Re = (DoG)/\mu_{air} \tag{3.5}$$

Up to this point the factors have been considered which must be taken into account in estimating the heater's h_c, this is fundamental for the use of eq (3.1). However the effect of energy losses in the ducts and heating systems must also be taken into account, these losses are basically produced by the obstacles presented to the air flow by the duct, heat exchangers and material to be dried. The total energy required in heating and ventilation is therefore increased by those losses although the heating load itself is by far the greater component in terms of energy requirements. A good illustration of the effect produced by the losses referred is found in the retrofitting of combustion equipment by electrical heaters in agricultural dryers. Axial flow fans are the most common and they exhibit the characteristic of increasing the volume of air and reducing the power requirements when the resistance to air flow in the duct is reduced. It has been reported that the conversion of a typical fuel fired coffee drying system to electrical heating reduces the resistance to the air in the duct so increasing the flow considerably [17]. This is so since large heat exchangers are replaced by a compact electric resistance battery which presents much less resistance to air flow than the previous system. This means that if a given drying system is replaced by an electric unit in these conditions the energy used by the fan will be reduced, however the increased air flow means that more energy has to be generated by the heater if the same air temperature is to be maintained.

Ideally the heating load for drying the product would be obtained from values of the required heated air flow and temperature, if possible from deep bed drying models as discussed in Chapter 2. These models need to consider the convective heat transfer coefficient in thin layers of the product.

The variables which cause the variation of h_o at the surfaces of the granulated material are similar to those reported above but much less information is available for this case. A classic formula for h_c of granulated material when air is blown perpendicular to a thin layer of product is of the form given in eq (3.6a), as shown by Williams-Gardner [170], Chilton & Perry [30] and other authors. A recent review of the classical formulae still in use can be found in Sokhansanj & Bruce [152].

$$h_c = a\ G^b \qquad (3.6a)$$

Based on these classical approaches Sokhansanj and Bruce propose the following relationship for estimating h_c of granulated products:

$$(h_c/Cp_{air}G)Pr^{2/3} = 3.26Re^{-0.85} \qquad 20 < Re < 1000 \qquad (3.6b)$$

The convective heat transfer coefficient is then estimated from the air flow parameters, dimensions of the particles and Reynolds number. The viscosity of heated air is approximately 1.96E-5 kg/m/sec [20], the corresponding value for the specific heat would be 1000 Wsec/kg/ C [84, 112]. The dimensional parameter of the Reynolds number used by Chilton & Perry is the diameter of a sphere having the same surface of the particle. The information available for agricultural products is the diameter of the sphere of equivalent volume (see for example

[111]). This value is used as a first approximation in the analysis which follows and it would appear that the results are in accordance with those reported by Sokhansanj and Bruce [152]. The equivalent diameters can be obtained from Mohsenin [111], which gives 8E-3 m for maize, 3.5E-3 m for rice and 3.9E-3 m for wheat (taking an average of seven varieties presented).

Using the above values it is possible to estimate the Reynolds number for the diameter of each product (Do), mass velocity (G) and viscosity (μ_{air}) of air. Although considerable data is available on the levels of air flow used in forced convection drying of agricultural products in terms of quantity of material being dried, e.g. m^3 of air per second per m^3 of material, per kg, per bushel, etc (see for example [10, 64]) this information is not readily expressable in terms of air flow per unit of perpendicular area of product. Nevertheless it is possible to conclude from the information given by [64] that when drying agricultural products in a cross flow dryer the air flow through the product may range between 0.25 and 0.41 m^3/sec per m^2. This is confirmed by the range of velocities in which thin layer drying studies have been made as reported in the previous Chapter. Considering the density of heated air as 1.19 kg/m^3 [64, 112], it is therefore possible to estimate the following range for the

Reynolds number when G is between 0.3 and 0.5 $kg/sec/m^2$,

$$122 < Re < 200, \text{ for maize}$$

$$54 < Re < 88, \text{ for rice}$$

$$60 < Re < 98, \text{ for wheat}$$

Thus $20 < Re < 1000$ and hence definite ranges of h_c can be found from the above and from eq (3.6b), as follows (the results are given in $W/m^2/\ C$).

$$50 < h_c < 61, \text{ for maize}$$

$$87 < h_c < 104, \text{ for rice}$$

$$81 < h_c < 97, \text{ for wheat}$$

3.3 Resistance Heaters

Resistive elements can be manufactured from alloys of Ni-Cr, Ni-Cr-Fe, Cr-Fe-Al, precious metals or non metallic materials. Those most used in the drying temperature range are Ni-Cr and Ni-Cr-Fe, the amount of nickel being a function of the temperature level required for the process [88, 98]. The common alloy for resistance heating elements is 80% Ni and 20% Cr (volume based percentage) [14, 44, 87].

One of the most important factors to be taken into account in the choice of element is its variation in resistivity with temperature, the greater the variation of this parameter over the temperature range of the process, the more complexity the control requirements become. Figure 3.2 shows that in the temperature range of interest Ni-Cr alloys have very appropriate characteristics.

The heating element is enclosed in a metal sheath made from steel, copper, brass or aluminum. These resistance heaters are very convenient due to their long working life and ruggedness. The heat which is produced by Joule effect in the heating element is conducted to the external metal surface through a medium which must be a good thermal conductor and a good electric insulator, this is normally granular magnesium oxide [87]. There is an inevitable temperature drop between the internal wire and the metal sheated enclosure. This type of heater can reach full heating power in less than ten minutes [170], and is the same metal sheathed medium wave infrared device which is discussed later in this work. Some manufacturers

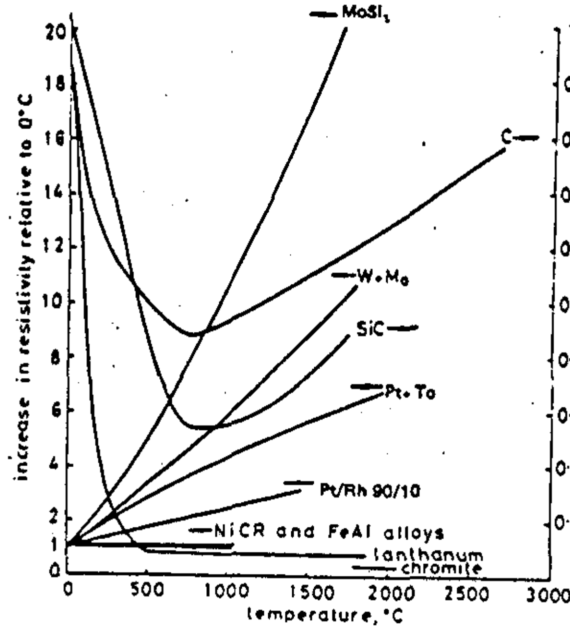

<u>Figure 3.2</u> Variation of Resistance with Temperature of Heating Element Materials[15].

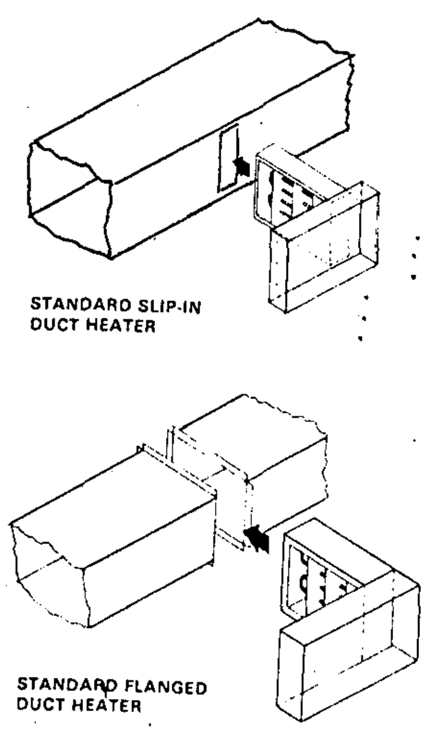

<u>Figure 3.3</u> Installation of Resistance Battery Heate [87].

claim such heaters can be cheaper than the open coil alternative since supporting of the latter becomes difficult when the size of the unit is large. Open wire elements also present problems associated with electric faults to ground and sheathed elements are preferred when moisture is present [87]. Other advantages of metal sheated elements are, for example, that hot spots produced by uneveness in air flows are attenuated during conduction over the metal sheath. The complete set of elements has an appreciable thermal mass, this reduces the switching operations required for temperature control leading to a longer element life and reduced wear on the contactors. In figure 3.3 some practical details of the installation of resistance batteries in heated air duct systems are shown.

3.4 Dimensioning of the Heater

As a first approximation, i.e. neglecting conduction and radiation mechanisms and the energy required to heat up the resistances, the energy supplied in unit time must be enough to raise the temperature of the air flow, i.e.

$$V^2/R = I^2R = \rho_{air}\dot{Q}Cp_{air}(T_a-T_i) \quad W \qquad (3.7)$$

where ρ_{air} and $\dot{Q}$ are the density and air flow rate respectively (m^3/h). T_a and T_i are the final and the initial temperature of air and V, R, I are the voltage, resistance and current flow in the heater. Both $\dot{Q}$ and T_a can be obtained from drying simulations as explained previously. The rate of energy transferred in unit time to the air must equal the rate of heat transfered from the heater to the air by convection, i.e. using eqs (3.1) and (3.7):

$$\rho_{air}\dot{Q}Cp_{air}(T_a-T_i) = Ah_c(T_h-T_a) \qquad W$$

where A is the area available for heat transfer from the heater, T_h is the temperature on the sheath and h_c is the convective heat transfer coefficient of the heater. All the parameters in the above relationships can be obtained from data on the drying simulations, tables or empirical equations such as eq (3.4). We are now left with a design compromise between A and T_h. The heating elements are normally specified in terms of surface power densities (i.e. the ratio between the power and surface area of each element), individual power and voltage. Therefore, knowing these characteristics and the power requirements (eq (3.7)), it is possible to estimate the number of individual elements and the total heat transfer area required.

Eq (3.7) shows that if the air flow is decreased and the heater is supplied at constant power the final temperature reached by the air is increased. In addition to this the reduction in air flow causes the convective heating coefficient to be decreased which, in turn, increases the temperature of the heater and damage to the latter is likely to occur in a short period of time if proper action is not taken. This can be seen by rearranging eq (3.1),

$$T_h = q/h_c + T_a$$

3.5 Economic Appraisal of the Replacment of Combustion Systems by Electrical Resistance Heaters

Electrical convective heating systems are well established and it is difficult to envisage any major breakthrough in this application. Limited improvements may still be made, for example, in the enhancement of heat transfer performance (which would increase the effective h_c of the system) by means of highly conducting sheaths and fins and by improved system geometry. Lower sheath temperatures might then be acceptable so increasing its useful life and reduce radiation losses to the ducts whilst still transferring the same heat to the air. Although this may result in lower capital costs and some gain in energy efficiency, these are not thought likely to be substantial improvements since the heaters are already quite efficient and relatively cheap. Moreover, as will be seen below, capital costs in these systems do not significantly enhance the return on investment which is critically affected by the relative costs of fuels and electricity.

The feasibility of replacing fuel oil in convective heating equipment by electricity and biomass has been analysed elsewhere [26, 27, 86] in terms of relative energy prices, installed power and load factor of the plants. The electrical technologies involved were resistance battery heaters and electrical boilers. These latter have the advantage that if high voltage versions are used, investment in transformers and low voltage ancillary equipment is avoided. There is also an economy of scale as compared with resistance heaters which are modular equipments. On the other hand resistance heater batteries are far more flexible, and have a faster response.

The present author [26, 27] has investigated cases in which electroheat and biomass combustion were retrofitted in place of the original fuel oil fired equipment in agro-industrial plants. The internal rate of return was estimated for a life period of 10 years and the pay-back period for a minimum acceptable 20 % effective return on the investment. These financial parameters were calculated in terms of the ratio between the price of one litre of fuel oil and average cost of one kWh of electricity or one cubic metre of firewood. The results obtained were then plotted as a function of K, a factor which expresses this ratio on a per unit basis.

The baseline, K=1, was the relative energy prices which existed in Costa Rica in October 1982 when the average cost of kWh of electricity was as shown in figure 3.4, the prices of fuel oil and firewood were ¢ 8.5/litre and ¢ 200/m^3 respectively (exchange rate; one dollar = ¢ 45). Figures 3.5 and 3.6 show the payback period for retrofitting a fuel-oil fired coffee drying plant. In figure 3.5 the electrical equipment is used only during off-peak hours and the capacity of the plant has been increased to allow for the required stand-by period. In figure 3.6 the unit is operated continuously and therefore a higher electricity charge is involved. Considering a minimum acceptable pay-back period of five years, it is seen that the investment would be acceptable if the equipment is not operated at peak times. Figure 3.6 indicates that an increase of approximately 30% in the cost of fuel oil (or an equivalent reduction in electricity) would have made the investment acceptable even if the plants were operated continuously.

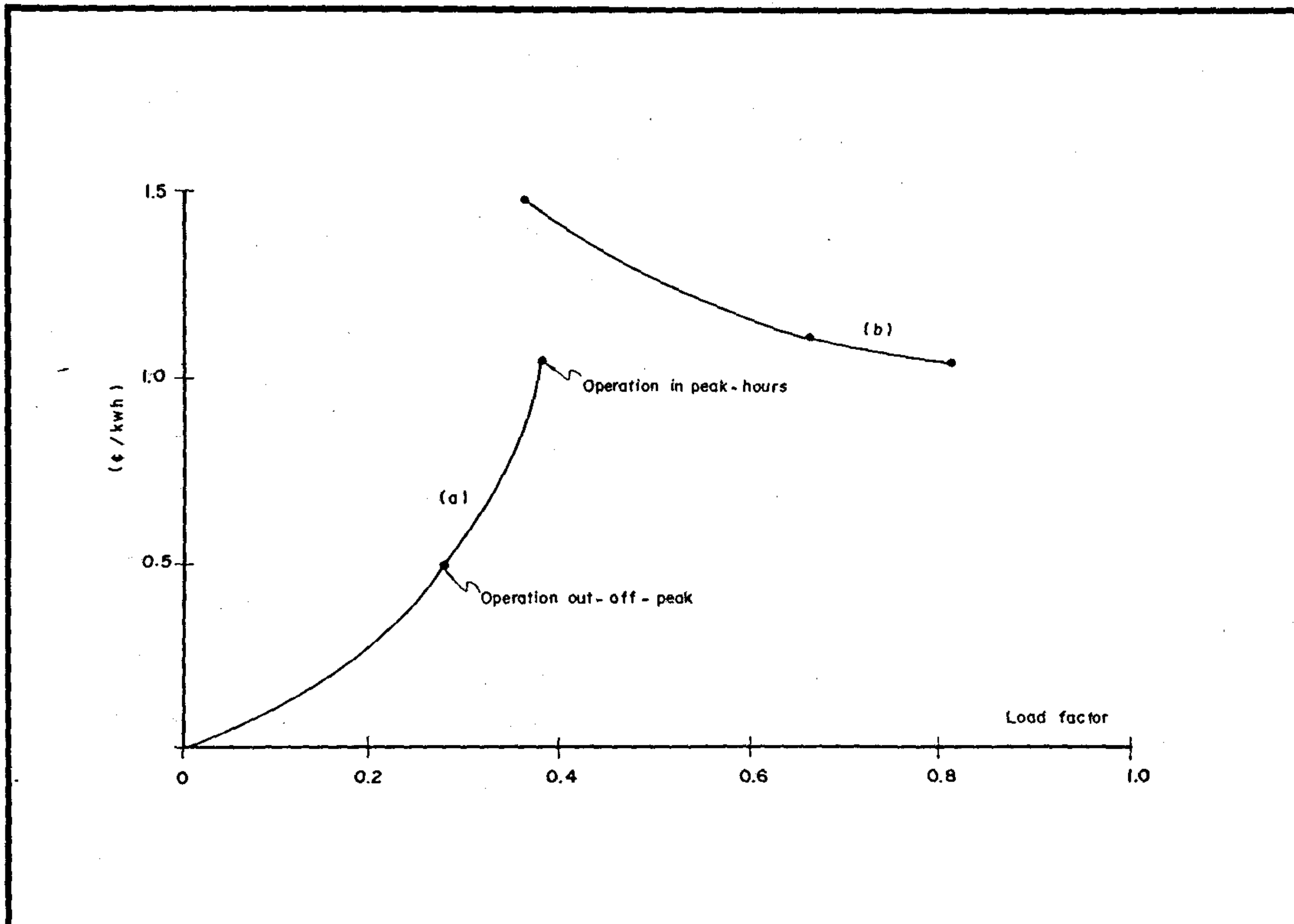

Figure 3.4 Electricity Costs applicable to electric drying plants in Costa Rica in 1982. (a) Off-peak seasonal tariff; (b) Normal industrial tariff [26].

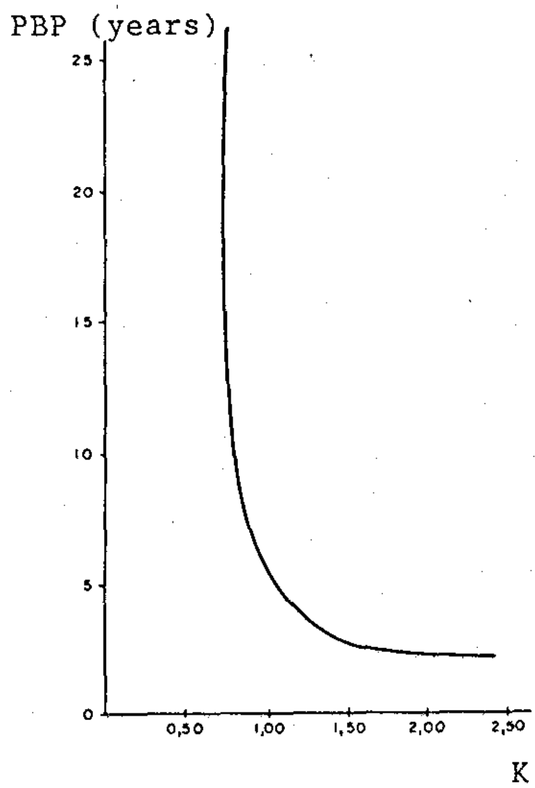

<u>Figure 3.5</u>
Compounded payback (i=0.2) for fuel-oil substitution by electricity in drying plant for 2,300 tonnes of coffee per year using preferential off-peak seasonal tariff and not operating in peak hours[26].

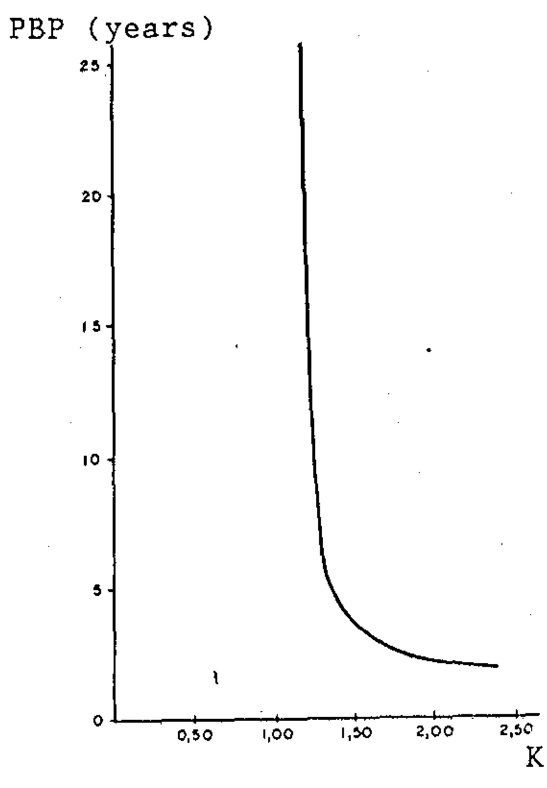

<u>Figure 3.6</u>
Compounded payback (i=0.2) for fuel-oil substitution by electricity in drying plant for 2,300 tonnes of coffee per year using preferential off-peak seasonal tariff and operating at peak hours [26].

If the price of internally produced fuel oil had been increased to the equivalent spot price in the Caribbean region (approximately 30% greater, [86]) the substitution would have been cost effective. The cheapest electroheat technology was found to be electrical boilers at US$ 36.7/kW for 1,500 kW plant and US$ 22.0/kW for 6,000 kW plant compared with modular convective equipment at US$ 70.0/kW (1982 levels, these include C.I.F. costs, taxes and agent commission in addition to the installation costs of the equipment and the step-down transformers if required).

A further important conclusion from the study referred to above is that, over a particular value of K, the pay-back reaches an almost constant minimum value. For electric boilers and resistance heaters in groups of 1,500 kW this occurs when K > 2.5, the payback period is then approximately 2 years. If electric boilers of 6,000 kW rating are operated at 0.8 load factor a payback period of 1.5 years is obtained with K > 1.5. In the case of Costa Rica the value of K > 2.5 corresponds to the elimination of the subsidy in fuel oil and a reduction of 50% in electricity charges. In Brazil much greater incentives were given to customers interested in these replacement projects (see Appendix I). Figures 3.5 and 3.6 indicate that such incentives might have been greater than strictly necessary for the projects to be feasible in so far as drying plants were concerned.

The replacement of fuel oil based drying systems by conventional electroheat technology has been discussed above, however firewood is also an attractive alternative. When choosing between mutually exclusive projects it is not enough that a given alternative proves to be profitable (i.e. the internal rate of return is greater than the minimum acceptable return on investment, pay-back is less than maximum period of return, etc), the incremental return on investment must also be appropriate. This is equivalent to solving the following equation [48]:

$$\sum_{t=0}^{n} (F_{tA}-F_{tB})(1+i)^{-t} > 0 \qquad (3.8)$$

where F_{tA} and F_{tB} are the annual cash flows of projects A and B over n years (both being cost-effective) and i is the minimum acceptable return on the investment. This is equivalent to saying that

$$\sum_{t=0}^{n} F_{tA}(1 + i)^{-t} > \sum_{t=0}^{n} FtB\ (1 + i)^{-t} \qquad (3.9)$$

or

$$NPV(A,i,n) \quad > \quad NPV(B,i,n) \qquad (3.10)$$

where the sums above are the net present values of cash flows of projects A and B over n years discounted at an interest rate of i.

This principle had been applied to a detailed assesment of coffee drying plants resulting in the conclusion that convective electric driers were only preferred to biomass systems if preferential off-peak seasonal charges were used and the cost of firewood was doubled (the equivalent of reforestation projects) [27].

The conversion of combustion-powered convection systems to electrical resistances still captures attention, as with the case of the Otter Tail Power Co, an electrical utility which supplies a power demand of more than 500 MW to the agricultural country of Minnessota, North and South Dakota (U.S.A.). This company has recently reported on a research project, based on such a retrofitting exercise, involving personnel from agricultural machinery and electrical resistance suppliers and two regional universities [58]. Although this project is reported as being succesful, as explained above this type of conversion is only influenced by the relative prices of fuel and electricity, since the heat transfer method used is common to both, i.e. as far as convection is concerned the only important variables are the velocity and temperature of air, not the way in which it is heated.

It would probably be more useful to concentrate on the study of more efficient air drying systems, e.g. the analysis of waste heat recovery and air recirculation in real dryers, and the design of computerized control systems for energy use monitoring and dryer automation. These may be the only fields in which significant improvements are likely to be obtained in so far as air drying systems are concerned.

4. INFRARED HEATING SYSTEMS

4.1 Introduction

This Chapter discusses the electrical methods used in radiative heating (infrared) applications and introduces design guidelines for such systems applied to the drying of granular materials.

Convective heat transfer, as discussed in previous Chapters, is a function of the temperature difference between the air and the surface of the material (eq (2.3a)). Hence, in order to dry the material, the air temperature must be higher than that of the product but the difference between these temperatures is inherently low in the falling rate period which means that a considerable volume of air needs to be used in order to transfer enough heat to the product. Some of the heat in the exhaust air can be recovered and this improves the energy efficiency of the process but there is a limit to this arising from the humidity of this air. Convection however is a reliable heating method and control is relatively straightforward. Another advantage is that the air can penetrate into the bed of granular material although the amount of useful work it performs is reduced as it transfers heat to the product and absorbs moisture as it does so.

As an alternative, radiative heat transfer can be used to increase the drying rate of many materials, including grain products, and some authors have suggested that considerable energy savings could result from doing so (see, for example [54]). Theoretically very high power densities can be achieved over relatively small areas but in practice the useful energy is reduced since the radiation emitted by the sources is distributed over a wide wavelength spectrum. However it has also been stated that only very thin layers of the product, in most cases a single particle thick, should be used in a stationary bed, or strongly agitated granules in a vibrated or fluidized bed, if the process is to be effective [54, 62, 63, 141]. Some authors even state that radiative heat transfer is not a reasonable alternative for drying agricultural products taking into account all factors involved [49]. More recently the interest in infrared drying of food products and granular materials in general appears to have been revived [45, 73, 140]. Here we are concerned only with those electrical sources which produce radiative heat by means of current flow through a resistive element which can either be exposed or contained in a transparent or opaque enclosure.

Most infrared drying studies have been based on experimental work and none of these appear to have reached the level from which drying models can be developed. For the purposes of the present work, a preliminary assesment of the competitiveness of infrared has been undertaken as described below. This is based on the experimental results of Hall and Headley [62] and the computer simulation of a commercial crossflow dryer. The real limitation in using infrared for through heating materials with a low thermal conductivity is that it is a surface mechanism, i.e. only an infinitesimal layer of the granule is heated. This results in major problems in avoiding excessive temperature build up at the surface and consequent damage to temperature sensitive products. All surfaces of the product must be equally exposed to the infrared source and this requires all the granules to have similar radiation exposure times. The energy available at the surface of the body must be transferred, by conduction mechanisms, to the interior of the particle. Nevertheless it is claimed that radiative heat transfer can be more advantageous than convection since no intermediate physical medium is required between the heat source and the load. The radiation can be focussed and instant control of the heating process can be obtained due to the low thermal mass of the effective heated load involved (i.e. large ;volumes of air do not need to be heated). However, although the control of the process can, in theory, be rapid, the temperature measurment required to instigate the control action presents technical problems since it is the actual temperature of the particles which would need to be measured.

4.2 Principles of Radiative Heat Transfer

Radiation is usually defined as the process by which energy is transferred from one body to another using an electromagnetic field as the transport mechanism. The position of the infrared band relative to the electromagnetic spectrum is shown in figure 4.1. When some of this energy is absorbed by a receptor body there is an increase in the temperature of that body due to the energy increase of its molecules. The heated body then acts as a secondary electromagnetic field source, reradiating some of the energy [63, 64]. The original energy source may emit its maximum energy between different wavelengths from that reradiated by the other body. Materials and radiation sources absorb and emit radiation in well defined patterns which are determined by the temperatures of the material and the source and the wavelength of the radiation.

Heat is not actually transmitted between the bodies but is

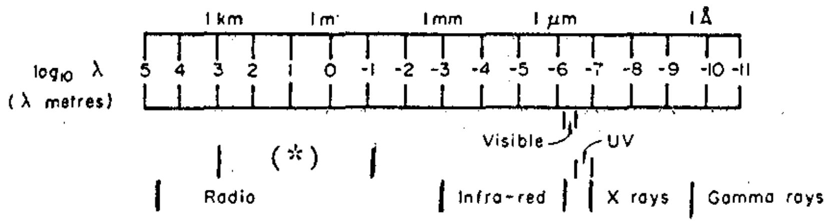

Figure 4.1 Spectrum of Electromagnetic Waves. (*) Radiofrequency and Microwave Range[57].

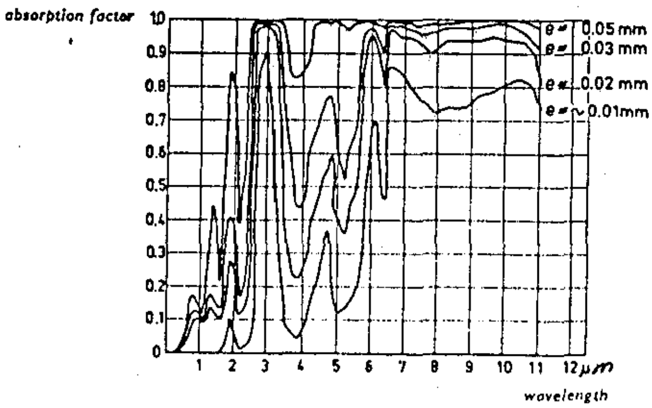

Figure 4.2 Spectral absorption curves of various thicknesses of water. Absorption factor = Absorptivity[92].

generated in the receptor when the field strikes a surface placed in the path of the wave propagation. For an ideal body with uniform absorption characteristics, each infinitesimal layer of the product is capable of absorbing the same radiation. However since the energy is absorbed first by the surface layers, the radiation which reaches the interior of the body is attenuated as it passes through the layers and the penetration depth of infra-red radiation is very small indeed. Some important conclusions follow from this. If a substantial net energy transfer is required then one of the bodies should contain more internal energy, i.e. be at a higher temperature, than the other, the former is the "source", the latter the "load" although it is clear that both act as receiver and emitter of electromagnetic energy. The body which is to be heated, i.e. the load, must be receptive to the electromagnetic energy which strikes its surface and, if through heating is required, the material must be very thin or time allowed for heat conduction within it. Both bodies should be placed in such a way that no obstructions exist between them. The relative position and arrangement of the bodies is of utmost importance and should be such as to guarantee that the maximum net heat transfer can be obtained with optimum energy efficiency. The parameters describing the relative position between the two bodies are expressed in terms of the view factors which are included in the radiative heat transfer relationships. In practice the medium between the bodies can have an important effect in the overall heating process, except when direct combustion methods are used, the most important absorbing medium in drying applications is water vapor.

The capability of a body to emit or absorb radiated energy is determined by its characteristics as expressed in terms of "emissivity" and "absorptivity" of its surface. These characteristics are affected by the wavelength of the field and the temperature, i.e. the energy state, of the body.

Since emission and absorption are based on the same physical phenomena involving the structure of matter, the capability of a particular body to emit or to absorb radiation is also similar if the wavelengths of the electromagnetic fields involved are the same. Hence it can be assumed that, for a given wavelength, the emissivity and absorptivity of the material are equal, irrespective of its temperature. This is Kirchoff's Law of Radiation. This concept can be applied in practice provided that the emmissivity and absorptivity of the real materials do not refer to radically different temperature levels since, in such a case, the wavelengths of the corresponding fields would be quite different.

Thermal radiation and radiative heat transfer can be confusing terms since heat, as such, is neither radiated nor transferred in the process. However these terms are in widespread use and are employed throughout this Report.

When radiative heat transfer is used for heating thin layers of materials which have a high thermal conductivity the heat is readily conducted through the body and the temperature gradients inside the material are negligible. However when materials with low thermal conductivity are subjected to these mechanisms the heat is not easily conducted from the surface of the body and the surface will reach a high temperature. This limitation in through heating of poor heat conductors can be a major problem in drying applications (see for example the drawbacks reported by Metaxas [107] when drying carpets) although the technique can make a major contribution to the heat treatment and curing of these materials. Since the penetration of the radiation in the body is very small, and the power densities are considerable, infrared finds its major applications in the rapid heating of very thin layers. Among these applications are the through heating of thin metallic bodies (see for example classical metal heating applications in [51]), surface treatment of relatively thick (and poorly conductive) materials (see for example wood heating applications in [52]) drying or curing paint and similar substances (see for example [92]) and moisture profiling of paper (see for example [54]) are those most commonly found.

The radiation incident on a body can be expressed in terms of three components: reflected, transmitted and absorbed, the latter is responsible for the temperature increase at the surface. The ratios between these and the total incident radiation are the reflectivity (ρ_r), transmissivity (τ) and absorptivity (α) respectively, these properties are referred to as the "optical" characteristics of the material. The sum of the above ratios must equal unity for any particular wavelength of the incident field and temperature of the body. Since the penetration of the radiation in the material is so small, transmissivity is usually neglected with a few exceptions such as air and glass which are transparent to infrared at certain wavelengths. Rough surfaces give rise to a diffusive behaviour causing the radiation to interact more than once with the body, hence a greater absorptivity is obtained with these than with polished or smooth surfaces. Thus the optical properties of the material are not only dependent on the wavelength and temperature but are also affected by the physical characteristics of the surface. In what follows it is assumed that the transmissivity of the products of interest is zero (this is based on experimental evidence, see for example [105]), which yields

$$\alpha + \rho r = 1 \qquad (4.1)$$

Using classical formulae resulting from Stefan-Boltzmann and Planck theories it is possible to conclude that the total rate of energy emitted from a body per unit time per unit surface area at a given temperature T is

$$Pd(T) = \int_0^\infty \varepsilon(\lambda,T)\{c\lambda^{-5}/[\exp(d/\lambda T)-1]\}d\lambda \qquad (4.2)$$

Evaluation of the above integral is difficult in practice mainly due to the lack of information concerning material properties and radiation sources. If sufficient data is available the expression can be approximated to a series of integrals in which an average emissivity is used for the particular wavelength range of interest. Some authors have assumed that the radiation source is a black body or has an emissivity nearly equal to unity (see for example [12]). The emissivity, and therefore the absorptivity, of agricultural products is quoted as lying between 0.6 and 0.7 [63]. Surfaces for which an average emissivity or absorptivity can be used over a given spectrum are said to behave like Grey Bodies in that spectrum, and the total rate of radiated energy per unit time per unit surface area is given by

$$Pd_{s} = \varepsilon\sigma T^{4} \qquad W/m^{2} \qquad (4.3)$$

In what follows it is assumed that both the product and source can be approximated to grey bodies over short wavelength bands. Hence, instead of using a constant value for the absorptivity and emissivity (which is the standard procedure where a grey body is concerned) different values have been assigned to these parameters within the main wavelength range of operation of the sources involved, i.e. where the bulk of the radiation is emitted from the source in accordance with Wien's Law;

$$\lambda\ T = 2.9E\text{-}3\ mK \qquad (4.4)$$

The data on the optical characteristics of the material, i.e. $\alpha(\lambda)$, $\rho_r(\lambda)$ and $\tau(\lambda)$ (which is negligible) were obtained from [105]. Data for source emissivity were obtained from the curves presented in a previous report [71]. In order to use the latter in the present analysis a regression analysis was performed with the data resulting in a set of equations for the source emissivity as functions of the wavelength as noted below.

An alternative to the approach used in the present report is to consider an approximate constant value for the absorptivity and emissivity as follows. Since Kirchoff's law states that the emissivity of a body at a temperature T is equal to its absorptivity for each wavelength, the absorptivity (or emissivity) of the equivalent grey body can be calculated using eqs (4.2) and (4.3), when the properties of the real material are known, i.e.

$$\alpha = \left(\int_0^\infty \alpha(\lambda,T)\{c\lambda^{-5}/[\exp(d/\lambda T)-1]\}d\lambda \right)/ \sigma T^4 \qquad (4.5)$$

However, in practice, only the variation of absorptivity with wavelength is usually known. Thus it appears justified to adopt this approximation (eq (4.5)) when the properties of the real bodies, i.e. the sources and loads in question, do not exhibit large variations within the wavelength range of interest, which is also the condition required for considering the grey approximation. Nevertheless it appears from [105] and [71] that this is not the case for the products and sources of interest here, for which a more rigorous approach is adopted in the following analysis.

In the above the emission relationships for real and grey bodies have been discussed. However a relationship is required for the radiative exchange between bodies, i.e. the net energy transfer which takes place per unit time. Two extreme cases of radiative heat transfer between grey surfaces can now be considered.

First consider the radiation exchange between two large grey parallel surfaces, i.e. the area of the plates is very large when compared with the distance between them. In this case all reflected radiation returns to the original source. The net exchange of radiation per unit time is given by [72]:

$$Q_g = [1/(1/\varepsilon_1 + 1/\varepsilon_2 - 1)]A\ \sigma(T_1^4 - T_2^4) \quad W \qquad (4.6)$$

When two small and well spaced grey surfaces exchange radiation it is assumed that no reflected radiation returns to the original source. The net exchange per unit time is then given by [38]:

$$Q_g = [\ \varepsilon_1 \cdot \varepsilon_2]A\ \sigma(T_1^4 - T_2^4) \quad W \qquad (4.7)$$

where the generalised view factors for the particular configurations are enclosed in square brackets.

At first glance it may be thought that eqs (4.6) and (4.7) lead to quite different results in all practical cases of interest, this is not the case as shown in table 4.1

Emissivities		Generalized View Factors	
		Small Surfaces	Large Paralell Plates
ε_1	ε_2	$\varepsilon_1 \cdot \varepsilon_2$	$1/(1/\varepsilon_1 + 1/\varepsilon_2 - 1)$
0.10	0.10	0.01	0.05
0.30	0.30	0.09	0.18
0.60	0.30	0.18	0.25
0.90	0.10	0.09	0.10
0.90	0.60	0.54	0.56
0.70	0.70	0.49	0.54
0.90	0.90	0.81	0.82
1.00	1.00	1.00	1.00

Table 4.1 Comparison between view factors in two extreme conditions of radiative heat transfer.

It can be concluded that, if one of the surfaces has a large emissivity, either eq (4.6) or eq (4.7) can be used. It will be noted below that in the short wavelength range of the spectrum both the emissivity of the source and the load are low. Therefore, although eq (4.7) can be used satisfactorily for most cases of interest in this report, it is eq (4.6) which describes most closely the physical configuration of the system and this has been used below. Hence the net radiation per unit time from an infrared source with area A and temperature T_s to a load at temperature T_m is taken as

$$Q = [1/(1/\varepsilon_s + 1/\varepsilon_m - 1)]A\,\sigma(T_s^4 - T_m^4) \quad W \qquad (4.8)$$

where ε_s and ε_m are the emissivities of the source and the material respectively. The above equation does not include the effect of an absorbing medium. If water vapor is present, as in drying applications, a term $(1-\alpha_v)$ can be included on the RHS of eq (4.8), where α_v is the absorptivity of water vapor. In practice it is important to ensure that the water vapor between the source and the load has a low absorptivity in the range of wavelength in which the infrared source delivers its maximum power. The radiation efficiency of the source will always be less than 1.0, due to conduction and convection losses. In some cases this efficiency can be as low as 0.5-0.6 in the longer wavelength region. These losses have not been included in eq (4.8) but they can be accounted for by the inclusion on the RHS of eq (4.8) of a term η_R, the radiation efficiency. It can be argued that in a well designed system, if the drying zone is enclosed by reflecting walls with good external insulation, almost the entire heat transfer given by eq (4.8) will eventually be absorbed by the load after many wall reflections, the remainder being transfered by convection to the air, this also performs a useful heat transfer function.

A further assumption in eq (4.8) is that both the source and load have similar areas. Although this is perfectly feasible at longer wavelengths it is less so in the medium and short wavelength bands even if appropriate reflectors are incorporated in the sources.

Most of the radiation emitted by short wavelength sources, i.e. infrared lamps and quartz tubes is produced in the 0.5-2.0 μm band, with a maximum around 1.0 μm . The report of Hardiman [71] indicates that the emissivity of tungsten varies between 0.3 and 0.45 in the band referred to. The same author notes that Inconel, which is a metallic alloy commonly used in the manufacture of the external metal sheat of resistance heaters, has an emissivity of 0.8-0.7 within the band 2.0-4.0 μm and 0.7-0.4 between 4 and 9 μm . Hardiman's data can be used to arrive at the following linear relationships which closely reproduce the emissivity of short wave (tungsten) and metal sheathed (inconel) infrared sources:

$$\varepsilon_s = 0.51-130.13E3\lambda, 0.5< \lambda<2.0\mu m$$

$$\varepsilon_s = 0.92-61.99E3\lambda, 2.0<= \lambda<9.0\mu m$$

These relationships are used below to describe the emissivity of the sources, i.e. the ε_s term in eq (4.8).

4.3 Infrared Absorption in the Drying Zone

Although the interior of the material contains most of the moisture in the material it only receives a fraction of the radiation absorbed by the product, most of the heat being dissipated at the surface. Therefore it can be argued that only the surface optical characteristics of the product should be taken into account, i.e. either the surface moisture or the hull present considerable absorptivity. The absorption characteristics of thin layers of water are shown in figure 4.2.

The absorption characteristics of moist air will now be considered. Absorption increases with the thickness of the air layer between the source and the load and with the relative humidity of the air. The absorption characteristics of a layer of water vapor 0.4 metres thick at 127 C and atmospheric pressure are shown in figure 4.3. Since moist air is a mixture of dry air and water vapor, and in a real dryer the separation between the heat source and the load is not likely to exceed 0.4 m if the unit is to be as compact as possible, the values shown in figure 4.3 can be taken as maximum levels of absorptivity in practical drying applications. If appropriate ventilation is provided inside the drying chamber the humidity of air will not reach saturation and the vapor absorption will be lower than that referred to above.

The values of reflectivity reported by Massie and Norris [105] for maize, rice, wheat, soya and other agricultural products are in the range 0.4 to 2.0 μm . These authors suggest that the reflectivity is little affected by the moisture content of the product although it may experience a slight increase when the moisture content is reduced. They conclude that, for all products, the lower values of reflectivity are found around 2.00 μm , the transmissivity is negligible particularly at the end of the band examined. Dagerskog and Osterstrom [40] investigated the reflectivity of food products between 0.8 and 2.4 μm , and found that it is low between 1.5 and 2.4 μm

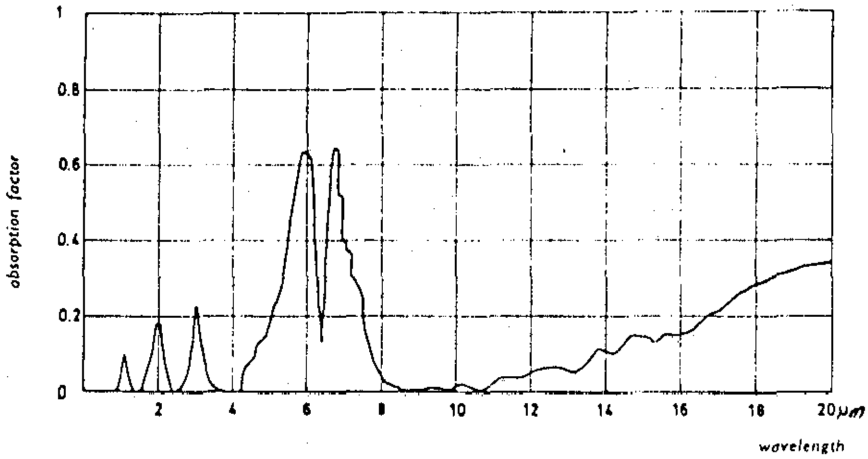

Figure 4.3 Spectral absorption curve of water vapour at ambient (atmospheric) pressure. Water vapour zone is 40 cm thick. Absorption factor = Absorptivity[92].

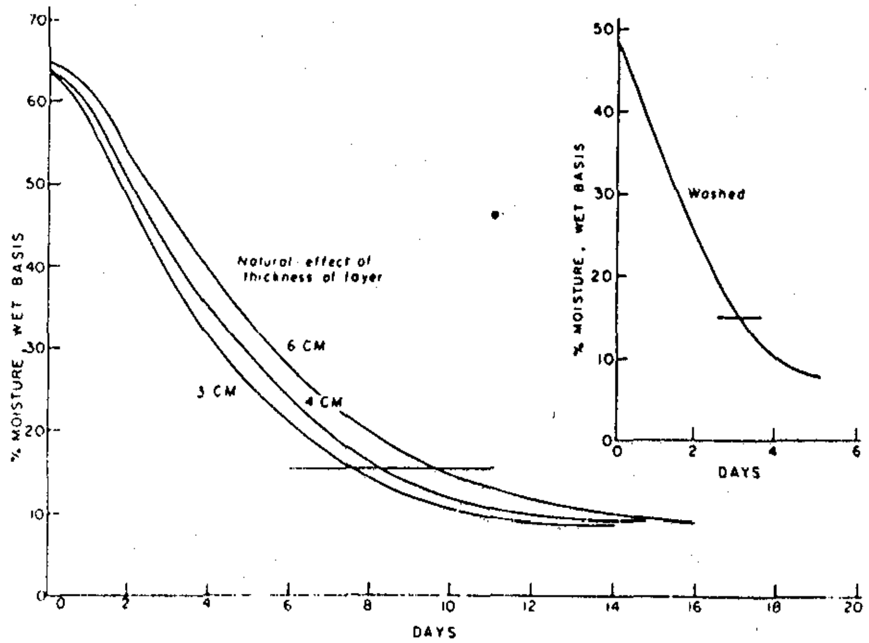

Figure 4.4 Drying curves of washed and natural coffee by solar radiation[42].

although the minimum values are obtained beyond 2 μm.These results have been summarised in table 4.2. Since radiative heat transfer is greatly affected by the source temperature the values for 0.5 μm have been included in the table. Infrared sources are limited to about 3,000 K which means that such systems cannot emit maximum radiation below approximately 1.0μm. Nevertheless, in the context of this Report, it is necessary to consider solar radiation which, for practical engineering calculations, can be taken as a black body at 5,800 K (see for example [57]), i.e. $\varepsilon_s = 1.0$ in this case.

	α WATER									
λ(μm)	Liquid	Vapor	ρ_r				$\alpha = 1-\rho_r$			
			Maize	Rice	Wheat	Soya	Maize	Rice	Wheat	Soya
0.50	0.04	0.00	0.16	0.28	0.16	0.22	0.84	0.72	0.84	0.78
1.00	0.10-0.13	0.10	0.65	0.71	0.63	0.62	0.35	0.29	0.37	0.37
1.50	0.11-0.40	0.00	0.22	0.45	0.25	0.25	0.78	0.55	0.75	0.75
1.95	0.10-0.85	0.18	0.15	0.33	0.18	0.15	0.85	0.67	0.82	0.82
3.00	0.90-1.00	0.22	0.20	0.45	0.25	0.25	0.80	0.55	0.75	0.75

Table 4.2 Absorptivity (α) and reflectivity (ρ_r) of water and crops as a function of wavelength (λ). For 3 μm it has been assumed that the reflectivity remains within the range observed over 1.5 μm as can be concluded from the results reported by [40].

Some of the above values of absorptivity of water vapor apply to only a very narrow wavelength band as shown in figure 4.3. Therefore a considerable amount of radiation will not be absorbed by the water vapor at the maximum level referred in table 4.2. In practice an efficient infrared unit should be well insulated and some way of recovering the heat available in the exhaust air should be incorporated not only because of the absorptivity of water vapor but also to recover the convection losses as will be discussed later. From table 4.2 it can be seen that the absorption characteristics of agricultural products vary little over the range considered except around 1.0μm where this type of material is highly reflective.

Since infrared have been considered in this Report as grey bodies at different wavelength ranges eq (4.4) can be used for estimating the source temperature at which the bulk of the radiation corresponds with the wavelengths of table 4.2, thus

$$T_s = 5{,}800 \text{ K} \quad \text{for} \quad \lambda = 0.50 \ \mu m$$

$$T_s = 2{,}900 \text{ K} \quad \text{for} \quad \lambda = 1.00 \ \mu m$$

$$T_s = 1{,}933 \text{ K} \quad \text{for} \quad \lambda = 1.50 \ \mu m$$

$$T_s = 1{,}487 \text{ K} \quad \text{for} \quad \lambda = 1.95 \ \mu m$$

$$T_s = 967 \text{ K} \quad \text{for} \quad \lambda = 3.00 \ \mu m$$

Using eq (4.8) and incorporating the relationships for the emissivity of the infrared sources for each wavelength range and the maximum absorptivity ranges of water vapor (α_v) as given in table 4.2, it is possible to estimate the maximum (i.e. considering that the load is being irradiated by a source of equal surface area) heat transfer at the above temperatures (T_s) to the load, which is assumed to be at ambient temperature, i.e. T_m = 293 K. If the temperature of the source is greater than 400 C this approximation involves an error no greater than 4 % as compared to the corresponding values obtained when T_m is assumed as the maximum level allowed in the product, i.e. 80 C.

In the solar case (T_s = 5,800 K, λ=0.5μm) not only the term ($1-\alpha_v$) should be included in the right hand side of eq (4.8) but also S, which is a factor that depends on atmospheric conditions and the position of the sun relative to an observer on earth, this point will be returned to later.

Considering first electrical sources, it is possible to obtain the following values for the heat transfer:

Product	2,900 K	1,933 K	1,487 K	967 K
Maize	804	229	56	24
Rice	710	198	52	18
Wheat	832	228	55	23
Soya	846	226	56	23

Table 4.3 Estimated maximum radiative heat transfer per unit time per unit surface area from infrared sources to agricultural products (kW/ m^2).

Alternatively, if the material is extremely wet, as may be the case in the initial stages of the pre-drying of washed coffee, only a thin layer of water is being irradiated. Therefore the spectral characteristics of this water are the factors to be taken into account (see figure 4.3). In this case the following values for the maximum radiative heat transferred per unit time per unit surface to a very wet layer of material are obtained when the corresponding values for α (of water) and α_v are taken from table 4.2 and the relationships for the emissivities of the sources are considered:

$$310\ kW/m^2 < q_{max} < 387\ kW/m^2 \quad \text{for } T_s = 2{,}900\ K$$

$$70\ kW/m^2 < q_{max} < 169\ kW/m^2 \quad \text{for } T_s = 1{,}933\ K$$

$$18\ kW/m^2 < q_{max} < 56\ kW/m^2 \quad \text{for } T_s = 1{,}487\ K$$

$$26\ kW/m^2 < q_{max} < 28\ kW/m^2 \quad \text{for } T_s = 967\ K$$

Although the radiative heat transfer may vary in accordance with the thickness of the water layer in damp conditions, it is evident from above that the short wavelength sources (T_s=2,900 K, λ=1μm) are the most appropriate for heating the material if large energy transfers are required irrespective of the state of the material. Hence in order to obtain high levels of radiation a high temperature source should be used even though the material may present considerably higher levels of reflectivity in the wavelength band concerned (see table 4.2).

It is possible to increase the effective absorptivity of the load if it is enclosed in a reflective container, polished aluminum can be used, polished steel is also an alternative due to its low emissivity (comparable with aluminum).

In practice however the levels of radiation estimated above for short wavelength sources are too high for applications involving the drying of non conductive materials which can be easily damaged by excessive temperature levels (e.g. food products). The radiation levels which can be tolerated by this type of material are closer to the lower range of the figures estimated above. Hence for these applications it is not necessary to have an emitting surface with the same area of that of the load, thus the radiation sources (e.g. metal sheathed elements) can be placed apart from each other in order to obtain the appropriate radiation levels (these are quoted later in this Chapter) on the surface of the material.

It appears that it would not be satisfactory to use infrared sources which produce most of their radiation beyond approximately 4 μm (this corresponds to using metal sheath elements below 500 C) since within the range 5 - 7μm the absorption of water vapour is excessive (see figure 4.3) and the temperature difference between the source and the material becomes insufficient to produce acceptable levels of radiation, most of the heat being transferred by convection. The emissivity of the source is also reduced. This also applies even if the absorptivity of the load is assumed to reach the maximum possible value, i.e. 1.0. Using eq (4.8) for $\varepsilon_m = 1$ and the relationship ε_s =0.92-61.99E3λ we obtain the following maximum rates of heat transferred to the product per unit time;

$$q = 10.2 \ kW/m^2 \ \text{for} \ T_s=725 \ K \ (\alpha_v=0.00)$$
$$q = 0.5 \ kW/m^2 \ \text{for} \ T_s=483 \ K \ (\alpha_v=0.63)$$
$$q = 0.2 \ kW/m^2 \ \text{for} \ T_s=363 \ K \ (\alpha_v=0.03)$$

As noted below, it is possible for a medium wavelength infrared system (2-4 μm) to replace a typical cross flow dryer, the former requiring approximately 50 m^2 of floor space with an installed power of nearly 10 kW/m^2 depending on the energy efficiency of the system. The use of low temperature levels at the surfaces of the metal sheaths would require far greater floor space in order to maintain the same throughput. This would affect the economic feasibility of the infrared system since it would result in a much lower throughput per unit of investment. In this case it might be preferable to use solar radiation which, although still a throughput-limited drying system, involves no running costs as far as energy is concerned.

Solar energy is in widespread use for drying agricultural products but, as can be seen from the curves for naturally dried coffee shown in figure 4.4, the drying periods are considerably greater than those achieved by mechanical methods (see Chapter 1 and Appendix II). Therefore, as noted in Chapter 1, it is clear that if the agro-industrial business can accept the costs of mechanical methods of drying these are to be preferred on the basis of increased production. Desrosier and Sivetz [42] report solar radiation measurements at Matao, in Sao Paulo state, Brazil, during part of the coffee harvest season. They found that the maximum daily radiation on a clear day was approximately 976.7 W/m², the corresponding value in a cloudy day being 418.6 W/m². The average taken over an entire daylight period of 11 hours was 607.8 W/m² when the day was clear. Thus an average S factor can be estimated for the atmospheric conditions and geographic location (south latitude of 21.5) referred to, as follows. If eq (4.7) is evaluated for $\varepsilon_s = \varepsilon_m = 1.0$ (i.e. the maximum energy absorbed from the sun, a black body) and considering $\alpha_v = 0$ (see table 4.2) we have Q_s = 642E5 W, hence

$$S = 607.8/(642E5) = 9.5E\text{-}6$$

Therefore the radiative heat transfer per unit time per unit surface from the sun to a damp layer of coffee in the above location can be as low as

$$q = 607.8 \times (\alpha) \quad W/m^2$$
$$= 607.8 \times 0.04 \quad W/m^2$$
$$= 24.3 \quad W/m^2$$

which might be increased to

$$q = 607.8 \times (0.8) = 486.2 \ W/m^2$$

as soon as the remaining water is contained within the beans (and the falling rate drying period begins).

Even if the effective absorptivity of the load is improved (e.g. by using a solar heat trap, which cannot however make α greater than 1.0) the resulting solar heat transfer will be much lower than the radiation levels which can be obtained with short and medium wavelength infrared sources. With the latter it would be possible to dry a layer of coffee in approximately one hour (see [140]), whereas the corresponding period for solar is in the range of several days (see figure 4.4).

4.4 Infrared Heating in Agro-industrial Plants

4.4.1 Available Infrared Sources

The incandescent lamp uses the flow of current through a tungsten wire and can operate over a wide range of temperatures, it is fairly efficient, approximately 85 % of the power input is converted into radiation. The maximum levels of radiation obtained are limited by the bulb and reflector arrangements resulting in installed powers of no more than 25 kW/m^2 [44, 54, 88]. When used as individual units they produce a very non uniform distribution of radiation in the space available [54, 92], this can be improved by adjusting the separation between sources and between the latter and the load.

Quartz tubes have replaced the conventional incandescent lamps over the last few years, although they are more expensive. Quartz glass has a higher transmissivity over longer wavelengths than normal glass hence these sources can also be effectively used to radiate energy at medium wavelengths. The devices are based on nickel-chrome or tungsten alloy wires enclosed in a quartz envelope. Installed powers range between 100 and 300 kW/m^2 [54, 88], and the shape of the quartz tube is very convenient for achieving a uniform distribution of the radiation over the material, particularly if it is used in a conveyor system where the load moves perpendicularly to the axis of the tube. The radiation emitted is approximately 85% of the power input in the short wave sources and between 60-65% in the longer wavelength types [31].

Medium wavelength quartz tubes have been mentioned above, however it is also possible to produce such radiation with the more robust metal sheathed heaters as used in convective heating applications. The maximum temperature which can be tolerated by the nickel-chrome heating element inside the heater is approximately 1,300 K, however when the temperature drop across the internal insulation is considered this reduces to no more than 1,100 K at the metal sheath (see for example Hardiman [71]). The wavelength for peak emission is between 2.5 and 3.5 and each element may be rated from 0.6 to 8 kW, the maximum installed powers obtainable are of the order of 60 kW/m^2 [31]. These radiation sources are said to be the most convenient types for heavy duty operations [170], they have longer lifetimes and produce a far better distribution of radiation over the material [54].

4.4.2 Guidelines for Designing an Infrared Dryer

Infrared drying equipment will always incorporate an air flow to extract the moisture, the temperature must not be lower than that of the load surface, since gained energy would be lost and lower rates of temperature increase would be obtained. In practice it may also be important to reduce natural convection losses, this can be done if the material is admitted to the drying zone through the minimum opening possible. Reflective materials should be used to construct the internal walls of the dryer and effective insulation should be provided for the equipment. The heat available from the cooling of radiation sources can be directed to the material hence carrying out useful work instead of being lost to the exhaust.

Hall and Headley [62] carried out an experiment in which the drying of a stationary single kernel layer of maize was investigated under two directions of a 0.1 m/sec air flow, the material being subjected to radiation from an infrared lamp. They found that a much faster drying was obtained when the air flow was in the same direction as the radiation, i.e. from the source to the load. The authors explained this by concluding that the heat absorbed by the water vapor is removed from the region between the infrared lamp and the material, then it is forced to flow through the material, thus enhancing the convective heat transfer. This would not be so if the air flow was in the opposite direction, in which case it would cool the material and carry away much of the sensible heat gained by the product. An additional point, not mentioned by the authors is that the convective heat available from cooling the lamp is being utilised since it interacts with the material.

In most infrared heating applications, a substantial amount of heat is produced in the surface layer of the product, much more than in conventional convection processes. This leads to high temperature gradients between the interior of a poor conductor and the surface so opposing the drying mechanisms as explained in Chapter 2. Ginzburg [54] recommends the use of intermittent irradiation of the material, this will lessen the severity of temperature gradients within the material.

Hall and Headley extended their experiments on the infrared drying of maize to the condition where no forced convection was applied. They used 2,500 K incandescent lamps with the load placed approximately 30 cms away from the source, the product depth was varied from a single kernel to 5 cm thick and a vibration of 1,200 cycles per minute with an amplitude of 0.6 cm was imparted to the layer of material. Data were obtained for three levels of radiated power, using one, two and three 375 W lamps. The effective installed power per unit surface area was not given by the authors, the radiative heat transferred was measured using the amount of evaporation from samples of water 2.5 cm deep. Three levels were thus defined, i.e. 2.4 kW/m^2 (one lamp), 3.4 kW/m^2(two lamps), 5.1 kW/m^2 (three lamps). It appears that these rates of heat transfer correspond closely to the actual installed power since the absorptivity of the water samples can be estimated as between 0.95 and 0.96 (see for example [38]). It can be seen from the results obtained that if the product is not to be dameged, stationary layers of maize cannot be dried with the above radiation levels from an initial moisture content of 25 % w.b. down to 13 % w.b. When the grain was vibrated it was found possible to dry 5 cm thick layers with no visual damage being observed. However Hall and Headley did not estimate the maximum radiation level for a given initial moisture content and depth of product, information which would have been useful for design purposes. The data obtained by Hall and Headley can be used to construct the curves of figure 4.5 which show the relationship between depth of layer, drying times and radiation levels used, and therefore constitute a simple infrared drying model for the conditions referred to above.

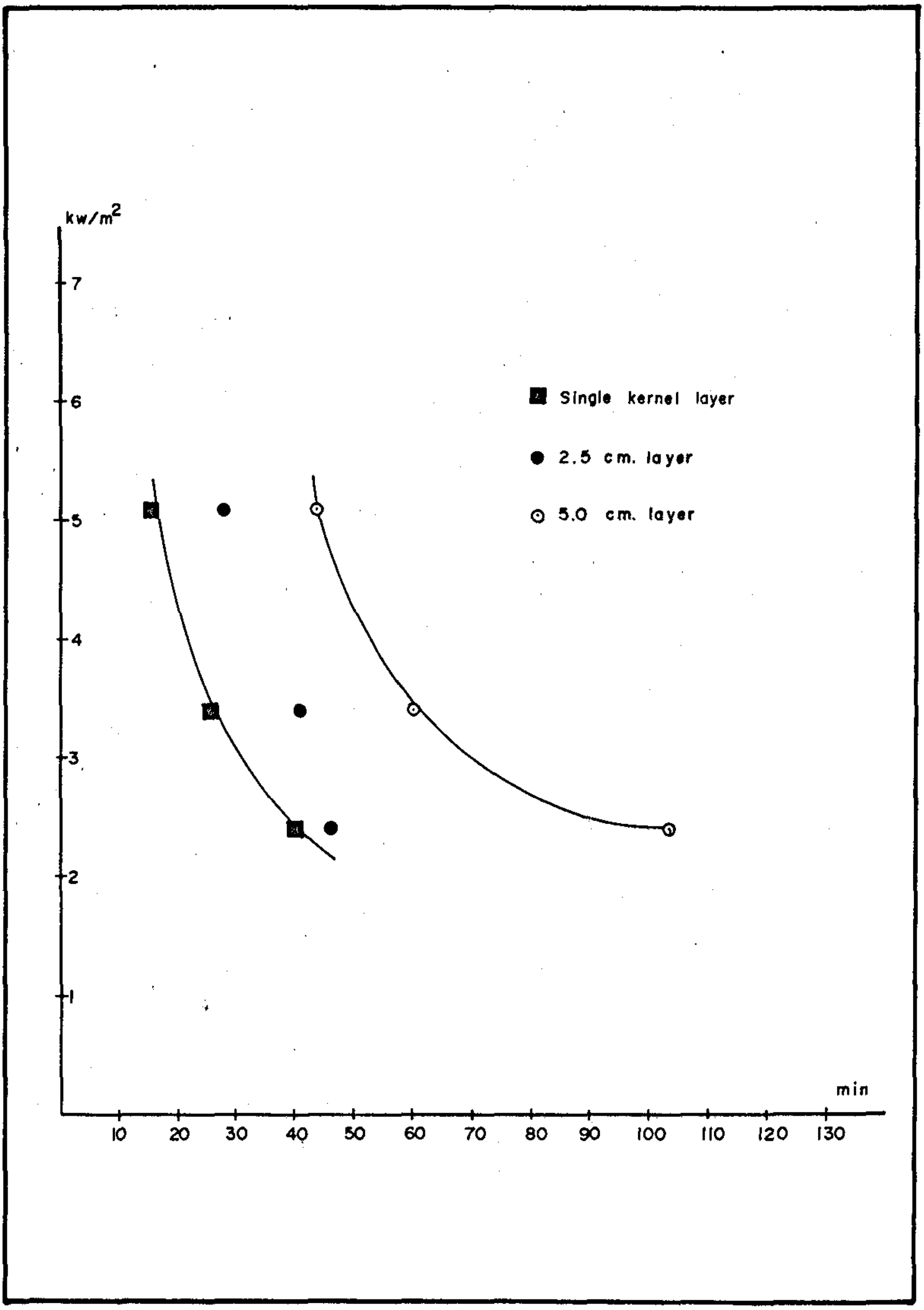

Figure 4.5 Drying time as a function of radiation levels.
Maize initial moisture content = 25 % w.b.
Maize final moisture content = 13 % w.b.
From data by Hall and Headley [62].

4.4.3 Review of Infrared Drying Plants for Agricultural Products

An installation engineered by Siemens is reported by Ginszburg [54]. The drying system consists of a receiving hopper into which the product is fed, and several vibrating sections transporting the material to a receiving bin storage section. The material is effectively intermittently dried since the infrared sources are not placed uniformly over the system and the product experiences periods of zero radiation, during which the moisture is extracted through suction boxes. The throughput is adjusted by means of varying the inclination of vibrating sections, this is done by a lever mechanism, the power input to the infrared sources can also be varied.

Infrared drying of rice has been undertaken experimentally in Italy by the Veneria di Lignana Agricultural Institute [54]. The material is loaded and then placed on a metallic 5.6x0.8 m^2 conveyor belt, the thickness of the layer of rice being carefully controlled. The product first experiences irradiation on the conveyor belt, it is then transported by a bucket elevator and screw conveyor to a further infrared treatment depending on its initial moisture content. The throughput of the process can be controlled by the speed of the bucket elevator and screw conveyor and by varying the power input to the radiation sources. The recirculated product experiences intermittent drying in this system.

A comprehensive study into infrared and convection drying of coffee and cocoa was carried out by Buxo and Felipes [24] in which layers of product from 8 to 15 cm thick were continuously stirred. The stirring of the product aimed not only to achieve better drying uniformity but also to polish the cocoa beans, a practice which has been carried out over the years by the feet of labourers. The infrared lamps were mounted approximately 30.5 cm from the product and a 24 kW resistance battery used to heat the air (approximately 0.4 m^3/sec per m^2 of material) up to 77 C. Since 36x250W lamps are used the installed power per unit surface can be estimated, this turns out to be approximately 1.9 kW/m^2. No problems were reported in drying coffee but cocoa suffered serious damage, drying was not uniform and infrared was thought to produce case hardening of this product, so making it very difficult to continue the drying process below 18 % w.b. Other problems were also reported, chiefly the cementing with gum of the bottom layers of cocoa and breakage of the beans by the rotating ploughs. Following these tests the infrared drying of cocoa was abandoned. The quality of the finally dried coffee was assessed locally and abroad and it was found that the infrared dried product attained better characteristics than the sun dried one.

Combined infrared and RF roasting of cocoa beans has been experimentally analysed in the U.R.S.S. and is reported by Ginzburg. The roasting system consists of two conveyor sections, the first is used to pre-heat a sigle kernel layer of the material under infrared action up to approximately 60-100 C, the material is then passed through a perforated plate RF system operated at about 20 MHz where it undergoes the last phase of the roasting. The upper plate system is connected to the RF unit, the lower electrode is the same conveyor belt which is properly earthed. The low thermal conductivity of cocoa beans, due to the high fat content, was seen as one of the main reasons why infrared should be used rather than convection. This is surprising since conduction is involved in both and, as has been discussed in Chapter 2, the higher temperature gradients produced inside the material when infrared is used (which are to a great extent due to the low thermal conductivity of the material) can actually present problems, as was presumably the case with the system of Buxo and Felipes.

The pre-heating of cocoa with infrared could probably be justified by savings in the higher costs of high frequency energy. Nevertheless the question in this case would appear to be whether to pre-heat the product with convection or radiation. It is worth noting that the material may leave the convection phase at a high temperature before being admitted to the next stage of roasting. Hence even though a new infrared-dielectric roasting unit might be an adequate alternative for processing a given product it may not turn to be a feasible investment if the convection equipment already installed is to be used in this application instead of radiation. Moreover, as will be noted in the next section, infrared does not appear to be competitive with convective techniques for drying cereal products, hence it is unlikely that an agro-industrial dielectric roasting plant in conjunction with an infra-red pre-heating system will be attractive to the industry.

4.4.4 Comparison between Radiation and Forced Convection

The effective radiation per unit time per unit surface to a vibrating layer of maize is

$$q = P_{ir}\eta_R \ (1- \alpha_v)$$

P_{ir} is the installed capacity per unit surface, η_R is the radiation efficiency of the source and α is the absorptivity of maize. Considering a layer of maize 5 cm thick, and taking P_{ir}=10 kW/m^2, which can be obtained with metal sheathed elements (η_R=0.65, the bulk of the radiation lies between 2.5 and 3.5 μm, which results in α=0.8 and α_v=0.22 from table 4.2) q can then be estimated as approximately 4 kW/m^2. This does not take into account the contribution of convection losses to the total heat transferred to the material since Hall & Headley [62] (on whose experimental results the analysis below is based) did not use any air flow on their drying experiment.

A model of the infrared drying of agricultural products such as those described in Chapter 2 for convective drying has not yet been developed. The kind of experimental work which is needed in order to study in more depth the feasibility of radiative heating techniques involves the quantifying of the effects caused by the intensity of radiation and perhaps the temperature, relative humidity and velocity of air. Ideally the intensity of infrared would be expressed as net energy transfer per unit time per unit surface. It is possible to use the results obtained by Hall & Headley and which yielded the information shown in figure 4.5. From the latter it can be estimated that a 5 cm vibrating layer of maize can be dried in nearly 53 minutes when an infrared system with 10 kW/m^2 of installed power (metal sheathed elements) is used (4 kW/m^2 effective as estimated above).

The corresponding throughput per m^2 can be estimated as

$$5E-2\ m^3/0.88\ h = 5.7E-2\ m^3/h$$

Consider a throughput of 2.7 m^3/h. In order to achieve this the area and installed power required are

$$(2.7\ m^3/h)/(5.7\times10^{-2}\ m^3/hr/m^2) = 47.4\ m^2, \text{ and}$$

$$47.4\ m^2 \times 10\ kW/m^2 = 474\ kW$$

Infrared requires a relatively large area, in this example a conveyor belt 2 metres wide needs to be nearly 25 metres long in order to dry 2.7 m^3/h of material without product recirculation. Considering a batch volume of 20 m^3 of maize then 7.4 hours are required to dry the product.

At this point it is appropriate to consider the effects of the technical and economical parameters on the economics of retrofitting a convective plant to infrared. The economic feasibility of the replacement can be assessed in terms of the compounded payback period (PBP) of the investment. This is the time in which the new plant investment and running costs can be recovered from the profits. If it is greater than the useful life of the equipment or the period in which the organisation requires to recover its investment then the project will not be cost effective. If the reverse is the case then the project will be worthwhile. The PBP may be found using the following equation in which profits are equated to financial costs

$$PBP\ HR(E_c C_c - E_{ir} C_{ir})/t_d v = \{Inv P_{ir} A/[1-(1+i)^{-PBP}]\}\ PBP$$

The terms E_c and E_{ir} are, respectively, the total energy requirement for drying the volume v of material in the cross flow dryer and that which is needed in the infrared system. HR and $t_d v$ are, respectively, the hours of operation of the drying plant in a year, and the time required for drying the volume v of product. C_c, C_{ir}, Inv and i are, respectively, the unit energy costs for the convective and infrared plants, the unit investment cost of the infrared plant and the annual interest charge. A is the surface area needed to dry the material. The investment cost of the infrared plant will be affected by the cost of the equipment and associated installation costs and also by the costs incurred in increasing the floor space required, if necessary.

It is first necessary to consider the operating conditions of the convective dryer, namely the temperature (T_a) and flow ($\dot{Q}$) of the drying air and the flow of product in the columns of the dryer. This information, together with the initial moisture content, temperature and other characteristics of the product, dimensions of the dryer and ambient conditions, used in conjunction with a simulation program for the crossflow dryer can be used to obtain the moisture content and temperature of the product and the absolute humidity and temperature of air along the height of the dryer. Thus it is possible to determine, by re-running the program several times if necessary, the time for the whole volume of material V to be passed through the columns of the dryer and discharged at the bottom at an appropriate final moisture content, this is the drying time t_{dv}.

This analysis can be illustrated as follows. Consider the comparison between an electric infrared unit and a convective dryer with different relative energy costs. For example, the crossflow dryer may be supplied with a relatively expensive fuel such as diesel oil or with cheap biomass residues obtained from crops and firewood. In the analysis the mechanical energy requirements of the fans are neglected when compared with the heating loads. Take for example a crossflow dryer 4 metres high and 3 metres wide with two 0.3 m thick drying columns. The total frontal area of the bed of material is $2x3x4=24\ m^2$, and the total cross sectional surface area of the drying columns is $2x3x0.3 = 1.8\ m^2$. If the velocity of product through the columns is adjusted to 3 m/h this yields a flow of product of $1.8x3 = 5.4\ m^3/h$. The temperature and flow of the drying air can be taken as, respectively, 80 C and 25,000 m^3/h, the ambient temperature and absolute humidity as 20 C and 0.01 kg/kg respectively. The initial temperature and moisture content of maize are 20 C and 25 % w.b. With these drying conditions the following results are obtained for the product at the bottom of the drying columns using the crossflow dryer simulation program supplied by Centreinar (Brazil) [136].

1st Pass: Moisture Content = 18.6 % w.b. Temperature = 67.5 C

2nd Pass: Moisture Content = 12.8 % w.b. Temperature = 71.3 C

This means that the material needs to pass twice through the drying columns in order to reach approximately 13 % w.b.

The time required for drying v m^3 of maize can thus be estimated as

$$2v/(5.4\ m^3/h)$$

which yields 7.4 hrs for v=20 m^3, i.e. a throughput of 2.7 m^3/h.

The energy required to operate the crossflow dryer would be:

$$E_c = Cp_{air}\rho_{air}t_d vQ(T_a-T_i)$$

Cp_{air} is taken as 0.28 Wh/kg/K [64], T_i is the ambient temperature. Similarly,for an infared system in which convection is not used;

$$E_{ir} = AP_{ir}t_d v$$

Agro-industrial plants have a low load factor due to seasonal operation, in what follows a value of about 0.3 is used, i.e. approximately 2,500 hours of operation a year [26,27]. A typical cost of capital is taken as 0.2 per year [86]. Under these conditions the curves shown in figures 4.6-4.9

are obtained which represent the pay-back period of the replacements as a function of the ratio K between the cost of the alternative fuel for the convective dryer and that of the energy used in the infrared dryer. Four scenarios have been studied, the first can be considered as the "standard ", and is based on the calculations performed in this Section (figure 4.6). The cases shown in figures 4.7 and 4.8 represent, respectively, a reduction to 80% and 65% of the installed infrared equipment with the dryer still performing the same drying task, i.e. these reductions can be interpreted as a more efficient utilization of the infrared sources (e.g. convection losses are used to increase the drying rate). It is important to note that figure 4.8 represents the ideal case in which the infrared sources operate at maximum possible efficiency, i.e. η_R=1.0. Finally, figure 4.9 illustrates the case where the "standard" infrared system is compared with a cross flow dryer in which a reduction of 20 % in energy consumption is obtained by means of air recirculation. Bakker-Arkema et al [10] and Bakshi et al [11] report on energy savings of up to 30 % when a cross flow dryer is fitted with an air recirculation system (see also table A.4, Appendix II). In the above calculations it has been assumed that the energy cost of the infrared dryer is C_{ir}= US$ 5E-2/kWh which is a typical charge for industrial use of electricity.

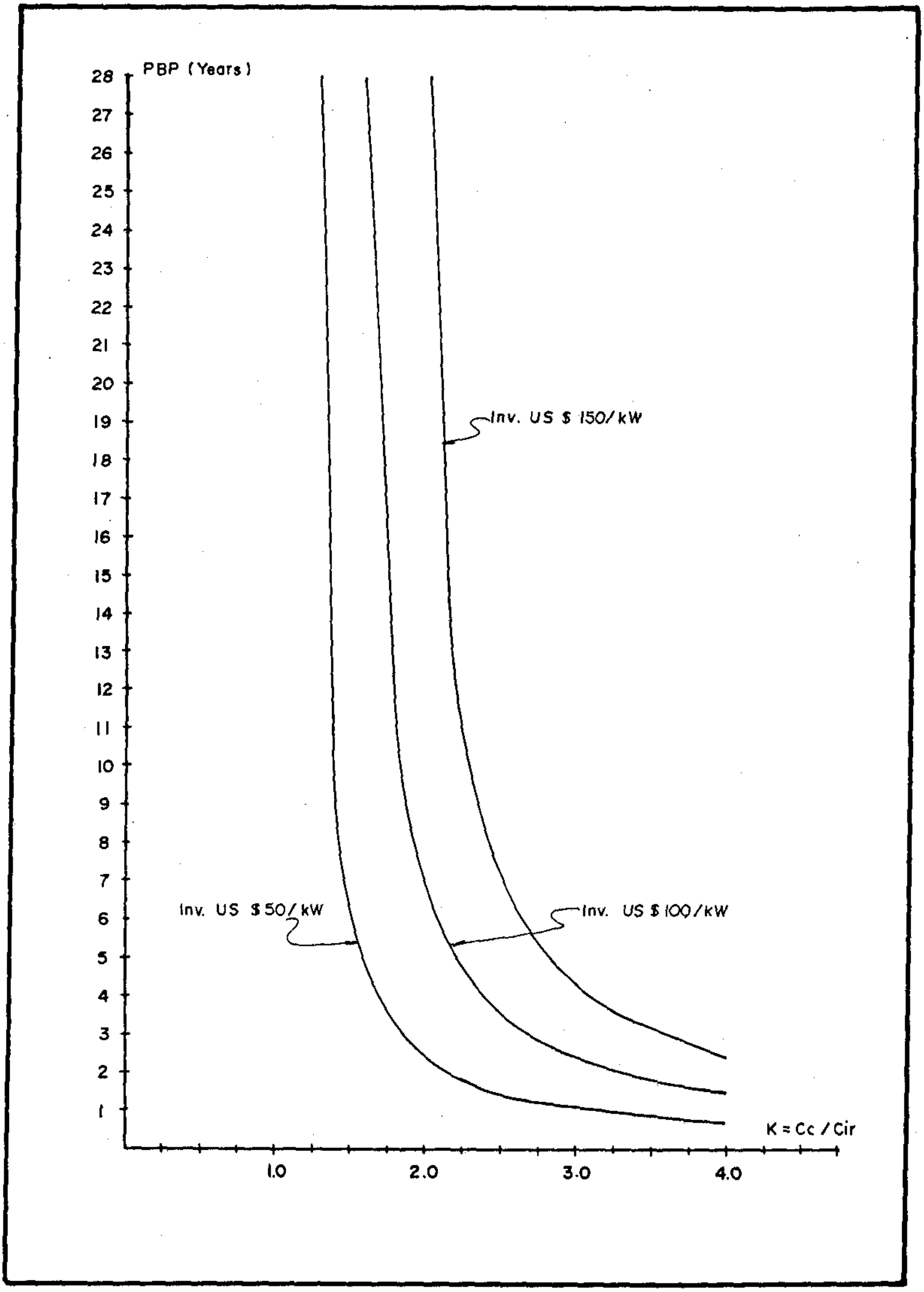

Figure 4.6 Compounded payback for retrofitting a 2.3 m^3/h throughput crossflow dryer into an infrared conveyor dryer. Load factor of the plant=0.3, installed infrared capacity=474 kW, return on investment = 0.2 per anum, C_{ir}=US$5E-2/kWh, Inv=investment costs in infrared dryer, C_c= energy costs of crossflow dryer (US$/kWh).

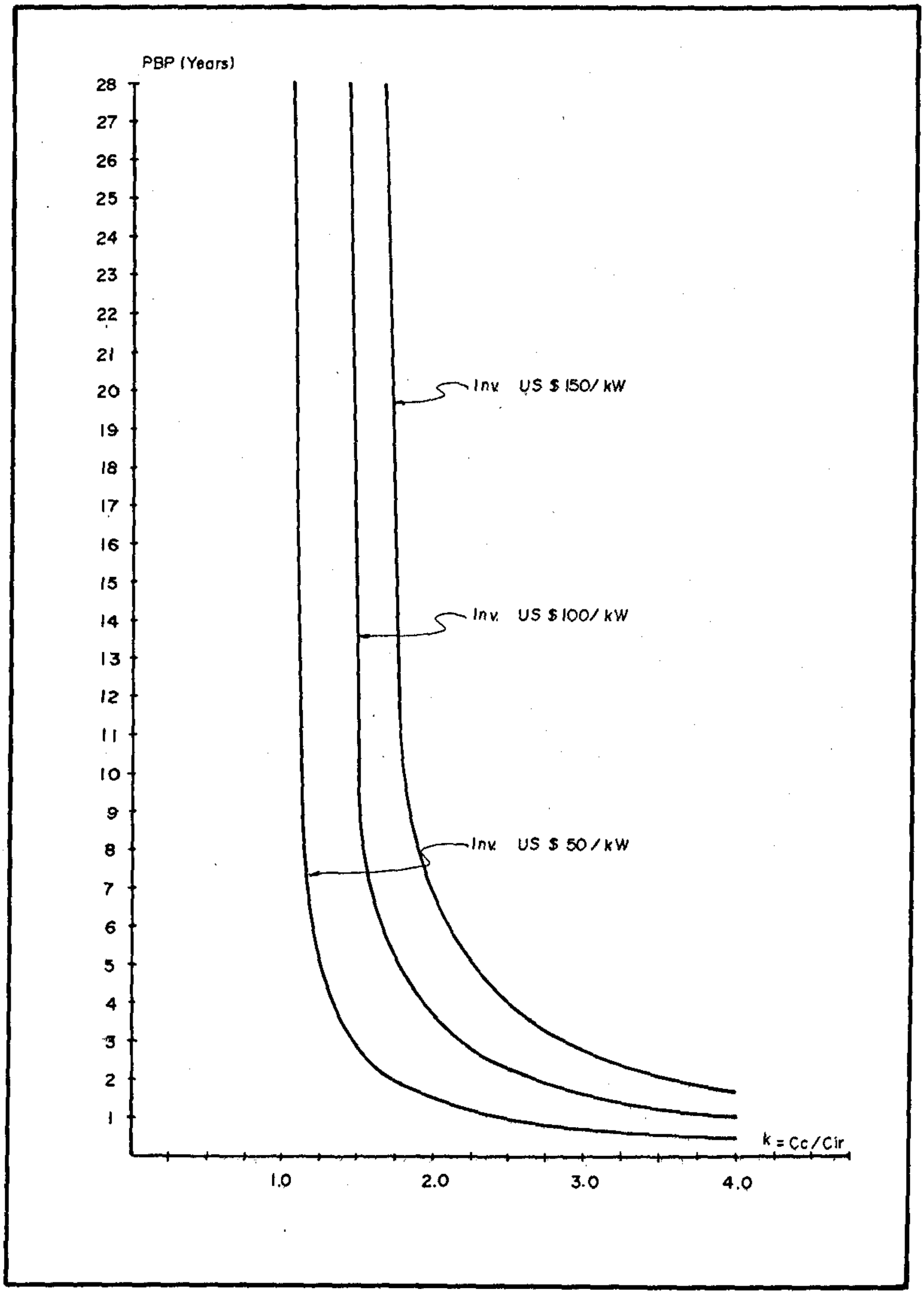

<u>Figure 4.7</u> Compounded payback for retrofitting a 2.7 m^3/h throughput crossflow dryer into an infrared conveyor dryer. Load factor of the plant = 0.3, installed infrared capacity = 379 kW, return on investment = 0.2 per anum, C_{ir}=US$5E-2/kWh, Inv = investment costs in infrared dryer, C_c= energy costs of crossflow dryer (US$/kWh).

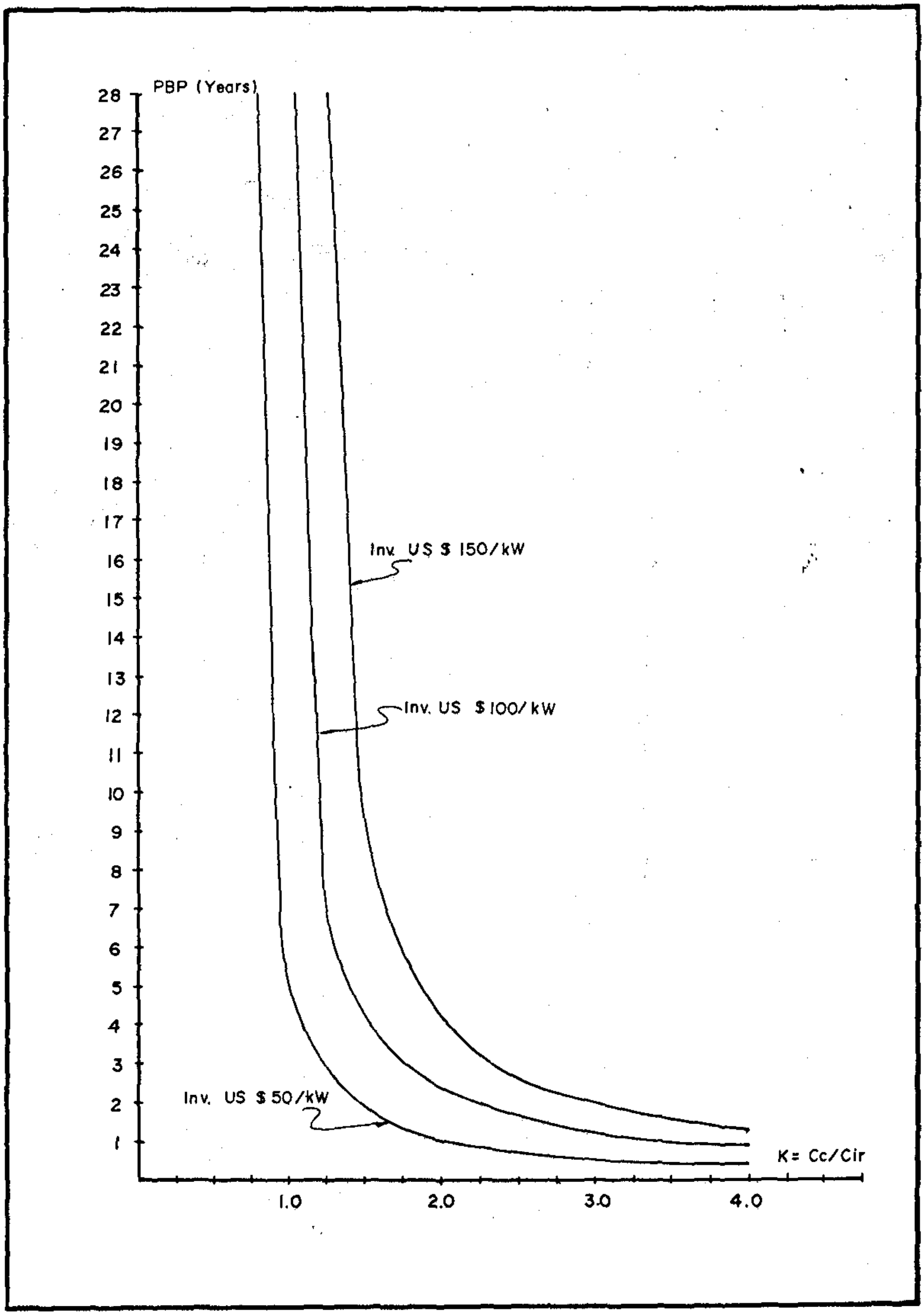

<u>Figure 4.8</u> Compounded payback for retrofitting a 2.7 m^3/h throughput crossflow dryer into an infrared conveyor dryer. Load factor of the plant = 0.3, installed infrared capacity = 308 kW, return on investment = 0.2 per anum, C_{ir} = US$ 5E-2/kWh, Inv = investment costs in infrared dryer, C_c= energy costs of crossflow dryer (US$/kWh).

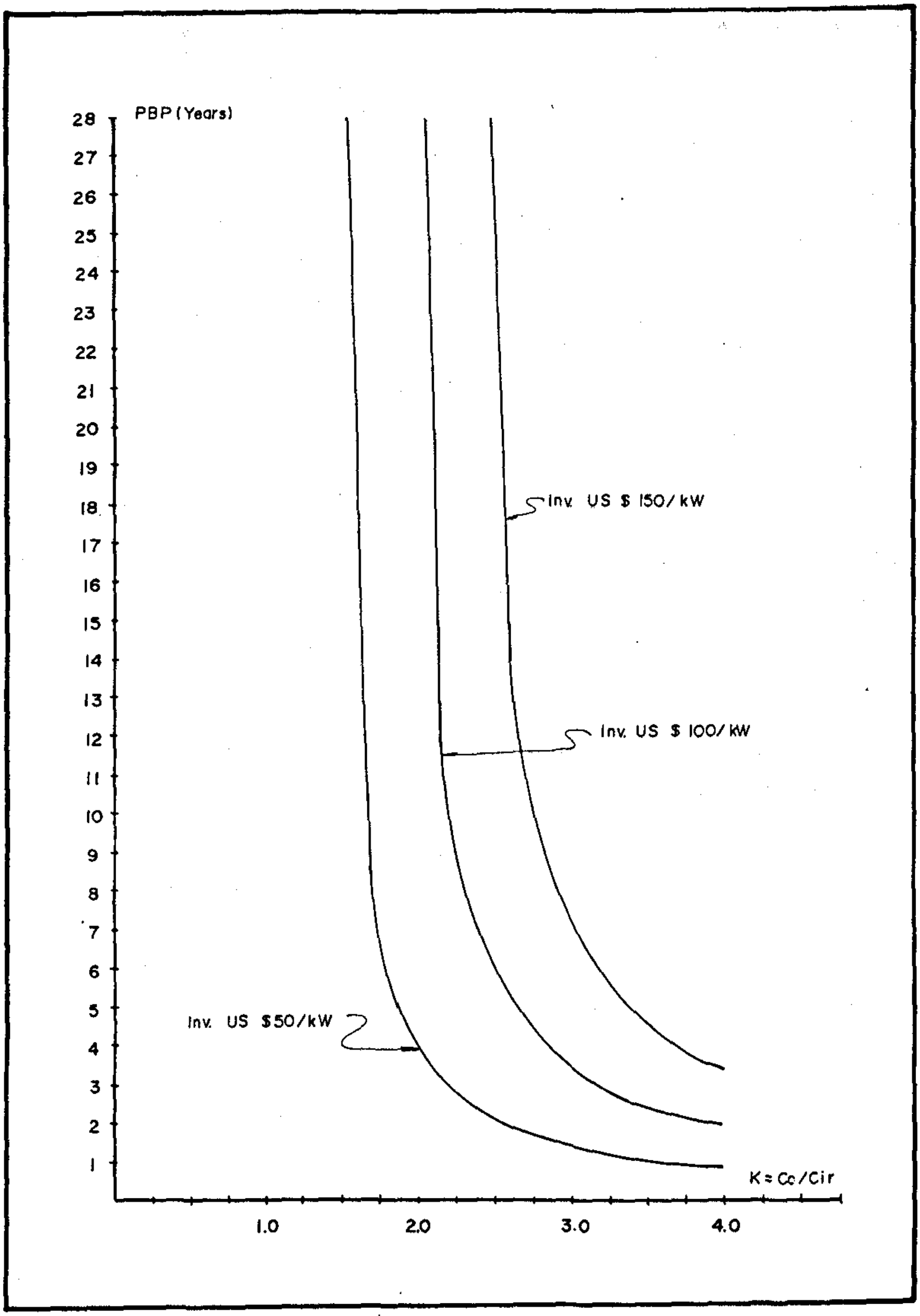

Figure 4.9 Compounded payback for retrofitting a 2.7 m^3/h throughput crossflow dryer into an infrared conveyor dryer. Load factor of the plant = 0.3, installed infrared capacity = 474 kW, return on investment = 0.2 per anum, C_{ir} = US$ 5E-2/kWh, Inv = investment costs in infrared dryer, C_c= energy costs of crossflow dryer (US$/kWh).

The effective unit costs of firewood and other biomass fuels are determined by the energy efficiencies of the combustion equipment and by the costs of the raw fuels plus storage and handling costs, which in this case are a relatively large portion of the total. From previous work, [26, 27] the costs of firewood can be expected to vary between US$0.5E-2/kWh and US$3.5E-2/kWh taking a thermal efficiency in the range 0.2-0.6 for the combustion system.

The investment cost of the infrared unit will be affected by equipment and installation costs and, possibly, by the associated costs of physical extensions of the plant. It was indicated in the previous Chapter that resistance battery systems using metal sheathed elements costed approximately US$ 70/kW in 1982. The infrared conveyor units proposed here also require metal sheathed heaters in their construction, these conveyor dryers however will require more metal parts than the compact resistance heaters used in convective applications since in the latter case the entire bank of heaters is installed in a relatively small section (see figure 3.3) of the air duct system already existing in the plant. In the above infrared estimations the range US$ 50-150/kW has therefore been used for the infra-red plant investment to compensate for this.

In practice this infrared substitution is not attractive, even at relatively low investment costs, unless $K > 1.0$, i.e. the unit energy costs of the convective dryer must be higher than those of the infrared unit. This is an improbable situation since the cross flow dryer can always be supplied by the same type of energy source used in the infrared system or with even cheaper fuels. It is evident that the key factor for infrared systems to be more attractive is the attainable throughput per unit area, this can be increased by using higher radiation levels on thicker layers of product in a vibrating conveyor. In this case the aim would be to attain in the infrared unit, without damaging the product by excessive temperature levels, a throughput which would require too much air flow in the cross flow dryer (and therefore higher energy consumption) However, from the analysis presented here it appears that the convective dryer can always match the throughput of an equivalent infrared dryer by means of increasing the air flow and the depth of the column.

An additional argument which might be raised against the use of electricity for the above infrared drying applications is the fact that the same results can be obtained by using combustion of biomass gases. The theoretical maximum flame temperatures achievable are in the region of 2200-2400 K although in practice these levels are not reached due to losses in the flames, moisture in the gases and the presence of non-combustible products in the mixture (see [37, 55, 90]. The flames have a high emissivity and can be approximated to a grey body, using eq (4.4) it will be seen that these gas systems correspond to radiation sources in the range 1.0 - 2.0 μm. Thus electric infrared equipment would be competing in unfavourable terms against biomass combustion systems which can produce the same levels of radiation at much lower running costs.

5. CONDUCTIVE HEATING SYSTEMS

Thermal conduction is governed by Fourier's Law, the rate of heat flow per unit time is proportional to the area of flow (measured normal to the direction of flow) and to the temperature gradient along the heat flow path, i.e.

$$q = - k(T_1 - T_2)/(x_1 - x_2) \quad W/m^2 \qquad (5.1)$$

The negative sign allows for the different directions of temperature and distance. The constant of proportionality k is the thermal conductivity of the material between x_1 and x_2.

If the diameter of each particle in a product bed is x_i then the steady state rate of heat flow per unit time through the thickness of the bed is (assuming that the later is much greater than x_i and x_i is very small),

$$q = (T_1-T_2)k/x_1 = (T_2-T_3)k/x_2 =$$

$$= (T_1-T_{n+1})/[(\sum_{i=1}^{N} x_i)/k] \qquad (5.2)$$

where $\sum_{i=1}^{N} x_i$ is the thickness of the bed

N = number of particles in the direction of the heat flow

$T_i - T_{i+1}$ = temperature difference across each particle

$T_1 - T_{n+1}$ = temperature difference across the bed

If a substantial heat flow is required the thickness of the bed must be small and the temperature differences large. In this case if a large amount of product is to be processed the required volume of the dryer and the heat transfer surface within it would have to be large. Alternatively large temperature differences would be necessary if the thermal conductivity of the material is low and this, in turn, may damage the product.

In some dryers a limited degree of conduction is applied to the product in order to increase the drying rate, especially at the final stages of the drying process, in doing this the energy efficiency of the dryer is also increased, since less air is used to heat the material to accelerate the diffusion of the internal moisture. The Guardiola tumble dryer allow some conduction to occur between the walls of the dryer and the material, these units have been fairly popular in the coffee drying industry throughout this Century though they require a substantial floor space in the plant and only produce small throughputs due to the temperature limitation of the product.

The requirement of a large surface area for conduction to be effective in the applications of interest can be illustrated as follows. Consider the cylindric conveyor dryer shown in figure 5.1. This system could be placed in the position of a standard screw conveyor at the bottom of a cross flow dryer. The outer shell of the screw dryer could be heated by electric means, e.g. by direct resistance or induction methods. If a temperature difference of 80-20=60 C is maintained across the moving layer of product then a maximum transference of (from eq (5.1) and figure 5.1)

$$Q = kA60/0.075 \quad \text{Watts}$$

is available for drying the material, where A is the surface area of the outer shell. Assuming k = 0.18 W/m K (value for cereal products, see [112]) and a 3 metre long screw dryer, no more than 270 watts could be transferred between the outer shell and the screw along the entire length of the dryer. As will be

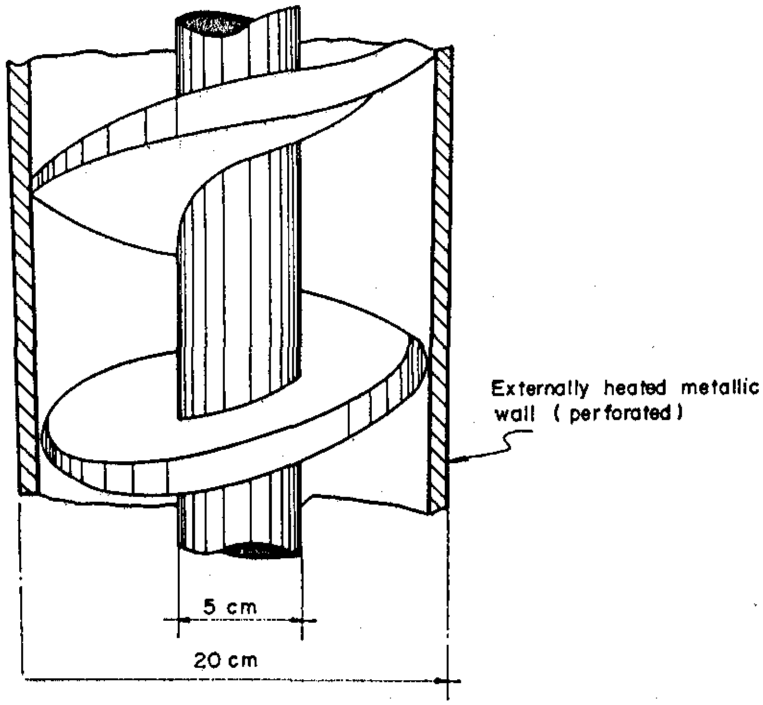

Figure 5.1 Screw Conveyor Dryer.

shown later, this is far too low for the drying applications of interest (Chapter 6).

Hence, if conduction were used, only single kernel layers of the product could be heated (e.g. in a tumble dryer). A technique which could directly heat the metal parts of the tumble dryer results in some advantages over conventional rotary methods (e.g guardiola) since only the minimum required amount of air flow would be supplied to the rotary dryer. Such an alternative is being pursued at the Electricity Council Research Centre (U.K.) using induction heating techniques (see [65]). This equipment is therefore equivalent to a tumble Guardiola dryer in so far as heat transfer to the product is concerned although it may yield a more energy efficient process since only the internal metal surfaces of the dryer are heated. However the limitation in the throughput of such a dryer remains as the main barrier when compared with convection (e.g. crossflow) plants.

6. DIELECTRIC HEATING SYSTEMS

6.1 Introduction

There are two basic methods for producing heat in a body. The first makes use of the conventional heat transfer mechanisms of conduction, convection and radiation. The second includes induction heating, direct resistance heating and dielectric heating. The first two of these are used for heating materials which have a low electrical resistivity, i.e. those which are good electrical conductors, such as metals and, in certain circumstances, glass and water. With both induction and direct resistance heating the energy is converted to heat inside the workpiece through the Joule effect but this is not as quite effective in insulators, i.e. dielectric materials. Such materials have high resistivities which would require much larger applied voltages, these will certainly exceed the insulator and surrounding air's breakdown limits. Most insulators however are subject to considerable polarisation effects when situated in a high frequency electric field and, as a consequence of this, the material becomes heated. The remainder of this Chapter is concerned with dielectric heating which relies on the transfer of energy through an electromagnetic field between a source and a load and then dissipating this energy, as heat, within the bulk of the load.

In the case of dielectrics the mechanisms of interaction with the field responsible for the heating effect produced are normally explained in terms of displacement of electrons with respect to the nuclei of atoms, displacement of atoms within molecules and reorientation of molecules. The latter component is due to the existence of permanent dipoles in the molecular structure of some materials [110].

The heat is produced in the dielectric, therefore if the surrounding medium and the enclosure in which the product is contained are not receptive to the field, the entire energy supplied is used in the load.

In considering the dielectric heating characteristics of materials it is not necessary to analyze the internal structure of the product since macroscopic quantities can be measured in the laboratory. These parameters are the lumped equivalents of all the interactions between the applied field and the material under the specific conditions in which the experiment is carried out. The parameters so obtained are the dielectric constant e' and the loss tangent $tg\delta$, the loss factor e'' is the product of these two quantities.In this respect, the loss factor measures the heating produced by all internal mechanisms [110, 142]. The dielectric constant ϵ' represents the response of the internal polarization mechanisms to the external field, i.e. the ability of the material to store potential energy by molecular and atomic interactions. This parameter is familiar to electrical engineers, it is the ratio of the magnitude of the current produced in a dielectric under the action of an external field to that which would exist if the same field were applied to a vacuum.

The internal power dissipated in an infinitesimal volume when an electromagnetic field is applied can be obtained from the integration at that point of the Poynting vector defined by

$$\vec{P} = \vec{E} \times \vec{H} \quad W/m^2 \tag{6.1}$$

where $\vec{E}$ and $\vec{H}$ are the electric and magnetic components of the field. From the definition of vectorial product, the vector defined by eq (6.1) is perpendicular to both $\vec{E}$ and $\vec{H}$. The magnitude of this vector expresses the power available per unit of transversal area therefore the computation of the power dissipated in a given material involves the integration of this vector within the product along the direction of the field propagation. Thus both the direction and magnitude of the electric and magnetic components of the field define the magnitude and direction of the Poynting vector and also establish the available power which can be transfered in a given volume. The general form of the energy dissipated per unit time within a dielectric volume v for a constant-magnitude internal field is given by Metaxas & Meredith [110] as:

$$Qd = 1/2\ w e_o e'' \int_V E_p^2\, dv \quad W \qquad (6.2)$$

where e_o is the permittivity of vacuum and E_p is the magnitude of the internal electric field $\hat{E}_p$, the latter being a peak value, w is the angular frequency of the field and v is the volume of the body whose effective loss factor is e".

In practice the equations defined in eqs (6.1) and (6.2) are not evaluated for each particle. If it is assumed that the bulk material experiences a constant magnitude and spatially uniform, i.e. a similar field is experienced by all particles in the drying zone then simplified formula can be obtained from eq (6.2),

$$Qd = 1/2\ w e_o e'' E_p^2 v \quad W \qquad (6.3)$$

where v is the volume of the bulk material in the drying zone.

Writing the above expression in terms of RMS values of the field instead of peak quantities and substituting the value for e_o we have

$$Qd = 0.556E\text{-}10fe''E^2 v \quad W \tag{6.4}$$

E being now an RMS quantity.

In some cases, it is difficult to obtain the above conditions hence in general the values obtained from eqs (6.3) and (6.4) are only a first approximation to the real system although in some circumstances they are adequate as will be shown later in this report. They are not satisfactory, for example, if the magnitude of the field reduces considerably as it penetrates the material and these equations should not be used if the penetration of the electromagnetic radiation is small as compared to the thickness or depth of the material to be processed.

6.2 Dielectric Properties of Agricultural Products

The dielectric constant and loss factor are respectively the real and imaginary components of the complex permittivity, i.e.

$$e^* = e' - je''$$

The capacitive effects are included in the real part of the permittivity and the dissipative or resistive effects are incorporated in the imaginary component. The magnitude of the permittivity, and consequently the dielectric constant, may be expressed in absolute values in which case very small values are involved, the units are farads/metre. However this magnitude is normally expressed in relative terms taking as reference the permittivity of vacuum, e_o, in this case the value of the dielectric constant is always greater than 1. This procedure is adopted throughout this Report unless otherwise stated.

The dielectric properties of agricultural products have been studied by S.O. Nelson and others in an attempt to correlate a characteristic of the material such as moisture content or ripeness with these properties and in order to study the response of the material to the heating effects. The majority of the technical literature in this field is concerned with cereal products though some data is available for peanuts and soya (see [121] and [124]) and for fresh fruits [118]. No information appears to be available for cash crops such as coffee and cocoa. The available data on the loss factor and dielectric constant of agricultural products is usually given in the form of tables, graphs or charts, which pose some restriction on its effective utilization. When data points are given they are usually few in number, thus it is difficult to use this information as a basis for statistical analysis. Since these properties are of particular importance for this Report it was considered that, as a first step, some of the available data should be transferred into analytical form, this was done using linear and non-linear regression analysis. In addition, an extensive program of experiments was carried out to measure the dielectric constant and loss factor of rice, coffee, maize, soya and wheat in the radiofrequency band. It was not possible to obtain the most popular yellow-dent maize in this Country to carry out the experiments for maize, therefore pop-corn was used. However the results obtained for the dielectric properties of this product lie closely to those reported by Jones et al [89] and S.O. Nelson for yellow-dent maize. More details on the experimental work and results are included in Chapter 8 and

Appendix IV.

The moisture content of the product at a given frequency band is the most important influence on the properties of interest although there is some evidence that the temperature and bulk density also have an effect (see [32], [89], [119], [120], [121], [122], [123], [124]). In the experiments described in Chapter 8 it was noted that the effect of temperature on the dielectric constant of the products of interest is much smaller than that caused by the moisture content. The corresponding effect on the loss factor is minimal. In the frequency band of interest, i.e. between 10 and 2,500 MHz the loss factor and the dielectric constant are inverse functions of frequency. At a moisture content of 25 % w.b. the decrease in the loss factor of maize when the frequency is increased from 10 MHz to 2.5 GHz, i.e. 250 times is around 70 %. Hence if it is required to increase the power dissipated (for a given field strength) it is advantageous to increase the frequency as can be seen from eqs (6.2)-(6.4). Alternatively, for a given dissipation, the field strength employed can be reduced if the frequency is increased so reducing the probability of electrical discharges occuring, as will be noted below.

Since the dielectric properties of the materials of interest are measured in bulk it is only possible to obtain the characteristics of an individual particle by means of extrapolation, some data for such dielectric constants is presented by Nelson [119, 120, 123]. More recently Nelson has obtained the dielectric constant of maize [123], wheat [120] and soya [121] in terms of frequency of the field, moisture content and bulk density of the material, the corresponding information for the loss factor is not yet available. The effect caused by the variation of the bulk density due to pressure was not considered to be important in the context of this work. In this case only the variation of the bulk density with moisture content is likely to be of importance, although it is known to be small [111], this was confirmed in the present study. However in industrial heating applications where the granular product may be submitted to different pressure conditions along its path through the dryer this effect may become worth considering. The most recently published dielectric constant results by S.O. Nelson for wheat and maize have been used in this report to estimate the dielectric constant of individual particles as a function of moisture content and frequency. This is possible since the same author had previously presented information on the variation of the kernel density with moisture content.

However it should be noted that the variation in the dielectric properties among different types of the same species can be of the order of 18 % [122], and can even vary considerably among different lots of the same product [124] when obtained by the same experimental methods and apparatus. Some variation can also be expected when working with material from different source and with different measuring techniques. The considerable variation in the dielectric properties of agricultural products is expected since it is known by agricultural engineers that the characteristics of agricultural materials vary among types of the same species, place of origin and year of harvest. Hence in practice it may be necessary to produce individual data for each particular product and application under consideration. In Chapter 8 the latest results of S.O. Nelson and those of Jones et al [89] are compared with the experimental values obtained in this report.

6.3 Power Calculations for Established Agro-industrial Drying Processes

If a general dielectric drying model were available and the maximum power levels which could be applied were known, it would be possible to design a dryer in which a given amount of product at a particular initial moisture content (M_i) would need to remain for a certain period of time in the drying zone to reduce its moisture content to Mr. Hence the throughput of the system could be estimated and, knowing the specifications of the equipment, it would be possible to calculate the corresponding investment and running costs. With the aid of the drying model it would be possible to vary the design parameters in order to optimise the performance and minimize the overall costs associated with the process, etc. However, as we have noted in previous Chapters, drying is a very complex process for which repetitive experimentation is the only practical way of assessing the feasibility of specific applications. This involves the design of appropriate experimental procedures and the installation of specialized rigs. In the case when many alternative systems can be used it is considered that the only method by which meaningful results can be obtained is to devise a method for pre-selecting the most promising techniques. This is necessary for dealing with dielectric heating applicators since many options appear to be appropriate at first glance. In the following sections the criteria used for selecting the alternatives are presented, those techniques which appeared to be most promising were subjected to further study.

The energy required to raise the temperature of the material, and the water which it contains and evaporate water, can be determined by estimating the required sensible and latent heat to heat up the wet material and evaporate the water. Over and above this additional energy is required to provide the energy to carry away the moisture, this component is however supplied by the ventilation equipment and is a small fraction of the total, furthermore it is similar for all the alternatives considered since it depends on the weight of water to be evaporated. In terms of energy required to drive the internal mechanisms of drying, the total needed is directly related to the mass of product, the temperature rise involved, the specific heats of the dry material and water, the latent heat of water and the initial and final moisture contents. Thus the energy needed per unit volume of finally dried product is:

$$E_{e1} = [\Delta T(Cp_d + M_i Cp_w) + h_v(M_i - M_f)]\ \rho_s \text{Wh/m}^3 \qquad (6.5)$$

where the moisture contents are expressed in per-unit dry basis terms. Rearranging eq (6.5) :

$$E_{e1} = \rho_s(\Delta T Cp_w + h_v)M_i + (\Delta T Cp_d - M_f h_v)\ \rho_s\ \text{Wh/m}^3 \qquad (6.6)$$

Therefore, for given values of temperature increase, specific heats, latent heat of water, final moisture content and bulk density of dry material the energy required is a linear function of the initial moisture content M_i. The properties were obtained from the references (e.g. [3], [111], [112], [42]) and are presented in appropriate units in table 6.1. Substituting these values leads to the developments of eq (6.6) for each of the products concerned (eqs (6.7) and (6.8)). It has been assumed that the final moisture content is 12 % w.b. This corresponds almost to the equilibrium moisture content of the products when stored. In eqs (6.7) it has also been assumed that the temperature rise for cereal products except coffee is ΔT = 60 C, for coffee the value of 40 C has been used. These correspond to maximum temperature rises, from ambient level to the temperature limits of the products, these are quoted in the corresponding technical literature (see [20], [42]) and various assessments [25, 27]. In eqs (6.8) it is assumed that the temperature differences are one tenth of these, i.e. 6 and 4 C respectively. Both cases are considered to represent a wide range of operating conditions, i.e. the product could be admitted to the dielectric drying plant at ambient temperature, or only after the end of a conventional convective drying phase in which the product has attained a temperature very close to that of the drying air. The specific heat and latent heat of evaporation of water have been taken as 1.16 Wh/kg/ C and 645.7 Wh/kg respectively.

Eq (2.33) shows that the product of the specific heat and bulk density of the material will affect the rate of temperature increase during drying, hence the latter has also been included in table 6.1 in terms of the dry material. As mentioned above, the differences due to moisture content are small and the same applies for the specific heat (see for example [111] and [112]). It was observed in the experiments (Chapter 8) that the variation in the bulk density remained restricted to no more than 10 %. The published values for the density of maize and wheat (table 6.1) agree very closely with the range observed in the experiments, although this was not the case for the other products. The differences for rice and soya were of the order of 25 % and those for coffee as high as 35 %. It is possible that such variations were due to different types of product. The average values from the experiments have been used for table 6.1 in the case of rice, soya and coffee.

Property	Coffee	Maize	Soya	Rice	Wheat
Sp. Heat (C_{pd}) (Wh/kg/ C)	0.46	0.40	0.44	0.30	0.31
Bulk density (ρ_B) (kg/m^3)	620	755	645	753	801
$C_{pd}\,\rho_B$ (Wh/m^3/ C)	285	302	284	226	248

Table 6.1 Specific heats and bulk densities of dry crops.

$$E_{coffee} = 429\ M_i - 43 \qquad kWh/m^3 \qquad (6.7a)$$

$$E_{maize} = 540\ M_i - 48 \qquad kWh/m^3 \qquad (6.7b)$$

$$E_{soya} = 461\ M_i - 40 \qquad kWh/m^3 \qquad (6.7c)$$

$$E_{rice} = 539\ M_i - 53 \qquad kWh/m^3 \qquad (6.7d)$$

$$E_{wheat} = 573\ M_i - 55 \qquad kWh/m^3 \qquad (6.7e)$$

$$E_{coffee} = 403\ M_i - 53 \qquad kWh/m^3 \qquad (6.8a)$$

$$E_{maize} = 493\ M_i - 64 \qquad kWh/m^3 \qquad (6.8b)$$

$$E_{soya} = 421\ M_i - 55 \qquad kWh/m^3 \qquad (6.8c)$$

$$E_{rice} = 491\ M_i - 65 \qquad kWh/m^3 \qquad (6.8d)$$

$$E_{wheat} = 523\ M_i - 69 \qquad kWh/m^3 \qquad (6.8e)$$

The specific heats and the latent heat of evaporation can both be taken as constant for the temperature ranges involved here (see for example [112]). The key parameters are the initial and final moisture contents and the throughput required. Given that there is a limit on the maximum value of field strength which can be used at a particular frequency, then the minimum drying time for a specified amount of material with known drying requirements can be found. This, in turn, determines the maximum throughput of the process. Alternatively, for a given throughput, the power input to the dryer needed to avoid excessive field strengths can be determined. However the field strength is not the only factor which needs to be considered. There are limits to the energy dissipation within the product if physical damage, such as rupture and cracking, is to be avoided. The appearance of the product and its milling properties must also be acceptable. Hamid et al [67] and Wear [166] suggest that the gross power densities used in the microwave drying of materials such as wheat and maize should not be higher than 400-500 kW/m^3. Some products may accept higher values without damage, that for rice for example, might be up to an order of magnitude greater. This can be deduced from experiments carried out by Wratten [175] to measure the dielectric properties of rice. Fanslow and Saul [46] carried out experiments on the microwave drying of maize using a range of power densities and different air flow rates to cool the product. The results showed that, for a given power density, the time for the first audible sound of cracking increased as the air flow increased. For example, with a gross power input density of 500 kW/m^3, the first sound was noted after 266 secs when the air flow was equivalent to 44 m^3/h but this increased to 430 secs when the flow rate was doubled. When the gross power input was increased to 2200 kW/m^3 the times for flow rates of 44 and 88 m^3/h were 32 and 62 secs respectively. It is unfortunate that these experiments were not extended to determine the maximum power density which could be used to cope with the entire drying process. However the work demonstrates the importance of surface cooling, an effect which will be examined later in this Report.

To obtain the actual power density within the material it is necessary to assume in the above previous results a value for the conversion efficiency from mains to high frequency energy. It is assumed here that all the available energy in the field is eventually absorbed by the product - after many reflections in some cases. Taking a typical value of 50 % for this efficiency the actual maximum allowable power density in the product becomes 230 kW/m^3 for maize and wheat and 2,300 kW/m^3 for rice. Wratten dried rice using an RF applicator under practical conditions, the rice being subjected to a range of temperature increase rates from 1.8 C/min to 130 C/min without exceeding the maximum temperature limitation of 80 C. No damage to the quality of the product was observed. The approximate net power densities used by previous workers are given in table 6.2. Values taken from the experiments described in Chapter 8 are included, the power density figures refer to the average values from the start of the process to the point where the maximum temperature is reached. In the case of the experimental data obtained for this Report the conversion efficiency from mains to load was actually estimated during the drying runs.

Taking the values in Table 6.2, the following maximum rates of energy dissipation per unit volume of material appear to be appropriate

350 kW/m^3 for coffee and soya
270 kW/m^3 for maize
240 kW/m^3 for wheat
1,000 kW/m^3 for rice.

Reference	Power Density(kW/m^3)	Mi(%w.b.)	Product	Damage	Pressure (torr)
Hamid et al 1969	185	20	Wheat	No	Atmos.
Wear 1977	280	25	Maize	Yes	25-50
Wear 1977	2,300		Rice	No	25-50
Wratten 1950	2,300	18	Rice	No	Atmos.
Fanslow & Saul 1971	1,000	18-23	Maize	Yes	Atmos.
Fanslow & Saul 1971	270	18-23	Maize	Yes	Atmos.
Butler & Gardner 1982	90	22	Maize	No	25-50
Butler & Gardner 1982	40	18	Rice	No	25-50
Experiments; (Chapter 8, 1987)					
	350	19-33	Rice	No	Atmos.
	300	25-36	Maize	Yes	Atmos.
	270	35-40	Wheat	Yes	Atmos.
	380	44-62	Soya	Yes	Atmos.
	390	44-65	Coffee	Yes	Atmos.

Table 6.2 Dielectric power densities for drying crops.

The drying energy requirements are given by eqs (6.7) and (6.8). If it is assumed that each m^3 of dry product must not experience more than a specified energy dissipation then the minimum drying time can be defined as the ratio between the energy values from these equations and the maximum power levels quoted. The maximum flow or product throughput is then the ratio of the volume to the minimum time required for drying, i.e.

$$\tau = V/[\text{eqs}(6.7) \text{ or } (6.8)/Qd_{max}] \qquad (6.9)$$

It is clear from the above expression that the lower energy requirements, i.e. those from eqs (6.8), give a higher limit for the maximum throughput. The ratio between the energy terms given in eqs (6.7) and those of eqs (6.8) is affected by the initial moisture content, this ratio varies between 1.1 and 1.6 over the following M_i ranges:

36 - 18 % w.b. for maize, rice, wheat and soya
and 50 - 30 % w.b. for coffee.

Thus if eq (6.8) is used to estimate the maximum throughput of a agricultural dielectric drying plant the values for the throughput may range from, say, 1.1 (at a high M_i) to approximately 1.6 (at a low M_i) times the values computed using eq (6.7). Substituting eqs (6.7) in eq (6.9), we have

for coffee :	$350/(429M_i-43)$	m^3/h	(6.10a)
soya :	$350/(461M_i-40)$	m^3/h	(6.10b)
maize :	$270/(540M_i-48)$	m^3/h	(6.10c)
rice :	$1,000/(539M_i-53)$	m^3/h	(6.10d)
wheat :	$240/(573M_i-55)$	m^3/h	(6.10e)

which leads to the values given in table 6.3.

Product	Maximum Throughput (m^3/h)				
(w.b.)	Mi=60%	Mi=50%	Mi=40%	Mi=30%	Mi=20%
Wheat			0.7	1.2	2.3
Maize				1.5	3.1
Rice				5.6	12.3
Coffee	0.6	0.9	1.4	2.5	5.3
Soya				2.3	4.8

Table 6.3 Maximum throughputs limited by power density (qualitative considerations) (drying zone volume 1 m^3).

The corresponding minimum drying times are given in table 6.4.

Since the drying periods refer to any amount of material these values are independent of the dimensions. The values in parentheses refer to the experimental results at 38.5 MHz (Chapter 8). The good agreement of the idealized figures with the real, i.e. experimental results must not be taken as an indication that in practice the drying times will always approach the idealized figures. The latter assume a free evaporation surface where it is only necessary to supply the required sensible and latent heat components. It has been shown above (Chapter 2) that in reality the situation involves a complex mass and heat transfer mechanism which induces moisture migration from the interior to the surface of the product. This is evident when, for example, the drying times of the cereal products are compared with those for soya or coffee. If drying were simply an evaporation process with no internal hindrances then from table 6.4 one would conclude that soya and coffee dry faster than rice and maize if the same electric field strength were used (the figures given in tables 6.3 and 6.4 for maize and soya correspond to 26 kV/m, peak). However in practice soya and coffee are much slower drying materials (see Chapter 8), this may be due to the fact that these are oil bearing products and the internal moisture finds it more difficult to diffuse through the particles.

Product	Minimum Drying Times (min)		
	M_i=50% w.b.	M_i=30% w.b.	M_i=20% w.b.
Wheat		50	21
Maize		40 (41*)	19
Rice		11 (9**)	5 (5***)
Coffee		24	11
Soya		26	13

Table 6.4 Minimum drying times governed by power density limitation due to quality considerations. Experimental results (Chapter 8): * drying from 27.4 to 12.6 % w.b. at 26 kV/m; ** drying from 32.9 to 11 % w.b. at 31 kV/m; *** drying from 19 to 10.7% w.b. at 31 kV/m.

The limitation imposed by qualitative considerations is dependent on the intended usage of each product.

6.4 Dimensional Considerations and Field Distribution

The total throughput of the system depends on the dimensions, i.e. cross sectional surface area and the speed at which the product passes through it. If the dimensions of the drying zone are limited by the space available, and the cross section is too small, the velocity may be unacceptably high and this, associated with a given minimum drying time may result in the drying zone being too long. Recirculation of the product will help but only at the cost of reducing the throughput for a given power input. Other considerations which need to be taken into account include drying uniformity which is of the utmost importance. Refering to eqs (2.7) and (2.33) it can be concluded that, in so far as dielectric heating is concerned, the same internal heating effect must be experienced by all particles if they are to have similar drying characteristics. Hence the design must be such that each particle experiences a similar field distribution. In addition to this, the concept of power penetration depth, or simply penetration depth, implies that, with a homogeneous substance, 63 % of the energy is dissipated within this depth. Therefore, for uniformity, the thickness of the material should be no greater, and ideally much less, than this value. Otherwise the only mechanism likely to ensure uniformity is conductive heat transfer. Dryden [44] has defined the penetration depth as:

$$d = 3.4E7/\{f[e'((1+(e''/e')^2)^{1/2}-1)]^{1/2}\} \text{ metres} \qquad (6.11)$$

where f is the frequency of the applied field. This expression is based on an incident planar wave and the equations for the field penetration depth given by Von Hippel [165]. The power dissipated is proportional to the square of the field strength, thus the attenuation factor of the power is twice that of the field. This concept is applicable for microwave fields since in the radiofrequency band the electric field is contained between two electrodes and the phenomena involved is similar to a circulating electrical current in the electrode system. Using the above equation it is possible to estimate the permissible thickness of the layers of product, the depth at which x % of the surface power is attenuated:

$$l = - d \ln (x/100) \quad \text{metres} \qquad (6.12)$$

where, for a given frequency of the applied field, d and therefore l, are dependent on the moisture content.

6.5 Electrical Breakdown

Electrical discharges developed across a gas may have useful applications, however here we are concerned with the adverse effects of such phenomena and the need to keep field strengths down to a value low enough to prevent them from occurring. This limitation has significant implications in so far as the power developed in the load is concerned. Damage to the product, and also to the equipment, may ensue and discharges of any type must be avoided. The breakdown field strength of clean, dry air under reasonable uniform field conditions and at atmospheric pressure and low frequency is approximately 3,000 kV/m. The value is affected by pressure but here we are usually concerned with pressures that are near atmospheric, it is also affected by frequency. However the most significant effect as far as dielectric drying is concerned is likely to be that caused by non-homogeinities, i.e. dust and moisture droplets in the environment and applicator and low electrical resistance pathts occuring for one reason or another in the bulk of the material. It will be noted from the experiments (Chapter 8) that breakdowns in the surrounding environment are likely to occur if the field strength in the surrounding air exceeds 200 KV/m (peak). This, therefore, is the maximum value adopted here. The corresponding rms value is approximately 141 kV/m, this is less than a tenth of the idealised figure quoted above. The approach used here was to estimate the field strength in the product for a particular value of power dissipation using eq (6.4). This internal field strength was then related to the "external field", i.e. that in the surrounding medium which is where the breakdown is likely to occur. The internal and external fields in and around an isolated sphere, cylinder or slab are related by the expressions [14, 18, 151]:

$$E_{air} = E(e'+2)/3 \quad \text{(sphere)} \tag{6.13a}$$

$$E_{air} = E(e'+1)/2 \quad \text{(cylinder)} \tag{6.13b}$$

$$E_{air} = Ee' \quad \text{(slab)} \tag{6.13c}$$

In the above relationships the value of e" has been assumed to be much lower than that of e′ as it invariably is in practice. Using the models developed for e′ and e" in Chapter 8, it can be shown that even in the worst case conditions, i.e. when the ratio e"/e′ is at its maximum value, this approximation will only cause an error of 5 % which is much smaller than that involved in measuring the dielectric constant and very much less than that caused by using the idealised relationships of eqs (6.13) in terms of a definite breakdown level.

Thus it is possible to express the maximum allowable applied electric field in terms of the power employed, the frequency, the volume of product in the drying zone and the dielectric properties of the material. Substituting eq (6.4) in eqs (6.13),

$$E_{air} = [Qd/(0.556E\text{-}10fe''v)]^{1/2}(e'+2)/3 \quad \text{(sphere)} \qquad (6.14a)$$

$$E_{air} = [Qd/(0.556E\text{-}10fe''v)]^{1/2}(e'+1)/2 \quad \text{(cylinder)} \qquad (6.14b)$$

$$E_{air} = [Qd/(0.556E\text{-}10fe''v)]^{1/2}e' \quad \text{(slab)} \qquad (6.14c)$$

6.6 Filling Factor

The filling factor is defined as the ratio of the volume of material to the volume of the applicator. The density of the material may be expressed in either of two ways, the bulk density is the weight of the material filling a container divided by the volume of that container. The alternative is to consider the specific density, i.e. the ratio between the weight and the volume of a single particle, in this case the voids between particles are not taken into account and therefore the shape of the particle becomes important. Assuming that the particle is spherical and of radius "a" then the maximum filling factor in an applicator whose shape is a rectangular cuboid is the ratio between a sphere of volume $4/3\pi a^3$ and a cube of volume $(2a)^3$, i.e. $\pi/6$ (assuming that "a" is small compared with the dimensions of the applicator). This implies that even with applicators involving other shapes the error is negligible since a large applicator can be taken to be the sum of very many small cubes. Thus the maximum filling factor in bulk terms is 1.0 whilst, using specific density it is $\pi/6$. Bulk density is used throughout most of this report, since the dielectric and other properties of the material were obtained from tests on bulk samples rather than individual particles. Hence the filling factor can vary between 0 and 1. For the purposes of this analysis the cases of a full (FF=1.0) and a partly full (e.g. particles moving in a rotating enclosure) (FF= 0.6) have been considered.

6.7 Frequencies Used

Specific frequency bands are allocated for use in industrial dielectric heating equipment, this is done in order to avoid interference with communications and similar apparatus. The frequencies concerned are not related to the dielectric properties of the particular material and therefore there is no guarantee that optimum frequencies can be chosen for a particular application. In the past the frequency bands available have been centred on 6.78, 13.56, 27.12, 40.68, 434, 915 and 2,450 MHz although the values 6.78, 40.68 and 434 MHz have not normally been used since they are subject to local agreements, more recently the 915 MHz band has also been placed in this category. In what follows several alternative systems are analysed in terms of the most appropriate frequency bands although it is recognised that the majority of the commercial high frequency heating units manufactured today are operated at either 27.12 (radiofrequency) or 2,450 (microwave) MHz. However since the application involved here represents a potential new market it has been considered important to assess the feasibilty of all promising alternatives.

Both microwave and RF heating are based on the same electromagnetic field phenomena and the effects are described by the same parameters, i.e. dielectric constant and loss factor. The main differences between them are the types of frequency converter and the design of the applicator. The RF frequency converter is usually a valve oscillator whilst for microwave heating it is normally a magnetron. The operation of the latter is well described in a comprehensive paper by Stuchly & Stuchly [155]. At RF frequencies the field can be contained within an open electrode system and can therefore be described as a static field [14] whereas at microwave frequencies the field propagates through space and must be contained within a metallic enclosure if it is to be useful in the heating context. The two, RF and microwave, are considered below.

6.8 Microwave Applicators

6.8.1 Introduction

When the microwave electromagnetic field is established within an empty applicator the spatial distribution of the electric and magnetic components will be determined by the frequency of the field and the geometry of the applicator. If the latter is partially or entirely filled with a dielectric material then this will also affect the field distribution. The power dissipated within the applicator is given by the integration of eq (6.1) and this will demand a certain amount of energy to be delivered from the source. Perfect matching of the source-applicator-load combination implies that all the energy from the source passes into the load and a 100 % heating efficiency is obtained. This is not possible to achieve in practice since part of the incident radiation is reflected depending on the dielectric properties of the material. Thus not only is 100 % efficiency likely to prove impossible but also some means must be found of disposing of the surplus reflected energy which otherwise may damage the source or be transmitted to the environment.

The field patterns within the applicator are complex and also dynamic in nature. However they are not random since they must satisfy the Maxwell equations at all points in space and time. Assuming a sinusoidal excitation of the field then the wave pattern can in general be expressed as the sum of an infinite number of single frequency waves or "modes". This large number however is limited by the ability of the source to produce such a range, by the ability of the coupling system and applicator to transfer them into the load and by the capacity of the load to absorb them. For any two sets of source-applicator combinations having slightly different parameters there will be different field distributions in each.

6.8.2 Waveguide Applicators

These are normally based on a single mode corresponding to one of the solutions of the Maxwell equations. For a given combination there is, however, a fundamental frequency, the cut-off frequency, below which no modes at all can propagate. The modes are classified as follows (where the magnetic and electric fields in each of the coordinates directions are denoted by H_x, H_y, H_z and E_x, E_y, E_z respectively), propagation being in the z-direction:

i) TE modes where $E_z=0$ and E_x, E_y, H_x, H_y and H_z are not necessarily so. The components of the electric field all lie on a direction normal to that of propagation, i.e. the axis of the waveguide. These are transverse electric modes.

ii) TM modes where $H_z=0$ and H_x, H_y, E_x, E_y and E_z are not necessarily so. The components of the magnetic field all lie on a direction normal to that of propagation, i.e. the axis of the waveguide. These are transverse magnetic modes.

iii) TEM modes where $E_z = H_z = 0$ and E_x, E_y, H_x and H_y are not necessarily so. These are transverse electromagnetic modes and do not exist in rectangular waveguides but they can be present in coaxial waveguides.

6.8.2.1 <u>TE_{mn} Rectangular Waveguide Fields</u>

The fields in a rectangular waveguide operating in the TE mode are shown in figure 6.1.

The cut-off constant is given by [8]:

$$k_c = m^2\pi^2/a^2 + n^2\pi^2/b^2 \qquad (6.15a)$$

where m and n are integers, a and b are the dimensions of the broad (x direction) and narrow (y direction) sides of the waveguide respectively.

The phase constant is given by (ibid):

$$\beta = (\mu e w^2 - k_c^2)^{1/2} \qquad (6.15b)$$

and is positive for a forward travelling wave, e is the permittivity of the medium in absolute terms (which can be approximated to $e = e'e_o$ if the dielectric materials of interest are filling the waveguide), w is the fundamental angular frequency of the field and μ is the permeability of the medium (equal to that of vacuum for air and non-magnetic materials). The limiting condition for propagation occurs when $\beta^2 = 0$ [9] hence the cut-off frequency is found from:

$$w_c = k_c/(\mu e)^{1/2} \qquad (6.15c)$$

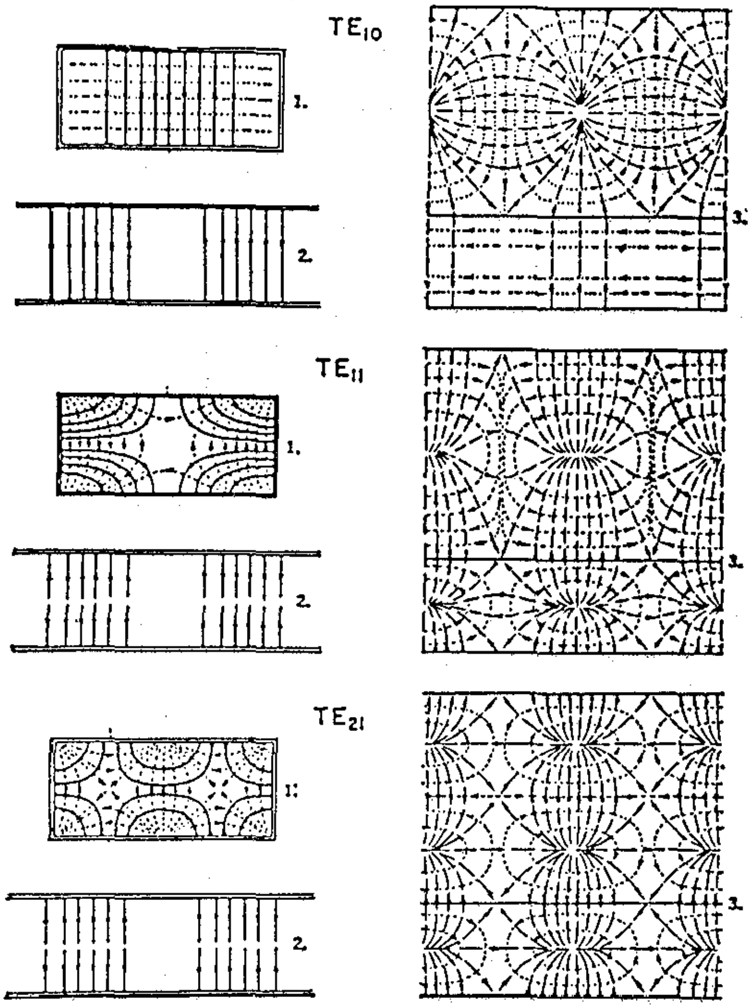

<u>Figure 6.1</u>
Field pattern within TE_{mn} rectangular waveguides[9].

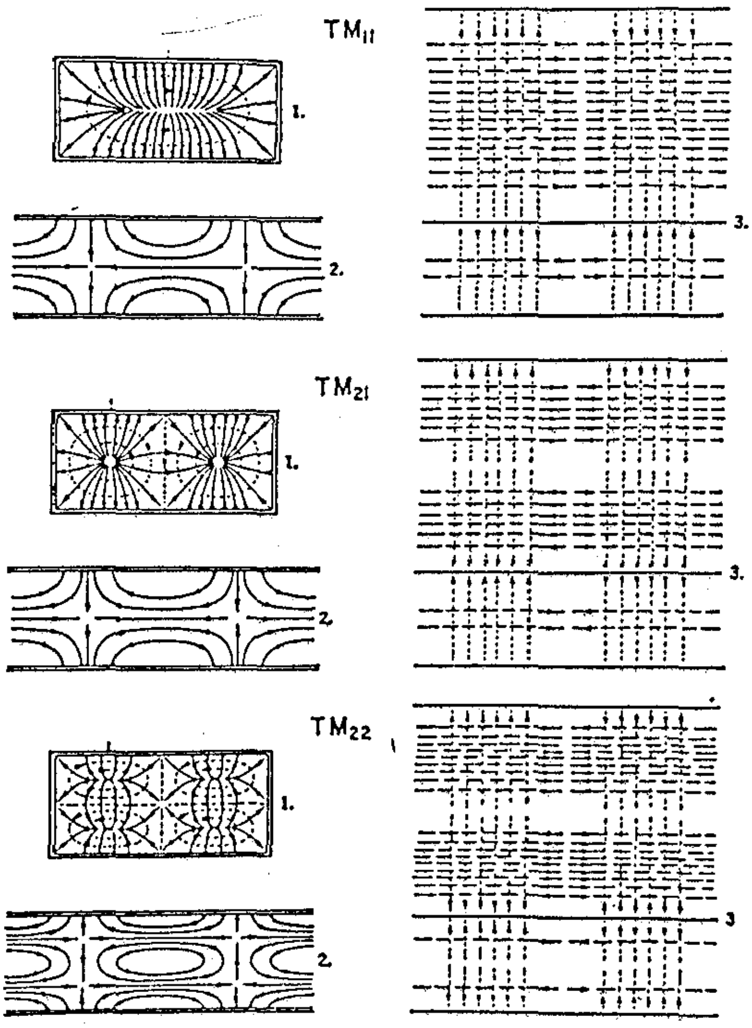

<u>Figure 6.2</u>
Field pattern within TM_{mn} rectangular waveguides[9].

Equations (6.15 a and c) indicate that the lowest cut-off frequency occurs when $n = 0$, $m = 1$, i.e. the TE_{10} mode. This mode implies that the E_x, H_y and E_z components are zero with the electric field having a maximum at $x = a/2$, hence the load should be placed at this point if the maximum power dissipation is to be achieved. The presence of a long load inside the waveguide gives rise to an attenuation of the wave in the direction of propagation.

6.8.2.2 <u>TM_{mn} Rectangular Waveguide Fields</u>

TM_{mn} fields have the form shown in figure 6.2. Equations (6.15) are also valid for TM_{mn} modes. In figures 6.1 and 6.2 the electric field (continuous) lines are shown, the intensity of this field is indicated by the closeness with which these lines are packed together.

6.8.2.3 <u>Circular Waveguides</u>

Waveguides can also be circular in shape and a large number of TE, TM and TEM modes can be supported in such a geometry.

The possibilities include circular pipes, coaxial lines and elliptical waveguides. The field patterns are again described by mathematical expressions obtained from the solution to Maxwell's equations with appropriate boundary conditions.

The field patterns for TE_{mn} and TM_{mn} modes in circular waveguides are as shown in figures 6.3 and 6.4. From figures 6.1-6.4 it will be noted that the higher the mode of oscillation the more high-field regions are produced. These excessively high field regions may be useful in certain applications in which, for example, filamentary loads are required to be heated but are likely to be less succesful in the present context which is concerned with producing a uniform field intensity over as large a volume as possible. There is the obvious possibility of passing the product down several low-loss tubes each centred on one of the high field regions but this would add extra costs and require more space to obtain a significant throughput. It would also present considerable problems in moisture extraction since the tubes would need to be perforated.

6.8.2.4 <u>TE_{10} Rectangular Waveguide Conveyor</u>

Metaxas and Meredith [110] recommend a travelling

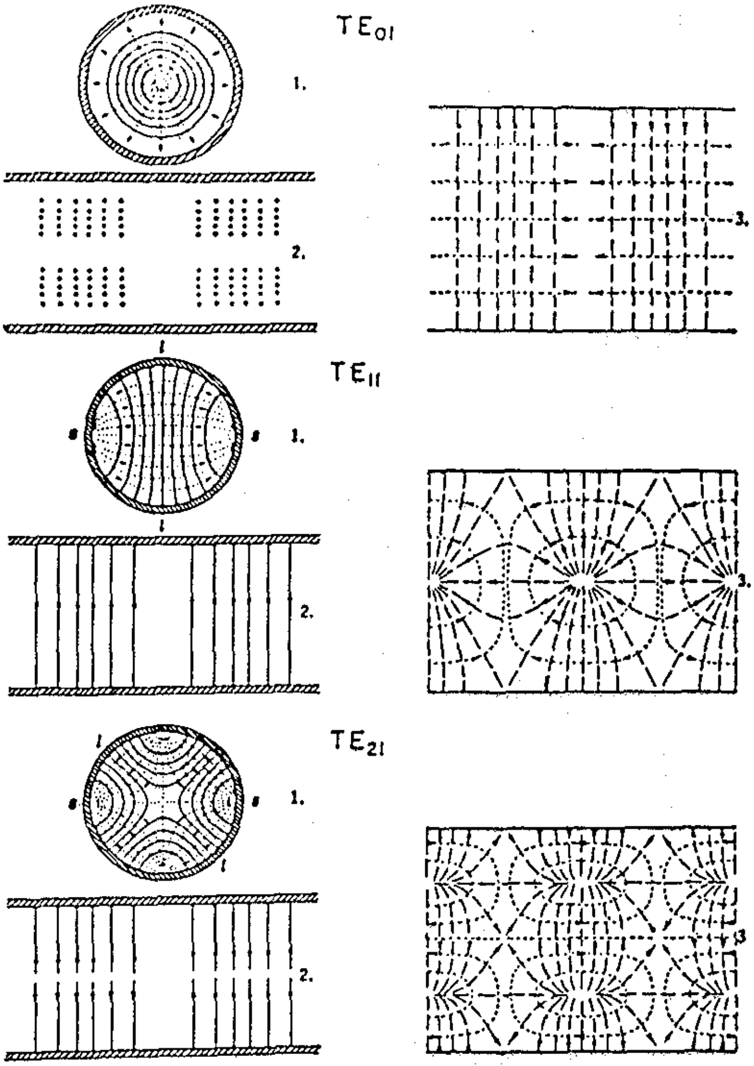

<u>Figure 6.3</u>
Field pattern within TE_{mn} circular waveguides[9].

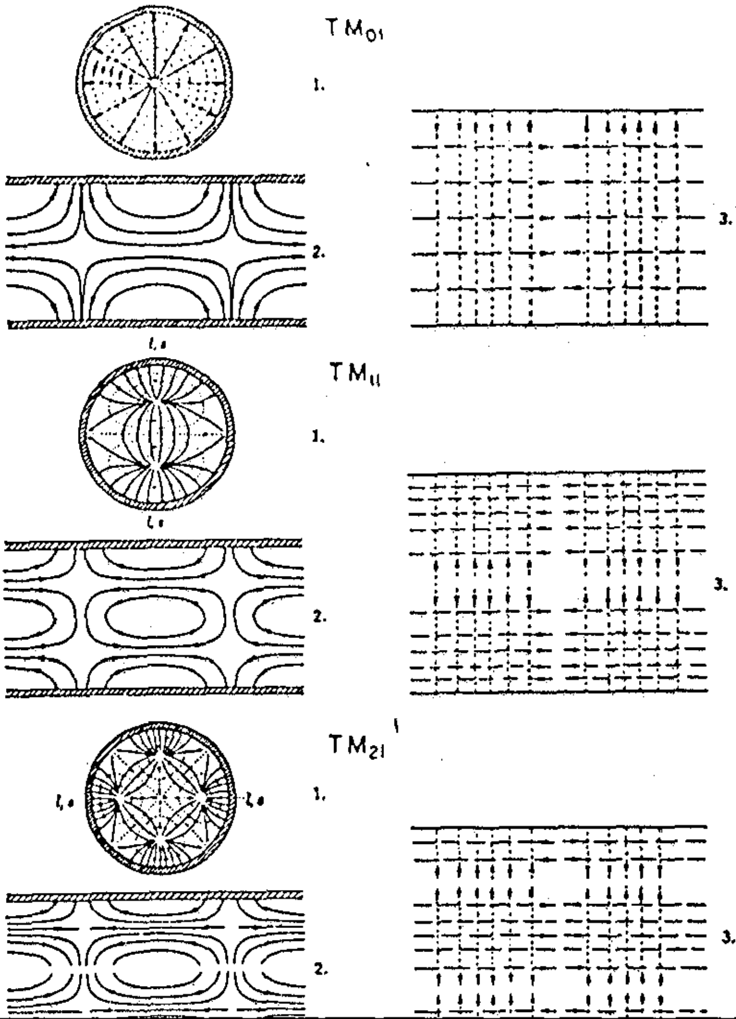

<u>Figure 6.4</u>
Field pattern within TM_{mn} circular waveguides[9].

waveguide applicator for heating laminar loads (e.g. paper), which can be used with a conveyor belt, the latter running in a plane parallel to the shorter walls at $x = a/2$ (i.e. in the region of maximum electric field strength), as shown in figure 6.5. The energy is fed from the magnetron at one end of the waveguide and the surplus passed to a dissipative load at the other. This arrangement allows for ventilation and, if a perforated belt is used, an effective through air flow in the granulated material can be achieved. Starting with the selection of the "b" dimension (see figure) it is possible to use the reference which indicates that the width of the conveyor must not exceed 3/8 of the free space wavelength if the TE_{10} mode is to be maintained as the dominant field component in the waveguide. Thus the greatest width possible (equivalent to b), i.e. at the lowest available microwave frequency of 434 MHz, is 26 cm. In order to select the "a" dimension the following relationship [135] can be used:

$$1.2a < \lambda_o < 1.8a$$

Where λ_o is the free space wavelength (= 3E8/f) in metres, which means that the TE_{10} mode only is propagated. If using the above relationship a is made equal to 0.4 metres the bulk of the material would be at x = 20 cm. Referring to

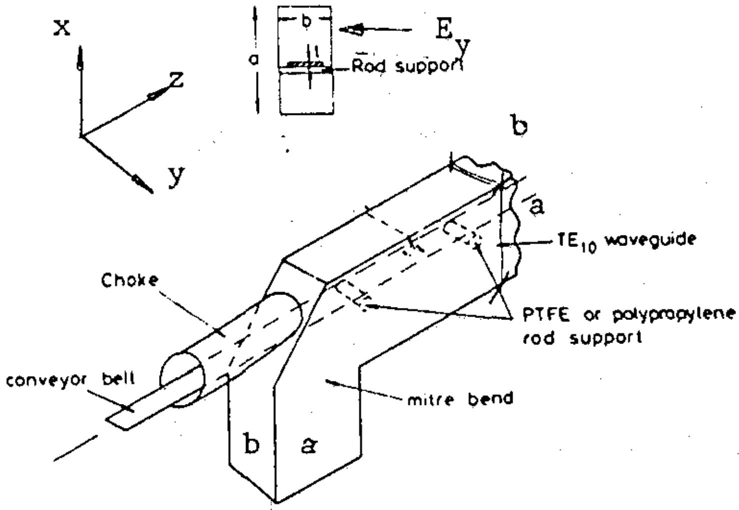

Figure 6.5 TE_{10} Rectangular Waveguide Conveyor [110].

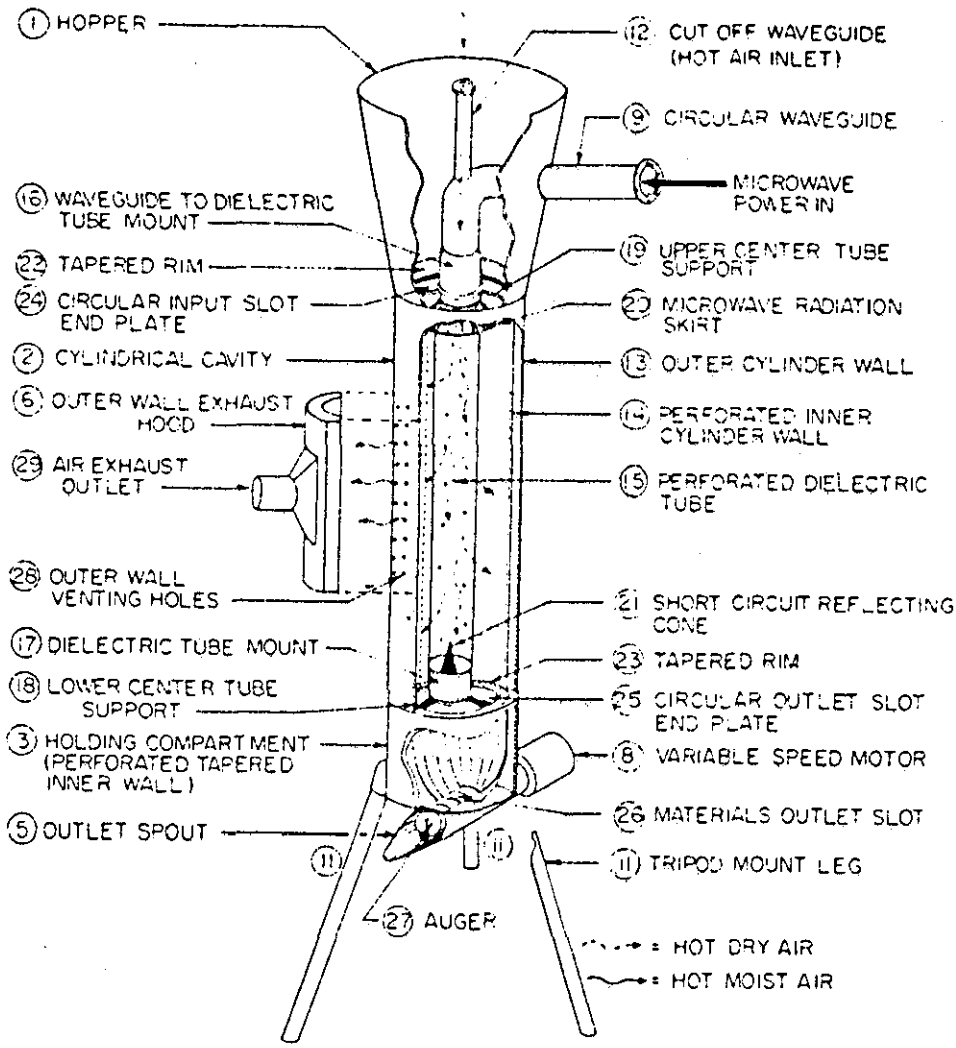

Figure 6.6 Circular Waveguide with Coaxial Dielectrics[69].

figures 6.1 and 6.5 and considering now the penetration of energy in the y direction, eq (6.12) can be used to estimate the permissible thickness for a 90% energy penetration in wheat and maize.

Product	d (metres)		x	l (metres)	
	M=12% w.b.	M=24% w.b.	%	M=12% w.b.	M=24% w.b.
Wheat	0.55	0.43	90	0.06	0.05
Maize	0.45	0.34	90	0.05	0.04

Table 6.5 Penetration depth (d) and depth of product at which x % of the dielectric power is absorbed (l)(f=450 MHz).

Table 6.5 and figure 6.1 indicates that the electric field changes direction along the axis of the waveguide, thus the width of the load on the conveyor belt can be made 21 (approximately 9 cm). The maximum depth of the layer of material on the conveyor is determined by the variation of the E_y component along the x, i.e. b direction. E_y is given by [8]:

$$E_y = j(-w\, m\pi/ak_c^2)H_1\sin(m\pi x/a)\cos(n\pi y/b)e^{-j\beta z} \qquad (6.16)$$

If the load has a thickness of 6 cm it is found from eq (6.16) that the field intensity varies between Emax and 0.864 Emax across the thickness. When the latter field variation is squared to give power figures it can be estimated that in a 6 cm thick bed of product the energy dissipation will not vary in more than 10 %. Hence the cross-section of the layer is 9x6=54 cm^2. The electric field is also attenuated along the length of the waveguide (z-direction). The attenuation constant is given by Marcuwitz [103]:

$$\alpha_a = (\pi \lambda_g e'')/\lambda_o^2 \quad \text{nepers/metre} \qquad (6.17a)$$

where 1 neper = 8.68 dB. Marcuwitz presents a method of calculating λ_g, the waveguide wavelength, for the configuration of interest, i.e. a waveguide containing a dielectric slab. The result is that λ_g is close to 1 m which, when substituted in the above relationship for α_a together with the regressions for e''_{wheat} and e''_{maize} derived from data presented by Nelson [122, 125] Nelson and Stetson [127] and taking the attenuation in dB per unit length give the results shown in table 6.6. The efficiency values do not include wall dissipation, the power transfer ratio Pi/Po per unit length is calculated using [110]

$$\alpha_a = 10 \log_{10} (Pi/Po) \tag{6.17b}$$

where Pi is the input power to the waveguide and Po is the power available per unit length.

Product (% w.b.)	α_a (dB/10 cm) M=12%	α_a (dB/10 cm) M=24%	Po/Pi per 10 cm M=12%	Po/Pi per 10 cm M=24%	Waveguide Efficiency (in 50 cm) M=12%	Waveguide Efficiency (in 50 cm) M=24% w.b.
Wheat	1.87	2.99	0.65	0.50	88.4	96.8
Maize	2.23	3.60	0.60	0.44	92.2	98.4

Table 6.6 Attenuation, power transfer and efficiency for the TE_{10} rectangular waveguide conveyor operating at 434 MHz.

The limits on throughput imposed by the need to stay within the electric field strength limits are shown in table 6.7. The internal electric field is calculated over the first 0.1 metre of the waveguide length (i.e. where approximately 50% of the waveguide power is dissipated), the maximum power which can be dissipated in the first 10 cm of the waveguide before breakdown occurs is obtained from eq (6.14c) taking the volume occupied by the material as 0.06x0.09x0.1 m^3 and an external field of 141 kV/m at 434 MHz. The actual maximum power per 0.5 metre of the waveguide is twice the value in the first 0.1 metre, very little energy being available at lengths greater than 0.5 m as noted from the efficiency figures in table 6.6. The maximum throughput is calculated using the allowable value of Qd_{max} and eqs (6.7) and (6.9). The applicator would not appear to be capable of processing the required amount of product.

Product	Qd_{max} (kW)				Maximum Throughput (m^3/h)		
(%w.b.)	M=12%	M=16%	M=20%	M=24%	M_1=16%	M_1=20%	M_1=24%
Wheat	19	19	17	15	0.4	0.2	0.1
Maize	24	21	19	18	0.4	0.2	0.2

Table 6.7 Maximum throughputs for the TE_{10} rectangular waveguide conveyor limited by breakdown considerations and operating at 434 MHz.

6.8.2.5 Circular Waveguide Applicators

In this construction the TE_{11} mode is dominant [103] and, as shown in figure 6.3, the electric field is highest, and relatively uniform, near the central axis. There is, however, an angular as well as a radial variation and also a z-variation, i.e. along the direction of propagation. If an appreciable quantity of product is to be processed under uniform conditions, it would be necessary to move the product relative to the cross-sectional components of the field, possibly by using an agitator manufactured from low loss material, the whole works being contained in an internal tube mounted along the axis. The internal tube could be perforated as to allow air to be blown through to assist in moisture evaporation from the surface of the product. The final construction would be very similar to the system shown in figure 5.1, and thus part of the screw conveyor of a cross-flow dryer could be substituted by such an applicator.

Hamid et al [69] proposed a sterilizer which might also be used to dry granular materials (fig 6.6). The product is fed from a hopper into the annular space between a double walled circular waveguide and an inner low loss perforated tube as shown in the figure. Both microwave energy and air are fed in through the inner tube and the air is extracted through perforations in the waveguide. The exhaust air is passed through a heat exchanger and used to pre-heat the drying air to improve the efficiency. The authors do not comment on heating uniformity and it may be that a screw conveyor such as that of figure 5.1 would be needed in order to obtain acceptable results. The external radius of the inner dielectric cylinder in the equipment proposed was 3.55 cm and that of the waveguide was 8.89 cm.

Figure 6.3 (TE_{11} dominant mode) and eq (6.1) show that the Poynting vector is always directed to the axis of the waveguide, therefore the penetration depth of the radiation is critical along the length. The values of penetration depth and load thickness (i.e. that in which 90% of the power is dissipated) are given in table 6.8 for a frequency of 2,500 MHz.

Product	d (metres)		l (metres)	
	M=12 % w.b.	M=24 % w.b.	M=12 % w.b.	M=24 % w.b.
Wheat	0.12	0.06	0.01	0.01
Maize	0.12	0.09	0.01	0.01

Table 6.3 Penetration depth (d) and depth of product at which 90% of the dielectric power is absorbed (l)(f=2,500 MHz).

The attenuation constant can be obtained by using the information given by Marcuwitz [103] for a circular waveguide with dielectric filling although the relative dimensions of the cylinders in this case are in the ratio 2:1. If the applicator dimensions are approximated to 10 cm and 5 cm the values shown in table 6.9 are obtained. These values are affected by the dielectric properties, the cylinder dimensions and the frequency.

Product	Waveguide Wavelenght (m)		α_m (dB/10 cm)		Po/Pi(10 cm)		Efficiency (per 0.3 m)	
(M, %w.b.)	12%	24%	12%	24%	12%	24%	12%	24%
Wheat	0.08	0.07	3.64	8.52	0.43	0.14	92.0	99.7
Maize	0.08	0.07	3.64	6.37	0.43	0.23	92.0	98.8

Table 6.9 Attenuation, power transfer and efficiency for a TE_{11} dominant mode circular waveguide screw conveyor operating at 2,450 MHz.

Table 6.9 indicates that most of the power is absorbed in the first 10 cm. The limit on throughput, imposed by the possibility of electrical breakdown, are given in table 6.10. The external field is calculated for the first 10 cm of the waveguide where between 57 and 86 % of the power input is dissipated. A filling factor of FF=0.6 in the space between the concentric cylinders is assumed which gives a total volume of material over the first 10 cm as 0.00141 m^3. The maximum power is found using eq (6.14c) at 2,450 MHz

$$Qd_{max} = (e''/e'^2)\ 5{,}373\ kW$$

and the maximum throughput from eqs (6.7) and (6.9).

Assuming an effective flow cross section of 0.0141 m^2 the throughput speed required to yield 4 m^3/h would be approximately 284 m/h (4.7 m/min) which is feasible for a screw conveyor. One such dryer could be fitted on each side of the crossflow dryer, the total output would thus be doubled. It should be noted however that due to substantial attenuation of the radiation in the waveguide it would not be possible to achieve the required residence time for drying in one pass through the applicator (see table 6.4)

Product	Qd_{max} (kW)				Maximum Throughput (m^3/h)		
	M=12%	M=16%	M=20%	M=24%	M_1=16%	M_1=20%	M_1=24%
Wheat	213	254	283	203	3.9	2.4	1.7
Maize	387.77	319.64	302.63	310.47	2.9	1.7	1.2

Table 6.10 Maximum throughputs for a TE_{11} dominant mode circular waveguide screw conveyor limited by breakdown considerations and operating at 2,450 MHz.

K.C.Gupta [59] has suggested a method of increasing the field uniformity, involving the insertion of an annular cylinder made from low-loss dielectric between the waveguide walls and the lossy load as shown in figure 6.7. In this case the central tube containg the load is 9.5 cm diameter, the annular dielectric layer being 0.34 cm thick. According to Gupta this thickness is critical. The product flows through the centre of the waveguide as opposed to the arrangement due to Hamid where it passes between the cylinders. The product could, if required, be enclosed in a second low loss tube so avoiding contact between it and the dielectric insertion. The outer dielectric layer is likely to be a good thermal insulator but it must have a high dielectric constant as compared with that of the product,

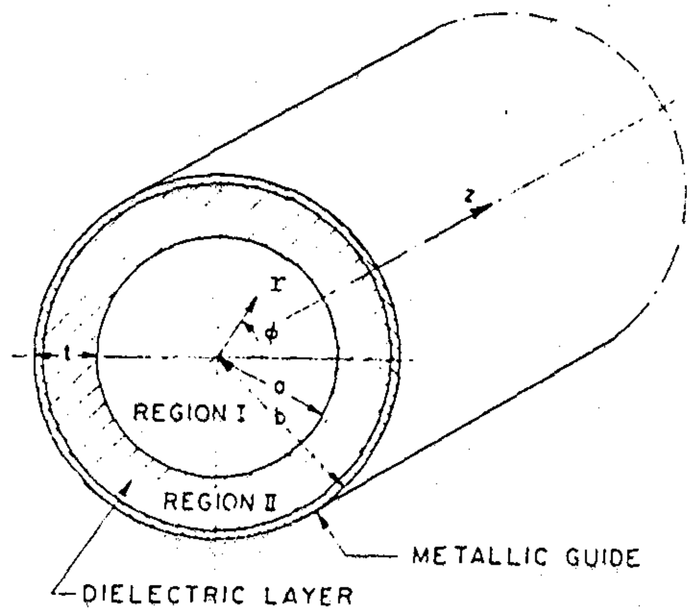

<u>Figure 6.7</u> Circular Waveguide with Coaxial Dielectrics[59].

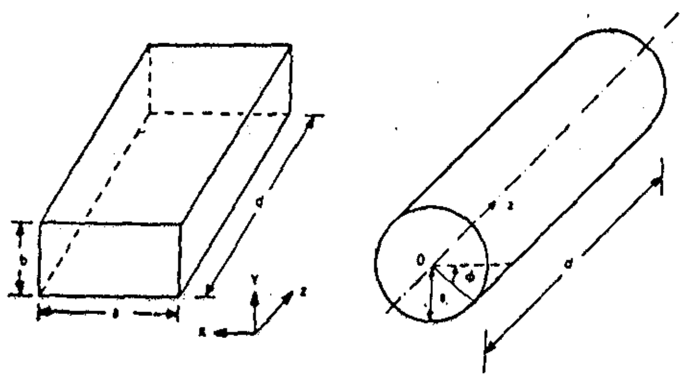

<u>Figure 6.8</u> Dimensions of Rectangular and Circular Multimode Resonators[60].

very little power would be dissipated within it and the efficiency will be high. Gupta has produced two estimates for the power distribution in the equipment which is designed to operate at 2,450 MHz. The first involves air as the load, i.e. the waveguide is empty apart from the low loss internal layer made from polystyrene with $e' = 2.5$. In the second case the guide contained frozen beef (e'=4) with an alumina (e'=9) dielectric layer. In the first case the power variation along the inner dielectric radius, i.e. the load, was 2 % as compared with 9 % in the second. The attenuation in the waveguide can be estimated from data available in Marcuwitz and is shown in table 6.11 together with the waveguide efficiency neglecting wall losses. It has been assumed that, in general, the ratio of the dielectric constant of the annular layer to that of the agricultural products is 2.5. Hence, using the corresponding e' models it is found that the dielectric constant of the required annular cylinder is approximately 8.0. The actual values in tables 6.11 and 6.12 are not quoted because Marcuwitz does not provide data when the ratio between the radii of these cylinders is so small, i.e. when a thin insulating layer is used. Nevertheless the trends indicate that the true values will be either smaller (<) or larger (>) than those shown.

Product (% w.b.)	Waveguide Wavelength(m) M=12%	M=24%	α_a (dB/10 cm) M=12%	M=24%	Po/Pi(10 cm) M=12%	M=24%	Waveguide Efficiency (per 0.3 m) M=12%	M=24%
Wheat	>0.05	>0.06	>2.28	>10.92	<0.59	<0.08	>79.5	>99.9
Maize	>0.04	>0.06	>1.82	> 5.46	<0.66	<0.28	>71.3	>97.8

Table 6.11 Attenuation, power transfer and efficiency for a TE_{11} dominant mode circular waveguide pipe operating at 2,450 MHz.

Gupta's estimates of the power uniformity suggest that an internal agitator would not be required to moving the product in the applicator. The throughput limitation imposed by breakdown considerations is shown in table 6.12, a filling factor of FF = 1.0 has been assumed implying that a 10 cm length (where more than one third of the power input is dissipated) includes a volume of 0.00069 m^3. Using eq (6.14c) the maximum allowable power limit in the waveguide is

$$Qd_{max} < (e''/e'^2)\ 2{,}984\ kW$$

Product	Qdmax (kW)				Maximum throughput (m^3/h)		
(%w.b.)	M=12%	M=16%	M=20%	M=24%	M_1=16%	M_1=20%	M_1=24%
Wheat	<118	<141	<157	<168	<2.2	<1.3	<0.9
Maize	<108	< 89	< 84	< 86	<1.6	<1.0	<0.7

Table 6.12 Maximum throughputs for a TE_{11} dominant mode circular waveguide pipe limited by breakdown considerations and operating at 2,450 MHz.

This type of applicator could be arranged vertically, i.e. attached to the side of the vertical dryer, and operated in conjunction with the bulk elevator. Again, the required residence time of the particle in the applicator implies that a multipass arrangement would be needed to give the necessary drying rate.

6.8.3 Resonant Applicators

6.8.3.1 Introduction

The main difference between resonant applicators and waveguide systems is the "static" as opposed to the propagating, electromagnetic field pattern in the former which is produced by multiple reflections at the cavity walls. The field distribution within the resonant applicator is difficult to predict, however if the characteristics of the load do not change during the heating cycle, the field pattern is constant in time unlike the waveguide systems where the field propagates. The field within the resonant cavity is highly non-uniform, the non-uniformity being more pronounced when the cavity is such that few oscillatory modes are sustained. A more uniform distribution is obtained when several modes are present since the field patterns due to each combine. Single mode cavities can be used to produce high heating rates in the load provided that the shape of the latter is such that it can be placed within the high field region. If uniform heating is required in a multimode cavity, then the load in the cavity must be moved relative to the field, by using a "mode stirrer" (which is similar to a rotating fan) which presents a variable reflective surface to the waves entering the cavity, a rotating antenna or by using several sources feeding into the cavity at different points. Kashyap and Wyslouzil [81] propose several methods for improving the field distribution in multimode cavities, some of these produce reasonable good results but, in general, this type of applicator always suffers from the drawback of non-uniformity.

Maxwell's equations must be satisfied at all points within the cavity and at the boundary surfaces. The resultant field distribution is the sum of all the incident and reflected waves produced by the different oscillatory modes.

Resonant applicators can be used in either batch or continuous processes. Heat dissipation in a material composed of a large number of small particles depends on the uniformity, or otherwise, of the physical properties of the particles as well as on the field distribution. The particles can be considered identical, at least to a first approximation, but the assumption of electric field uniformity is likely to lead to error. Since the particles are small the internal field within each can be regarded as uniform since the penetration depth of the energy is large compared to the dimensions of an average particle. In a continuous process the field can vary in a direction along the direction of movement without necessarily detracting from the uniformity of drying although variations in the plane perpendicular to this direction are likely to cause problems. In batch processes the product should be moved in all directions if uniformity is to be achieved, i.e. a fluidized or tumbled system should be established in order for all particles to be exposed to similar field patterns.

The resonant frequency is a characteristic of a particular oscillatory system, ideally it does not depend on any energy absorbing components in the system, their effect is to decrease the amplitude of the resonant peaks. The "sharpness" of the resonant peak is expressed in terms of the Q factor, one definition of which is the ratio of the resonant frequency to the bandwidth corresponding to the frequencies at which the stored energy in the system is half of the total possible. An alternative definition is the ratio of the stored energy at resonance in the system to the rate of energy dissipation in the system. In the general multimode case a large number of resonant oscillations are produced each corresponding to a particular resonant frequency and Q factor. The load is the energy dissipative component in the system and its introduction into the cavity causes a decrease in the Q factors of all the modes within the cavity.

Since the Q factor is proportional to the ratio of the energy stored to the energy dissipated in the cavity, the ideal situation for achieving high energy efficiency is to design for high Q factor values when the cavity is empty and low Q values when the load is inserted. It will be noted below that the first requirement can be met by using high conductivity materials and ensuring that low resonance frequencies are not established within the cavity. The loaded Q however is largely dependent on the properties of the material which change during the process.

6.8.3.2 Multimode Resonant Applicators

These are designed to produce a large number of resonant modes around a particular mean frequency. The electric field distribution, and consequently the heating effect, is improved as the number of modes is increased. The full theoretical analysis of these systems is very complex, hence designs are largely based on empiricism. However a simplified analysis is given below which serves to illustrate the general trend. Considering a TE_{101} mode in a rectangular cavity (the last subscript indicates the number of variations of the resulting field in the z-direction, i.e. 1 in this case), Atwater [8] gives the following expression for the resonant frequency:

$$w_R = [\pi/(\mu e)^{1/2}](1/a^2 + 1/d^2)^{1/2} \qquad (6.18a)$$

The field patterns are illustrated, in figures 6.8 and 6.9. The E-field has only a component in the y-direction and is greatest

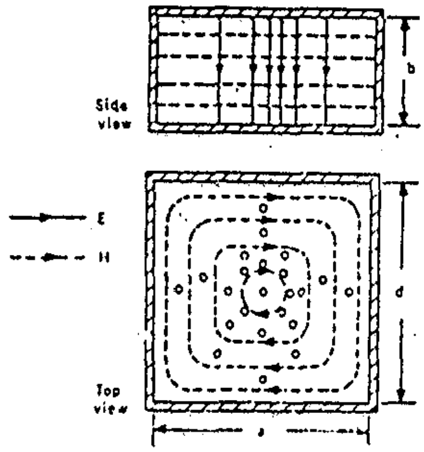

Figure 6.9

TE_{101} mode field pattern in a rectangular resonator [60].

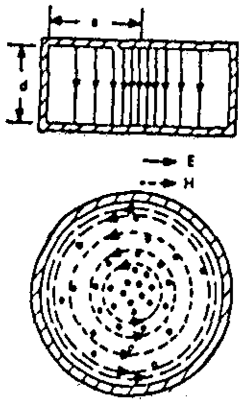

Figure 6.10

TM_{010} mode field pattern in a circular resonator [60].

at the centre of the x-z plane, the magnetic field has two components, H_x and H_z, this mode is based in the TE_{10} waveguide mode.

In general d is given by [60]:

$$d = p\lambda_g/2 \tag{6.18b}$$

Alternatively, for the TE_{101} mode, (ibid);

$$d = \lambda_R/\{2[1-(\lambda_R/2a)^2]^{1/2}\} \tag{6.18c}$$

λ_R is the resonant wavelength. In the general case for a cavity of dimensions a, b and d the resonant frequency is obtained from [8]:

$$w_{Rmnp} = [\P/(\mu e)^{1/2}](m^2/a^2 + n^2/b^2 + p^2/d^2)^{1/2} \tag{6.18d}$$

where m,n and p are integers. Thus the lowest resonant frequency is that corresponding to the TE_{101} mode but higher frequencies are desirable since these reduce the possibility of breakdown and the wall losses (so increasing the unloaded Q factor).

Circular cross-section cavities are also possible, the simplest mode is the TM_{010}, this is discussed below in the section on single mode resonators. The characteristical dimensions and field patterns are shown in figures 6.8 and 6.10, they are similar to those established in rectangular TE_{101} cavities. The resonant wavelength is [60]:

$$\lambda_R = 2.61 \ a \tag{6.19}$$

where a is the radius. The length, d, of the cavity is arbitrary to a certain extent, as will be seen in the next section.

As explained earlier, the Q factor is one of the most important parameters, a reasonable approximation [18] to this quantity (unloaded) is :

$$Q_o = \mathcal{V}/(A\,\delta_s) \tag{6.20}$$

where $\mathcal{V}$ is the volume of the empty cavity (m^3), A is the wall area (m^2) and δ_s is the skin depth (metre) of the induced currents in the walls. The latter is dependant on the properties of the wall material and on the frequency, it decreases (and the unloaded Q factor increases) as the frequency and/or the conductivity increases. The unloaded Q factor of a cavity operating in the TE_{101} mode and rectangular in shape is given by [60]:

$$Q_o = [\pi(\mu_o e_o)^{1/2} 2b(a^2+d^2)^{3/2}]/\{4R_s[ad(a^2+d^2)+2b(a^3+d^3)]\} \quad (6.21)$$

where R_s is the surface resistivity of the walls.

The unloaded Q factor of the TM_{010} mode circular cavity is [80]:

$$Q_o = (a/\delta_s)/(1+a/d) \quad (6.22)$$

Metaxas and Meredith [110] have devised a simplified expression for the Q factor of a cavity containing a spherical load. They assumed that the load occupied a significant portion of the cavity and that wall losses were negligible, the following were also assumed :

i) The microwave energy was fully absorbed by the load.

ii) The load dimensions were equal to, or greater than, the the free space wavelength within the material.

iii) The external and internal fields were uniform and related to each other by the dielectric constant of the load as expressed by eq (6.13a).

These conditions could be considered to be satisfied in the applications of interest here if a large number of small particles are being agitated in a rotary cavity or the bulk of the material is passed through a cavity fed from several sources, i.e. all the particles experience a similar heating effect provided that the penetration depth of the radiation is large enough as compared to the thickness of the product. The resultant Q (loaded) is given by

$$Q_L = (e'/e'')[1+(e'+2)^2(1-FF)/(9e'FF)] \qquad (6.23)$$

where FF is the filling factor.

Thus, in order to obtain a low loaded Q, the filling factor must approach unity. This has disadvantages however, there is for example, the problem of penetration depth which requires that only a small amount of material should be placed in the cavity if heating uniformity is to be mantained. This effect has been noted by Wear [166] when drying grain in a cylindrical cavity. It must be remembered that ventilation is necessary and hence the cavity cannot be completely full of material.

Nevertheless, as noted below, when much lower frequencies are used, i.e. in RF applications, it is possible to retain the material between two electrodes in which an unity filling factor can be obtained.

There are four multimode resonant cavity techniques which might be considered for this particular application:

i) Rotating cavity partially filled with material

ii) Multimode conveyor

iii) Pneumatic or fluidised bed systems

iv) Moving bed drying systems.

Alternatives (i) and (iii) are very similar as also are (ii) and (iv). The first two only will be considered here since it is considered that the results are equally applicable to the other two, the latter are however briefly commented on later. The rotating cavity is appropriate for batch processing whereas the multimode conveyor is essentially a continuous heating system using a perforated low-loss conveyor belt to allow ventilation. In the case of the rotating cavity an air extractor fan, to remove the moisture, could be located on the axis of the rotating cavity opposite to the microwave source and air inlet. The drying air would enter through a slot in the waveguide which feeds the power into the cavity.

Figure 6.11 shows the conveyor system. Since the power feed is at the top of the cavity and the conveyor belt is full of material there is little reflection from the bottom, i.e. the inferior walls of the cavity. The permissible depth of product, obtained from tables 6.5 and 6.8, ranges from 1 cm at 2,450 MHz to about 6 cms at 434 MHz. The allowable width of the bed of product at 2,450 MHz is very small and microwave sources are not generally available at 434 MHz which is no longer a standard frequency for power applications. The figures for the penetration depth and allowable bed depths at 1,000 MHz are presented in table 6.13 from which it is noted that a 3 cm product layer is appropriate for obtaining a high degree of heating uniformity. No problems of non-uniformity are anticipated with the rotating cavity at higher frequencies since the incident radiation reacts with each of the small particles and total penetration would be achieved.

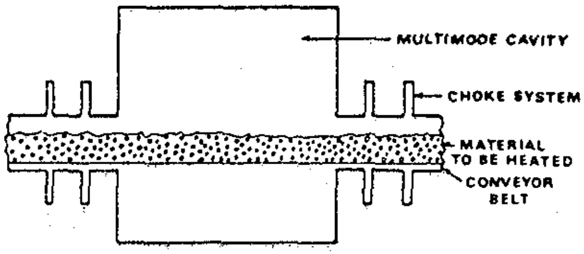

Figure 6.11 Resonant Conveyor[61].

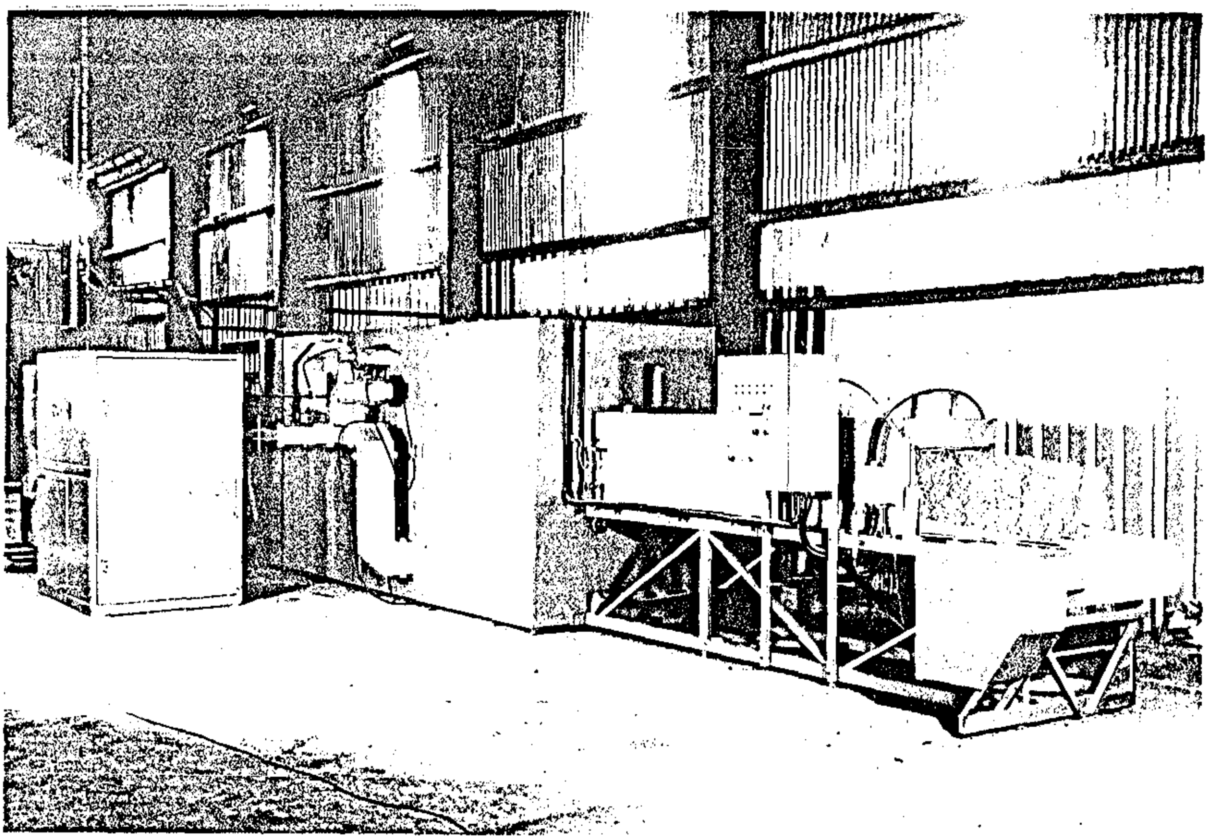

Figure 6.12 Commercial 60 kW microwave conveyor for crop processing (after Magnetronics, UK).

Product	e′		e″		d (metres)		l (metres)	
(% w.b.)	12%	24%	12%	24%	12%	24%	12%	24%
Wheat	2.75	3.75	0.27	0.50	0.23	0.18	0.02	0.02
Maize	2.77	4.17	0.22	0.35	0.35	0.29	0.04	0.03

Table 6.13 Penetration depth (d) and depth of product at which 90% of the dielectric power is absorbed (l) (f=1,000 MHz).

The cavity dimensions which give the TE_{101} mode at a frequency of 915 MHz can be determined from eq (6.18a), once one of the dimensions is established. If a=2 m then the length of the cavity calculated from eq (6.18a) is d = 0.17 m which is obviously very small for practical purposes. This dimension can only be increased by using lower frequencies and a smaller "a" dimension. Putting a = 1 m and considering f = 168 MHz for the lowest resonant frequency then d = 2 m, this value increases to d = 4 when a minimum frequency of 155 MHz is accepted, and so on. The height b, is not relevant in the case of the TE_{101} mode since there is no electromagnetic field variation in this direction although it is, of course, important if other modes are established in the cavity. In any event the height should not be too large relative to the depth of product since this reduces the filling factor and hence results in a larger Q of the loaded cavity and also greater wall losses.

From Metaxas and Meredith [110] the maximum overall efficiency (mains to load) can be estimated as:

$$\eta = \eta_g \, \eta_t (1 - Q_L/Q_o) \qquad (6.24)$$

where η_g is the efficiency of the microwave source and η_t is the transmission efficiency from the magnetron to the cavity, i.e. the connecting waveguide. It is assumed that optimum matching has been achieved. Note that η can be calculated for given values of η_g and η_t when the values for Q_o (eqs (6.21) or (6.22)) and Q_L (eq (6.23)) are substituted in eq (6.24).

Table 6.14 indicates the limitations in throughput of the multimode conveyor when operated at 915 MHz, the product volume has been taken as 1x0.03x4 m^3, the corresponding power relationship is found from eq (6.14c),

$$Qd_{max} = (e''/e'^2)\ 122E3 \quad kW$$

Product	Qd_{max} (kW) (in 4 m)				Maximum throughput (m^3/h)		
(% w.b.)	M=12%	M=16%	M=20%	M=24%	M_i=16%	M_i=20%	M_i=24%
Wheat	4,410	4,644	4,574	4,407	82	50	35
Maize	3,615	3,350	2,814	2,313	61	32	19

<u>Table 6.14</u> Maximum throughputs for a rectangular multimode conveyor limited by breakdown coniderations and operating at 915 MHz.

The results in the table assume no variation in the field intensity along the length of the dryer, this is justified if a number of sources plus mode stirrers feeding into the cavity at different points along its length are considered.

The actual dimensional constraints for an increased throughput are less dependent on the limitations imposed by the cavity than on the space available within the plant since, by varying the speed of the conveyor, large quantities of material will pass through the drying zone. Nevertheless, too fast a speed of the conveyor will require long drying sections or multipass systems. Consider for example the case in which the conveyor speed is such as to mantain the throughput at 4 m^3/h. The product would need to be passed through a cross sectional area of 1 x 0.03 m^2 which implies a speed of 2.22 m/min. The time which a given portion of the material spends in the drying zone is the ratio of the dryer length to the conveyor speed, i.e. 4/2.22 = 1.8 min, which is not enough to complete the drying operation as shown in table 6.4. It is evident that if recirculation is not used this would require very large dryers even when the initial moisture content is low (see table 6.4), therefore a multipass system would need to be provided for all those products.

A rotary multimode cavity would operate in a similar fashion to a guardiola dryer. The product would be loaded into the cavity and microwave power applied until the required conditions were achieved. Considering the same minimal oscillatory modes as above, i.e. 155 MHz for a 4 m long conveyor, the cavity dimensions, and the filling factor would need to be chosen to give the required throughput and drying time. The cavity radius can be estimated from eq (6.19) as 0.742 m. If a length of 2 m with a filling factor of 0.6 is taken then a 4 m^3/h throughput is achieved with a drying time of 31.1 min which may be satisfactory for all of the products in table 6.4 if the initial moisture content level approached the 20 % w.b. mark. The throughput limitation can be estimated taking the material volume as $\pi \times 0.742^2 \times 0.6$ =

2.075 m^3 and considering an input field at 2,450 MHz and using eq (6.13a),

$$Qd_{max} = 5.6E6\ e''/(e'+2)^2\ \ kW$$

from which it is noted that breakdown limitations are not significant, the throughput is limited by quality and dimensional considerations.

Batch and continuous multimode would both appear to be feasible for drying the above products although both would require some modifications to the drying plant.

The installation of a 60 kW conveyor unit for crop heating, i.e. sterilising, pasteurising, etc. has been reported recently by Meredith [106] as shown in figure 6.12. This unit is said to be capable of processing between 1 and 2 ton/h of relatively dry product through a temperature rise from ambient to 80-110 C. These throughput levels correspond to something between 1-2 m^3/h of maize or wheat heating, and much less if the energy requirements for drying are taken into account. The floor space requirements are not small (it is reported that the total length of the unit will exceed 10 meters), these excessive lengths may be due to the fact that the unit has a single 60 kW magnetron (which would cause the field to be concentrated in a section of the length) and also due to other operations carried out in the product.

An Australian company has recently claimed to have produced the world's first multimode microwave dryer, commissioned in June 1986 [117]. The demonstration model is 15 m long, 2.3 m wide and 2.3 m high, and uses a 1.5 m wide conveyor belt. It is powered by 64 magnetrons giving a maximum capacity of 400 kW. This unit has been used for drying agricultural products and mineral materials such as sand, coal and clay.

6.8.3.3 Single Mode Resonant Applicators

Many types of single mode resonant applicators are possible. The only one studied here is the TM_{010} circular cavity shown in figure 6.13. The filling factor of such cavities is inherently small and they are not suitable for processing large diameter loads since this results in large dimensions and high loaded Q factors. Thus if large quantities of material are to be processed then large dimension cavities would be needed so increasing the cost. Metaxas [108, 109] has examined the TM_{010} circular cavity thoroughly. As noted before the

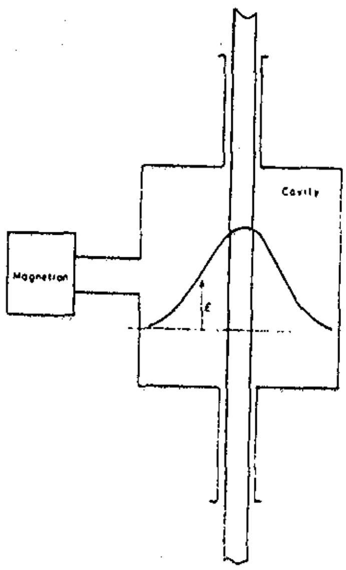

Figure 6.13 TM_{010} Single Mode Circular Resonator[44].

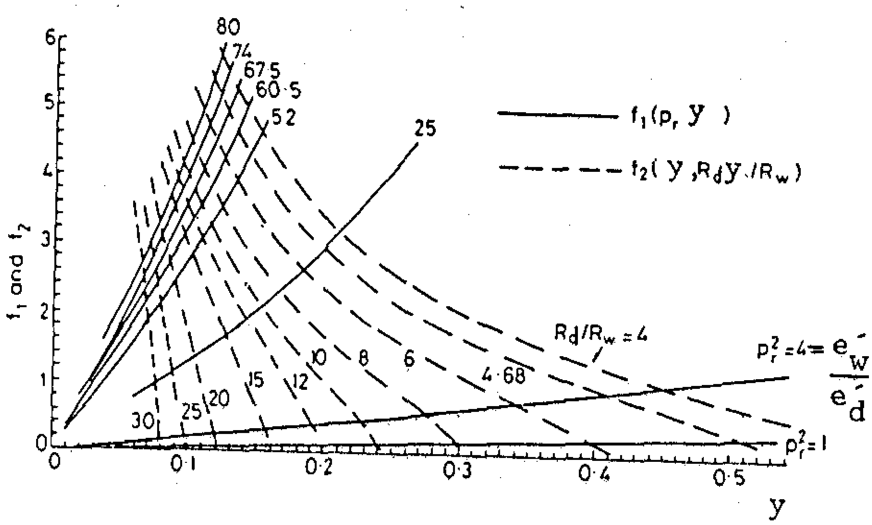

Figure 6.14 Curves for solving conditional equation[110].

field strength is a maximum at the centre and falls to zero at the walls. The field is symmetrical in the radial direction and does not change with the angle. The energy is launched into the cavity via a TE_{10} rectangular waveguide. The diameter of the tube must be very small compared with that of the cavity if uniform heating is to be achieved. The work carried out by Metaxas did not involve diameters that would be required for this application but the theory is applicable to the heat treatment of two coaxial dielectrics and results in a conditional equation for resonance in which both sides are dependent on the radii of the two cylinders, their permittivities and the frequency. The results are plotted in figure 6.14. Although the cavity length may be chosen to fit the application, it does have an influence on the Q factor, the latter increasing as the length is increased as can be inferred from eq (6.22). This would help in enhancing the efficiency of the cavity, but it would produce a sharper resonance and therefore a small load radius is required to obtain acceptable heating uniformity in the material. There is no point in using a long cavity when the attenuation of the field along it is significant. In the following analysis it is assumed that the length is 0.2 m. The minimum radius of the internal tube depends on throughput considerations and can be calculated by assuming that the product falls freely through the tube, i.e. it achieves a maximum velocity equal to

$$(2gh)^{1/2}$$

where h is the distance between the top of the elevator and the cavity. If the latter is mounted 2 m below the top of the elevator then the minimum radius for achieving a 4 m^3/h throughput is $r=(1.1E-3)/[\pi(2x9.8x2)^{1/2}]^{1/2}=0.75$ cm (1.1E-3 m^3/sec is equivalent to 4 m^3/h). It would not be realistic to envisage an adequate flow of most of the products of interest through a tube less than 1.5 cm in diameter.

Since moisture needs to be extracted from the internal tube, air would have to be used as the external coaxial dielectric ($e_d'=1$). When air is chosen as the outer dielectric the values of y (fig 6.14) become

$$y = 2\pi fr/c \qquad (6.25)$$

Reference to figure 6.14 indicates that as the dielectric constant of the product (e_w') increases the value of y decreases and therefore a lower value of the radius r needs to be adopted. Hence taking the large value of 4 for maize at 2,450

MHz with an external to internal radius ratio (R_d/R_w) of 20, we obtain (fig 6.14) y = 0.12 which, when substituted in eq (6.25) for f = 2,450 MHz gives r = 0.23 cm, which is not enough to allow the product to flow or to obtain an acceptable throughput. If the frequency is reduced to 915 MHz the value of r becomes approximately 0.62 cm and 1.32 cm at 430 MHz. However the use of low frequencies has the disadvantage of lower efficiency and a reduction in the ratio of the radii implies a greater variation of the power density across the load tube, although this should not be too important since the material would pass through the applicator several times. The minimum acceptable value of this ratio is difficult to determine since it is affected by the particular heat and mass transfer developed in each material. The average used by Metaxas when heating filamentary loads was around 15. Based on the dielectric properties of the materials at 1,000 MHz and considering fig (6.14) and eq (6.25) it is found that at 915 MHz the internal radius required is 0.8 cm with a cavity radius of 12 cm. The length would be as assumed before, 0.2 m, which is in accordance with Metaxas who uses a value which is a little less than the cavity diameter. The maximum power, limited by breakdown considerations, is estimated from eq (6.14b), i.e.

$$Qd_{max} = e''/(e'+1)^2\ 41 \quad kW$$

The limits in throughput are shown in table 6.15 from which it is clear that this cylidrical cavity is unsuitable for the application concerned.

Product (% w.b.)	Qd_{max} (kW) (in 0.2m) M=12%	M=16%	M=20%	M=24%	Maximum throughput(m^3/h) M_i=16%	M_i=20%	M_i=24%
Wheat	0.8	0.9	0.9	0.9	15E-3	9E-3	6E-3
Maize	0.7	0.7	0.6	0.5	13E-3	7E-3	4E-3

Table 6.15 Maximum throughputs for a TM_{010} cylidrical cavity limited by breakdown considerations and operating at 915 MHz.

6.9 Radio Frequency Applicators

6.9.1 Introduction

There is relatively little information in the literature directly related to RF heating as compared to, for example, microwave heating. What is available is mainly concerned with wood and plastic joining processes and, more recently, with paper and textile drying. Most of the work reported relies mainly on empirical design techniques although progress has been made at the Electricity Council Research Centre (UK) in the modelling of dielectric heating processes and in the design of equipment for laminar materials as well as the measurement of the relevant properties of the materials concerned. In addition to this, sources such as Brown et al [21] discuss the field patterns obtained by using particular electrode systems.

Lower frequencies result in more uniform field distributions, though RF systems also require higher field strengths for an equivalent power dissipation and electrical breakdown may become a problem. The most usual frequency is 27.12 MHz, although 13.56 MHz is also in use. Much lower frequencies have been used in the past for RF heating purposes, and higher frequencies were also popular (e.g. around 40 MHz). Uniform field distributions over much larger volumes are possible with RF and this effect is enhanced as the frequency is reduced.

A potentially serious problem which can occur with RF is with the voltage standing waves which can be set up in the applicator. The distance between peaks decreases as the frequency increases and at RF it is a fraction of a metre. The effect is increased if a dielectric other than air exists between the electrodes. If this dielectric has a relative permittivity of e then if a voltage V_o is applied at one end of the system the voltage at a distance "x" from the source is [14]:

$$V_x = V_o/[\cos 2\pi(e^{1/2}x/\lambda_o)] \qquad (6.26)$$

Eq (6.26) applies for a transmission line, but similar results can be obtained in rod and plates systems. The effect is therefore influenced by the moisture content of the product and by the frequency. Table 6.16 shows the value of x (in cms) if the voltage variation is limited to 5 %.

Product	x(cm)(13.56 MHz)					x(cm)(27.12 MHz)					x(cm)(40 MHz)				
(%w.b.)	12	21	30	39	48	12	21	30	39	48	12	21	30	39	48
Wheat	65	55	47			35	29	25			25	20	17		
Maize	58	50	45			30	26	23			22	18	16		
Rice	64	55	48			33	29	25			23	20	17		
Coffee	64	55	48			35	30	26	23	20	25	21	18	16	14
Soya	65	53	44			35	28	23			24	20	16	14	12

<u>Table 6.16</u> Distance at which the variation between applied voltage (V_o) and terminal voltage (V_x) is 5% in an open electrode system.

These dimensions are small for practical drying applications. However if the electrodes are fed at different points, for example, at the centre, i.e. at x/2 and again at x/4 and 3x/4, the length which can be used is, in effect, quadrupled. These feeds should all be the same length and also be as short as possible.

The relationship between the load and the generator in RF systems is important since the two must be tuned to obtain maximum performance. The system contains equivalent resistances, inductances and capacitances which, at the high frequencies used, have distributed characteristics.

Consider an effective voltage V in a radiofrequency applicator in which a constant interelectrode separation d′ is maintained. The equivalent of this system is shown in figure 6.15, the total current I can be separated into two components: I_r (which accounts for the energy dissipated as heat in the material) and I_c, a purely reactive current which circulates through the system. The energy dissipated per unit time is given by

$$Qd = V\ I_r \quad W \tag{6.27}$$

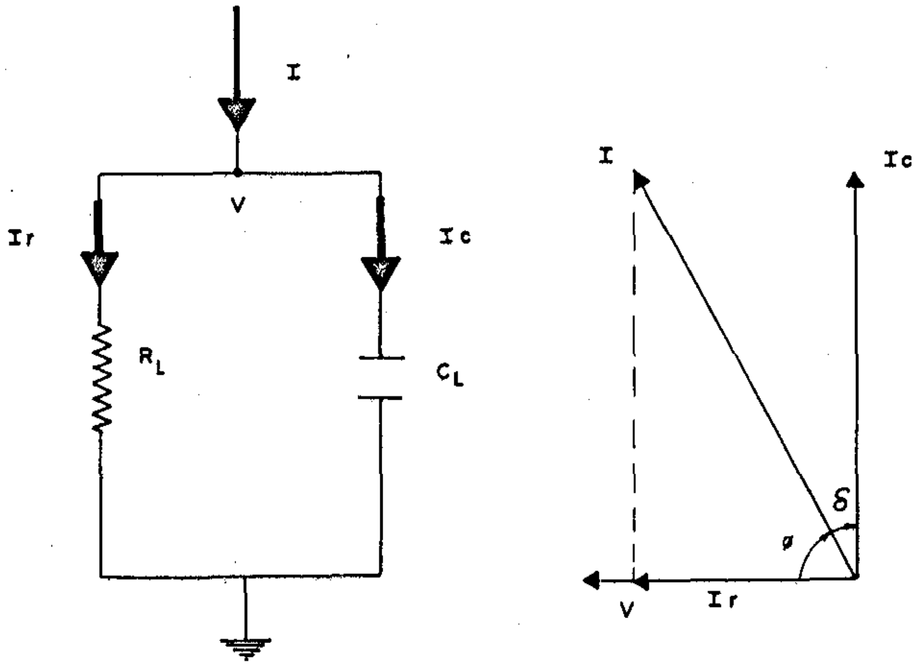

<u>Figure 6.15</u> Equivalent circuit and phasor diagram of a loaded parallel electrode RF system.

$tg\delta$ is the ratio of the magnitudes of the resistive and reactive components of the total current, i.e.

$$I_r = I_c tg\delta \qquad (6.28)$$

The magnitude of the reactive current is,

$$I_c = VwC_L \qquad (6.29)$$

where C_L is the effective capacitance obtained when a material with dielectric constant e' is inserted, i.e.

$$C_L = e_o e'(\mathbf{v}/d')(1/d') \qquad (6.30)$$

and $\mathbf{v}$ is the volume of the material. When eqs (6.28) to (6.30) are substituted in eq (6.27) we have,

$$Qd = (V/d')^2 w e_o e' \mathbf{v} tg\delta \qquad (6.31)$$

which reverts to eq (6.4) if we define an effective internal field strength in the bulk of material, $E = V/d'$, and if $e'tg\delta$ is substituted by e''.

The reactive power (i.e. that which is not converted into heat) is given by

$$Q_{reactive} = V^2 w\ C_L \tag{6.32a}$$

Substituting eq (6.30) in (6.32a) yields

$$Q_{reactive} = v\ w e_o e' E^2 \tag{6.32b}$$

The quality factor of the loaded RF system can be expressed as the ratio of the two quantities in eqs (6.32b) and (6.31),

$$Q_L = e'/e'' = 1/tg\delta \tag{6.33}$$

Eq (6.23) tends to the above relationship when the filling factor approaches unity, as expected. Q_L is the load Q factor, since the load fills the entire volume available in the applicator, although in practice the electrodes and connections will have an effect on Q_L which has not been considered above. Alternatively, the loaded Q factor can be defined as the ratio between the reactive power in C_L and the real, or active power in R_L (see figure 6.15), which yields

$$Q_L = (V^2 w C_L)/(V^2/R_L) \quad (6.34a)$$

$$Q_L = w C_L R_L \quad (6.34b)$$

Thus the quality factor of a given loaded RF applicator is directly related to the ratio between I_c and I_r, i.e. the reactive current required per unit of resistive current, the latter is responsible for the production of the required heat in the material. Hence when the material is placed in the RF system it should draw as much resistive current as possible as compared to the reactive component (i.e. a low loaded Q factor). This clearly means that the efficiency of the applicator is improved since less "unproductive" current is involved and therefore lower energy losses are produced in the RF feed lines and connections. Alternatively, smaller feeders and ancillary equipment are required to handle the same amount of useful, i.e. active power.

In the above the applicator and load stage has been discussed, in general the complete system consists of an RF oscillator, a coupling circuit, the applicator and the load to be heated. A short discussion of the RF system follows below. This refers to tank circuit resonators, which are the most commonly used type of construction, other systems are described elsewhere (see for example [43]). The oscillator is supplied with a DC voltage usually obtained by transformation and rectification (see figure 6.16). The system is composed by the rectification section which feeds the valve(s) and the tank circuit, the latter is a resonating L-C circuit in which the RF oscillations are produced. The resonant frequency is:

$$w_R = 1/(L_T C_T)^{1/2}$$

where C_T and L_T are the equivalent capacitance and inductance of the tank circuit. For resonance to be maintained at w_R the total impedance across terminals 1-2 should remain resistive, i.e. the current drawn from these terminals should be in phase with the a.c. voltage V_R (figure 6.16). Figure 6.15 indicates that if a direct connection is made from the oscillator terminals to the electrode system the reactive component C_L takes the system out of resonance. In practice the resonant frequency is determined by the combined effect of all the inductances and the capacitances in the system connected to the oscillator terminals. This frequency must remain stable under loading conditions and the design should be such that the energy efficiency is as high as possible. The source can be matched to the load by adjusting the parameters of the coupling circuit, and varying them during the operating cycle if

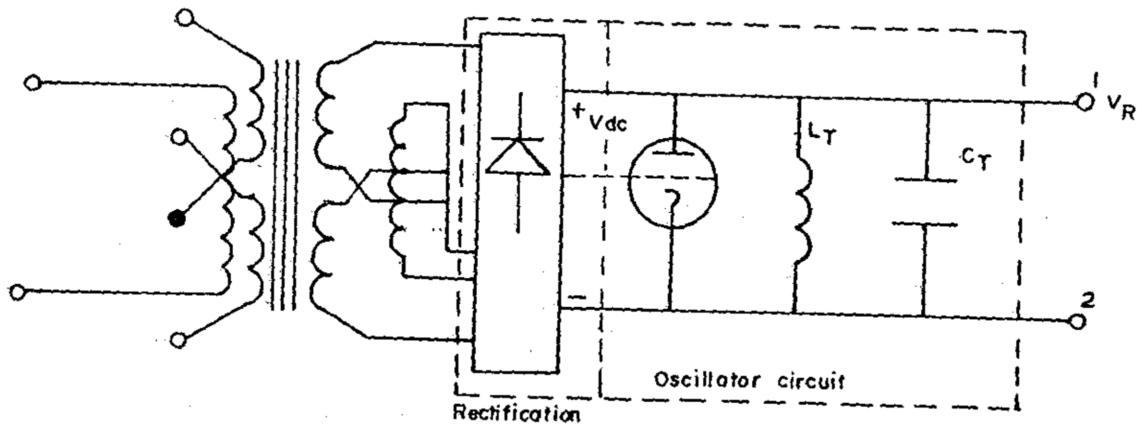

Figure 6.16 Diagram of RF Power Generator.

necessary, the amount of adjustment being determined by the extent to which the variation of the parameters of the load affect the desired resonance. The RF power can be fed directly into the applicator, such an arrangement is a simple solution when the parameters of the load do not vary appreciably during the heating cycle or if the change produced in the resonant frequency can be tolerated. In practice the frequency shift can be minimized by using a large tank capacitor C_T compared with the dielectric load capacitance. The applicator efficiency is affected by the term $(1-Q_L/Q_o)$ where Q_o, the unloaded Q factor, is determined by the applicator arrangement and the material from which it is constructed, it can be written as:

$$Q_o = w_R C_o R_o \qquad (6.35)$$

where w_R is the resonant frequency. C_o and R_o are, respectively, the capacitance and resistance of the unloaded applicator system.

In addition to the above, the efficiency of the total system will be affected by the losses in the tank circuit and the electrodes and by the currents circulating in the low frequency part of the equipment. If high values of C_T and

C_o are used to obtain a better frequency stability and a large Q_o (see eq (6.35)) and thus attain a higher efficiency, then the resulting RF current will increase due to the lower reactance which is "seen" at the oscillator terminals and tank circuit. This will not only cause the losses due to the Joule effect to increase, but it will also require high currents from the mains to supply the rectification section, tank circuit and applicator even though the latter may be lightly loaded. In this case, if the RF generator is supplying a batch drying process, a low overall energy efficiency will be obtained during most of the operation (see Chapter 8). The valve efficiency is likely to be of the order of 70 % (see for example [114]), a theoretical maximum of 75 % has been suggested [77]. When the complete system is taken into account, i.e. transformers, rectifiers, RF valves and tank circuit, electrodes and load, an overall efficiency of 40-60% is likely (see Chapter 8).

It is possible to use a coupling circuit with variable components (see for example the variable coupling circuits presented by [14], [43] and [77]). Many arrangements are possible but ideally the overall effect is equivalent to the introduction of a variable reactance into eq (6.34a), which yields

$$Q_L = [V_R^2 w_R f(LCR_w)]/P_o \tag{6.36}$$

where V_R and P_o are the oscillator output voltage and power in RMS values and $f(LCR_w)$ is a capacitive component which accounts for the equivalent capacitance of the applicator (including load) and also for the variable reactances of the coupling circuit. This term is affected by the inductances, capacitances, resistances and frequency of the system. The resulting system at the terminals 1-2 of the oscillator can therefore be represented by an equivalent circuit in which the load resistance R_L is in parallel with a capacitor $f(LCR_w)$. Hence for a given frequency tolerance and load variation the value of Q_L can be optimised by adjusting the reactance X of the coupling circuit (figure 6.17) in order to produce the required operating conditions and optimum energy efficiency. If the operation is to be satisfactory throughout the drying process then the method adopted to make the necessary adjustments to the L-C components of the coupling circuit must have a response which is faster than the change in load parameters. The adjustments in the coupling circuit will have to respond to a control strategy, probably based on a microprocessor system.

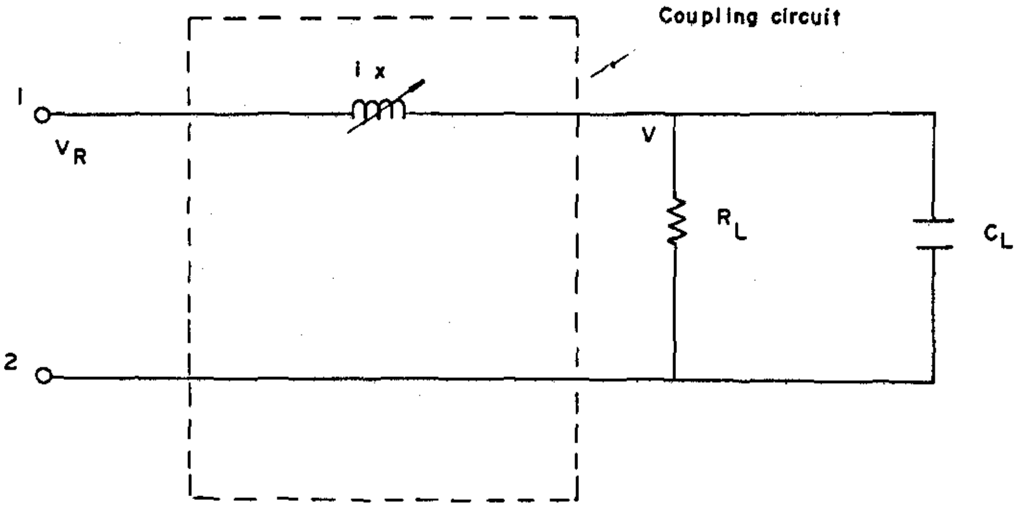

Figure 6.17 Diagram of RF Coupling and Applicator/Load Circuit.

Consider finally the circuit shown in figure 6.17 which represents the general circuit seen from the oscillator terminals when a variable coupling network is used. In order for the resonance of the tank circuit to be maintained in theory the impedance across the terminals must be a pure resistance. After the required algebra is carried out it is found that the value for the coupling reactance X must always be adjusted to

$$X = [(wC_LR_L)R]/[1+(wC_LR_L)^2] \tag{6.37}$$

Considering eq (6.37) and calculating the voltage V across the load as a function of the voltage at the oscillator terminals, we have

$$V = V_R\{R_L/[1+(wC_LR_L)^2]-jX\}/\{R_L/[1+(wC_LR_L)^2]+j(X-X)\}$$

Substituting eq (6.37) and the expression for Q_L as given in eq (6.34b) in the above equation for V results in

$$V = V_R(1-jQ_L)$$

which is equivalent to

$$V = V_R\ (1+Q_L^2)^{1/2}\angle\psi\ , \tag{6.38}$$

where $\psi = -tg^{-1}(e'/e'')$.

Hence the voltage in the load V lags the voltage V_R at the oscillator terminals by the arctg of e'/e''. Moreover, the magnitude of V is $(Q_L^2+1)^{1/2}$ times greater than the terminal voltage V_R. Both this magnitude and phase difference are solely dependant on the dielectric properties of the material.

6.9.2 Cross Flow Conveyor Systems

Most RF conveyor applicators fall into one of the categories illustrated in figure 6.18. They have been applied succesfully in drying paper and textiles but in such cases the material is very thin. Thin materials often employ a "strayfield" system in which adjacent electrodes have opposite polarity and a significant horizontal component of the field is produced. This system produces a horizontal field component which is particularly useful in the case of paper and other fibrous materials which have a higher loss factor in this direction. If the plate system is to be used in drying applications, an airgap between load and the upper electrodes must be used or, alternatively, the plates could be perforated. In any case, if the material is carried on a conveyor belt, an

(a) Through Field Plate System

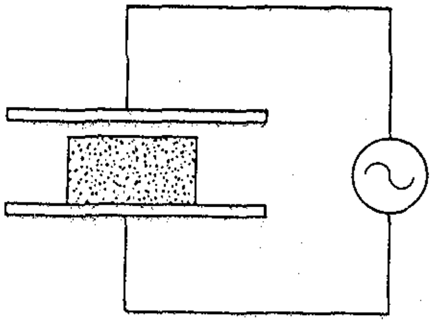

(b) Simple Rod Electrode System[14].

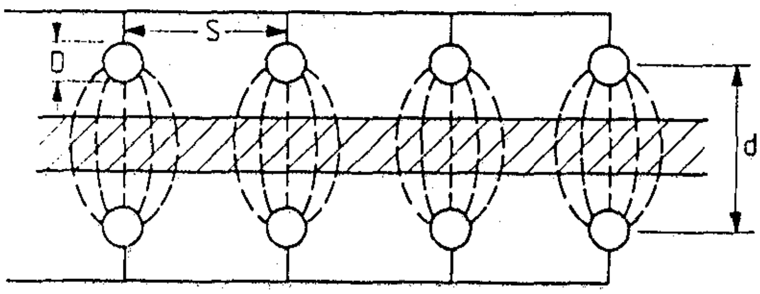

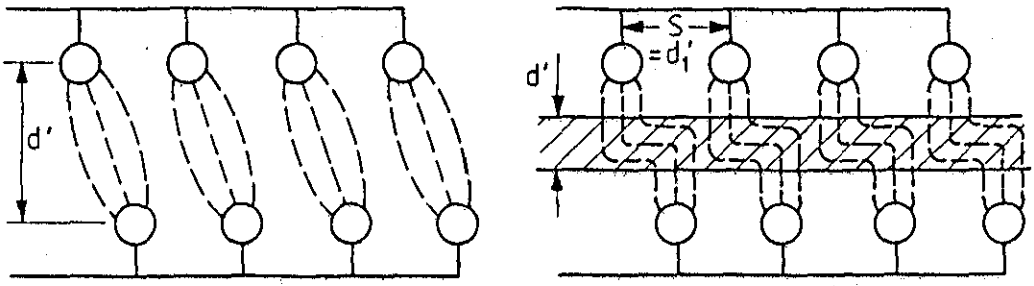

(c) Staggered Through Field Electrode System[14].

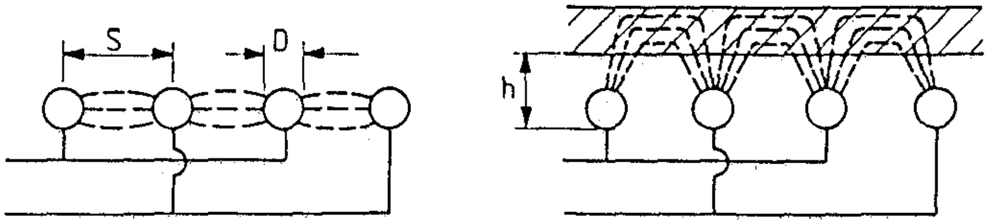

(d) Strayfield Electrode System[14].

Figure 6.18 RF Electrode Systems.

airgap needs to be present.

It has been reported that if the diameter of the rods is more than 1/3 of the spacing "S" and the thickness of the material is less than 0.9 (d′-D) (see figure 6.18b) then the field produced by the rod system is very similar to that created by flat plates [14].

Consider the case of a rod system with 8 feeding points in a bar which is connected perpendicularly to the rods as shown in figure 6.19. With this arrangement an acceptable length (table 6.16) for each rod would be 0.5 metres if the energising frequency is 27.12 MHz, the corresponding figures for a 13.56 MHz system would be 4 feeding points on the centre bar and 1 metre length for each rod. This arrangement is shown in figure 6.19 with the lower electrode earthed. A conveyor belt whose length is 4 m and whose width is 1.0 m can then travel through the rod or plate system, whichever is used, provided that the frequency of operation is 13.56 MHz. In this case the depth of the product on the conveyor is not determined by the power penetration depth, it is controlled however, by the need to obtain a reasonable flow of air over the surface of the particles. In the analysis of the following RF systems it is assumed that the depth of the bed is 0.1 metres.

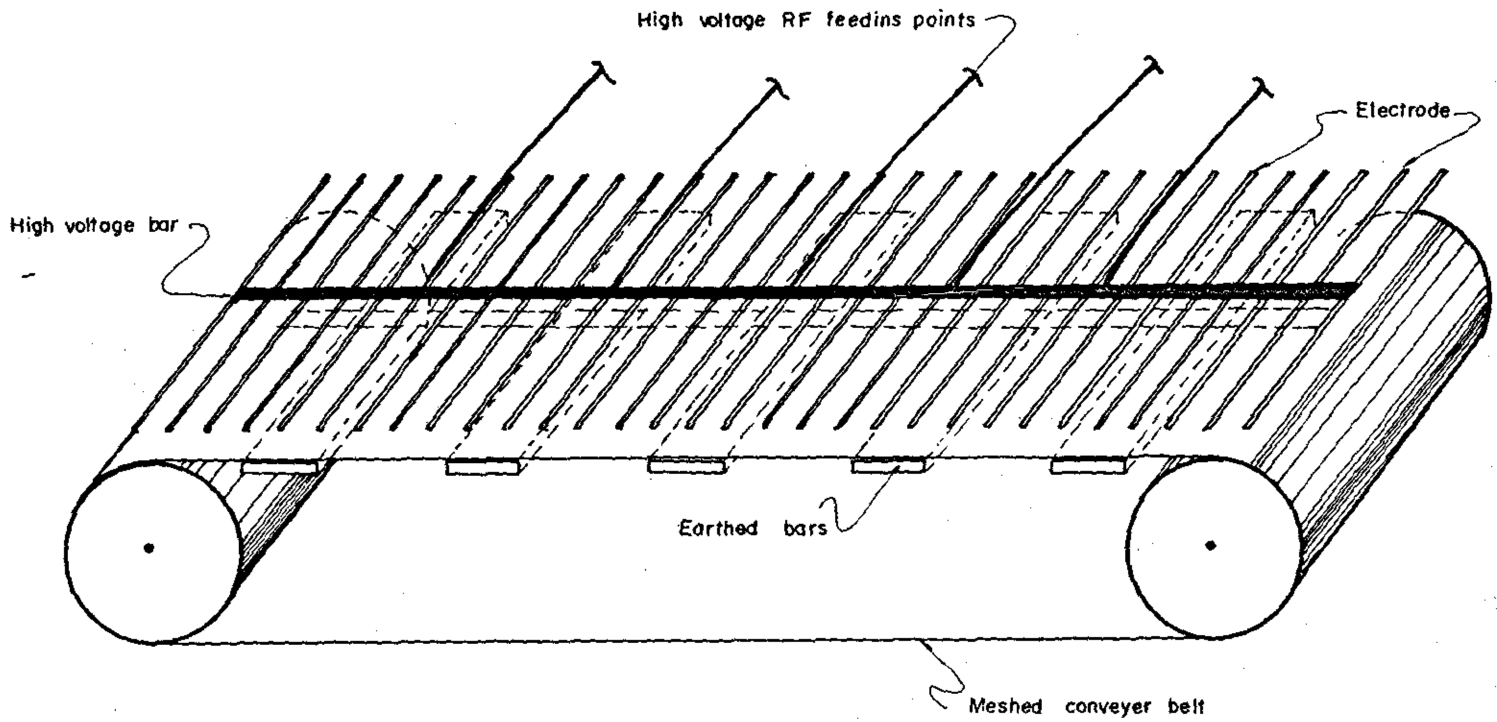

Figure 6.19 RF Crossflow Conveyor System.

The throughput limitations imposed by the need to avoid breakdown are given in table 6.17 for 13.56 MHz at which frequency the maximum power limit is (a bed of material 1.0x4.0x0.1 m^3 has been considered)

$$Qd_{max} = (e''/e'^2)\ 6E3 \quad kW$$

Product (%w.b.)	Qd_{max} (kW) M=12	M=21	M=30	M=39	M=48	Maximum Throughput (m^3/h) M_i=21	M_i=30	M_i=39	M_i=48
Wheat	158	136	116			1.4	0.6		
Maize	138	146	132			1.4	0.7		
Rice	197	200	194			2.2	1.1		
Coffee	244	272	280	275	262	3.4	1.7	1.1	0.7
Soya	205	267	287						

<u>Table 6.17</u> Maximum throughputs limited by RF breakdown for a conveyor operating at 13.56 MHz.

The corresponding values for 27.12 MHz and 40 MHz are shown in tables 6.18 and 6.19, in all cases the bed dimensions were 0.1x1.0x4.0 m^3. The effect of standing waves becomes more severe as the frequency is increased, this may pose difficulties in the design of the electrodes. The maximum power and throughput values in tables 6.17-6.19 are, for a given thickness, dependent on volume.

Product (%w.b.)	Qd_{max} (kW) M=12	M=21	M=30	M=39	M=48	Maximum Throughput (m^3/h) M_1=21	M_1=30	M_1=39	M_1=48
Wheat	318	280	241			2.9	1.3		
Rice	374	390	383			4.1	2.1		
Maize	290	300	265			3.0	1.4		
Coffee	452	537	570	570	549	6.4	3.2	2.0	1.3
Soya	423	573	623			5.1	2.7		

Table 6.18 Maximum throughputs limited by RF breakdown for a conveyor operating at 27.12 MHz.

Product (%w.b.)	Qd_{max} (kW) M=12	M=21	M=30	M=39	M=48	Maximum Throughput (m^3/h) M_1=21	M_1=30	M_1=39	M_1=48
Wheat	469	418	362			4 (6)	2 (13)		
Rice	532	565	561			6 (4)	3 (8)		
Maize	457	457	395			5 (5)	2 (11)		
Coffee	625	777	845	855	830	9 (3)	4 (5)	3 (9)	2 (14)
Soya	633	878	963			8 (3)	4 (6)		

Table 6.19 Maximum throughputs limited by RF breakdown for a conveyor operating at 40 MHZ.

Tables 6.17-6.19 show that, as expected, higher frequencies are to be preferred. The figures in parentheses in table 6.19

are the estimated minimum drying times (in minutes) imposed by breakdown limitations at 40 MHz. These have been obtained as discussed in Section 6.3 and they involve the energy terms of eq (6.7) and the maximum power levels which can be applied in the applicator from initial (M_i) to final (M_f=12) moisture content as indicated in table 6.19. Table 6.4 and the experimental results for 38.5 MHz (Chapter 8) indicate that the estimates presented here for coffee and soya are optimistic since these are very slow drying materials. As opposed to the other products, it appears that the drying of rice is limited by breakdowns and not by quality damage. The RF conveyor will be capable of drying rice at large throughputs, e.g.in excess of 4 m^3/h without recirculation of the material. The residence time in the dryer would be approximately 6 min (M_i between 20 and 30 % w.b.) with a conveyor speed of 0.67 m/min. For the other products recirculation will be a more acceptable alternative, due to the dimensions involved, than a single pass system.

The electrode voltage required can be obtained from [14]:

$$V = E\,(d_{ag}e' + d'') \qquad (6.39a)$$

where E is the effective field strength in the bulk of material, d_{ag} is the airgap thickness and d" is the thickness of the material. Expressing the field in the airgap, E_{air}, in terms of E using eq (6.13c) and substituting in eq (6.39a) yields

$$V = E_{air}\ (d_{ag}e' + d'')/e' \qquad (6.39b)$$

Thus the airgap should be as small as possible if the electrode voltage is to be kept low. Assuming an airgap of 1 cm the electrode voltages, at 27.12 MHz, are given by the following (the values are obtained using eq (6.39b) in which E_{air} is substituted into eq (6.14c):

$$V = (q_d/0.556E\text{-}10x27.12E6e'')^{1/2}(0.01e'+0.10)$$

where q_d is the net dielectric power density in the product. The values of the electrode voltage for q_d=250 kW/m^3 are shown in table 6.20.

Product	Electrode Voltage (RMS, kV)				
(%w.b.)	M=12%	M=21%	M=30%	M=39%	M=48%
Wheat	3.9	3.1	2.7		
Rice	3.3	2.6	2.1		
Maize	5.2	5.5	6.6		
Coffee	3.2	2.3	1.8	1.6	1.4
Soya	3.3	2.1	1.5		

Table 6.20 Electrode voltages in a RF conveyor when operating at 27.12 MHz with a dielectric power density of 250 kW/m^3

The voltage at the oscillator terminals (V_R) with variable coupling arrangement can be obtained using eqs (6.39), (6.38) and (6.33), which results in the values given in table 6.21.

Product	Oscillator Voltage (RMS, kV)				
(%w.b.)	M=12%	M=21%	M=30%	M=39%	M=48
Wheat	1.6	2.4	2.5		
Rice	1.9	2.3	2.1		
Maize	3.5	5.1	6.4		
Coffee	1.7	2.1	1.8	1.5	1.4
Soya	1.8	2.0	1.5		

Table 6.21 Oscillator voltage required to maintain the electrode voltages in table 6.20

6.9.3 Cross Flow Vertical System

Consider a crossflow dryer, 3 m long and 4 m high. If a rod system of the same dimension is placed on each side of such a unit, with a gap between electrodes of 10 cm, then a substantial quantity of material could be processed with the need for only limited additional space. Alternatively, this system could use a set of perforated capacitor plates or even two metallic mesh sheets. The air for carrying away the moisture could be obtained from the outlet of the crossflow unit. The rods could be mounted horizontally with an insulating mesh between the electrodes to hold the product. Each rod would then be 3 m long and would have three feeding points at 13.56 MHz and six at 27.12 MHz. These feeds could be supplied by perpendicularly mounted high voltage busbars using the arrangement shown in figure 6.20, i.e. three of those bars would be required at 13.56 MHz and six at 27.12 MHz. Earthed bars, similar to those shown in figure 6.19, would be attached to the dryer outlet and the whole structure grounded. The air could be extracted through the outer electrodes using an insulated extraction unit. This air could be mixed with fresh air from the environment before it re-entered the dielectric unit. The waste heat from the electrode system and that from the cooling of the valves and tank coils could be used to supply part of the heat required for

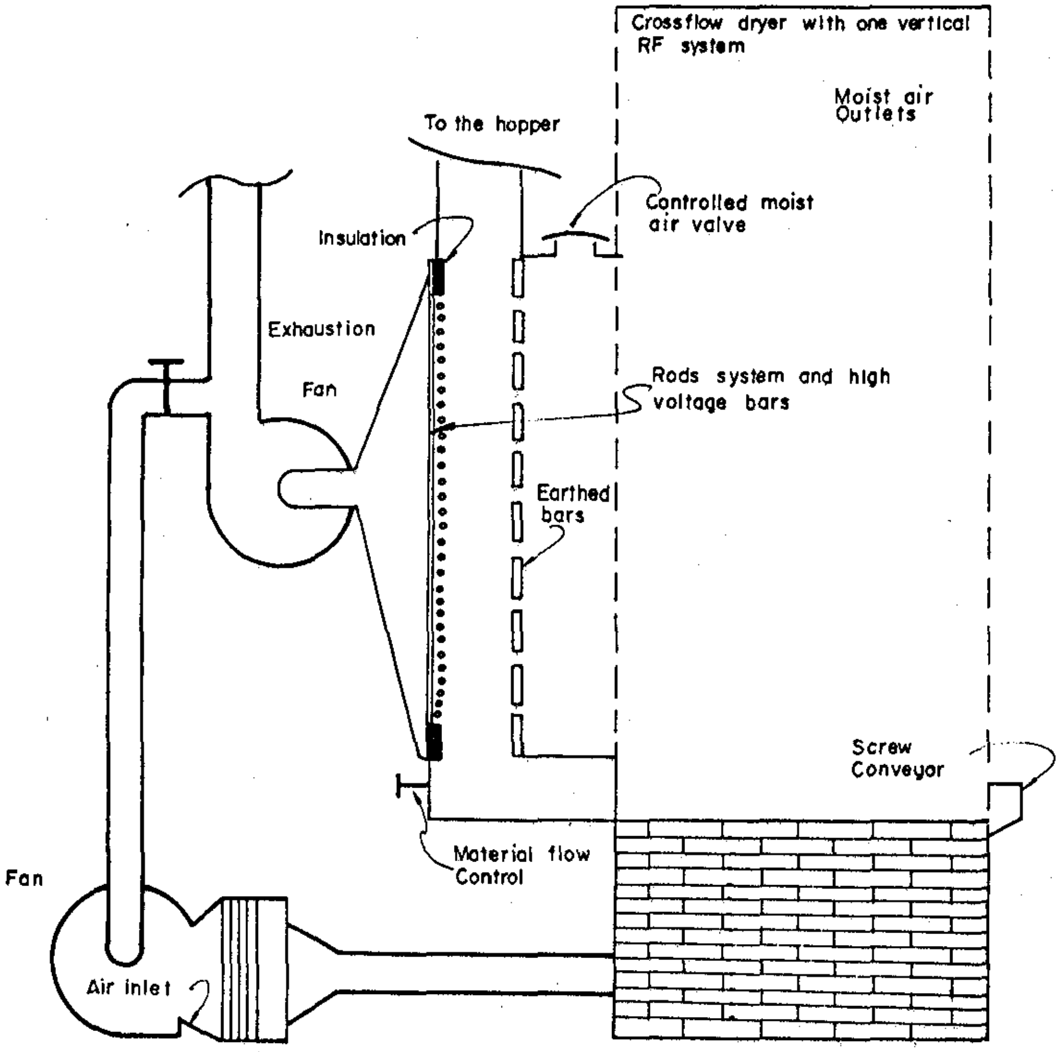

Figure 6.20 RF Vertical Crossflow System with Heat Recovery Arrangement.

the convective part of the process. The system is as shown in figure 6.20, the product would be fed from a hopper which received the material from the elevator after having been carried in the screw conveyor at the bottom. The operation of the system with, say, coffee would be as follows. The crossflow dryer starts full of wet product, the convective or pre-drying stage then begins and the partially dried product is discharged at the bottom and recirculated if required. As soon as the moisture content has been reduced to the required level for dielectric heating to be used, then the product could be conveyed to a hopper above the electrode system from which it would move to the dielectric drying section. In the meantime the crossflow dryer would be filled with a new batch of wet product and the process repeated. Both the convective and dielectric drying operations would be carried out simultaneously but with different batches of material.

The throughput limitation imposed by the need to avoid breakdown is shown in tables 6.22-6.24. The maximum power is obtained using eq (6.14c), taking the volume of product in the drying zone to be 0.1x3.0x4.0 m^3, in the 13.56 MHz case the expression obtained is

$$Qd_{max} = 18.1E3 \; e''/ \; e'^2 \qquad kW$$

The corresponding expression for 27.12 MHz is

$$Qd_{max} = 36.2E3\ e''/\ e'^2 \qquad kW$$

and, for 40 MHz;

$$Qd_{max} = 53.4E3\ e''/e'^2 \qquad kW$$

In this case the maximum power and throughput are three times those obtained in the cross flow conveyor configuration. This is due to the fact that in the latter the volume of material is one third of that considered for the cross flow vertical system. Both arrangements are, however, equivalent in terms of throughput per unit of material being dried.

Product	Qd_{max} (kW)					Maximum Throughput(m^3/h)			
(%w.b.)	M=12	M=21	M=30	M=39	M=48	M_i=21	M_i=30	M_i=39	M_i=48
Wheat	473	409	349			4.2	1.8		
Rice	591	601	581			6.5	3.3		
Maize	414	439	396			4.3	2.2		
Coffee	732	817	841	825	787	10.3	5.2	3.2	2.1
Soya	616	800	860			7.5	3.9		

Table 6.22 Maximum throughputs limited by RF breakdown for a vertical crossflow system operating at 13.56 MHz.

Product (%w.b.)	Qd$_{max}$ (kW) M=12	M=21	M=30	M=39	M=48	Maximum Throughput(m^3/h) M_i=21	M_i=30	M_i=39	M_i=48
Wheat	955	840	723			8.6	3.8		
Rice	1.1E3	1.2E3	1.2E3			12.4	6.3		
Maize	871	900	796			9.1	4.3		
Coffee	1.4E3	1.6E3	1.7E3	1.7E3	1.6E3	19.1	9.7	5.9	3.8
Soya	1.3E3	1.7E3	1.9E3			15.4	8.1		

Table 6.23 Maximum throughputs limited by RF breakdowns for a vertical crossflow system operating at 27.12 MHz.

Product (%w.b.)	Qd$_{max}$ (kW) M=12	M=21	M=30	M=39	M=48	Maximum Throughput(m^3/h) M_i=21	M_i=30	M_i=39	M_i=48
Wheat	1.4E3	1.3E3	1.1E3			13(6)	6(13)		
Rice	1.6E3	1.7E3	1.7E3			18(4)	9(8)		
Maize	1.4E3	1.4E3	1.2E3			14(5)	7(11)		
Coffee	1.9E3	2.3E3	2.5E3	2.6E3	2.5E3	26(3)	13(5)	8(9)	5(15)
Soya	1.9E3	2.6E3	2.9E3			23(3)	12(6)		

Table 6.24 Maximum throughputs limited by RF breakdowns for a vertical crossflow system operating at 40 MHz

The values in parentheses in table 6.24 are the estimated minimum drying times.

This applicator would be capable of giving a considerable throughput, e.g 4 m^3/h, in one pass through the electrode system. For the interelectrode cross sectional area of the above equipment, the corresponding velocity of the product is 0.22 m/min which, considering the height of the system, implies that each particle stays in the drying zone for 18 min. Table 6.4 and the experimental results (Chapter 8) indicate that all cereals could probably be dried in one pass through the system. If one applicator is mounted at each side of the dryer, the velocity required for maintaining the same throughput would be 0.11 m/min in each unit which means that the product would need to stay for a little over half and hour in the drying zone. By doing this, wheat and maize may be dried from higher initial moisture contents. The drying of rice would present no real problem, but coffee and soya would yield much smaller throughputs and require recirculation. Consider, for example, the case of coffee when drying from 50 to 40 % w.b. at near breakdown conditions and 38.5 MHz. From Chpater 8 it can be estimated that it would take 25 mins to dry each particle, therefore for a 4 m^3/h throughput to be obtained the product would need to pass six times through a single RF vertical system as above and three times if a twin arrangement were adopted.

The voltage required on the electrode system for constant power can be estimated from eqs (6.14c) and (6.39b) with $d_{ag}=0$, yielding the values shown in table 6.25. The corresponding voltages at the output of the oscillator are shown in table 6.26.

Product (%w.b.)	Electrode Voltage (RMS, kV) M=12%	M=21%	M=30%	M=39%	M=48%
Wheat	3.1	2.3	1.8		
Rice	2.6	1.9	1.4		
Maize	2.5	1.8	1.5		
Coffee	2.6	1.7	1.3	1.0	0.8
Soya	2.6	1.5	1.0		

Table 6.25 Electrode voltages in a RF vertical crossflow when operating at 27.12 MHz with a dielectric power density of 250 kW/m^3

Product (%w.b.)	Oscillator Voltage (RMS, kV) M=12%	M=21%	M=30%	M=39%	M=48%
Wheat	1.3	1.7	1.7		
Rice	1.5	1.6	1.4		
Maize	1.7	1.6	1.4		
Coffee	1.4	1.5	1.2	1.0	0.8
Soya	1.4	1.4	1.0		

Table 6.26 Oscillator voltage required to maintain the electrode voltage in table 6.25.

6.9.4 Cylindrical Systems

Cylindrical applicators were discussed earlier in this Chapter in connection with microwave systems where the dimensions are critical. These constraints do not apply in the case of RF although the ventilation arrangements must be adequate and the required electrode voltage not too high. The field uniformity in a perforated low loss tube full of dielectric material (as in figure 6.21a) can be arranged to be fairly uniform if suitably shaped electrodes are used, assuming that the voltage is constant along the plates and that the properties of the material are also constant. The former can be compensated for as indicated above and the variation due to the properties of the material should not be too significant if the electrodes are as shown in figure 6.21b, which shows that the shape of the plates required to produce an uniform field in the material is not greatly altered if the dielectric constant changes from, say, 2 to 8, which is the maximum variation expected in this application (see the models developed for ε' in Chapter 8). A perforated, low-loss tube, 20 cm in diameter could maintain a throughput of 4 m^3/h if the product velocity was 2.1 m/min, which gives a residence time of 2 mins for the particle to be dried in one pass. It will be noted from table 6.4 and Chapter 8 that, in most cases, this

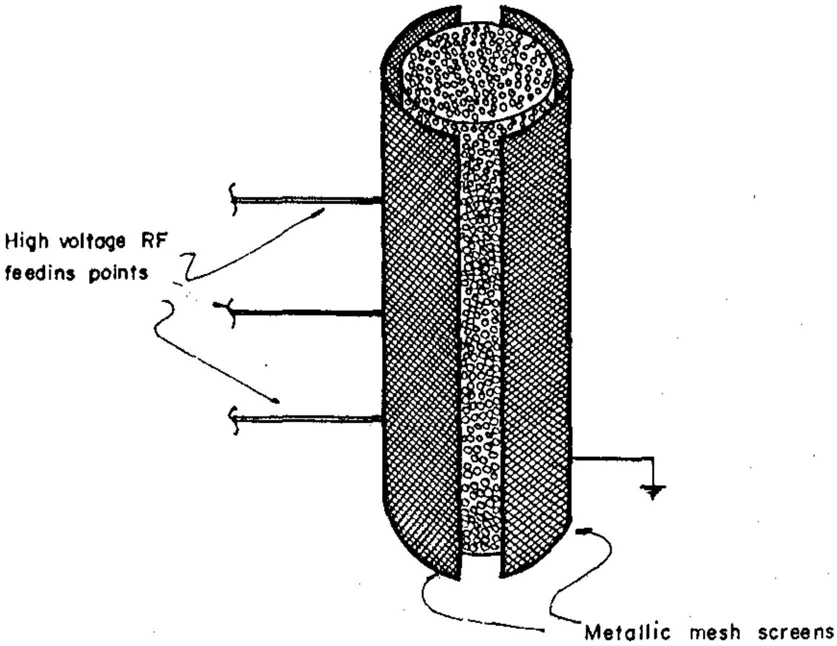

<u>Figure 6.21(a)</u>
RF Cylindrical System.

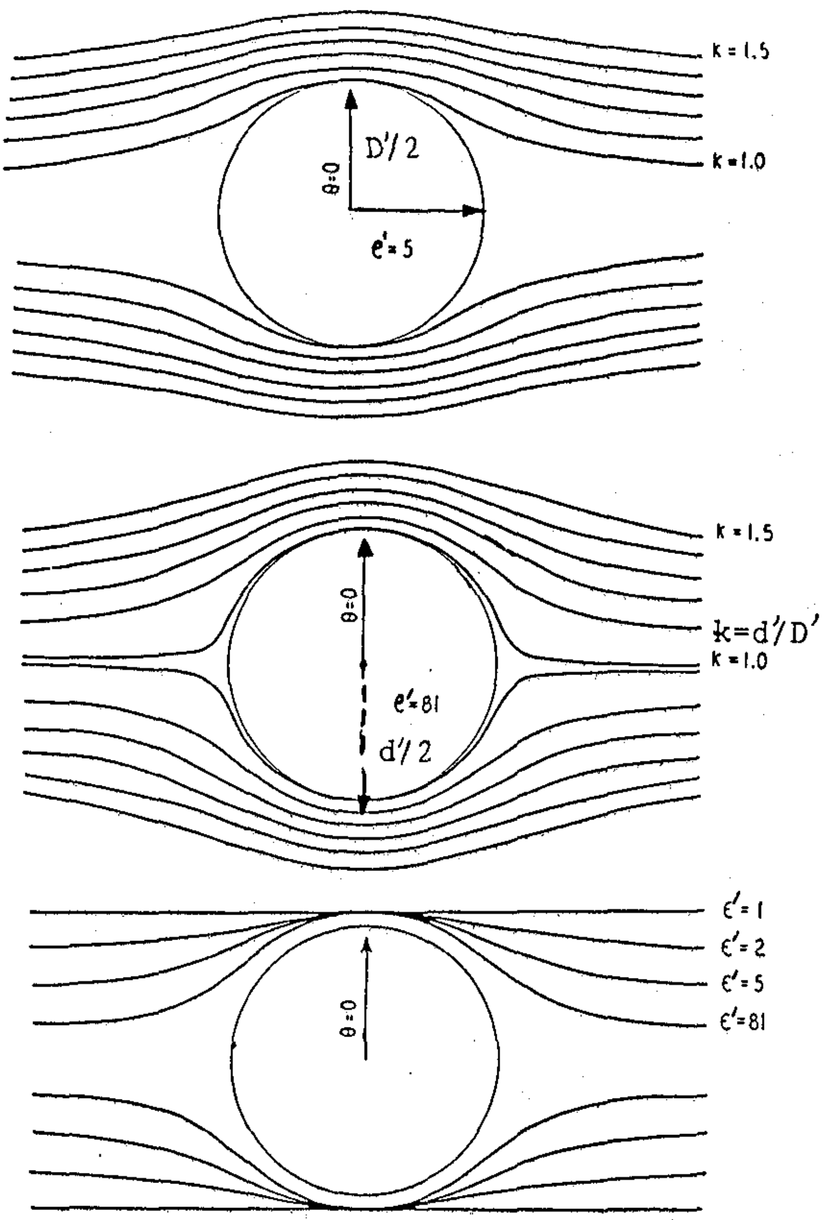

<u>Figure 6.21(b)</u>
Equipotential plates which will produce a uniform electric field in a cylinder:

i) When e´= 5.

ii) When e´= 81.

iii) For several e´ values when d´/D´=1. [21].

would imply product recirculation unless a smaller moisture reduction was involved. The tube would need to be placed between two curved electrodes of an approximately 0.2x3 m^2 area. The internal electrode would be earthed and the external supplied from the RF source via 3 feeding points if the working frequency were 13.56 MHz (6 if the frequency were 27.12 MHz). The plates would need to be insulated and adequate ventilation would have to be provided (figure 6.21a). The voltage between the electrodes can be estimated from [21]:

$$V = E(e'+1)\{d'r/D' - [(e'-1)/(e'+1)]\, D'r/d'\} \qquad (6.40)$$

where D′ is the diameter of the tube, d′ is the maximum distance between the electrodes and r is the radius of the tube.

The throughput limitation imposed by breakdown considerations is shown in tables 6.27-6.29 when the product volume is assumed to be $\pi \times 0.1^2 \times 3$ m^3 and the relationships for maximum power are based on eq (6.14b), i.e.

$$Qd_{max} = 5.7E3e''/(e'+1)^2 \quad \text{kW for 13.56 MHz}$$

$$Qd_{max} = 11.3E3e''/(e'+1)^2 \quad \text{kW for 27.12 MHz}$$

$$Qd_{max} = 16.7E3e''/(e'+1)^2 \quad \text{kW for 40 MHz}$$

Consider eqs (6.13) and (6.14). For a given maximum field value in the air gap (which in this Report is considered to be 200 kV/m peak), the corresponding value in the bulk of material will be larger in the cylindrical case than in the slab, thus a greater throughput can be obtained in the former arrangement. The formulae above apply to a dielectric cylinder and the accuracy increases as the distance between the electrodes increases for a given load radius. Hence the values in the following tables are likely to be somewhat higher than those which might be obtained in practice, since the relationship between internal and the external field in a dielectric cylinder allows a larger value of field strength in the bulk of material to be greater in a given limit to the external field.

Product	Qd_{max} (kW)					Maximum Throughput(m^3/h)			
(%w.b.)	M=12	M=21	M=30	M=39	M=48	M_1=21	M_1=30	M_1=39	M_1=48
Wheat	83	84	80			0.9	0.4		
Rice	106	123	130			1.2	0.6		
Maize	81	96	93			0.8	0.4		
Coffee	131	167	189	198	199	1.8	0.9	0.6	0.4
Soya	109	168	203			1.3	0.7		

Table 6.27 Maximum throughputs (limited by RF breakdown) for a cylindrical system operating at 13.56 MHz.

Product (%w.b.)	Qd_{max} (kW) M=12	M=21	M=30	M=39	M=48	Maximum Throughput(m^3/h) M_1=21	M_1=30	M_1=39	M_1=48
Wheat	155	164	159			1.6	0.8		
Rice	193	232	252			2.1	1.1		
Maize	162	191	183			1.7	0.9		
Coffee	220	307	366	397	407	3.1	1.6	1.0	0.6
Soya	208	346	428			2.5	1.3		

Table 6.28 Maximum throughputs (limited by RF breakdown) for a cylindrical system operating at 27.12 MHz.

Product (%w.b.)	Qd_{max} (kW) M=12	M=21	M=30	M=39	M=48	Maximum Throughput(m^3/h) M_1=21	M_1=30	M_1=39	M_1=48
Wheat	218	237	234			2.2	1.1		
Rice	267	329	364			3.0	1.5		
Maize	241	281	266			2.5	1.3		
Coffee	287	426	526	583	605	4.0	2.0	1.2	0.8
Soya	298	515	649			3.6	1.9		

Table 6.29 Maximum throughputs (limited by RF breakdowns) for a cylindrical system operating at 40 MHz.

Except for coffee and soya, the above tables indicate that the 20 cm tube is not adequate to cope with the levels of throughput needed if breakdowns are to be avoided.

In practice, however, coffee and soya will dry much more slowly (see Chapter 8) than any of the above materials, hence it appears that a single cylindrical system attached to the side of the crossflow dryer would not compare with a medium throughput conventional plant.

In addition to this the required voltages for this system are far greater than those needed for the cross flow systems presented above. The electrode and oscillator voltage at 27.12 MHz and q_d=250 kW/m^3 for a system in which d'=0.25 m and D'=0.20 m are shown in table 6.30 and 6.31 respectively.

Product (%w.b.)	Electrode Voltage (RMS, kV) M=12%	M=21%	M=30%	M=39%	M=48%
Wheat	9.9	8.4	7.7		
Rice	8.6	7.0	6.2		
Maize	8.8	7.3	6.9		
Coffee	8.3	6.3	5.2	4.6	4.3
Soya	8.5	5.7	4.5		

Table 6.30 Electrode voltage required in a RF cylindrical system when operating at 27.12 MHz with a dielectric power density of 250 kW/m^3

Product (%w.b.)	Oscillator Voltage (RMS, kV) M=12%	M=21%	M=30%	M=39%	M=48%
Wheat	4.0	6.5	7.2		
Rice	5.0	6.2	6.0		
Maize	5.9	6.7	6.8		
Coffee	4.5	5.6	5.1	4.6	4.3
Soya	4.5	5.4	4.5		

Table 6.31 Oscillator voltage needed to maintain the electrode voltage as in table 6.30; RF cylindrical system with variable-coupling operating at 27.12 MHz.

6.10 Other Applicators

Other possible dielectric drying systems, some of which have been mentioned earlier, are described below. The microwave moving bed and fluidised dryers are, respectively, similar in operation to the conveyor and rotary types described above. The moving bed, with or without a vacuum feature, has been proposed in the past. The fluidised system does not appear to have been used for dielectric drying applications although Perkin [132] reports on two U.K. patents involving this principle. All would require a comprehensive re-design of conventional drying plant which brings them outside the terms of reference of this work.

6.10.1 Microwave Moving Bed Dryer

This was suggested by Hamid et al [68] as a development of an earlier proposal by the same authors [66, 67]. The original objective was to use high frequency energy for pest control of agricultural products, the experiments being carried out with relatively dry grain. The authors suggested that layers greater than 10 cm thick would present penetration problems which they originally suggested might be overcome by agitating the material during the process. The initial development was based on the arrangement shown in figure 6.22a which used a vertical waveguide with the product falling through a series of plastic baffles, this solved the penetration problem but led to increased tuning difficulties. The next prototype (figure 6.22b) had only one baffle and the tuning problems were claimed to be solved. The final development was the application to grain drying using microwave in combination with hot air (figure 6.22c). The authors have also proposed an RF alternative to the latter arrangement. This is equivalent to the cross flow vertical system already discussed above.

6.10.2 Vacuum Dryer

The main feature of vacuum processing is that the boiling point of the water is lowered so as to allow moisture extraction without the need for high product temperatures. Thus, the material can be dried at this lowered boiling temperature in this way avoiding damage to the product. When dielectric heating methods are used for drying, the temperature of the material could well exceed the maximum level tolerated by the product if an acceptable throughput were to be achieved. This is a limitation in the use of dielectric heating for drying temperature sensitive products. In such applications, if high power densities are required, the only way to prevent the temperature from exceeding the limit is to stop the heating for

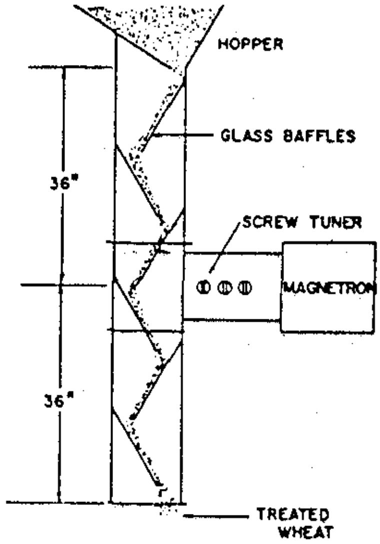

(a)

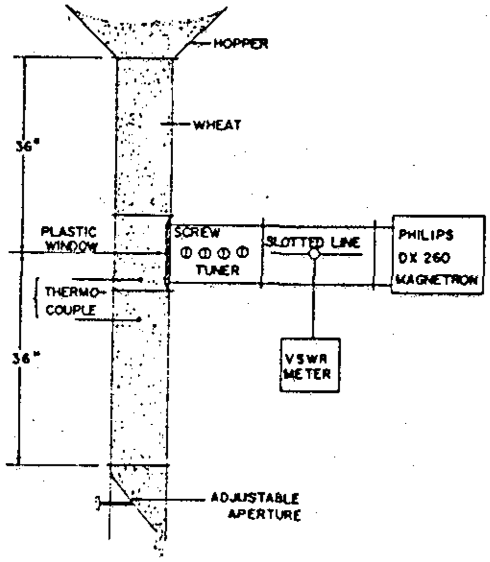

(b)

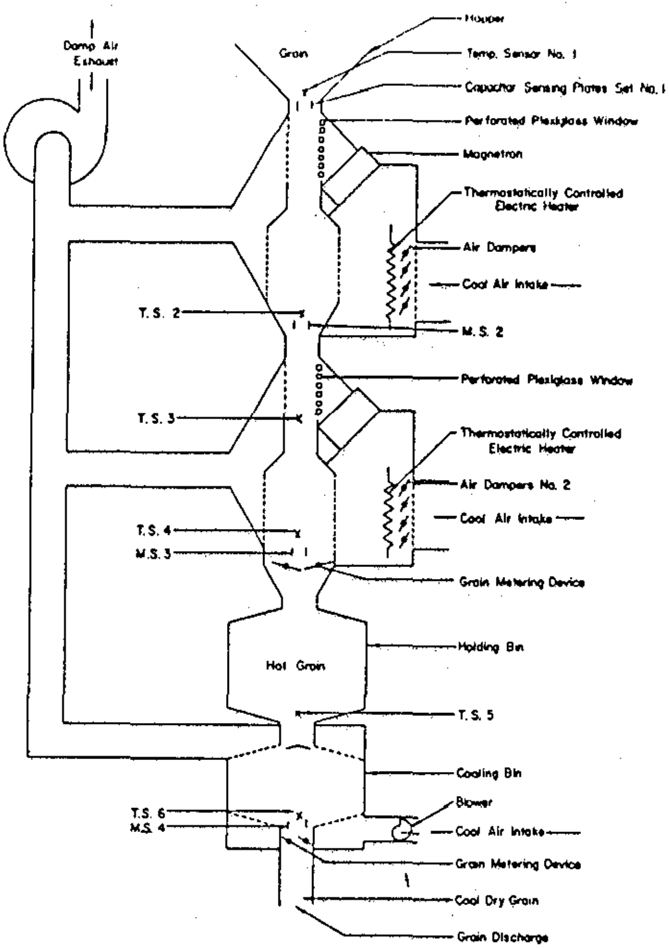

(c)

Figure 6.22
Microwave Moving Bed Systems[66,67,68].

brief periods of time, i.e. intermittent drying, during which the material is force cooled. From Chapter 8 it will be seen that the products involved here respond differently to the same applied field in regard to the temperature rise. This restriction is not applicable when a vacuum is used. Moreover, the addition of air to the vacuum drying chamber is not required and this avoids the wastage of powered granules.

Dielectric heating has been used in vacuum drying as an alternative to radiative and conductive techniques although the problem here is one of electrical breakdown which, at the pressures used, might be expected to occur at field strengths as low as 1/3, or even 1/300, of the values required at atmospheric pressure (see for example [110]). This constraint limits the use of RF techniques in these applications since it reduces the throughputs which can be dealt with. Nevertheless, the process might still be attractive as compared with traditional conductive and infrared vacuum techniques since floor space, labour, investment costs and maintenance are all reduced for a higher quality product (see for example [34], [53], [70], [78], [79], [157]). However, in most cases, such equipment would be difficult to combine with an existing drying plant and a complete re-design would be necessary.

At present the equipment costs appear to be too high to be accepted by the market. A prototype microwave vacuum dryer working at pressures of between 25 and 50 torr has been built and tested for drying agricultural products. The system operates with two or 4 6 kW, 2,450 MHz magnetrons but handles only a small fraction of the output of an average crossflow dryer. The performance details of this prototype have been presented in many publications (see for example [23], [145], [166]). When the initial experiments with the prototype were carried out the results obtained were not particularly good and showed evidence of considerable heating non-uniformity. In the unit finally chosen the internal tube carrying the material has a much smaller diameter than that of the cavity and the microwave sources are positioned such that reflections are maximised before the energy is passed into the tube (figure 6.23). The processed volume is small and major modifications in existing drying practices would be required [145] if it were to be used. Energy requirements for drying maize from 22.4 to 13.5 % w.b. are 4.2 MJ/kg of evaporated water (1 kWh = 3.6 MJ) [23].

6.10.3 Fluidised Bed and Pneumatic Dryers

In these systems the removal of moisture is accomplished by diluting the material in a stream of heated air. The process is

NOTE: Microwave inlets are not on the same horizontal plane. They are spaced in a vertical spiral to evenly distribute the energy.

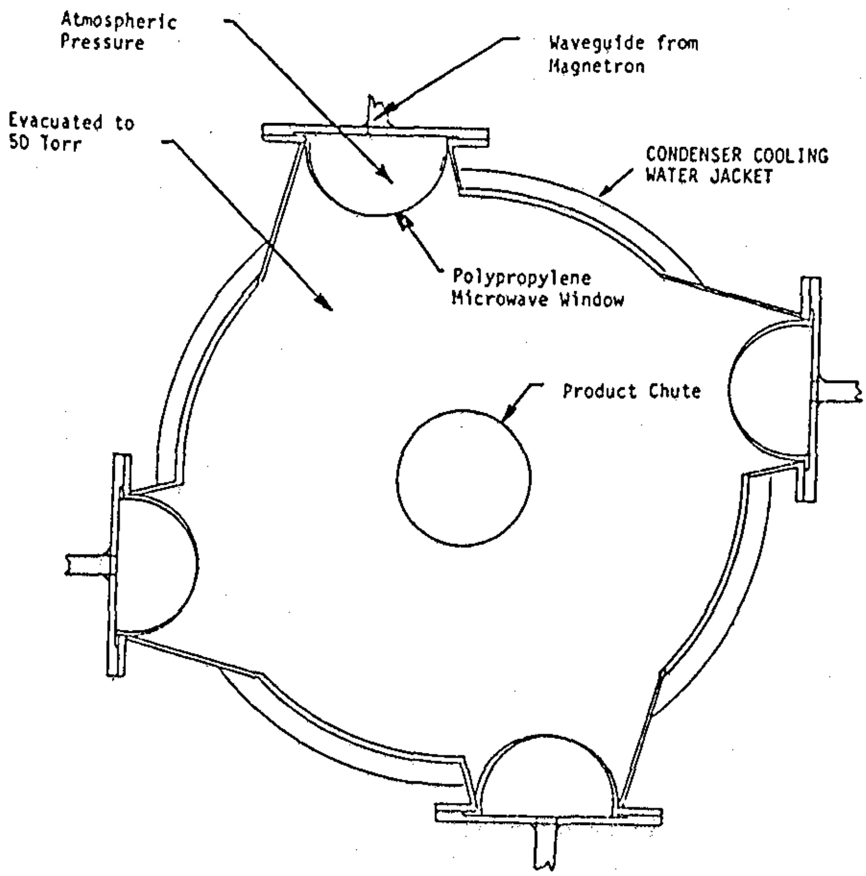

Figure 6.23 Top view of product tube and microwave insertion ports in vacuum chamber[166].

carried out in an enclosure where the material is mixed with the air and which incorporates a collecting device to separate out the dry product. Heat and mass transfer are very efficient and the residence time is short as compared with normal convective techniques although some product damage may result. Moisture content and temperature levels of individual particles are fairly uniform throughout the fluidised bed (see for example [162]), which is not the case in deep bed convection plants as noted above (Chapter 2). Desrosier and Sivetz [42] have reported on failures using the fluidised bed technique applied to coffee possibly due to wide differences in the size of individual particles. Whilst it is likely that the addition of dielectric heating would bring about an improvement, a radical re-design of existing plants would be needed.

7. DISCUSSION OF ALTERNATIVES AND CHOICE OF DRYING SYSTEM

7.1 Energy Applied from Outside the Product

As far as convective heating systems are concerned, resistance units using metal sheated elements are convenient. They can be accurately controlled and provide a high degree of flexibility and reliability for the drying process. They can easily be adapted to existing plants and save valuable space in the latter.

Another electroheat option is to supply the heated air by means of a central electric boiler supplying steam to several heat exchangers in the plant. Although this is not so flexible and convenient as resistance heaters, it results in a considerable economy of scale and, if high voltage units are used, it may be possible to avoid using transformers by connecting the boiler directly to the distribution voltage.

Electrical equipment required for convective heating applications is already developed and highly efficient systems are available at relatively low costs per unit of installed power. This technology does not offer major contributions in terms of enhancement of heat transfer in the process itself apart from the well known advantages of electrical systems when compared with the combustion alternatives. Its use is nevertheless attractive when low prices of electricity are offered to industry. The relative prices of energy products is therefore the main variable to be taken into consideration since, as noted above, the investment costs of this type of electrothermal equipment are much lower than petrol and biomass fired combustion systems.

The relative advantage of electrothermal processes over combustion systems has induced some confusion to the evaluation of many retrofitting projects. Convective electric heating equipment is sometimes seen as the only electrical alternative to combustion and as a novel technique for drying. This is not so since, as far as convection is concerned, the most important variables are the temperature and flow of air independent of the energy source used to heat up the air. There still is much work to be done in enhancing the performance of most convective dryers. This work, however, is likely to be concentrated in the development of more energy efficient processes by means of mathematical modelling to simulate schemes for drying different products.

Radiative heating techniques are an alternative to many convective heating plants, it is possible to obtain very high rates of heat transfer to the material with short and medium wavelength sources, far greater than when solar radiation and natural convection are used. Forced convection systems are limited by the maximum temperatures and velocities of air which can be achieved in practical dryers. Where agricultural products are concerned, the use of infra-red is limited to only a fraction of its potential (e.g. table 4.3) due to the temperature limitations and the low thermal conductivity of the product. This constraint removes from infrared the major potential advantage which is to increase the throughput by means of increasing the rate of heat transfer to the product up to the point where the amount of heated air required by convection to match infrared would be prohibitive.

Even though infrared might be more effective than convection at a given stage in drying a particular product, the rates of radiative heat transfer which can be achieved with flames produced by combustion of biomass gases are equivalent to those from infrared electric equipment which emits the major part of its radiation in the range 1.0-2.0 μm. Therefore the conditions in which the latter is to be prefered are equivalent to those discussed above for convection systems. In the case of infrared systems, however, the use of electrical equipment instead of combustion is more difficult to justify since in the latter case only the burner systems are required and the heat exchange sections are not needed.

Taking into account the above and considering that conduction is not convenient for drying most of the products of interest due to their low thermal conductivities and sensitivity to high temperature levels, it is considered that as far as the scope of this report is concerned, internal heating is the only option which should be pursued further as a potential alternative to convection in drying applications.

7.2. Energy Dissipated Within the Product

Several alternatives for the dielectric drying of granular products were presented in the previous Chapter. There are so many unknown variables to be taken into account that a precise evaluation of the options is not possible based on quantitative criteria alone. Most of the applicators proposed have not been developed and there is a substantial lack of information concerning the performance of the systems even at an experimental level. The maximum throughput levels which can be achieved in each application will be determined by the final use and characteristics of the product as well as the dielectric, thermal and physical properties which have been used in the assesment presented above. Nevertheless it is considered that the criteria previously proposed can be applied to the pre-selection of the best drying systems. By incorporating the different models for the dielectric properties of the materials into the formulae and criteria developed in Chapter 6 it is possible to analyse several operational characteristics of the proposed systems. These characteristics can be studied under different conditions of the electric field breakdown strength and frequency, filling factors, thermal and physical properties of the materials, temperature increases from beginning to end in the drying process, maximum levels of dielectric power density, constructive details of the applicator, etc. The calculations required in Chapter 6 are tedious and laborious but the results can be conveniently examined on a computer spreadsheet in which all the parameters refered to can be easily modified so giving increased analysis capability. The tables displayed in the previous Chapter come from this analysis considering the most likely conditions.

Based on the above results the following systems appear to be the best alternatives:

1. Circular waveguide conveyor;

2. Microwave multimode conveyor;
3. RF cross flow conveyor;
4. RF cross flow vertical system.

Considering first type 1, the screw conveyor appears to be more appropriate than the tube, in both cases eq (6.14c) has been employed due to the difficulty in deciding which formula should be used to relate the internal to the external field during breakdown. This choice may give a conservative estimate of the maximum throughput which can be achieved (see a discussion on this effect in Section 6.9.4). The same can be said in regard to the vertical cross flow system. However, for the latter there is experimental evidence that using eq (6.14c) for this configuration gives fairly good agreement with the actual breakdown occurrences (see Chapter 8). In any event, if eq (6.14c) gives conservative throughput levels, this will result in an increased advantage with options 1 and 4 above. Type 1 applicators would require a single microwave source. Although, in theory, a perfect matching of several sources would produce a desired mode of oscillation at microwave frequencies, in practice this is difficult to obtain. This affects dramatically the economics of single-source microwave drying systems because the price of an installed kW of microwave power increases with the power levels required. Thus, at present, large power (greater than 100 kW net output) microwave heating units need to be based on the use of multiple power sources in multimode cavities. This is convenient in economic terms and also enhances the uniformity of the field distribution in the drying zone. In practice a circular waveguide (type 1) is limited to a fraction of the maximum power levels considered in the previous Chapter (table 6.10) since a large source would result in a non-feasible investment.

The single-source circular waveguide conveyor is a promising alternative for small and medium size plants in which each dryer would process something in the range of 500 tonnes of rice per year (considering a 0.3-0.4 m^3/h unit operating 2,000 hours per per year). In this case a single 60 kW magnetron could be used for the circular waveguide.

RF valves are supplied with output power levels in excess of 400 kW (at 27.12 MHz) (see for example [43] and [114]). Therefore, no problems are anticipated when processing large volumes of material since either single or multiple power units could be used if necessary. This is not a problem since Brown Boveri Ltd has been selling for many years RF heating equipment rated at 900 kW for chipboard manufacturing industries.

One point concerning the RF crossflow systems described above is the relatively low voltage levels which are required on the electrodes even when large dielectric power densities are employed. If this power density is in the range of 300 kW/m^3 the voltage on the electrodes does not need to exceed a few kV. This results in very low oscillator voltages indeed, especially if a variable-coupling system is incorporated between the oscillator terminals and the electrodes. Low voltage oscillators require lower anode voltages on the valve resulting in cheaper RF power components, rectifiers and transformers.

Hamid et al [68] estimated the costs of a complete RF drying system at 40 % of those of an equivalent microwave unit. Perkin arrived at similar figures when comparing RF and microwave power sources larger than 150 kW, he assumed the lifetime of RF power sources to be twice that of microwave units [133]. In a more recent report the same author states that whenever the two alternatives, i.e. microwave and radiofrequency, could be used in a given application, RF is to be preferred due to the lower investment costs and system simplicity [132].

In terms of floor space requirements, the crossflow vertical system appears to be the most favourable option, followed by the two types of conveyor. It is considered that both microwave and RF conveyors would need approximately the same space and require some modifications to the plant.

The four types of applicators listed above can achieve relatively large throughputs, the RF systems are capable of drying certain materials (e.g. cereals) with no recirculation. The processing of coffee and soya would have to be done using several passes through the latter applicators since those products are much slower drying materials (see Chapter 8). The multimode conveyor is the unit which gives the largest throughputs per unit of material in the drying zone. This, however, may only be important for materials which can withstand high levels of internal energy dissipation, since other products would be limited, by qualitative considerations, to levels of throughput smaller than those defined by electrical breakdown considerations. The RF vertical cross flow system is also capable of processing large amounts of product, a twin vertical system is a convenient alternative for obtaining high throughputs in limited space. In practice it should be competetive with the multimode conveyor as far as throughput is concerned, provided that the products are not dried from extremely wet conditions. For example, if coffee was introduced at M_1= 48% w.b. into the RF cross flow system, the throughput of the apparatus would have to be reduced to one fifth of that which could be obtained if the beans were introduced at, say, M_1= 21% w.b. if breakdowns are to be avoided.

Considering the factors discussed above, it is possible to rank the four pre-selected applicators in decreasing order of merit in accordance with the criteria shown in table 7.1. The numbers refer to the order of the applicators in the list at the beginning of this section.

Criteria	Order of Merit		
	First	Second	Third
Cost of power source	(3,4)	2	1
Life of power source	(3,4)	1	2
Large throughput with limited floor space	4	(2,3)	1
Need for recirculation	(3,4)	2	1
Energy efficiency of the applicator and source	1	(2,3,4)	

Table 7.1 Ranking of Dielectric Drying Systems.

Options 4 and 3, i.e. the cross flow RF systems, appear to be the most acceptable alternatives, they are extremely flexible, capable of handling large ranges of throughput in the same applicator and, being electric equipment, they could easily be controlled or automated. Once the basic applicator, i.e. the electrodes and ancillary systems is installed further changes in the power levels would only require the installation of more power capacity and adjustment to the voltage levels and tuning components. The dielectric drying capacity could evolve more in the drying plant in response to changing economic scenarios. If the pre-drying, or convective (heated air), part of the operation is supplied by combustion it would be important to prevent the passage into the high field zone of carbon rich particles and gases which would increase the probability of breakdown. A heat exchange system would eliminate most of these risks.

A more in-depth examination of the feasibility of options 3 and 4, i.e. the drying by dielectric (RF) techniques assisted by cross flow convection is thus justified by the arguments presented above. It will be shown below that although the results obtained can be directly applied to the RF cases, they would also be valid for an ideal cross flow microwave system in which sufficient power uniformity were achieved. In most cases this would require the use of multiple source feeding and also that the thickness of the bed of material in the drying zone be much smaller than the power penetration depth. In the next Chapter the experimental methods and apparatus used are presented, the drying rig was developed for use with high frequency energy sources operating in the radiofrequency band.

8. EXPERIMENTAL WORK

8.1. Measurement of Dielectric Properties

8.1.1 Introduction

The dielectric constant and loss factor of the materials involved are important parameters in this study. They have been used throughout this Report in the evaluation of the operational characteristics of dielectric drying systems and, in conjunction with other experimental data, for designing the experimental rig and in the study of the performance of the drying process.

8.1.2 Experimental Equipment and Methods

The dielectric properties of soya, maize, coffee, rice and wheat were measured in the radiofrequency band using a TF 329G Marconi Q-factor meter and a dielectric sample holder (figure 8.1) which was specially constructed as a coaxial capacitor following similar methods and procedures suggested by other workers (see, for example, [21], [89]). Three centre frequencies were selected for the measurements: 13.5, 27 and 40 MHz. These are the most important frequencies for radiofrequency heating applications although the first two, and especially the second,

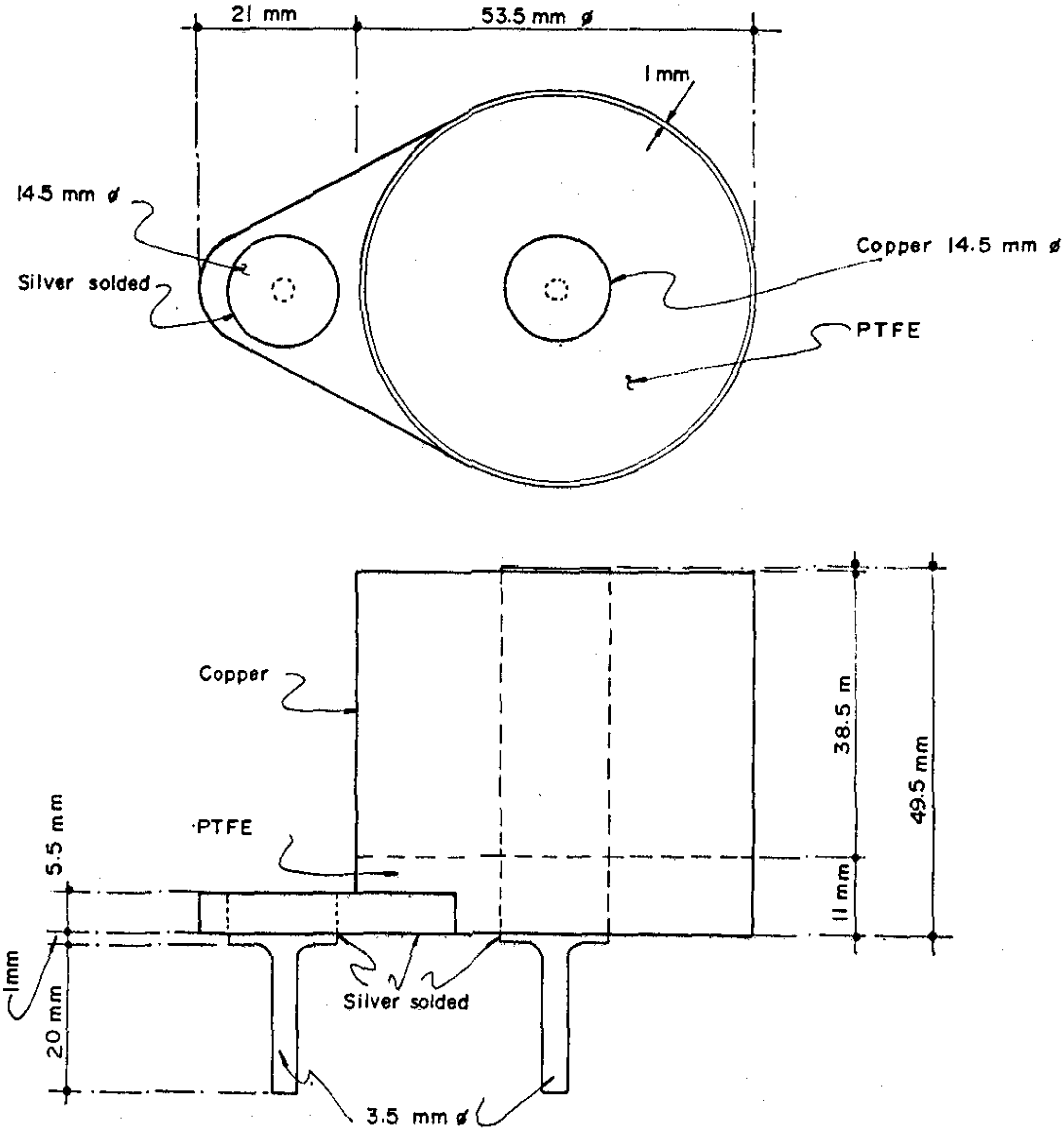

Figure 8.1 Coaxial Dielectric Sample Holder.

are more usual in present day applications. Most of the existing data refers to cereal products, namely wheat and maize, a few data points for rice are also found in [175]. There is also recent information on the dielectric constant of soya [121] in addition to the results presented by Jones et al [89]. The model used by Nelson for the dielectric constant of soya requires the density of the material as a function of moisture content to be known. No data has been found in the literature for coffee, this is understandable in view of the fact that almost all the data published is for crops produced in the U.S.A. It was not possible to obtain significant quantities of the most common yellow dent type of maize in the UK and pop-corn was used instead. The dielectric properties of this material are, however, very close to those of yellow dent maize obtained by Jones et al [89] and S.O. Nelson as will be seen below. Maize, rice (long grain), wheat and soya beans were obtained from local shops, the unroasted ("green") coffee (identified as "Brazilian") was also acquired from a local coffee roaster. The experiments were carried out between the Autumn of 1986 and the Spring of 1987.

Some authors have used freshly harvested products for drying studies (for example [150]) and the measurement of the dielectric properties of the material (see for example [175]).

In this procedure the material is usually collected and then frozen until required. Most workers however have added water to the dry product and then stored it at low temperatures (between 4-10 C) to obtain a moisture equalization and prevent fermentation or mold attack (see [16], [32] and [122]. Nelson [122] states that the differences between the properties of rewetted agricultural products and freshly harvested ones are minimal. The method followed in this study was to soak the dry products for 36 hours at 15 C after which the water was drained and the material stored in sealed glass jars for 3-10 days at 5 C. The product was stirred several times during the soaking period and agitated for a few minutes every 8-10 hours during the first day of storage. After the storing phase the jars were opened and the measurements begun as soon as the temperature of the product reached equilibrium with the external ambient value (18-24 C).

The moisture content of the material, expressed on a per-unit wet basis (w.b.), is

$$M = [(W_{wet}+W_{dish})-(W_{dry}+W_{dish})]/[(W_{wet}+W_{dish})-W_{dish}]$$

Where W_{wet}, W_{dry} and W_{dish} are the weight of the wet and totally dry material sample and the weight of the dish used to hold the sample on the balance and to dry it in an oven. A balance with a minimum reading of 0.1 g was used and the weight of the totally dried sample was obtained after the material had spent 72 hours in an oven at 110 C.

The capacitance and Q factor measurements were performed for various moisture content and temperature levels. In each experiment at least 14 pairs of values were obtained for the dielectric constant and loss factor from very wet to almost totally dried (down to 2% w.b.) material at ambient temperatures, and from ambient to high temperatures (up to 115 C) with the dry product. The same experiment was repeated at least 5 times when studying the variation with moisture content, and at least 3 times in the temperature effect study.

The experiments investigating the effect of temperature were carried out after the product samples had been heated by an air blower and placed in the coaxial capacitor which incorporated an insulated cover and cap. These modifications to the sample holder may have contributed to the small difference (less than 5 % at 40 MHz and approximately 1.5 % at 27 MHz) between these results and those obtained from the average values of the unloaded holder Q factor observed in the earlier moisture variation experiments. No differences in the two sets of results were observed at 13.5 MHz. These small variations were accounted for in the calculations and all the initial capacitance and Q factor measurements at different frequencies were repeated for each individual temperature variation experiment.

The cap was provided with three small holes at different positions through which a temperature probe was inserted at three points along the diameter of the sample holder. The final temperature was defined as the mean value of the three readings.

The readings taken from the experiments were fed into a microcomputer spreadsheet which calculated the dielectric constant and loss factor using as inputs the values of weight, volume and temperature of the product samples together with capacitance, Q factor and dry weight. A sample printout of the spreadsheet used is shown in Appendix IV. The experimental arrangement is shown in figure 8.2.

8.1.3 Experimental Results and Discussion

For a given product and frequency the same experiment was repeated several times with different samples of material. The resulting figures for e′ and e" will not all fit in a smooth

Figure 8.2 Experimental apparatus used for measuring dielectric properties.

curve since, as noted above, variations should be expected when working with different samples of non-homogeneous materials and also due to the measuring method used which incorporates in the calculations small differences of electrical parameters. These in themselves are very sensitive to stray capacitance effects.

In order to fit the data to a mathematical expression, two approaches were adopted in studying the moisture effect.

First, the points remote from the bulk of the data were excluded from the regression analysis. This procedure was not followed with the temperature dependent data since many fewer data points were obtained in these experiments. The exclusion of data points involved a certain degree of subjective judgement which may affect the final results. Several curve functions were examined, namely linear, inverse, exponential, quadratic (parabola) and cubic. The resulting models were then compared in terms of the standard deviation (S_e) and the square of the coefficient of correlation (I^2). S_e is the mean of the differences between observed and predicted values. It measures how closely the model describes the actual observed quantities. The units are the same as those of the dependent variable. I^2 is a ratio that expresses the degree in which variations in the values of the dependent variable can be explained by those of the independent ones, its value ranges from 0 to 1. The values for I^2 need to be carefully related to those of S_e. For example, a given correlation may yield a very low S_e and I^2 and still represent a good result despite a low value of I^2 (which ideally should approach 1). This would be the case of a constant, when the value of the dependent variable is certainly not affected by those of the independent ones. The models finally chosen are presented in Appendix IV. In this Appendix the corresponding graphs showing the variation of e′ and e″ with moisture content at 40 MHz are also shown. The a,b,c and d entries in the tables A.6-A.13 refer to the constants in the equations which are usually of the cubic type, i.e. $e', e'' = a + b(M/100) + c(M/100)^2 + d(M/100)^3$ but in some cases a more simple straight line $a+b(M/100)$ was found to be adequate. The moisture content, M, is expressed in % w.b.

The variation in the dielectric properties with temperature is far less (at least one order of magnitude) than that caused by the moisture content. The dielectric constants of all the products studied increases by up to 25 % when the temperature is increased from ambient to 100-115 C. In the case of soya this variation is of the order of 10 %. The effect on the loss factors is much less and is generally negligible with the exception of wheat in which case the variation in the loss factor is of the same order of that of the dielectric constant, i.e. around 25 % in the temperature range considered above.

Secondly, it was considered that expressions which described the variation of the loss factor and dielectric constant of each product with moisture content (M) and frequency (f) of the applied field would give a more general type of model, although some degree of precision might be lost. In this case all the data obtained from the experiments were used with no exclusion of extreme data points.

Two families of multiple regression models were used to fit the data: the parabolic type, i.e.

$$e', e'' = b_1 + b_2 f + b_u f^2 + b_3 M + b_v M^2$$

and the straight line,

$$e', e'' = b_1 + b_2 f + b_3 M$$

in both cases the frequency, f, is in MHz.

For each of the above forms several transformations were applied, e.g. natural logarithmic (LN(x)), cubic, etc yielding various curvilinear model combinations. The straight line type of models proved to be an acceptable choice, these are listed in Table 8.1 below.

Product	Moist.Range	Model	S_e	r^2
Maize	7-35 %w.b.	$e'=(2.50-3.03E-2f+0.14M)$	0.46	0.866
Maize	7-26	$e''=(8.69E-3-2.97E-3f+0.29LN(M))^3$	0.05	0.976
Rice	4-26	$e'=(1.42-6.25E-2LN(f)+1.68E-2M)^3$	0.38	0.830
Rice	4-26	$e''=(0.67-7.38E-2LN(f)+1.70E-2M)^3$	0.43	0.720
Soya	4-26	$e'=(1.40-9.25E-2LN(f)+2.35E-2M)^3$	0.35	0.913
Soya	4-26	$e''=(0.48-7.56E-2LN(f)+3.26E-2M)^3$	0.38	0.928
Coffee	12-45	$e'=(1.56-0.12LN(f)+1.71E-2M)^3$	0.37	0.919
Coffee	12-45	$e''=(0.83-0.14LN(f)+2.17E-2M)^3$	0.51	0.723
Wheat	8-26	$e'=(1.45-9.71E-2LN(f)+2E-2M)^3$	0.50	0.657
Wheat	8-26	$e''=(0.65-7.87E-2LN(f)+1.41E-2M)^3$	0.41	0.771

Table 8.1 Expressions for the variation in the dielectric constant and loss factor of agricultural products with moisture content and frequency. Frequency range: 13.5-40 MHz. Temperature range: 18-22 C for soya, coffee, maize and rice; 20-24 C for wheat.

Inspection of the equations in Table 8.1 indicates that the dielectric constants and loss factors increase with the moisture content and decrease with the frequency of the applied field in all cases.

The mathematical expressions obtained for the dielectric constant of maize and wheat were then compared with those developed by S.O. Nelson. These consider the frequency and moisture dependence as above and also the effect of bulk density [120, 123]. There appear to be no published models of the dielectric constants of other products which can be included in this comparison, nor is any model for the loss factor available. Some data obtained from the curves derived by Jones et al [89] were also included in the comparative analysis.

On inspection of the variation in e′ with moisture content at the three major RF bands, i.e. 13.5, 27 and 40 MHz it was noted that, above approximately 16-18 % w.b. the models depending on both frequency and moisture practically coincide. At low moisture contents, 10-12 % w.b. the difference between the two is a maximum, in general of the order of 20-30 %. The moisture dependent models for each frequency (presented in Appendix IV) exhibited similar percentage differences compared with the Nelson′s results. For wheat the moisture dependent expressions are in closer agreement with Nelson and for maize this is true of the models depending on both frequency and moisture (presented in table 8.1). The data reported by Jones et al is, generally, in very good harmony with both models developed in the present work. For maize the frequency/moisture model is in close agreement with the earlier workers. In the case of wheat the moisture dependent models are marginally more appropriate.

8.2 Dielectric Drying Experiments

8.2.1 Introduction

High frequency methods appear to be promising techniques for many drying processes but there is still a need for more engineering design data related to the performance of these systems before costly prototypes are built. Power, temperature and breakdown limitations of the processes may limit the throughputs for certain materials and the effects produced by different air and ambient conditions together with the high frequency field parameters also need to be examined with regard to their effects on the resulting drying rates. For these reasons an experimental dryer was constructed and used in actual drying tests as described below.

8.2.2 Experimental Apparatus

An experimental high frequency drying system was developed using RF generators operating at around 40 MHz. The rig was designed in such a way that convection, environmental and high frequency parameters could be determined for incorporation in the design of drying equipment. The unit was designed and built between the Autumn of 1986 and early Summer 1987 and has been succesfully operated since that date. The main objective as far as the work reported here is concerned was to analyse the feasibility of the process and to arrive at design methods and parameters for future prototypes.

For the radio-frequency system the power density term $f(\vec{E},M)$ can be found from eq (6.31). It is affected by the electric field, frequency and moisture content. In order to avoid deep-bed air drying effects affecting the situation, a small thickness must be used, in this study a layer of product 5 cm thick was adopted in order that the air conditions could be assumed to be reasonably uniform across the bed. The following variables are required in order to predict the drying time of a specified product in the dielectric heating system:

E; electric field strength in the bulk of material (kV/m)

M_t; target moisture content of the product (% wet basis)

M_i; initial moisture content of the product (% wet basis)

M; moisture of product at time t (% wet basis)

t; time (mins)

The target moisture content is defined here as that required to give the required product quality. In air drying studies the equilibrium value can be used but where internal heating methods are involved as here, then, in theory, the material can be dried down to zero moisture content regardless of the ambient conditions. For coffee, for which equilibrium moisture equations were unavailable, a constant target moisture content of 13 % w.b. was used. In the case of the other products M_t was taken as the ideal equilibrium moisture contents for storage under normal ambient conditions (temperature and relative humidity) prevailing in the laboratory. The equilibrium moisture contents were evaluated using the Henderson type models given by Chung et al [33]. For this purpose a Casella Assmann Hygrometer was used to assess environmental conditions during the experiments.

In all the dielectric drying experiments carried out in this study the air temperature was the ambient value and the air flow was maintained approximately equal to that found in typical agricultural drying plants. Any heating of the surface of the product affords no enhancement to the internal drying mechanism, it merely increases the amount of energy supplied to the surface (see Chapter 2). However increasing the flow of air may help to force cool the material although it will not increase drying in the falling rate period. The same is true of the relative humidity of the air in the drying zone since only in extremely damp conditions are its effects significant (see for example Allen [5]. Many previous workers have only considered the effect of the relative humidity on the equilibrium moisture content but when dielectric heating is used, the equilibrium moisture contents cannot be defined. Hence the importance of the relative humidity of air is likely to be reduced further in most applications. In any event the experimental drying apparatus used here was designed in such a way that all the above effects could be studied later if required.

The prototype was designed around a pair of capacitor plates between which the material was contained (see figures 8.3 and 8.4). This was the only practical method which was found possible to simulate a real plant which, in practice, might be of the conveyor or moving bed (vertical) type. The results obtained are considered to be directly applicable to the RF cross flow drying systems examined in Chapter 6 and also valid for an ideal cross flow microwave system in which sufficient power uniformity can be achieved. The latter would require the results to be expressed in terms of the dielectric power densities instead of the electric field strength. This is discussed further later in this report but to be fully relevant to the microwave case then a multiple source feeding arrangement would be required and also the thickness of the bed of material in the drying zone would need to be much smaller than the power penetration depth.

The dimensions of the capacitor plate system need to be small to guarantee that the standing voltage effect is negligible for all the frequencies likely to be used in the rig and the frequency used should not be so low as to cause electrical breakdowns when operating the unit at the required power levels. Depending on the dielectric properties of the granular material under consideration and on the throughput required, the equipment finally developed could be used in the frequency range of, say, 5 to 50 MHz. The higher frequencies are limited by the dimensions of the plates and at lower frequencies breakdown is the major problem. This could be overcome by increasing the spacing between the plates or by reducing the voltage levels although this would considerably reduce the drying rates obtained.

The plates must be larger than the cross sectional area of the product sample in order to avoid field distortions at the edges. From table 6.16 it is seen that 0.3x0.3 m^2 is an appropriate dimension for the capacitor plates if the voltage variation has to remain below 10 % when the RF feed is connected near one extremity of the plate. The plates also need to be perforated since air must flow through the product to carry away the surface moisture (see figure 8.4). A duct system was designed to carry the air and connected to the perforated plates which form the electrode system. The cross sectional area of the duct from the air intake to the outlet of the drying zone is identical to that of the sample of material, i.e. is 0.2x0.2 m^2.

The plates were made from stainless steel. One of the plates, and the associated section of air duct, was connected to earth, the other electrode (the high voltage plate) and duct section were insulated (see figures 8.3 and 8.4). The earthed plate and duct section are movable in order to allow the interelectrode spacing to be varied. The earthed section of duct incorporates the air intake and the instrumentation which is

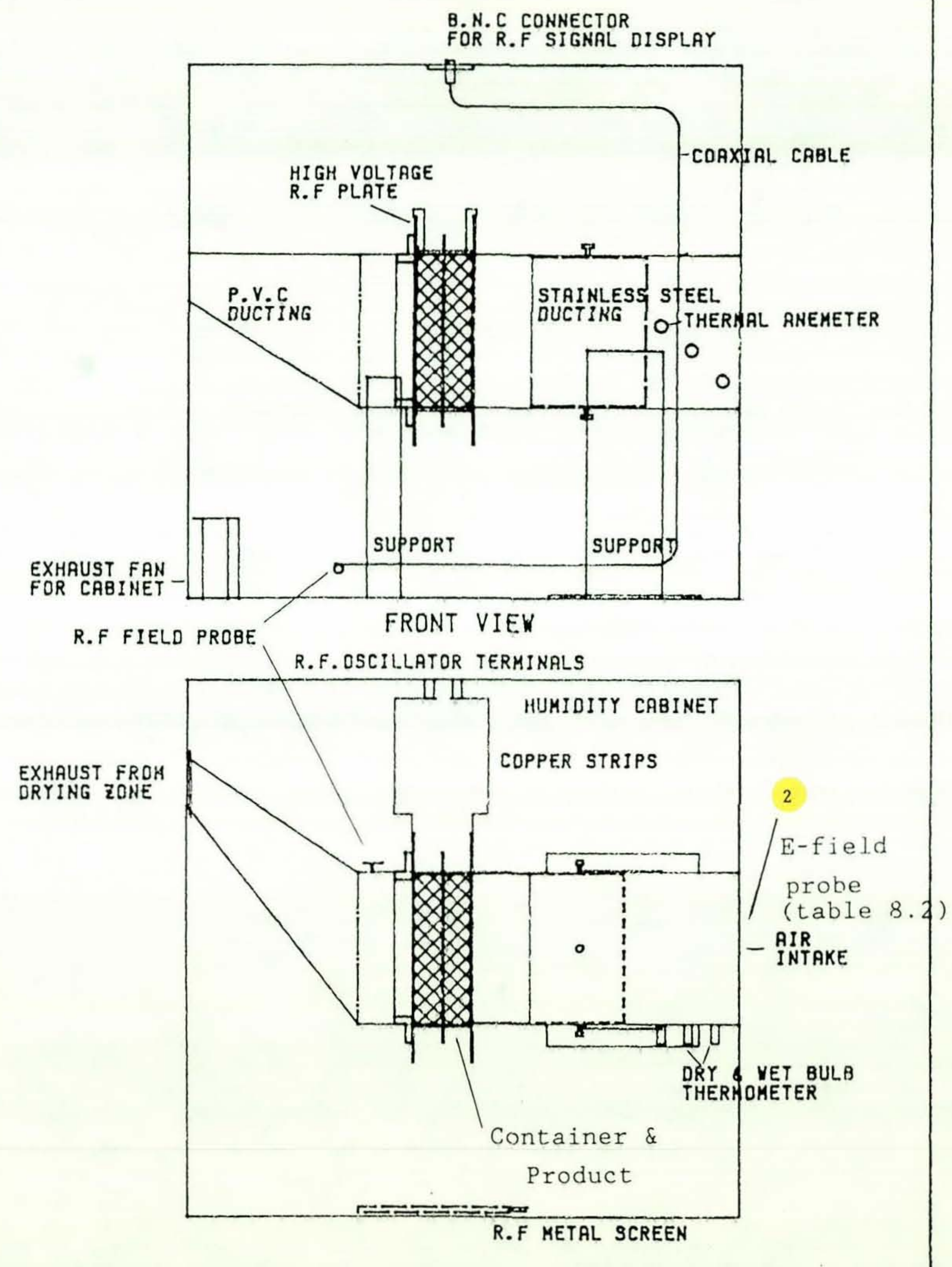

DIELECTRIC DRYING RIG	VIEW INSIDE HUMIDITY CABINET
25 SEPTEMBER 1987	PROJECT F.P.CALDAS
SCALE 1:8	Figure 8.3 DRW. P.BARRINGTON

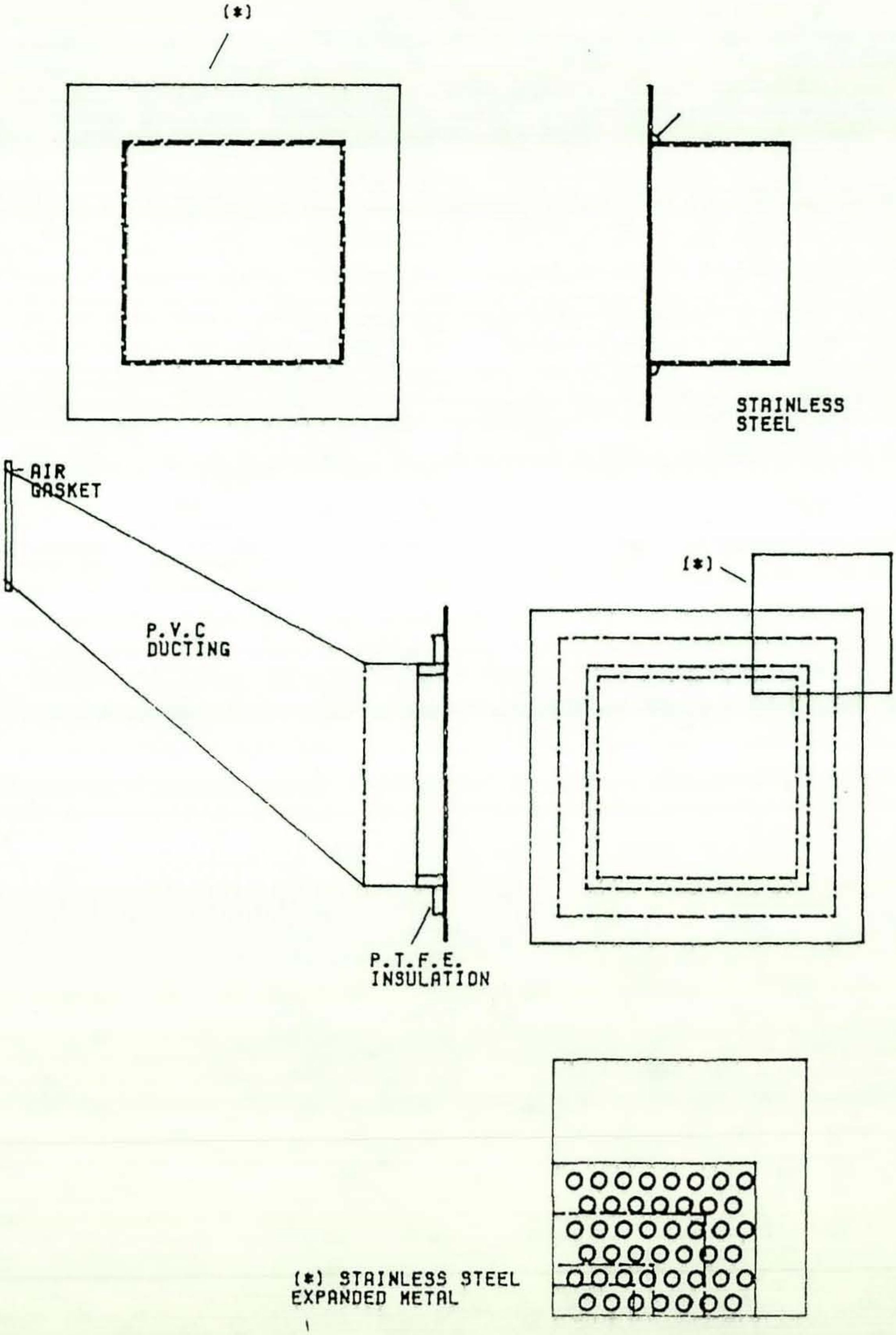

DIELECTRIC DRYING RIG — DUCTING AND PLATES

25 SEPTEMBER 1987 — PROJECT F.P.CALDAS

SCALE 1:8 — Figure 8.4 — DRW. P.BARRINGTON mounted here in order to avoid interference from the RF field. The duct is manufactured from aluminum. The second duct section begins at the junction of the drying zone outlet and the high voltage plate. It carries the exhaust air from the drying zone and is manufactured from P.V.C. The duct system and plates are joined by fixing screws in order to allow for ease of electrode replacement

The air flows used correspond to those found in typical convective dryers, i.e. 0.25-0.41 $m^3/sec/m^2$. With a cross section of the duct equal to $0.2 x 0.2\ m^2$ then the air flow needs to be within the range of:

$$(0.25\text{-}0.41\ m^3/s) x 0.2 x 0.3 = 0.01\text{-}0.02\ m^3/s,$$

which is equivalent to an average velocity of

$$(0.01\text{-}0.02)/0.04 = 0.25 - 0.50\ m/s$$

The thickness of the layers of material in typical convection plants would be larger than those which would probably be adopted in high frequency units. As mentioned previously in this report, typical cross-flow beds can be as thick as 30 cm or more and it is unlikely that in a full-sized dielectric drying plant the bed of granulated material would be so thick, as this would require higher applied voltages (see Chapter 6). In turn this would mean that a given installed ventilation plant would be able to produce a greater air flow due to the lower resistance of the material bed. Hence, in practice, the air flow velocities would be somewhat greater than those given above for typical convective dryers.

This range of air velocity is too low to be measured with a Pitot Tube (see for example [1], pgs F13.14,15). A thermal anemometer would be preferible. An AVM501TC Prosser velocity meter was used in this case. This type of instrument measures the velocity of air by determining the electric current required to keep constant the temperature of the sensor element in response to the heat transfer which takes place between the element and the air flow.

In order to retain the product between the electrodes and to allow the weighing and other experimental procedures to be carried out, it was necessary to design a suitable container. The dimensions of the container were fixed according to the size of the plates and the separation between them, the construction material needed to have zero, or very low, loss. Before finally selecting the container material, several alternatives were considered. As well as a low loss factor the material is required to have a relative permittivity close to that of the product and be able to withstand temperatures of the order of 150 C. Several nylon products were tested but failed on the temperature requirement. It has also been reported that the loss factor of Nylon changes excessively with temperature (see for example [110] and [165]). A study of the data for the dielectric properties of materials given in Von Hippel [165] indicated that bakelite, mica, silicon based plastics, and polyvinyl resins would be adequate as far as dielectric properties and temperature requirements were concerned. Experiments with bakelite proved however that this material could not withstand the temperature levels required, the same occurring with many commercially available plastics including PVC. PTFE was then tested. A 1 cm thick block was placed for several hours on a metal plate whose temperature was maintained between 230 and 250 C. The surface of the material in contact with the hot plate was kept at approximately 205 C, the opposite side reaching nearly 100 C. The PTFE experienced no physical deterioration and therefore it was concluded that this material was adequate for use in the construction of the container and other insulated parts of the experimental rig (see figures 8.3 and 8.5). PTFE proved to be an ideal material. The same container was used throughout all the experimental drying runs and at the end of

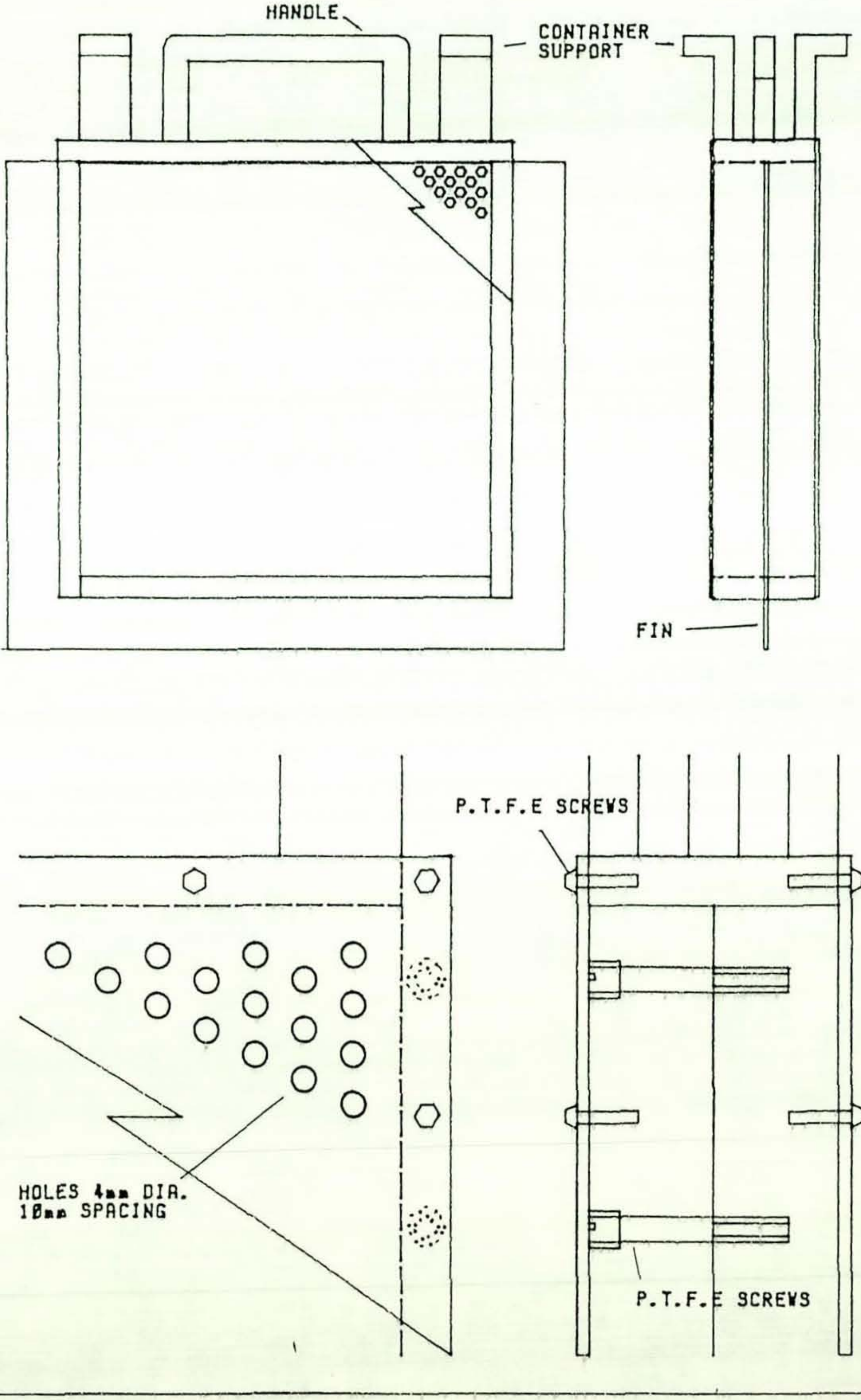

DIELECTRIC DRYING RIG		PRODUCT CONTAINER
25 SEPTEMBER 1987		PROJECT F.P.CALDAS
SCALE 1:8	Figure 8.5	DRW. P.BARRINGTON

these it was still sound. The only PTFE replacement required was after nearly 60 drying runs when a severe electrical breakdown melted part of a thin section of the material between two ventilation holes. This required the substitution of one of the perforated sides of the container. This same section had previousls withstood the high temperatures produced by at least half a dozen breakdowns. PTFE is, however, difficult to machine and, since all the parts of the container, including the joining screws, needed to be made from this material, this part of the work was time consuming.

The container was held tightly between the plates to prevent air gaps and consequent breakdowns. It was important to ensure that the cross-sectional area of the material perpendicular to the air flow did not exceed the dimensions of the air duct. This was done in an attempt to ensure uniform drying conditions in the material. Initially when using the container it was found that condensed water on the sides perpendicular to the plates produced local electrical discharges. In order to overcome this a plastic fin was included in the design. This increased the electrical breakdown distance. For convenience this fin was first made from a strong commercial PVC plastic but this had to be changed to PTFE since, after a few drying runs, the PVC was heated by the RF field and this induced further breakdowns.

As shown in the figures, the RF experimental rig was enclosed in a metal-walled compartment. This was done not only for convenience and electrical safety but also to isolate the system from the outside environment in so far as radiofrequency radiation was concerned. In order to allow the experiments to be carried out under different ambient temperature and humidities, the compartment was, in fact, a Gallenkamp Humidity Cabinet. An exhaust fan for the cabinet was added. This was quite separate from the much larger exhaust fan used to extract the air from the drying zone which is omitted from the diagrams since it is installed away from the cabinet near to the window of the laboratory. The smaller exhaust fan was installed in order to extract toxic gases from the products and, possibly, the PTFE following electrical breakdowns. The front glass door through which the electrode system and load could be inspected included a metal screen which was effective in limiting RF emissions as discussed below.

Interlocks were fitted to interrupt the RF power supply when the door of the cabinet was opened.

After the mechanical and structural problems had been solved the next step was to choose an adequate high frequency power generator. A 27 MHz power source was not available but two alternatives were possible: one at 2 MHz and the other at nearly 40 MHz. The former was an induction heating source which was particularly attractive to the present application due to the closeness of its nominal RF power output to the estimated maximum heating requirements of the process. However, it was considered that the frequency was too low and that breakdown problems may have arisen. Therefore an Intertherm DH83/2 water cooled unit, with a nominal resonant frequency of 38.5 MHz and capable of supplying a maximum of 6 kW RF output was used. This RF generator required a nominal 12 kW three phase supply plus earth and neutral lines in addition to an adequate water supply to cool the valves.

Once the high frequency generator was installed it was necessary to decide on the feeding arrangements for the RF electrode system. The use of a transmission line was first considered. This presented advantages in terms of quick replacement of RF generators but transmission line theory shows that the load must be correctly matched. The load value which allows maximum energy transfer when the load is connected to a generator by a transmission line is the square root of the ratio between the inductance and the capacitance (defined between the two conductors) of the line. Deviations from this value, which is known as the characteristic impedance, will cause wave reflections and resultant standing voltages on the line greater than the voltage on the generator terminals. This effect is likely to produce overheating and possibly breakdown on the line so reducing the energy transfer and overall efficiency.

The use of coaxial cables capable of delivering RF energy rated at 6 kW at several thousand volts was investigated. These cables are normally manufactured with characteristic impedances of 50 or 75 ohms as compared with the load impedance which, in this case, varies from 100 to more than 4,000 ohms as noted below. The use of these cables would require the design and construction of a variable coupling unit between the end of the line and the load, this was not considered to be a practical solution in view of the limited time available. It was finally decided that the terminals of the RF generator should be attached to the capacitor plates by means of an electrical connection as short as possible. This was achieved by mounting the high frequency unit of the RF generator at the back of the humidity cabinet (see figure 8.7). An opening was made on the back of this cabinet through which the two terminals of the RF generator were introduced, the teminals were connected to the electrode system using copper strips. One of the terminals of the RF generator was earthed to the metallic body of the oscillator, this was also connected to the earthed electrode plate.

The RF voltage on the electrodes was varied by means of a three phase variac which changed the mains A.C. and consequently the high voltage supply to the full-wave rectifier bridge which supplies the D.C. input to the anode of the RF valve (see figure 8.6). Care was taken to supply the auxiliaries of the RF generator system with their nominal voltage. A wattmeter was connected after the auxiliaries across two of the lines which supplied the rectification stage. A domestic energy meter was also incorporated (between one of the lines and neutral) in addition to a removable ammeter which monitored the current in different feeders.

Figure 8.6 shows that the coupling from the tank circuit to the electrode system is not direct but is carried out through what is, in effect, a coupling coil.

Ideally both the voltage and the frequency at the electrodes should be continuously monitored but the voltages involved here are too high for direct measurement with conventional RF voltmeters. Several alternatives were considered

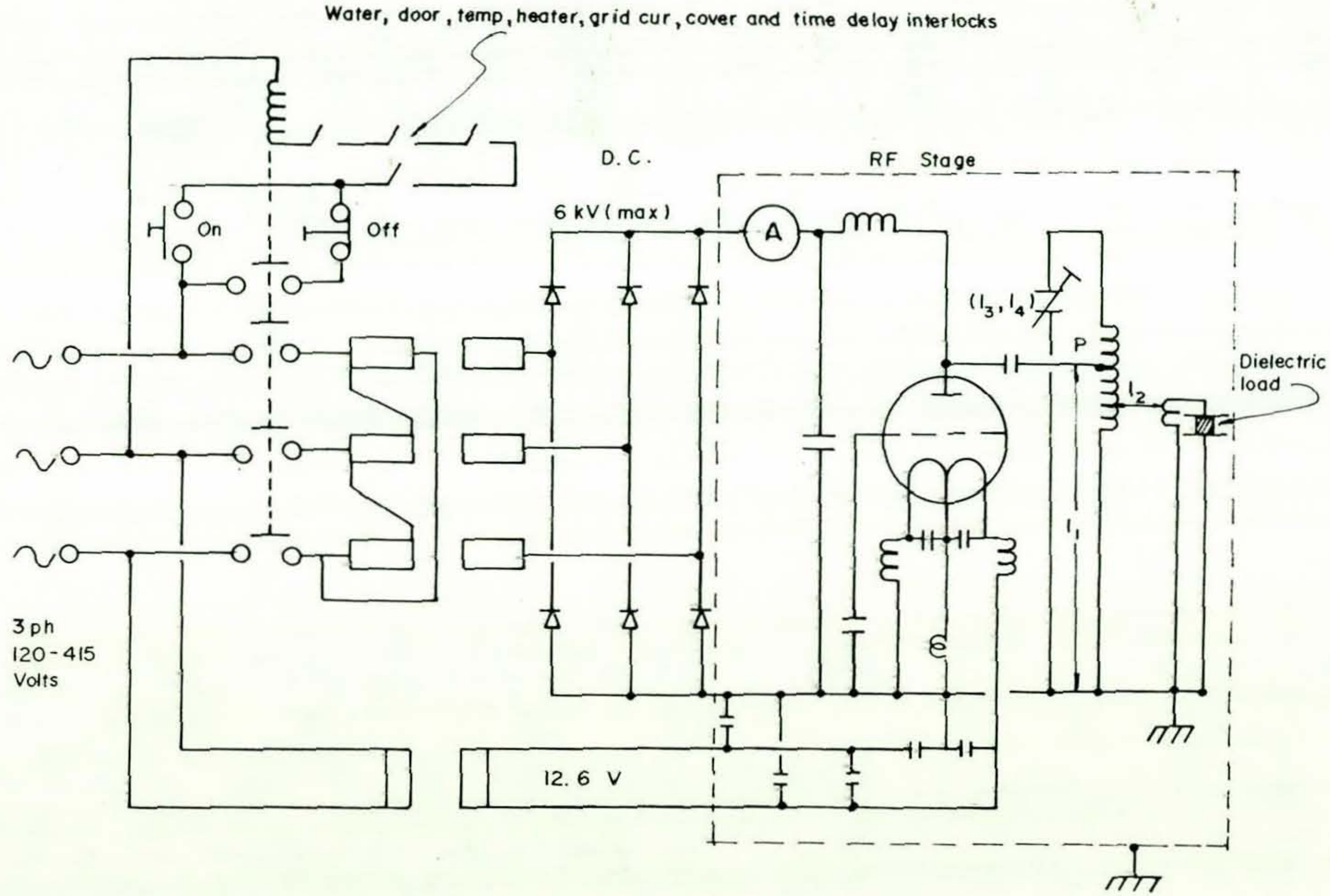

Figure 8.6 Electric circuit of the RF experimental system

(by Mr D. Hackett, Loughborough Univ.).

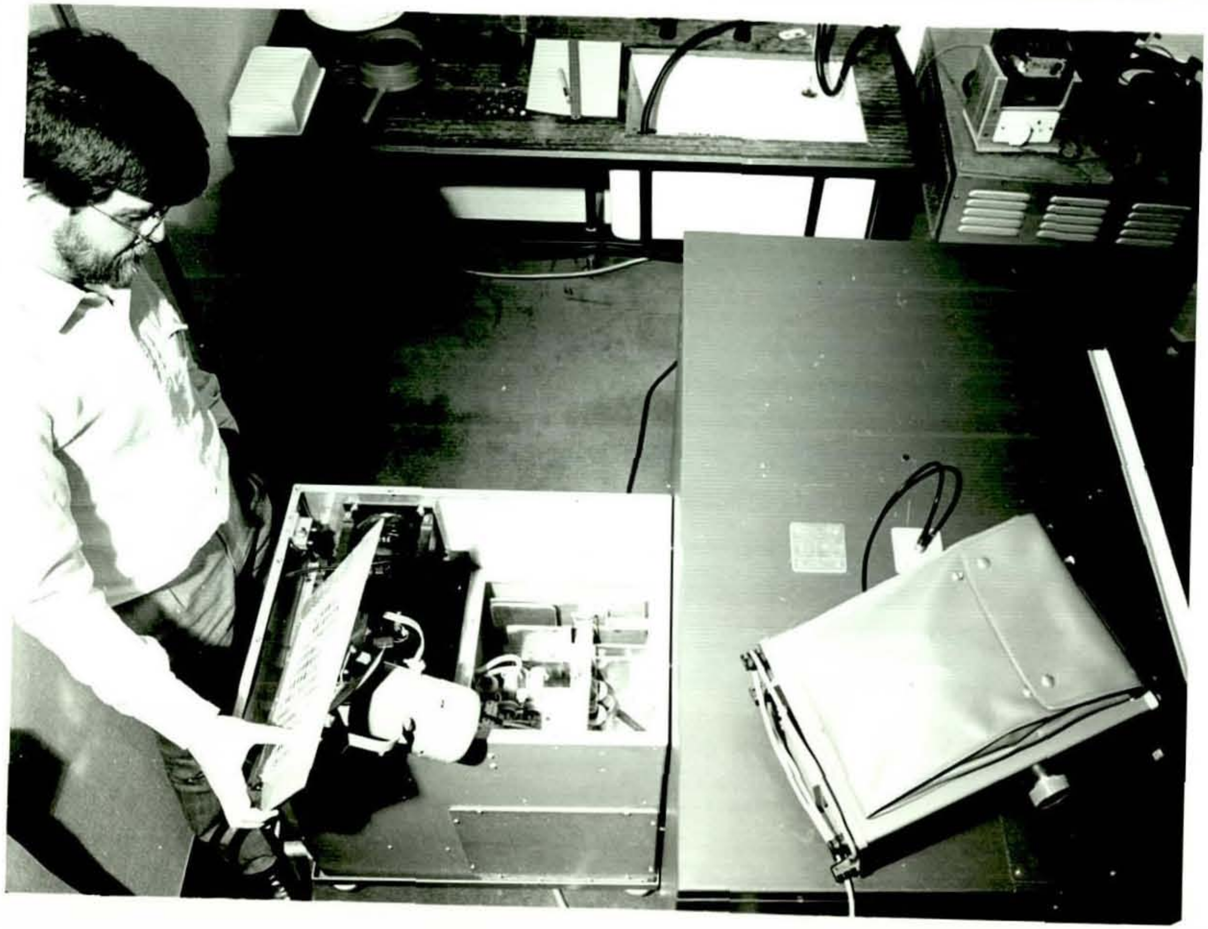

Figure 8.7 Connection between the RF stage of the high frequency generator (left) and humidity cabinet (right).
3 : Location of E-field probe (see table 8.2).

for measuring this voltage by voltage division, many of these were not reliable and would have presented some hazard to the operator. An RF field probe was finally adopted, this was terminated in an inductor coil which was used to detect the electric field. The probe was introduced in the cabinet, and placed in the electric field adjacent to the electrode system. The small RF voltage produced could then be related to the applied high voltage on the plate. Voltage and frequency were then measured using an oscilloscope connected to the probe by means of a B.N.C. connector and coaxial cable (see figure 8.3). The best possible placement of the probe inside the cabinet was dependent on the direction of the axis of the coil and its distance from the electrode system. This was due to the variation of the dielectric properties of the material during the heating cycle, which affected the pattern of the stray fields surrounding the electrodes and consequently the probe measurements. Ideally there would be minimal differences between these measurements when the electrode system is empty or loaded. In order to find the best location for the probe, seven alternative positions were studied, for each one of these voltage measurements were taken with the oscilloscope at three different voltage levels on the plate with the system both loaded and unloaded. The load in this test was a plastic bag filled with water. Even in the location finally selected the voltage reading was found to vary over a 2:1 range depending on the stray field effect and the coil direction relative to the field. As will be seen below these readings do serve a useful purpose but they should not be taken as reliable absolute values.

More details of the experimental apparatus and its arrangement are shown in figures 8.9-8.15.

8.2.3 Voltage Calibration and Radiation Tests

Once the experimental equipment and the high frequency generator was installed and ready for use safety and RF interference tests were carried out.

It is generally accepted that a level of radiation equivalent to that emanated from the human body in a normal sedentary state (100 W/m^2) is safe for permanenet exposure, although some authors quote exposure levels of 10 W/m^2 between medium and high RF frequencies (30-300 MHz). This reduction in the allowable limits is due to the increased receptivity of the human body within this band [13, 56, 110].

A HI-3001 Holaday meter was used to assess the radiation levels on the exterior surfaces of the equipment and in the surrounding working area. This instrument was supplied with two electric field probes plus a set of earphones which produce a sound proportional to the meter reading. Two sets of measurements were taken: One with no load and the other with the container full of product. In both cases the RF generator was operated close to its maximum output and with the highest possible voltage on the electrode system. The electric field is highest, and so is the concentration of the field lines, where the permittivity of the medium is greater. Hence it was considered that the largest stray field effects would occur at no load conditions, this causing the maximum levels of radiation from the equipment. The results obtained are presented in table 8.2. Only the maximum values of field strength were recorded. The conversion from E-field to effective power quantities is based on a table supplied by the instrument manufacturer. The numbers in parenthesis refer to the values with the container full of product and those in brackets correspond to the figures in which the probe locations during the measurements are shown.

It is evident that the equipment does not emit excessive levels of radiation even when operated at full voltage and no load. When the drying runs are being carried out the emissions are greatly reduced as can be seen from the table. The greatest source of stray field radiation is the connection made at the generator terminals, the maximum levels occur when the RF generator is at full voltage but no power is being drawn from the tank circuit. When the load is connected to the generator terminals the level of radiation is very low. In this case the power rectification stage (D.C.) of the RF generator is the major emitter. The effectiveness of the RF metal screen in the window, which faces directly on to the electrode system, is evident from the Table below.

Probe Location	E-field Strength (V/m)	Effective Power (W/m^2)
1.On the Window {8.10}	28.3 (3.9)	2 (0.04)
2.On the Air Intake {8.3}	70.7 (3.9)	13 (0.04)
3.On Generator and Cabinet Joint {8.7}	173.2 (44.7)	80 (5.3)
4.On Door Joints {8.10}	100.0 (15.8)	27 (0.7)
5.Working Area (in between Variac and Cabinet) {8.10}	4.5 (3.9)	0.05 (0.04)
6.Rectifier Valves {8.10}	104.9	29
7.Water Hoses {8.10}	67.1	12

Table 8.2 Radiation emitted from the equipment.

Following the above safety tests the interference problem was next investigated. The RF generator used operates at a frequency which is no longer approved for ISM purposes and therefore interference with local communication systems was seen as a potential difficulty. The radiation emitted from the rig was in the band between 38 and 39 MHz and its effects were detected around the experimental equipment. Tests were carried out in the adjacent parts of the building using a radio receiver. The operational characteristics of the equipment were varied during these tests but nothing was detected which could be attributed to the experimental rig which was then cleared for operation. The system was operated almost every day for three months during which no complaint regarding radio interference was received.

Before starting the experiments, the tank circuit elemnts were adjusted to avoid as much as possible harmonics and amplitude modulation in the RF signal; this setting was left unchanged during all the following voltage calibration and drying runs. The tank circuit design allowed for minor variations in the operating conditions. The generator was able to produce an output between approximately 35 and 39 MHz, depending on the relative positions of the internal inductive and capacitive components. This adjustment affected the waveform of the output signal from the tank circuit. It was concluded that the optimum conditions for operation were near to 38.5 MHz which was the setting adopted. The setting is shown in figure 8.6 in terms of four physical positions of the adjustment: l_1, l_2, l_3 and l_4. The corresponding details of the tank circuit arrangement are shown in figure 8.8. l_1 is the distance (220 mm) between the connection of the RF coupling capacitor (point P in figure 8.6) to the tank circuit inductor and the metallic wall (at earth potential), l_2 is the distance (70 mm) between the inductor and the coupling coil, l_3 (32 mm) and l_4 (20 mm) are the distances between the adjustable tank capacitor plates.

In order to estimate the applied RF high voltage on the electrode system, calorimetric experiments were carried out with plastic bags filled with water. The bags were made from a thin, *heat resistant low-loss polyester* similar to those used for containing food being cooked in domestic microwave ovens. The bags were somewhat larger than the internal volume of the PTFE containers and, when filled with water, occupied almost the whole internal volume available except that needed for the bag seals. These seals experienced no heating effect nor did the PTFE parts of the container which were not in contact with the water even though all parts were subjected to similar electric

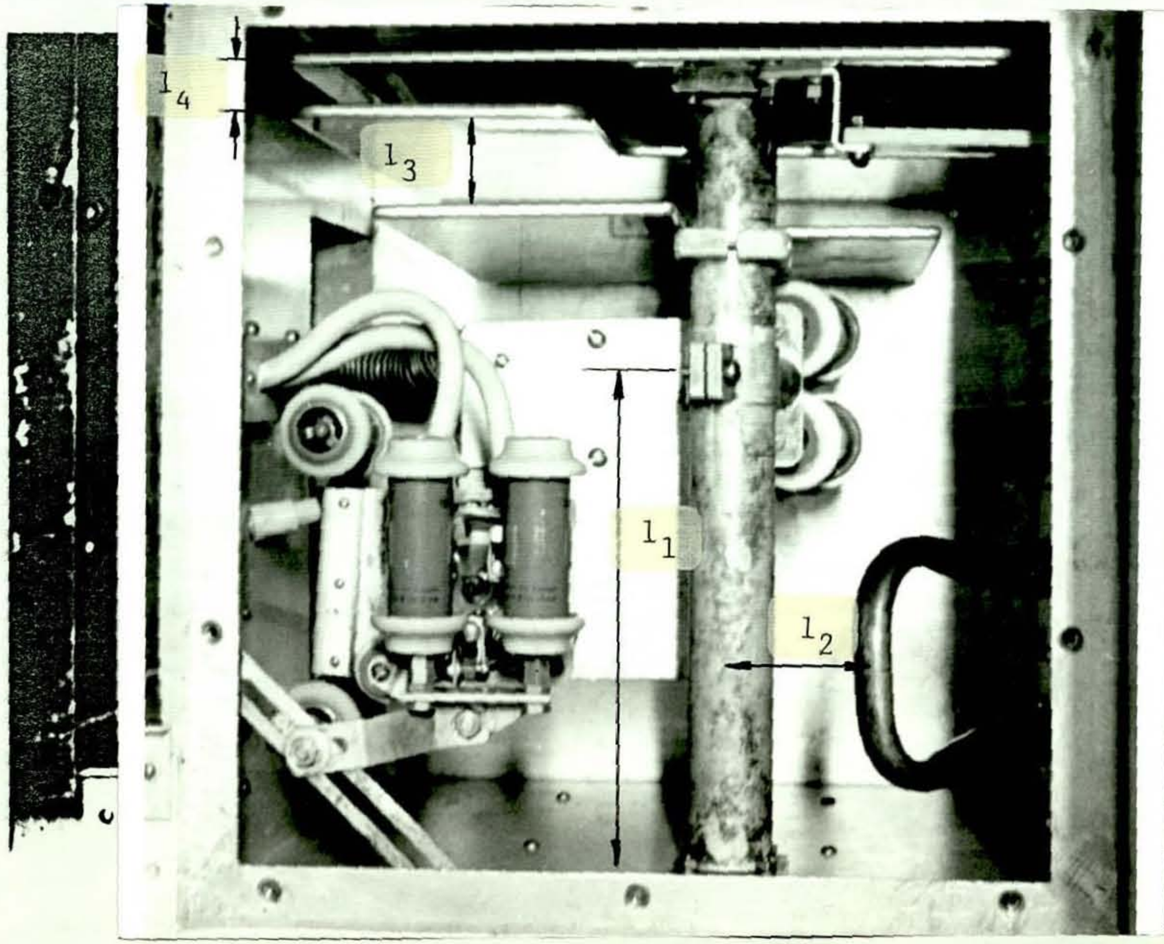

Figure 8.8 Tank circuit of RF generator; the coupling coil is connected to the electrode system (right). Dimensions: l_1= 220 mm, l_2= 70 mm, l_3= 32 mm, l_4= 20 mm.

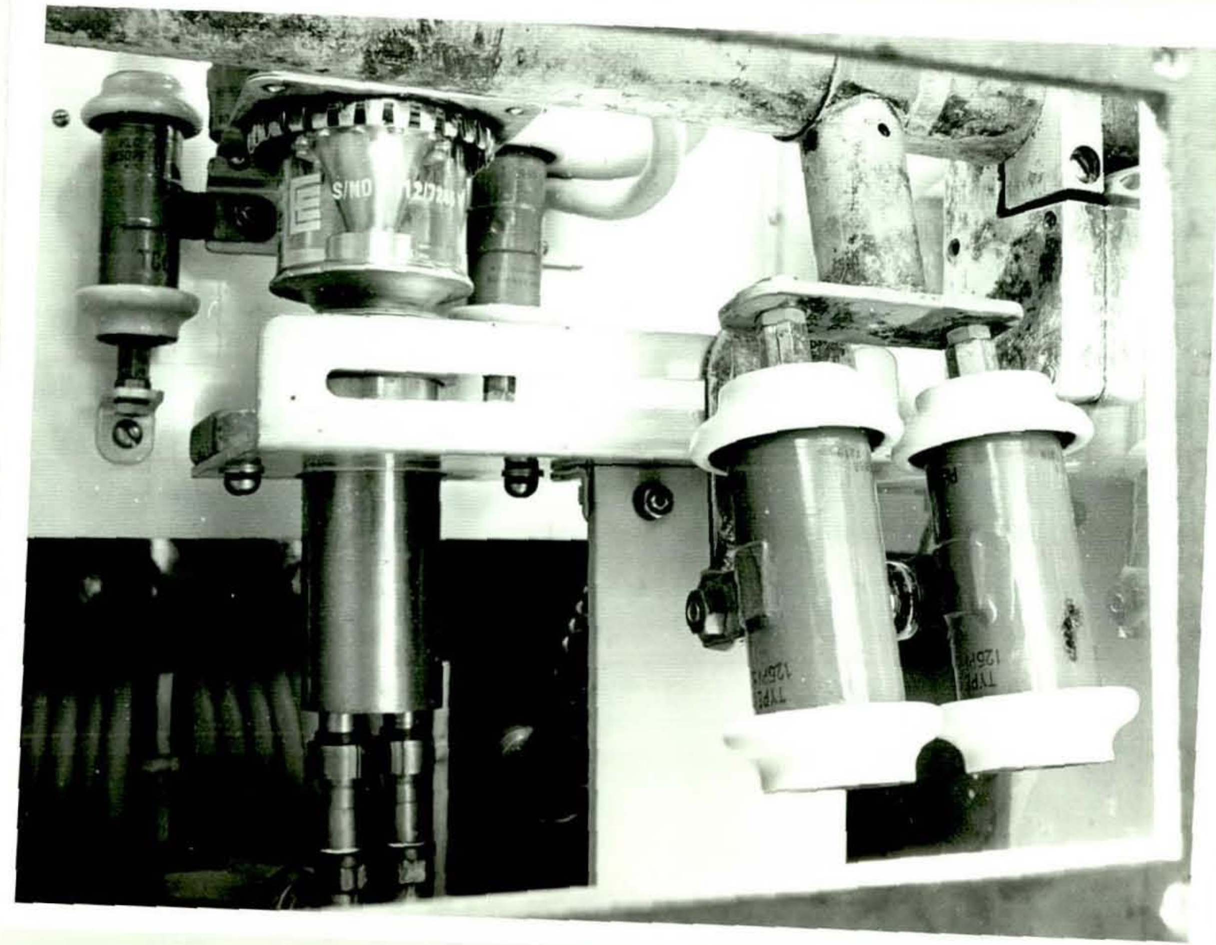

Figure 8.9 RF Valve and tank circuit's inductor and coupling capacitors as seen at the coupling coil's position.

Figure 8.10 Experimental drying system. The power (mains and rectification) section of the high frequency generator is shown in the RHS of the picture together with various instruments and the variac. 1, 4, 5, 6, 7: Location of E-field probe (see table 8.2).

Figure 8.11 Experimental drying rig inside the humidity cabinet; the air velocity sensor and temperature (dry and wet bulb) probes are shown inserted in the earthed (RHS) section of the air duct.

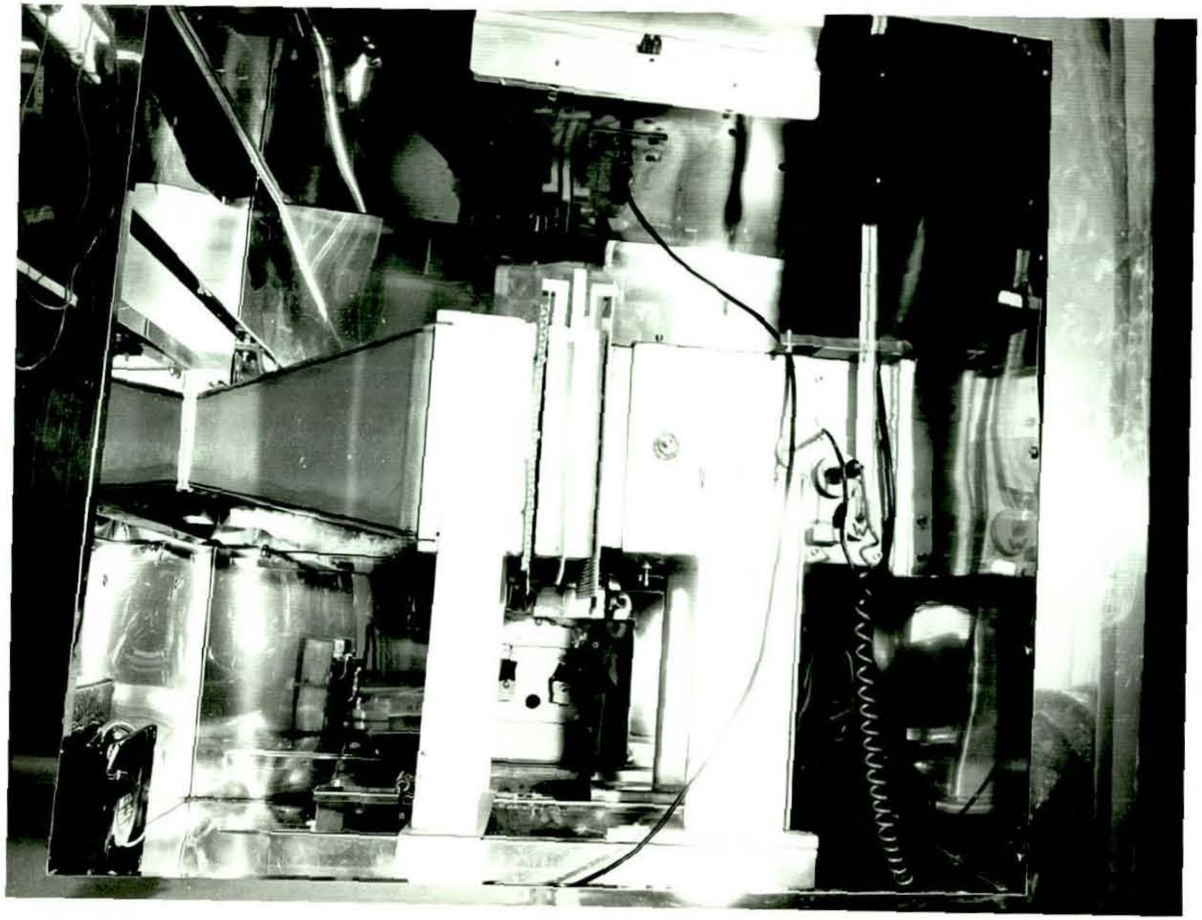

Figure 8.12 Internal details of the air duct system, electrodes, PTFE container and placement of probes. The connection between the electrodes and the terminals of the RF generator (i.e. coupling coil) is noted behind the system.

Figure 8.13 Arrangement adopted in the dielectric drying experiments to estimate the various load parameters.

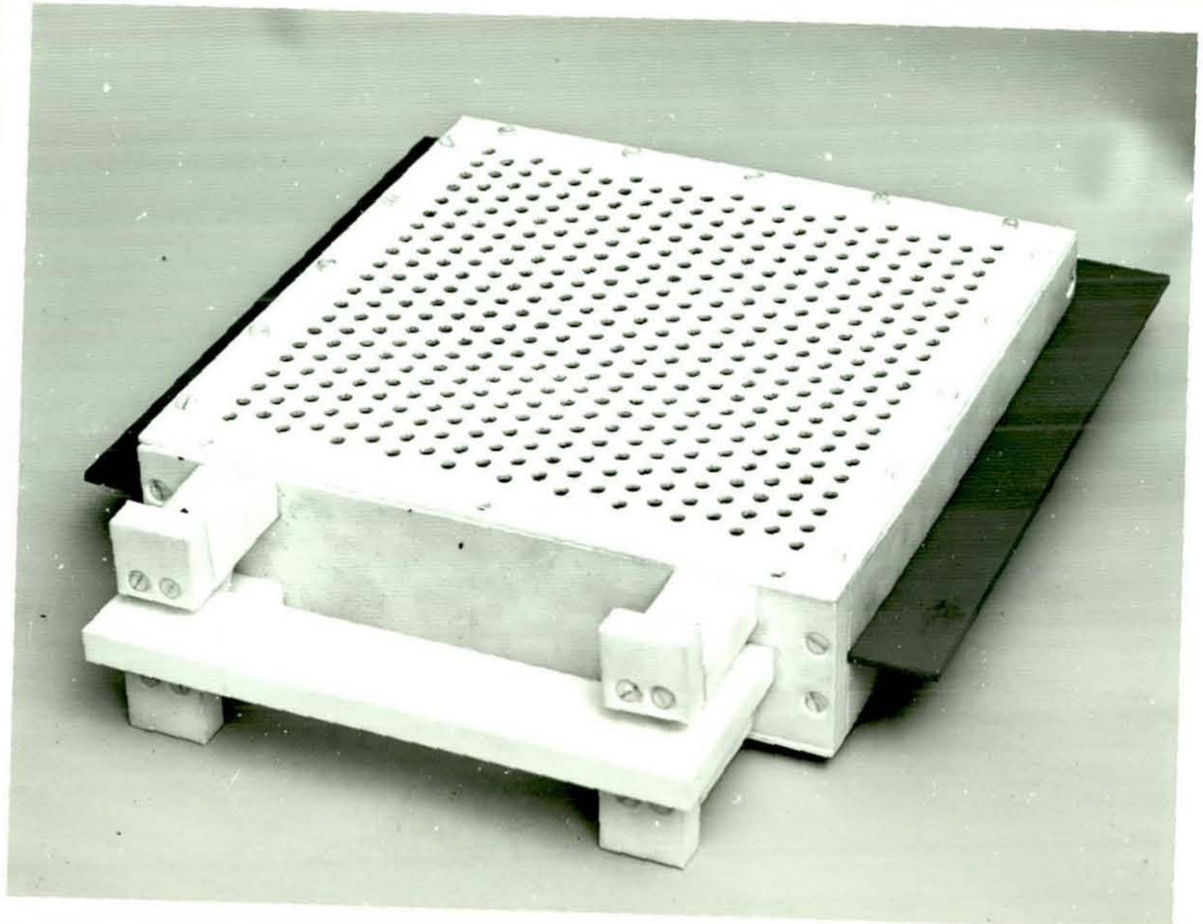

Figure 8.14 PTFE container used to hold the granular material.

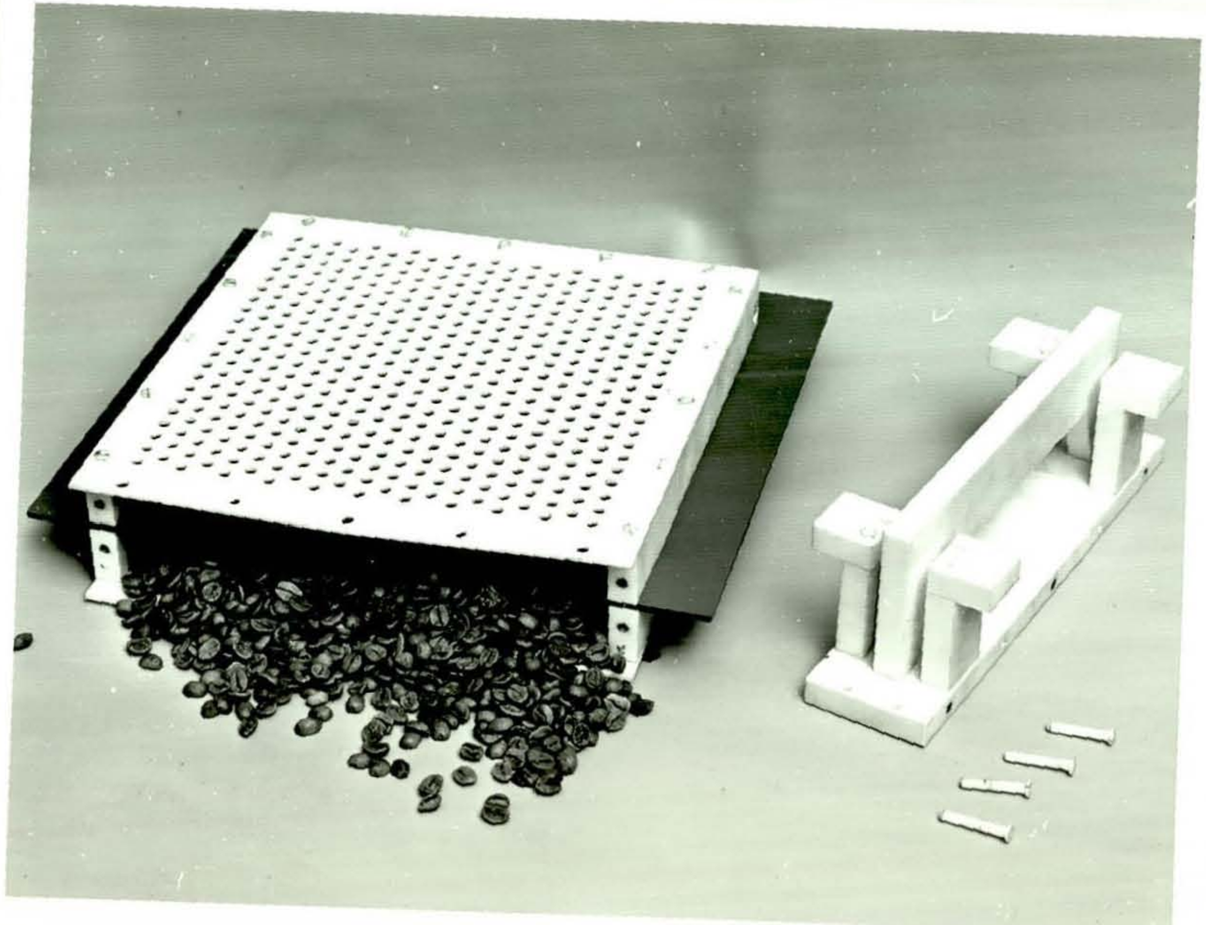

Figure 8.15 PTFE container used to hold the granular material.

field conditions.

The bag containing water was put in the PTFE container which was then placed between the electrode plates. Different input voltages, using the input variac, were then applied for fixed time periods. The temperature rise of the water (T_f-T_i) was measured in each case and the energy used to heat up the water was obtained from:

$$E_w=Cp_w\rho_w(T_f-T_i)V_w \quad Wh \qquad (8.1)$$

where C_w, ρ_w and V_w are, respectively, the specific heat, density and volume of water. In the temperature range used in this experiment the specific heat and density of water are virtually constant, i.e. 1.16 Wh/kg/ C and 1,000 kg/m^3 respectively.

Considering the water as a homogeneous dielectric, an equation for the energy term can also be written as (eq 6.3):

$$E_w= \pi f e_o(V_p/d')^2e''_w V_w \Delta t \quad Wh \qquad (8.2)$$

where f and V_p are the frequency and peak value of the RF voltage between the electrodes, d′ is the separation between the capacitor plates and Δt the period of time for the individual test.

Ideally the RF voltage on the electrode plates would be perfectly sinusoidal with its amplitude, V_p, affected only by the input voltage from the mains. Unfortunately, this is not the case in practice and although the RF signal was sinusoidal during light load operation, under other conditions it contained a small percentage of harmonics. However the major problem was an amplitude modulation of the RF voltage which was first noted when the setting of the tank circuit elements was being made. Changes in the position of the tank circuit elements had some effect on the harmonic components of the signal and these effects were kept as small as possible but the amplitude modulation could not be reduced by any adjustments made to the tank circuit. The only way this modulation could be eliminated was to use input voltages in the nominal range recommended for the RF generator (380-415 volts). Since the amplitude modulation appeared to be produced by a 300 Hz source it was concluded that it was caused by the full wave (6 diode valves) rectifier bridge. This applied a far from ideal DC voltage to the valve when the mains input was outside the recommended range.

The above effect was taken into account in eq (8.2) by considering that only a fraction of that energy would be available. The fraction was expressed mathematically using an amplitude modulation, or modulation depth factor, $K_{a.m.}$. This parameter, estimated from oscilloscope readings, is the ratio of the area under the curve of the modulated RF signal to that of the ideal unmodulated signal (i.e. $V_p(1/f)$). The energy finally available is then given as

$$E_w = \pi f \varepsilon_o (V_p/d')^2 (K_{a.m.})^2 \varepsilon''_w V_w \Delta t \quad \text{Wh} \qquad (8.3)$$

After combining eqs (8.1) and (8.3) and inserting the values for the various parameters (Δt being expressed in minutes) we have for V_p:

$$V_p = (435.3/K_{a.m.})[(T_f - T_i)/(\varepsilon''_w \Delta t)]^{1/2} \quad \text{Volts (peak)} \qquad (8.4)$$

The electrode voltage, V_p, was determined from the results of almost 70 calorimetric tests for various mains input voltages, $K_{a.m.}$ was assessed for each one of these experiments, it was noted that this parameter was substantially constant during the heating cycles but varied linearly with the applied mains voltage. $K_{a.m.}$ is discussed further below, in the drying runs it varied not only with the voltage applied but also with the change in the dielectric properties of the load. Correlations for V_p as a function of the input mains voltage, the voltage on the RF field probe, the variac setting and the mains input power are also presented later in this Chapter.

It should be noted that V_p is expressed in terms of peak value and should not be confused with the RMS values used elsewhere in this report. Under ideal conditions there would be a definite constant relationship between these two figures, this not being the case here due to the effects reported above. However, using eqs (8.2) and (8.3), it is possible to define an amplitude V_{psin} for the unmodulated sinusoidal RF voltage which would produce the same effective heating as that of the modulated wave, i.e.

$$V_{psin} = V_p K_{a.m.}$$

The RMS value of this energy-equivalent sinusoidal wave is given by

$$V = V_p K_{a.m.}/(2)^{1/2}$$

This quantity reduces continuously with the decrease of

$K_{a.m.}$ during the drying runs.

8.2.4 Experimental Procedure

Several product samples were rewetted by soaking them in water for 36 hours after which the surplus water was drained off and the material stored in hermatic 1 litre glass jars at a maximum temperature of 10 C. Each drying run required approximately 2.5 litres of granular product to fill the PTFE container. Before commencing the experiments, the jars were left open to reach ambient temperature after which the PTFE container was filled, closed and placed between the capacitor plates. In the meantime the water cooling system of the RF valve was turned on and the air temperature and relative humidity measurements made at the air intake section. Following these measurements, the velocity of the air flow to the material was measured, taking care to adust the air speed probe with its axis parallel to the air flow. This probe needed to be inserted in the duct for each measurement and withdrawn afterwards due the likelihood of damage by the stray RF field.

After performing the above procedure, the container was taken out of the rig and the air flow switched off. The temperature and weight of the material in the container were measured with the temperature probe on top of the scale dish (see figure 8.13) in order to observe the temperature without delaying the weighing operation. The weight of the temperature probe was compensated for in the moisture content computations as was that of the container. The height of the product in the container was then measured. This was required in order to estimate the product volume shrinkage during the drying process. This approximate method gave an error of up to 10 % when compared with more precise volumetric measurements. Unfortunately, it was not possible to make more accurate measurements in the few minutes available to take the readings, as this would have required removing the product from the container which would have affected both the weight and the temperature of the samples.

The above measurements were defined as having taken place at zero time. The container was then placed in the electrode system and the initial reading of the energy meter was taken. A mains voltage input value was selected, taking note of the variac position, this voltage was maintained constant during the drying run. The generator was then switched on and an interval allowed for the valve heaters to reach operating temperature. The airflow was then started and the RF applied to the electrode system. The stop watch was then started and the first stage (of up to 19 in some cases) of the drying begun.

During the drying operation a series of measurements were made with the oscilloscope. These were voltage amplitude and frequency on the RF field probe, frequency of the modulation and amplitude modulation factor ($K_{a.m.}$). At the same time the input power was also monitored by means of the connected wattmeter.

At the end of the initial period the D.C. supply to the anode was switched off and the PTFE container was taken out of the rig and placed, with the temperature probe in position, on the balance. The air flow supply was also disconnected. Weight, temperature and volume measurements were taken again after the maximum temperature had developed, as the surface took a few minutes to reach its final value after the air flow was removed. These measurements were considered to have taken place at a time given by the elapsed interval measured by the stopwatch from the starting time. After the maximum temperature reading had been recorded, the container was replaced in the electrode system with the warmest side facing the air intake section of the duct. This was done to enhance the temperature distribution in the bulk of material. The RF generator was started and a new drying period commenced.

All the measurements were repeated for as many drying stages as necessary until the RF generator tripped out due to high anode current caused by overload, electrical breakdown or too light a load.

Once the drying run had been completed, the air speed probe was inserted once more in the air intake section of the duct and a final air speed reading taken. This was done to check the air flow change due to variation in the product volume. The final reading on the energy meter was recorded and the container then emptied. The product was examined for signs of damage (figure 8.15) and then placed in the oven at approximately 110 C for three days to establish its dry weight.

The above procedure was followed in each one of the sixty drying runs carried out with the experimental drying system. Depending on the product, the initial moisture content and the field strength used, each drying run took from half to a full day to complete.

The measurements taken during the experiments were fed into a microcomputer spreadsheet in order to calculate the performance parameters, i.e. RF plate voltage, moisture content variation, initial and target moisture contents, volume (in absolute and relative (p.u.) terms) and bulk density of the product, gross and net dielectric power densities, power utilization factor, load resistance, capacitance, impedance and Q-factor, equivalent RMS electrode voltage, amplitude modulation factor ($K_{a.m.}$), instantaneous and average energy efficiencies and throughput. Much of this information could only be determined for each particular test when the weight of the dry product was obtained but other data is directly obtainable during the drying runs. A sample printout of the spreadsheet used is shown in Appendix IV.

8.2.5 Experimental Results and Discussion

8.2.5.1 Electrical Parameters

The results obtained from the experimental dielectric drying unit yielded abundant data concerning the process most of which is summarized in the following paragraphs. However, as noted above, the amplitude modulation problem produced some uncertainties which are likely to affect the information obtained. The consequence of this modulation was a continuous reduction in the RMS electrode voltage as the drying cycle progressed as evidenced by the decrease in $K_{a.m.}$ with diminishing loads. This effect is produced by the rectifiers and is accentuated by the fact that the RF source used was not designed to cope with such an extensive range of load conditions. For most of the time only a small fraction of the nominal capacity of the generator was employed. In terms of the ratio between the measured input power and the nominal 12 kW input the nominal power utilization varied from as low as 5 % up to 75-80 % for short periods. For most of the time the generator did not exceed about one third of its capacity. This problem is largely due to the fact the the process was one of batch drying which inevitably resulted in a large load variation. In the real continuous process situation each oscillator will see a very nearly constant load across its terminals which is very nearly constant. This will avoid the above problems and will allow each generator to be tuned to operate under optimal load conditions.

The amplitude of the voltage measured by the RF field probe changed during the drying experiment. This was probably due to the change in the stray field pattern as the load is reduced, i.e. as the material is dried. The probe voltage was considerably affected by the relative angular position between the axis of the coil on the probe and the electrode system and also by the distance between the probe and the eletrodes. The best possible configuration was kept constant during the experiments. The above factors had no effect on $K_{a.m.}$, which was only influenced by the input voltage and loading conditions. Some correlations obtained for $K_{a.m.}$ are presented in table 8.3. In order to obtain these the input voltage V_i and the load resistance R_L were chosen as independent variables. The selection of V_i is inevitable since this obviously affects $K_{a.m.}$. The choice of R_L is based on the fact that the RF generator appears to "lose" the load when this is too small and this phenomenon is followed by a reduction of $K_{a.m.}$.

Model	S_e	I^2
$K_{a.m.}=-0.29+9.11E-3V_i-3.31E-5V_i^2+4.28E-8V_i^3$	0.12	0.502
$K_{a.m.}=0.36+1.30E-3V_i-6.32E-5R_L$	0.10	0.541
$K_{a.m.}=0.93+1.23E-3V_i-9.28E-2LN(R_L)$	0.09	0.555
$K_{a.m.}=0.32+2.19E-3V_i-2.23E-5V_i^2-1.25E-4R_L+1.52E-7R_L^2$	0.09	0.566

Table 8.3 Amplitude modulation factor as a function of the applied mains voltage (V_i, volts RMS) and load resistance (R_L, Ohms)

A relatively low S_e was obtained for all the above models of the amplitude modulation factor. $K_{a.m.}$ was measured on the oscilloscope, an estimate of the areas had to be made at each drying stage and a very short time was available to do this. Over four hundred of such readings were taken in the experiments, all of which have been included in the above regressions. However, the coefficient of correlation is relatively low and the inclusion of the load resistance in the above models enhanced the correlation by only a small amount. It is, therefore, difficult to finally determine at this stage which parameters affect $K_{a.m.}$ apart from V_1. The problems may lie between the rectification and the high frequency sections of the oscillator in response to the decreasing load levels.

A variation on the magnitude of V_p of the same proportions as that observed for the voltage on the RF field probe was not considered to be feasible, the load was small in relation to the capacity of the generator and the electrodes were directly connected by short copper strips to the generator terminals. For a given input mains voltage, and therefore a constant D.C. valve anode voltage, the resultant (RF) voltage and current in the resonant tank circuit should not change appreciably, as demonstrated by the fact that the measured D.C. current drawn from the rectifier to the anode of the valve is kept constant. The same is also the case for the measured input power to the rectification section, which remains fairly constant once the mains voltage is set on a given level. A given level of anode voltage and current (D.C.) in the valve yields, a definite value for the internal resistance of the valve, i.e. the effective resistance between the anode and the cathode. This can be found from the manufacturer's data. Hence, the change in the load (which is continuosly decreasing, i.e. the effective resistance and impedance increase) will be the only factor affecting the current drawn from the tank circuit. Since this current will decrease during the drying process a smaller (RF) voltage drop will be observed between the tank circuit and the electrodes. This will cause an effective increase in the plate voltage (and not a decrease), the magnitude of which is difficult to determine.

Regression formulae for the amplitude of the electrode voltage V_p (kV, peak), RF field probe voltage V_{pr} (V, peak), input power P_i (kW), input voltage V_i (V, rms) and variac setting P.V. (%) are shown in table 8.4. The first expression in the table is the result of the calorimetrical experiments already discussed. A very high correlation coefficient was obtained, although the scatter, measured by S_e, was not negligible. If this calibration is adopted for the amplitude of the electrode RF voltage as a function of the input voltage and correlate the latter with the variac setting and the RF field probe voltage, then the next two expressions for V_p in table 8.4 can be obtained. The correlation with the variac setting is much better than that with the probe voltage, the latter being the amplitude of the maximum recorded voltage.

Model	S_e	r^2
$V_p=-0.19+1.17E-2V_i-2.85E-5V_i^2+2.92E-8V_i^3$	0.24	0.959
$V_p=0.39+0.44V_{pr}-0.06V_{pr}^2+4.34E-3V_{pr}^3$	0.18	0.835
$V_p=-3.4+0.16P.V.-1.61E-3P.V.^2+5.71E-6P.V.^3$	0.03	0.999
$V_i=21.08+9.85V_p+232.24V_p^2-73.09V_p^3$	56.79	0.955
$V_i=-542.34+20.82P.V.-0.16P.V.^2+4.24E-4P.V.^3$	10.25	0.999
$V_i=63.23+68.19P_i-5.21P_i^2+0.17P_i^3$ (for all products)	21.00	0.996
$V_i=67.91+62.08P_i-5.22P_i^2+0.21P_i^3$ (for cereals)	5.91	0.999
$V_i=81.74+52.71P_i-0.88P_i^2-0.11P_i^3$ (for coffee & soya)	19.24	0.997

Table 8.4 Experimental relationships for the variation in amplitude of electrode voltage with changes in input voltage.

Neither the frequency of the amplitude modulation (approximately 300 Hz) nor that of the RF voltage (38.5 MHz), i.e. the "carrier" of the former signal, varied during the experiments. The high stability of the RF frequency under such a wide load variation implies that the tank circuit capacitance is very large as compared to that of the load.

8.2.5.2 Load Parameters

The load varied widely during the experiments. This was mainly caused by the change in its dielectric properties and in a lesser degree due to the volume shrinkage within the PTFE container as noted from eqs (8.15) and (8.6) below. The volume was greatest at the beginning of the drying cycle and decreased as the moisture content dropped, the range observed being as shown in table 8.5 in p.u. terms. The figures in parentheses refer to the corresponding moisture content.

Product	Maximum Volume	Minimum Volume
Rice	1.0 (33 % w.b.)	0.7 (10 % w.b.)
Maize	1.0 (36 % w.b.)	0.7 (14 % w.b.)
Wheat	1.0 (39 % w.b.)	0.7 (18 % w.b.)
Soya	1.0 (60 % w.b.)	0.6 (30 % w.b.)
Coffee	1.0 (60 % w.b.)	0.6 (31 % w.b.)

Table 8.5 Maximum volume variation during drying (p.u.) and associated moisture contents.

The electrical characteristics of the load can be expressed in terms of its effective resistance, capacitance, impedance and Q factor. The load resistance can be defined by equating eq (6.31) to V^2/R_L, which gives

$$R_L = d'^2/w e_o e'' V \qquad \text{Ohms} \qquad (8.5)$$

The expression for the load capacitance is obtained from eq (6.30):

$$C_L = e_o e' V/d'^2 \qquad \text{Farads} \qquad (8.6)$$

Apart from the effect produced by the variation of dielectric properties, R_L and C_L are also affected by the change in volume, the frequency of the RF field, the electrode separation and their dimensions. The load Q factor was calculated by using eqs (6.34b), (8.5) and (8.6).

The maximum variations in the capacitance and impedance of the load are as shown in table 8.6. The moisture range is shown in parentheses. The capacitance increases with the moisture content following the increase in the dielectric constant (eq (8.6)), whereas the impedance is lower at higher moisture content. Higher values of capacitance and lower impedances were obtained during the drying experiments, but it was not possible to estimate these values beyond the moisture range for which the models of e′ and e″ have been defined. The same holds for the resistance and Q factor of the load, the changes in these parameters are shown in figures 8.16 and 8.17.

Product	Capacitance Range (picofarads)	Impedance Range (Ohms)
Rice	6.5-8.2 (11-32 % w.b.)	635-255 (11-32 % w.b.)
Maize	12-44 (12-36 % w.b.)	338- 88 (12-36 % w.b.)
Wheat	4.5-6.2 (18-40 % w.b.)	2841-465 (18-40 % w.b.)
Soya	6.1-8.6 (30-48 % w.b.)	578-251 (30-48 % w.b.)
Coffee	16-30 (27-48 % w.b.)	248-130 (27-48 % w.b.)

Table 8.6 Maximum variation of the load capacitance and impedance during drying and associated moisture content values.

8.2.5.3 Other Characteristics of the Drying Process

The drying experiments were carried out at various electrode voltage levels with air flows ranging from 0.7 to 1.1 m^3/sec per m^2 of the cross sectional area of the 5 cm thick layer of granulated material. This range includes the conditions for all the five agricultural products considered in

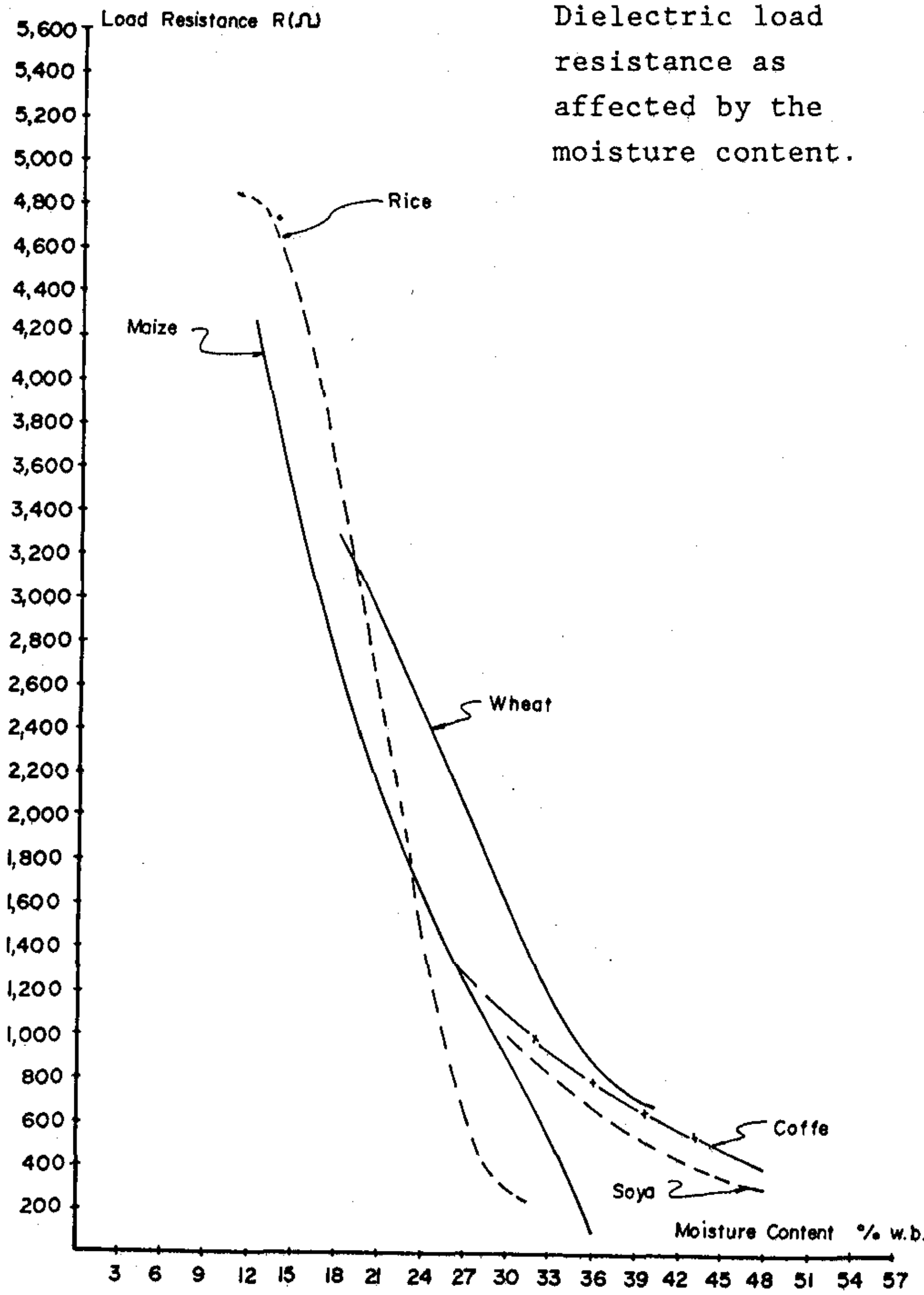

Figure 8.16
Dielectric load resistance as affected by the moisture content.

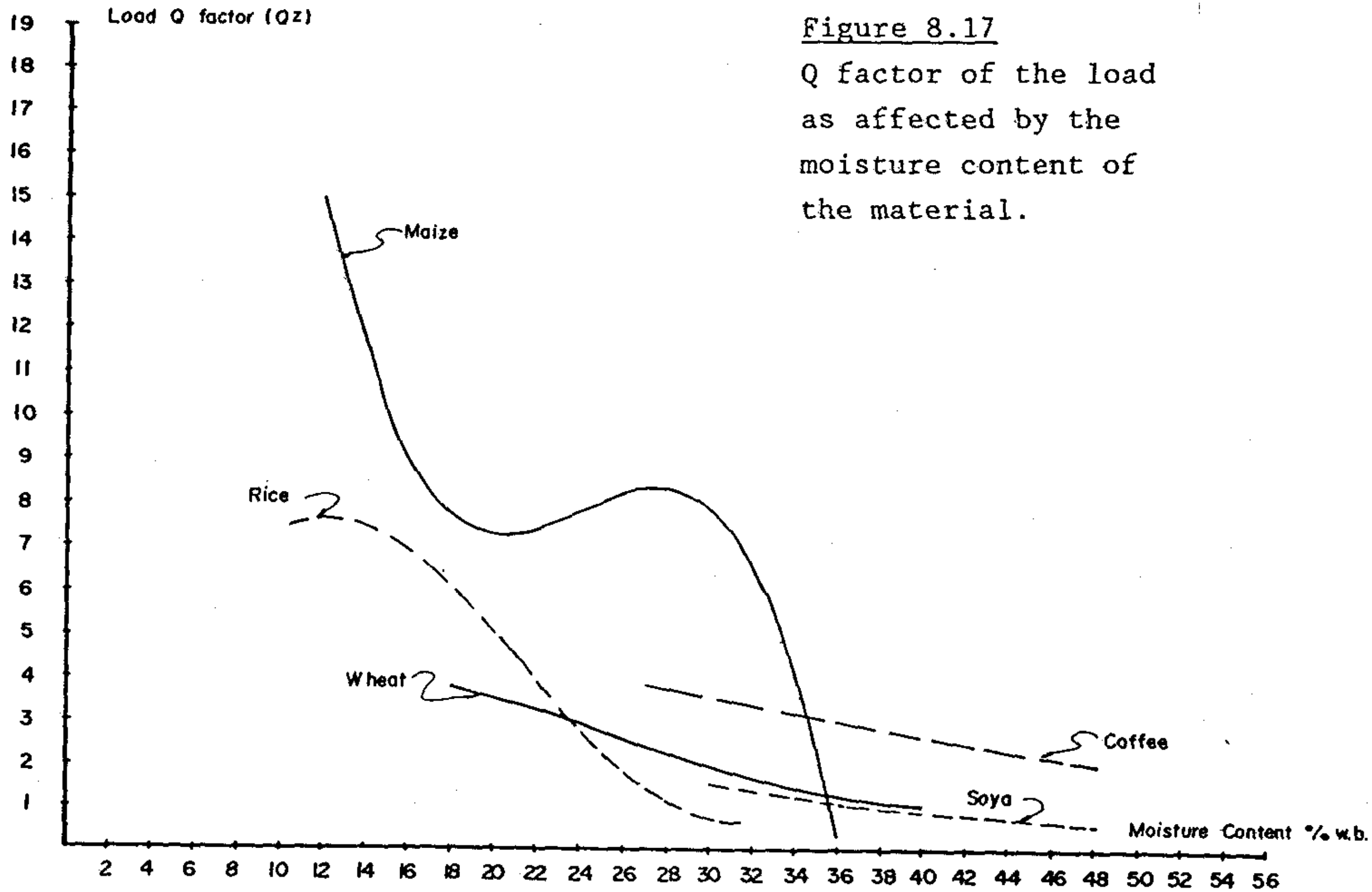

Figure 8.17
Q factor of the load as affected by the moisture content of the material.

this report and also the air velocity increase due to the shrinkage of the material in the container. This latter variation was less than 10 %. The air temperature varied from 18 to 23 C during the period in which the experiments were carried out and its relative humidity ranged between 0.4 and 0.5.

It was found that the cereal products could be dried in the equipment over a wide range of moisture contents. Maize and rice were dried from as high as 33-36 % w.b. down to 10-12 %. The corresponding drying range for wheat was 40-17 % w.b. Coffee and soya were dried from as high as 60 % w.b.. It was not possible, however, to continue the drying process with these products below approximately 27-30 % w.b., as the generator would stop oscillating. Details of the drying parameters are shown in table 8.7.

q_d has been calculated using the wattmeter readings and eq (6.31). Since the latter requires values for the dielectric properties of the material, it was not possible to calculate the levels for soya and coffee above approximately 45-48 % w.b. Although changes in V_p produced a considerable effect in q_d, the latter is much more affected by the large changes in rig efficiency and the dielectric properties of the product as the moisture content changes. The maximum temperature reached by the material was also strongly dependent on the value of V_p used. There is also evidence that, for a given moisture range, η_d increases as V_p is increased but it is difficult to assess how much of this is due to the reducing efficiency of the equipment as the load is reduced and how much is caused by an enhancement of the drying process itself.

Product	V_p (kvolts)	q_d (kW/m^3)	η_d (p.u.)	T_m (C)
Rice	0.85 - 1.66	1 - 1,002	0.12-0.30	12 - 111
Maize	0.85 - 1.54	1 - 764	0.03-0.21	15 - 127
Wheat	1.02 - 1.66	12 - 552	0.10-0.53	16 - 97
Soya	0.85 - 1.54	6 - 1,371	0.23-0.48	12 - 90
Coffee	1.24 - 1.80	42 - 2,173	0.28-0.61	12 - 96

Table 8.7 Maximum variations in electrode voltage (V_p), net dielectric power density (q_d), average drying efficiency (η_d) and temperature of the material (T_m) during the drying experiments.

The drying efficiency η_d has been calculated for each drying run and is the ratio of the energy requirements as given by eq (6.6) to the energy consumed during the drying run as measured by the wattmeter and energy-meter. Since the variation in input power P_i during drying was small the calculations based on the power and energy meters were practically identical. The resultant efficiency is an "average" value obtained by considering the whole drying run from an initial moisture content M_i to the final M_f, the latter being the minimum level just before the RF generator stopped operating.

An alternative form of energy efficiency has also been considered. This is the instantaneous value at a given point in the drying cycle, which can be written as

$$\eta_e = \pi f \varepsilon_o (V_p/d')^2 (K_{a.m.})^2 \varepsilon'' V / P_i \qquad (8.7)$$

This latter quantity has been used to estimate the net dielectric power density applied at a given point in time. The variations in η_e with moisture content for each product is shown in figure 8.18. Since the efficiency is considerably affected by the loading conditions of the RF generator, it was considered that a parameter involving the load variation should be used as an independent variable in order to estimate the

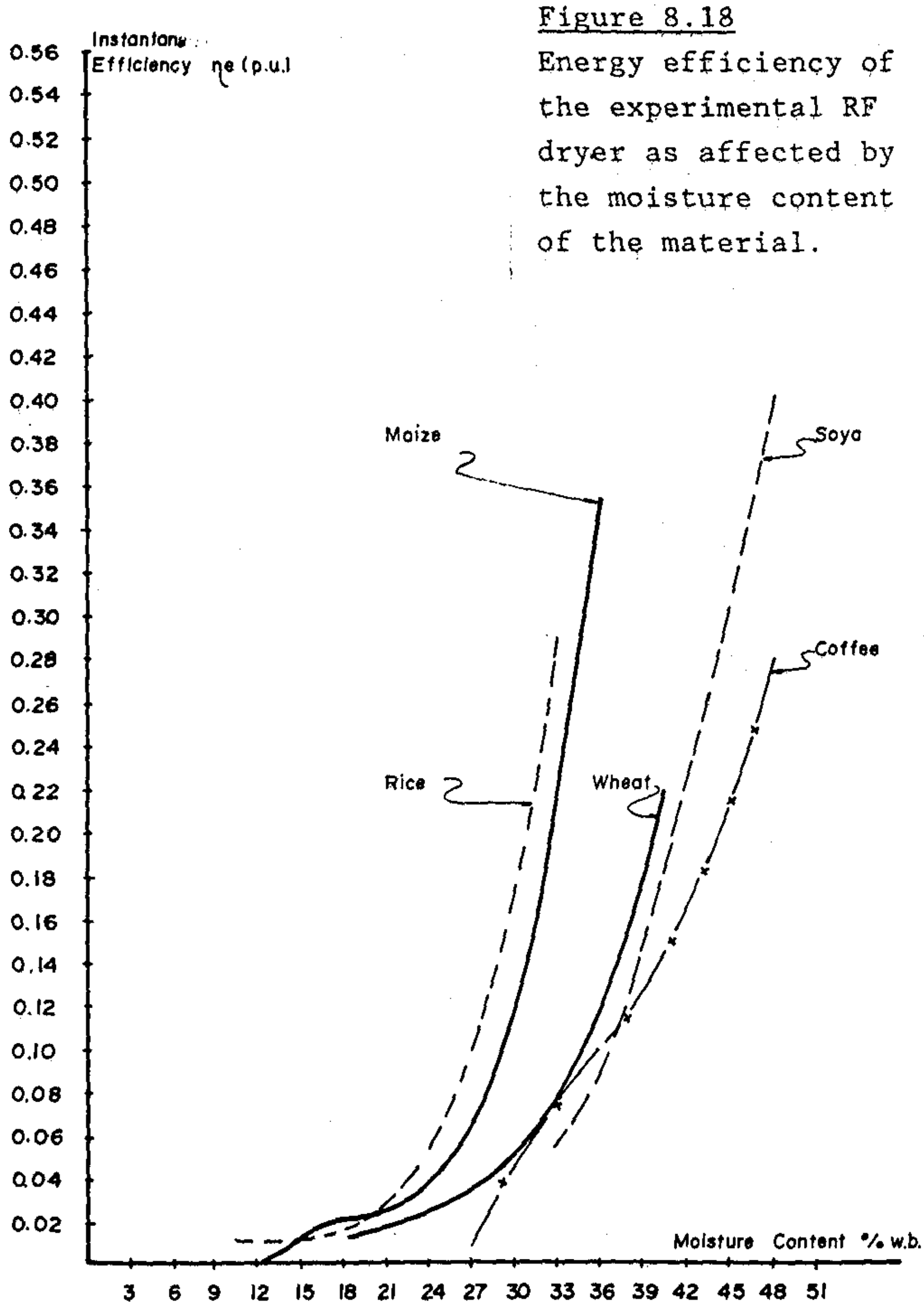

Figure 8.18
Energy efficiency of the experimental RF dryer as affected by the moisture content of the material.

efficiency of the experimental rig regardless of the product used. Among the alternatives R_L and Q_L were examined as possible candidates. With the help of figures 8.16-8.18 it was possible to select the most convenient parameter, primarily by investigating if a correspondence existed between the intersections of the R_L and Q_L families of curves and those of η_e over similar moisture content ranges. Whilst the results were clearly divergent when Q_L and η_e were considered, this was not the case when the latter was related to R_L. This correspondence was very close if the cereals were considered as a separate group. The regression analysis performed shows a very definite dependence of the efficiency on the effective load resistance. The final relationships between η_e and R_L are shown in figure 8.19 and are summarised in table 8.8.

Product	Model	Se	r^2.
(a)	$\eta_e=0.39-4.40E-4R_L+1.62E-7R_L^2-1.84E-11R_L^3$	0.042	0.965
(b)	$\eta_e=0.93-2.38E-3R_L+2.16E-6R_L^2-6.58E-10R_L^3$	0.042	0.963
(c)	$\eta_e=0.32-3.05E-4R_L+9.77E-8R_L^2-1.01E-11R_L^3$	0.017	0.994

Table 8.8 Equations for the instantaneous energy efficiency of the rig as a function of the equivalent load resistance. (a): all five products; (b): soya and coffee beans; (c): cereals (rice, maize, wheat).

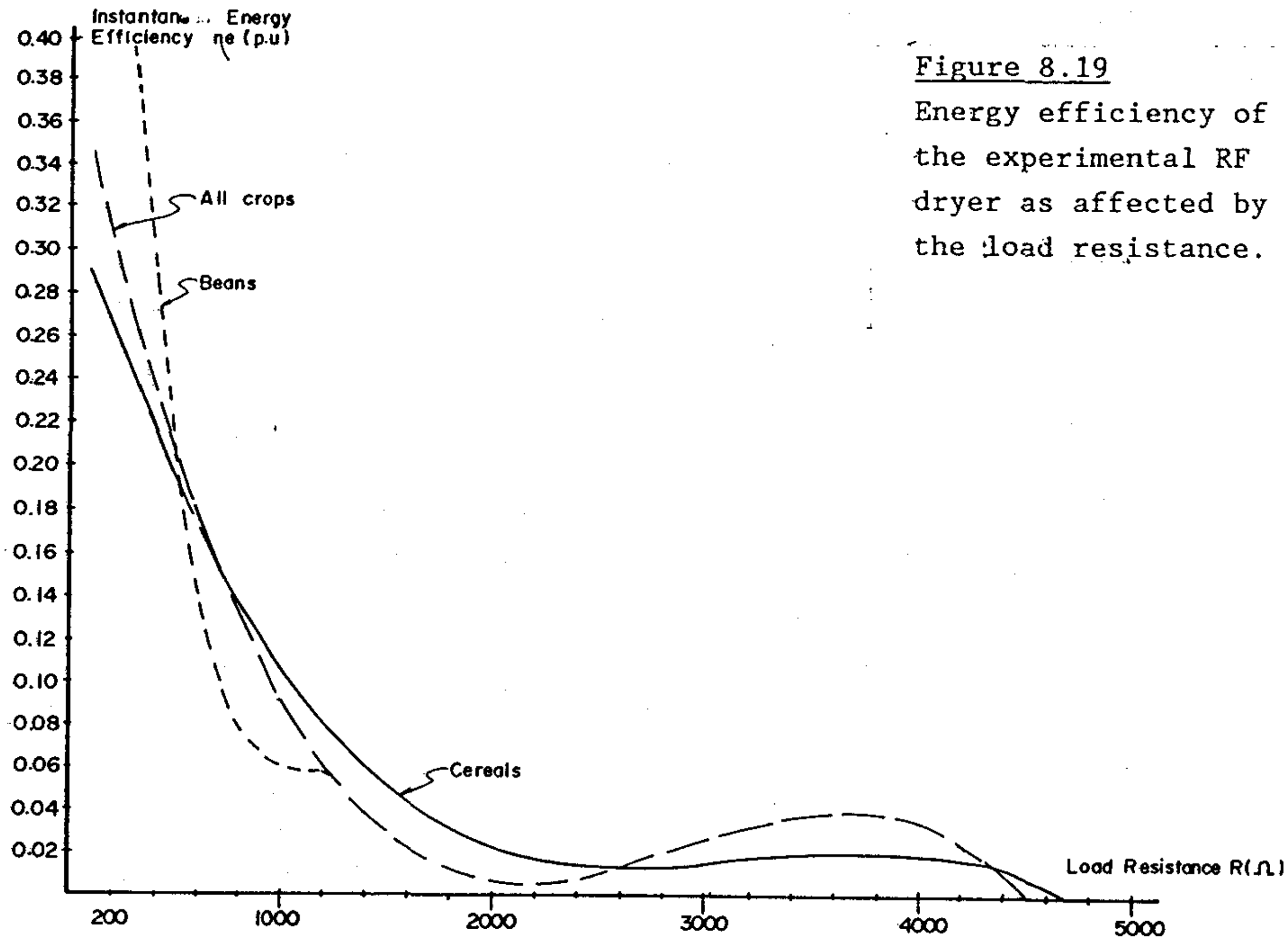

Figure 8.19

Energy efficiency of the experimental RF dryer as affected by the load resistance.

Considering the two efficiencies discussed above, η_d and η_a, if the high frequency energy absorbed by the product at any given moment (which defines η_a) is totally used to heat up the material and evaporate water (which defines η_d), the following relationship must hold under ideal conditions;

$$\eta_d = 1/t_d \int^{t_d} \eta_a \, dt \qquad (8.8)$$

Hence, the value of η_d approaches that of the average value of η_a taking into consideration the drying period t_d if no experimental errors have occurred. However, in practice, errors may be incurred in the determination of several of the parameters which have been used to calculate η_d and η_a. Amongst these parameters, η_d uses the specific heat, bulk density and volume of the completely dried product. In this Report the published values for the specific heat have been used and some variation might be expected. The published values for the bulk density of dry maize and wheat agree very closely with the range observed in the experiments and, therefore, the former values were used. This was not the case, however, for the other products, the differences for rice and soya were of the order of 25 % and those for coffee as high as 35 %. The average values obtained from the experiments were preferred in these cases. The volume used in the calculations was that of the product at the end of the drying run, which was measured (approximately) as described above. In any event, it should be higher than that of the totally dried material.

With regard to n_e, three variables are of utmost importance: $K_{a.m.}$, V_p and e". The first two have an increased effect since their square is used in the calculations. The variation of the amplitude modulation factor has not been entirely predicted in this Report and individual measurements were used instead of the smoothed model obtained by regression analysis. The value of V_p is also not very precise, although the calorimetric method seems to be the best presently available. Finally, the models for e" are accurate for moisture contents of up to, say, 35-40% above which the Q factor and capacitance method gives a high diversity in the results, some readings indicating much higher values for the e" than those finally predicted by the regression analysis.

Although a detailed study of the above equation and associated errors, taking into account the experimental data, has not been carried out in this Report, it is evident that the value of η_d is generally between the extremes for η_e in a particular drying run. Apparent exceptions to this rule, are the cases when η_d is higher than the maximum recorded value for η_e, might have been caused in part by the factors discussed above. For example, the real value for η_d may be lower than that calculated in the experiments due to imprecision in the estimation of the specific heat, the volume and the bulk density of the dried product. Similarly, η_e may have been undervalued due to e", V_p and $K_{a.m.}$. The effect caused by imprecision in the estimates for $K_{a.m.}$ seems more likely, as the variations show no particular trend. When a drying run was repeated, any differences appear to be attributable to changes in the values of $K_{a.m.}$ in the two experiments. In any event, it is not always possible to interpret a difference between η_d and η_e as being caused by such errors. It was not possible to estimate η_e for moisture content levels above those for which the experimental models of e" were defined. The first (and highest) value of η_e is obtained at the end of the first stage of the drying run. In most cases this takes up a relatively long time with the product losing a considerable amount of water within a moisture range where drying appears to be more efficient. The misleading effects of these factors is evident when one examines the tests performed with shorter time intervals between measurements or lower initial moisture content levels. In these cases the resulting values of η_d were much closer to or even within the η_e range.

The efficiency given by the manufacturer of the high frequency generator is 0.5 from A.C. mains to RF output. Mullard [114] quotes the efficiency of the valve used in the experiments (Mullard TY7-6000 W) as 67 %. Hence, it can be assumed that about 25 % of the energy input is lost before the valve stage, i.e. in the rectifying section, and the remainder in the tank circuit. These losses are produced by the stray components of the RF field and by Joule losses in the tank circuit, the latter being dependent on the RF penetration depth in the metal components. Since we have an indirectly coupled RF output, in theory it would be possible to vary the impedance seen by the valve, i.e. the combination of the tank circuit, electrodes and dielectric loads. Ideally, for best operating conditions, this value should be matched as closely as possible to the internal resistance of the valve, i.e. the effective resistance between anode and cathode. Physically this matching could be done by varying the separation of the coupling coil and tank circuit components and by introducing adjustable reactive components between the tank circuit and the electrodes. The construction of such a tuning system would improve the operating conditions of the existing experimental equipment, since it might be used to reduce the effects of extreme load variations. The design of such a unit, which would need to use empirical methods, could incorporate a computerized control system. This is a subject for future work.

Turning to the temperature rises during drying, it was noted that, between 1.24 and 1.54 kV (electrode voltage amplitude, V_p), the temperature of rice exceeded 80 C at the end of the drying process, but this did not appear to affect the quality of the product. Drying rice at levels higher than 1.66 kV did, however, cause a few kernels to crack. Previous work reports on the high resistance of this product to the levels of dielectric power used in these experiments. It may be concluded that the high temperatures reached caused this cracking rather than the dielectric power density (q_d) itself which was less than 1,000 kW/m^3. The temperature of maize exceeded 80 C at lower V_p levels (1.24 kV). Since both products have similar loss factors at 38.5 MHz this presumably occurred due to the lower (specific heat x bulk density) product ($C_{pd}\rho_m$) observed for maize (see table 6.1) which, according to eq (2.33), will produce a greater temperature increase. The maize quality was, however, not affected up to approximately 1.4 kV after which cracking began resulting in a few damaged kernels. This cracking of the maize kernels always occurred at an estimated q_d greater than 200-250 kW/m^3. At approximately 1.44 kV the wheat temperature reached values higher than 80 C, although the product suffered no damage, at least up to 1.54 kV, which in this case corresponded to q_d levels as high as 500 kW/m^3. From table 6.1 it is noted that $Cp_d \rho_m$ is about 20 % lower for wheat than it is for maize. When the loss factors are considered, however, the values for maize are much higher than those for wheat (38.5 MHz), especially within the moisture range (greater than 22-24 % w.b.) where the maximum rate of temperature rise occurs. It would only be possible to quantify the contribution of these opposing factors to the temperature increase rates if information regarding the conduction of heat within individual particles were available (eq (2.33)). In any event, the higher values of the loss factor of maize causes it to be more responsive than wheat to the high frequency field.

When drying soya and coffee beans it was noted that, above approximately 1.33 kV, the temperature of the former exceeded the 80 C mark. This occurred at approximately 1.41 kV for coffee. In both cases, however, the maximum levels reached were much lower than those in the case of cereals. Since soya and coffee have approximately the same $Cp_d \rho_a$ value (table 6.1) this difference in the temperature increases may be attributed to the larger loss factor of soya at 38.5 MHz. In comparing soya with maize it is noted that $Cp_d \rho_a$ is of the same order for the two products although the loss factor of maize at 38.5 MHz appears to be greater than that of soya above 30 % w.b., which is the drying range for soya and coffee in the experiments. The volume of soya shrunk considerably during the drying process, this was the only apparent change in the product up to approximately 1.41 kV and 400 kW/m^3. At this stage the surface of some of the beans became scorched and this was followed by burning and breakdown. In the case of coffee, some of the beans split when working at voltage levels of the order of 1.24-1.34 kV with q_d at 500 kW/m^3. This corresponded to temperatures slightly higher than 60 C, which was taken as the maximum allowable level when drying this product by convection methods. The volume of the coffee beens also shrunk considerably during the drying process.

It was evident from the experiments that all the products were affected, to some degree, by the maximum temperature reached during the process. It was also noted that the material initially exposed to the air flow developed much lower temperatures than the maximum levels reported above. On the air intake side of the PTFE container the temperature of the material ranged from a little higher than ambient to no more than 50 % of the maximum value reached on the opposite side. This was compensated for in the experimental procedure by changing the exposed side of the container at the end of each stage to ensure that all particles would be subjected to similar heating effects.

With regard to the energy usage in the high frequency drying process, the energy required per unit of evaporated water lessens as the initial moisture content increases. Higher voltage levels on the electrodes will also reduce the specific energy consumption, although care must be taken not to exceed the maximum levels referred to above. Drying rice at 1.24 kV from 25 to 14 % w.b. requires 6.3 MJ/kg of evaporated water. If M_i is increased to 33 % w.b., the consumption decreases to 3.7 MJ/kg. These energy consumption levels are within the range reported in commercial crossflow dryers (see for example [10] and table A.4).

8.2.5.4 Drying Models

As a final result of the experiments one would like to arrive at models predicting the times involved in the high frequency drying of a particular product. Ideally these models would be as general as possible in order to increase their future usefulness. As noted above, the amplitude modulation effect observed in the experiments not only increased the complexity of the calculations but also caused the results to be less generally applicable. Another experimental drawback was that the RF generator was not able to dry coffee or soya beans below relatively high moisture content levels. The results presented below, therefore, are conservative estimates for the drying process and should only be applied within short moisture content ranges.

The drying time estimates are conservative since they are based on variables such as the RF electrode voltage which in the ideal case would not have imposed amplitude modulation and thus a particular value of V_p would produce a constant field strength and not a continuously reducing one which was the case in the experiments reported here.

In order to arrive at the models, the data obtained for the moisture content variations over time were subjected to regression analyses in which the common empirical air drying models given by eqs (2.14) were all considered. It was found that the exponential type of model was the most appropriate, i.e.

$$(M-M_t)/(M_i-M_t)=\exp(-k_d t_d^{k_q}) \qquad (8.9)$$

It might be worthwile in further dielectric drying studies to explorev a new concept for the value of M_t as has been done in the air drying case noted above, where the equilibrium moisture content has been substituted by a "dynamic" value. This adjustment could well improve the precision of the dielectric drying model. The moisture ranges for each product are given in table 8.9. The resulting (average) correlation factors and standard deviations when the data are fitted to eq (8.9) are also included in the table.

Product	M_i (% w.b.)	M_t (%w.b.)	M_f (%w.b.)	S_e	r^2
Rice	19 - 33	11.5	down to 11	0.16	0.93
Maize	25 - 36	13.7	down to 13	0.14	0.90
Wheat	35 - 40	9 - 11	down to 18	0.12	0.93
Soya	44 - 62	11.5	down to 30	0.10	0.90
Coffee	44 - 65	13.0	down to 29	0.11	0.78

Table 8.9 Ranges of initial moisture content (M_i), target moisture content (M_t), final moisture content (M_f), standard deviations and square of correlation coefficients for the high frequency drying models (38.5 MHz) (eq (8.9)).

From eq (8.9) above it is noted that when $t=0$ then $M=M_i$. Moreover, when $t \rightarrow \infty$ then $M \rightarrow M_t$. Therefore M_t, the target moisture content, is the value of M in the limit, when $t \rightarrow \infty$. In air drying studies this limit value is the equilibrium moisture content M_e of the product at the corresponding temperature and relative humidity. As noted above some authors have introduced the concept of a "dynamic equilibrium moisture content", as opposed to the true value as defined in Chapter 2. The former is simply the value of M_e which fits best the data to eq (2.14). In the dielectric case, however, the final moisture is not limited by the equilibrium value with air, but it can continue to any required level, even $M \rightarrow M_t=0$. The zero limit has not been used in the present study for M_t due to the following reasons:

i) The available RF generator stops working at a much higher moisture content than the ideal zero limit, hence if the latter value had be taken this might have distorted the fitting of the above equation, which in the ideal dielectric case (i.e. if it were possible to dry the samples in the dielectric rig down to $M=0$) would have $M_t=0$.

ii) In the present case M_t should be in accordance with a practical minimal value, i.e. the equilibrium value for storage.

Using the above analysis, the resultant values for the drying constants k_d and k_q can be correlated with the electrical parameters of the experimental sytem, i.e. amplitude of the RF electrode voltage, input mains voltage and power and variac setting. This was done by obtaining a regression formulae for the drying constants as a function of the input mains voltage V_i and then substituting V_i by one of the expressions given in table 8.4, e.g. those involving V_p or P_i. The latter gives very high correlations with V_i.

Linear, quadratic and exponential models were tried for both drying constants. They all gave good correlation but the exponential model was selected since this was considered to be more useful for extrapolation purposes and also for practical reasons. The cubic, and to some extent the quadratic, models give good results in the mathematical sense but may fail in practice due to the fact that these expressions have a greater degree of freedom. Hence, even though the coefficients are calculated for minimum errors, often the final result has no practical significance.

The following expressions were therefore chosen to estimate the values of k_d and k_q:

$$k_d=a_d\exp(-b_d/V_i) \tag{8.10a}$$

$$k_q=a_q\exp(-b_q/V_i) \tag{8.10b}$$

The results of the corresponding regression analysis are given in table 8.10.

Drying Constant	Regression Coefficients	S_e	r^2
k_d, Coffee	a_d = 0.14, b_d = 94.2	4.7E-3	0.70
k_q, Coffee	k_q = 0.35		
k_d, Maize	a_d = 0.97, b_d = 275.3	6.6E-2	0.87
k_q, Maize	a_q = 0.50, b_q = 33.4	1.6E-2	0.75
k_d, Rice	a_d = 1.18, b_d = 262.8	2.4E-2	0.99
k_q, Rice	a_q = 0.53, b_q = 42.3	5.1E-3	0.98
k_d, Soya	a_d = 0.19, b_d = 127.2	1.5E-2	0.75
k_q, Soya	k_q = 0.35		
k_d, Wheat	a_d = 0.49, b_d = 215.3	1.4E-2	0.91
k_q, Wheat	a_q = 0.44, b_q = 23.8	6.9E-3	0.76

Table 8.10 Regression analysis data for the models of the dielectric drying constants (38.5 MHz)(eqs (8.10)).

Taking eqs (8.9) and (8.10) in conjunction with the coefficients given in table 8.10, it is possible to predict the drying times when the experimental system is operated at 38.5 MHz. Some results are shown in tables 8.11 and 8.12. Some higher voltage results have been obtained by extrapolation. The moisture values in table 8.9 are the maximum used in the experiments, the drying models may not be valid outside these limits. A much greater precision in the predictions results when the models are used with shorter moisture ranges and for higher voltage levels.

Product	M_i	M_f	t_d	V_p	E_p	Max E_{pair} (1)	Max E_{pair} (2)
Rice	33	18	12	1.2	22.2		135
Rice	30	18	4	1.8	33.3		170
Rice	25	18	4	1.2	22.2		95
Rice	25	18	35	0.8	14.8		60
Rice	25	18	2	1.6	29.6		125
Maize	35	18	44	1.2	22.2		140
Maize	30	18	10	1.8	33.3	203	185
Maize	25	18	14	1.2	22.2	112	140
Wheat	40	30	6	1.2	22.2		130
Wheat	40	30	3.5	1.5	27.8		165
Wheat	40	30	12	1.0	18.5		110
Wheat	35	18	78	1.2	22.2		120
Wheat	35	20	19	1.8	33.3		180

Table 8.11 Dielectric drying times (t_d, mins) at 38.5 MHz for cereal products at various initial (M_i) and final (M_f) moisture contents (%w.b.), electrode voltages (V_p, kvolts) and field strengths (E_p, kvolts/metre). Max E_{pair} is the estimated maximum field strength in the surrounding air: (1) considering the dielectric constant of the material individually for each particle (sphere), and (2) considering the dielectric constant of the material in bulk (slab).

Product	M_i	M_f	t_d	V_p	E_p (2)	Max E_{pair}
Soya	50	40	16	1.2	22.2	170
Soya	50	40	10	1.8	33.3	255
Soya	55	45	33	0.8	14.8	125
Soya	55	45	11	1.2	22.2	185
Soya	55	45	8	1.6	29.6	250
Coffee	50	40	31	1.2	22.2	170
Coffee	50	40	21	1.8	33.3	260

Table 8.12 As Table 8.11 but for soya and coffee.

The above Tables show, that for a given field strength, rice is the product which is processed fastest, followed by maize and wheat. Soya and coffee are seen to be slow drying products in high frequency terms. This may be due to the fact that these products contain a substantial amount of oil and tars which might hinder, to some extent, the diffusion of moisture. The slowness of soya and coffee drying is evident when the values in table 8.12 are compared with those for wheat. From these results it is noted that reducing the moisture content by 10% takes much longer for coffee and soya than it does for wheat, although the drying process is faster when carried out at higher moisture content levels.

Soya and coffee are not only slow drying materials but they also appear to be less responsive to changes in electrode voltage levels. Consider, for example, the case of rice being dried from 25 to 18 % w.b. and soya from 55 to 45 % w.b. initially with V_p=0.8 kV. An increase of 50 % in V_p causes a considerable reduction in the drying times of both. With soya this reduction is about two-thirds of the value at 0.8 kV whereas for rice it is reduced to 11 % of the former value. A further increase of 33 % in V_p will produce approximately a 30 % reduction in the drying time of soya, the corresponding effect on rice will be a 50 % reduction. Coffee shows a similar response to electrode voltage changes as soya in the range considered.

Another factor which has a considerable effect on the drying times is the value of the initial moisture content level M_i. When M_i of rice is increased from 25 % to 33 % w.b. it triples the time required for drying the material down to 18 % w.b. at V_p= 1.2 kV. An increase of only 20 % in the initial 25 % w.b. value requires a 50% increase, to 1.8 kV, in voltage, in order to achieve the same drying time. This doubles the maximum field strength level in the surrounding air which increases the probability of breakdowns occuring. A similar effect is observed for maize, e.g. at 1.2 kV an increase of 40 %

in the initial moisture content level of 25% w.b. triples the drying time.

8.2.5.5 Breakdown Occurrence

Rice and wheat were dried with a maximum V_p level of 1.66 kV, the maximum for maize and soya was 1.54 kV. In the latter case electrical breakdowns imposed the restriction on increasing voltage levels, whereas for maize the splitting of the kernel was the key factor. Coffee was dried using up to 1.8 kV on the electrodes and, although breakdowns occurred in some cases, it was still possible to safely perform many drying runs at such high voltages. With soya this was not possible since any attempt to go beyond the 1.5-1.6 kV value caused a breakdown. Breakdowns were apparently induced by two different mechanisms: Partial carbonization in the drying zone and also due to high values of the dielectric constant of relatively cold material samples.

The first type developed with soya and, especially, coffee. It was characterized in the case of soya by a smell at the air exhaust end also by the visual evidence of a minor burning on the surface of some beans. The latter occurred first. Some soya drying runs were performed at 1.4 kV at which this light superficial burning was evident but breakdown did not develop. Breakdown always ocurred with soya at 1.54 kV and moisture contents of 50-45 % w.b. With coffee, breakdown developed only in some cases above approximately 1.6 kV. Here this was clearly induced by overheating of the product and combustion of tars, the latter producing smoke at the exhaust outlet a few seconds before the breakdown. Moisture content of the product was in the range of 45-40 % w.b. Other coffee drying runs were carried out with no problems at higher voltages and moisture contents. An interesting case occurred when a breakdown was induced at 1.8 kV, not due to carbonization of the product (the maximum temperature was 80 C) or high moisture content (55-50 % w.b.) but caused by the burning of the PVC container fin. This was subsequently replaced by a PTFE component.

Soya produced examples of breakdowns directly caused by high values of the dielectric constant. One case occurred at 1.54 kV half a minute after drying started when the temperature of the product was at ambient and its moisture content of the order of 45 % w.b. When drying wheat a similar breakdown occurred only once, at 1.66 kV, when the moisture content was close to 40 % w.b.

An estimate of field strengths in the air surrounding the material is given in table 8.13 for the cases discussed in the above paragraphs. Similar to the values presented in table 8.12, the results may be conservative when the moisture content is higher than 35-40 % w.b. due to the measurement limitations of the capacitance-Q factor methods for estimating dielectric properties over that range of moisture content.

Product	Moisture (% w.b.)	V_p (kvolts)	Max E_{pair} (kvolts/m)
Soya	45	1.54	200
Soya	50-45	1.54	220
Coffee	50-45	1.66	240
Coffee	45-40	1.54	195
Wheat	40	1.66	185

Table 8.13 Estimation of the field strength in air preceding breakdown development.

It would appear that the probability of breakdowns developing increases when the field strength in the surrounding air exceeds the 200 kV/m (peak) mark. This value has been taken as the maximum allowable level for a breakdown-free drying process in the calculations performed in Chapter 6.

9. CONCLUSIONS AND RECOMMENDATIONS

This Report has explored the possibilities of using novel drying techniques to obtain potential improvements over conventional processes, which are usually based on convection methods. The work has been concentrated on electrotechnologies, in which methods for evaluating the feasibility of new techniques, especially high frequency drying, have so far not been well developed. Both economic and technical factors are introduced and used to establish criteria and to develop experimental methods and equipment in order to make a particular contribution to the study of drying by high frequency methods.

It has been shown that in order for infrared to compete economically with convection in crop drying applications the levels of throughput per unit of radiated area must be increased over those which have been proposed in technical literature so far. This requires applying much higher radiation levels per unit volume of material than what has hitherto been done. This has not exceeded 5 kW/m^2 of effective radiation on a thin layer (up to 5 cm thick vibrated layer). This will be difficult to attain bearing in mind the temperature sensitivity and low thermal conductivity of the materials concerned, which are easily damaged at 80 C or even 60 C in some cases. As far as applications in agro-industry are concerned, electrical infrared presents an additional disadvantage, the same levels of radiation can be obtained at a lower cost with biomass gas systems. Conduction gives rise to similar problems when dealing with poor heat conductors and the thickness of the layer or bed of the material must be kept low. Ideally the heat should be applied to single granules and the temperature levels need to be high. This would require large dryers to process an acceptable amount of material and would involve long drying times due to the temperature limitation.

The cost of industrial high frequency heating equipment is high, in part this is due to the restricted nature of the market relied upon so far. Research and development in this field is very limited and most of the new applications proposed are based on well established designs. The high frequency drying rig developed in this work is a valuable tool for future pre-prototype study at an affordable cost to the research worker. The experimental work has focussed on the study of a crossflow dielectric configuration which appears to be the most convenient for drying granular materials in a large throughput continuous mode. The reasons for selecting this configuration are discussed in Chapter 7 and are based on the analysis presented in Chapter 6. Basically this is due to lower investment costs, longer life and greater throughputs of the crossflow dielectric scheme for a given dimension of the drying zone. The arrangement uses dielectric power assisted by crossflow convection, the frequency being in the low or medium RF band, i.e. in the range 10 MHz to more than 40 MHz.

The design, construction and operation of the experimental dryer involved a consideration of electrical (mains and RF), mechanical and thermal variables. Other factors were also taken into account, e.g. safety requirements relating to human exposure to RF voltage and radiation and interference with radio communication systems. The assessment of RF breakdowns and maximum dielectric power density levels were also considered. The rig was used to study the high frequency drying process under different operating conditions, e.g. a range of RF voltage and input power levels. Amongst the variables studied were drying times, moisture content and temperature variation, volume shrinkage, dielectric power density, energy efficiency, energy usage and electrical parameters of the load. In order to evaluate the performance of different dielectric dryers and to design the experimental system it was necessary to measure the dielectric properties of all the products used over the frequency, temperature and moisture ranges of interest. The data have been presented in the Report and used to develop mathematical models of the parameters in terms of the moisture content of the product and the frequency of the electric field. Most of this information is hitherto unpublished.

The factors which most affect the economic feasibility of drying a given product with high frequency techniques can be determined with the aid of the methodology introduced in Appendix II. By far the most important factor is the reduction in drying time as compared with convection. The dielectric drying time is greatly affected by the electric field strength or dielectric power density levels, but it cannot be reduced beyond definite values if electrical breakdowns or damage to the sample is to be avoided. The specific minimum drying times of different material samples as limited by breakdown and quality considerations are given in Chapter 6 and 8. The values given in Chapter 6 are obtained on a theoretical basis but appear to agree very closely to the experimental figures (Chapter 8) for cereals. In the case of soya and coffee, the theoretical approximation yielded optimistic results. This is due possibly to the oil rich material hindering the diffusion of internal moisture outwards. It is shown in Appendix II that the unit investment costs and energy efficiencies of the convection and dielectric plants also affect considerably the feasibility of the latter type of equipment. A comparison between the energy efficiency of different convective and dielectric drying plants is given in Appendix II. A more detailed study of the energy efficiency of the experimental high frequency dryer is found in Chapter 8.

The experimental system developed allows processes to be examined, especially those involving products which dry much more quickly in an electric field as compared with conventional methods. Amongst the materials studied in this work rice appears to be the only one with a real promise of being dried economically using dielectric techniques, even then a considerable reduction in investment costs will be required. In the conservative estimate made in Appendix II it was found that, in the case studied, the unit investment costs would have to be reduced down to levels presently found in the domestic microwave segment of the market (approximately US$ 200/ kW). In practice this reduction may not have to be so drastic, but more exact figures can only be obtained with the help of accurate data on the drying of rice in commercial crossflow plants. Reliable and already checked information is available for maize but it was not possible to obtain the same for rice. Further studies are needed with this material, in the experiments it was not possible to study the process at its highest throughput mode (minimum drying time), i.e. just before breakdown or quality damage occurs. This was possible with all the other four materials under consideration but the experimental RF unit was not capable of providing a power density of more than approximately 1 MW/m^3 in the bulk of the product. There is experimental evidence that rice withstands far greater dissipation levels than those attained in Chapter 8 (see Chapter 6). Rice dries much quicker than other materials under the same conditions, e.g. at 38.5 MHz and a field strength of 33 kV/m the drying time is reduced to 14 % of that for coffee.

The experimental results concerning the dielectric drying times were obtained using a sample of material held between a perforated RF electrode system operated at 38.5 MHz. Different RF field strength levels were applied to the electrodes and the effect on the drying time and other variables were recorded and expressed mathematically in empirical equations. This arrangement aimed to give a set of technical and economic criteria which can be used at the pre-prototype level in order to decide if further developments stand a real chance given the material drying characteristics. The results would be, at the moment, the best possible approximation of the high frequency drying in the final prototype, which may be of the conveyor or vertical crossflow dielectric types (see Chapter 6). The latter are continuous rather than batch systems, hence the experimental results (batch) simulates the conditions prevailing on a section of the real dryer with given RF and other operational conditions. Therefore, the same results can only be expected in the overall drying zone of the real apparatus if similar conditions occur throughout the same. Different pressure conditions of the bulk of material in a large, commercial vertical arrangement may have an effect on the dielectric properties of the material (Chapter 6). This was not included in the experimental work. Different ambient and air conditions can be changed in the experimental rig developed with a few modifications in the latter. This was not possible to do in this research due to time and resource limitations, but they are likely to have minor effects in the dielectric drying process itself (Chapter 8) except perhaps in excessively damp ambient conditions, when breakdowns around the electrode system would present a problem. This latter effect is worth studying in detail if this technology is to be used in tropical latitudes. The maximum field strength levels prior to breakdowns were estimated in the experiments and agreed very closely with the technical literature (around 200 kV/m peak).

Amongst the measurements of variables perhaps the most critical of them are the high RF voltage levels on the electrodes, which could not be measured directly with the commercially available electric instruments. In this case calorimetric estimations are commonly used. Nearly 70 of such experiments were carried out to calibrate the unit, they yielded a highly correlated set of data although the scattering was not negligible. It is important to note, however, that all calculations involving the RF voltages yielded sound results, including the air field strength for breakdown assessment.

The experimental work used a 38.5 MHz standard power source already available in the laboratory. In the future this could be adapted to improve the source/load power transfer and to obtain more information on RF parameters prior to the drying stage. The drying equations at other frequencies can be obtained with the same methodology presented in Chapter 8 if appropriate power sources are made available. The dielectric properties were measured over the 13.5-40 MHz band and these results are readily available to be used in other studies involving drying in this frequency range. Alternatively it may be instructive to consider dielectric power densities (q_d) rather than, as here, voltage or field strength. This would yield a more general type of model which would be independent of frequency over a large range, and not, as was the case here, limited to the 38.5 MHz band. In order to carry out such experiments a procedure similar to the one carried out here might be followed with the addition that, at every measuring stage, the input power level would be adjusted, this would require a very flexible RF source. The electrical resistance of the load can be estimated using the models for e" and eq (8.5) and used to determine the instantaneous energy efficiency making use of regressions formulae similar to those presented in table (8.8). The required input power level would need to be adjusted to:

$$P_i = q_d V / \eta_e$$

where q_d is the dielectric power density at which the drying run is being performed.

The experimental apparatus could also be used in more fundamental types of research, for example in checking part of the theoretical solution of the heat and mass transfer equations presented in Chapter 2 once all the thermo and physical parameters are known (eqs (2.27) and (2.33)). This might be done as part of a research programme whose objective was to measure the mass difusivity and thermal gradient coefficient. It might be preferable to begin the research with materials having an uniform microscopic structure and progress to more complex substances such as biological products.

The work reported here is especially relevant to industrial energy planning strategies in those countries which have a particular economic dependence on imported oil, but which have abundant hydro and other primary energy sources which need to be converted to electricity in order to be used in industrial process heating applications. At the microeconomic level, they are of industrial importance in the conversion of existing heating processes to new technologies so increasing appreciably the throughput and the revenues from the business. This work has presented a methodology which can be used for checking, up to the pre-prototype level, the feasibility of introducing the proposed equipment in accordance with the developing macro and micro economic scenarios. This methodology made possible the evaluation of different techniques, including the technical and economical points for and against each and why the crossflow dielectric, and particullarly RF configuration, was chosen to further research and development.

APPENDIX I

A.1 Energy Resources and Usage

The so-called oil crises of 1973 and 1979 produced a remarkable impact in the economy of the World which, for the first time in recent history, realised that fossil fuels were extremely valuable commodities. Those not having significant oil reserves or geopolitical power saw their development jeopardized by the inevitable effect on the terms of trade relating their export products to imported oil and capital goods. Some Latin American and African nations were particularly affected by the economic conditions established after these two crises, especially those countries whose economies were largely based on imported oil products. The question was; How to pay for the ever increasing costs of imported capital goods, produced in the inflationary economy of the developed countries and how to cope with the additional burden of expensive fuel for running the economy ?

Those developing nations which possessed large oil reserves had the opportunity to create considerable capital reserves and initiate their own independent plans for industrialization.

Political conditions allowed them to obtain advantages from the petrol multinationals and to acquire increased support from the developed nations in which the oil-rich countries deposited much of the capital accumulated during the oil boom of the 70's. With such large amounts of money available for investment the overwhelming majority of banks turned to the developing nations, offering attractive credits with the ultimate objective of promoting social and economic progress.

The major investments were concentrated on the modernization and expansion of industry and in the infrastructure required for this sector of the economy, e.g. roads, electricity, ports. Some countries undertook large energy projects in order to become less dependent on energy imports. Amongst the Latin American countries, Brazil and Costa Rica made significant investments in the development of internal energy resources. Brazil, for example, developed a significant sugar-cane alchohol programme and also accelerated the use of its hydro electric potential. These two nations, Brazil and Costa Rica, shared similar energy crises but within different political, economic and social scenarios. Both have large hydro electric and biomass potentials, the former also has uranium deposits and Costa Rica possesses some geothermal energy.

The Brazilian government has estimated that hydroenergy will account for most of the electricity produced in the country, at least until the year 2015 [96]. There is still a large portion of the country which has no electricity supply, especially in rural areas. It has been reported that, although the average rate of increase of electricity consumption in rural areas was 23 % per annum between 1976 and 1981, only 10 % of the total number of settlements is supplied with electricity [4].

Costa Rica is a small nation and electricity is close to almost all towns and settlements of the country. Only a few of the major agro-industries are not connected to this service. It has a population of almost 2.5 million with, basically, an agricultural economy. It is dependent in imported capital goods and has no known petroleum resources although its hydro potential is remarkable considering the size of the country, only 50,000 km^2. More than 8,500 MW of identified and feasible hydroelectric potential is estimated to be available, although only 500 MW of this capacity has been developed. Hydro electricity provides approximately 98 % of the electric energy demand in this country [86]. The official estimates given by goverment institutions place the renewable biomass potential very close to that of hydro electricity. In 1966 the participation of biomass in the consumption of energy in industry accounted for nearly 60 % of the total. In 1981 this participation was just 35 %, whereas in the same period the contribution of petroleum products went up from 35 % to 50 % and electricity from 7 % to 16 %. This process of energy substition is shown in table A.1. In 1981 13 % of Costa Rican imports were petroleum products (ibid).

Energy Source	1966	1971	1981
Coal & Coke	0.1 %	0.1 %	0.1 %
Biomass	57.6	49.2	34.6
Electricity	7.3	10.1	15.5
LPG	0.3	0.6	1.1
Kerosene	-	-	1.1
Diesel Oil	10.0	16.5	11.3
Fuel Oil	24.7	23.5	36.6

Table A.1 Energy Consumption in Costa Rican Industry [26].

As far as the consumption of petroleum products in Costa Rican industrial sector is concerned, the major utilisation is for fuel oil with a relatively small use of diesel, mainly used in burners, for drying cereal grain products. In 1982 it was estimated that one third of the fuel oil consumed by industry was used for generation of steam and two thirds for direct heating processes (10% for medium temperature applications, mainly drying, and 58 % for high temperature furnaces, largely concentrated in the three cement plants operating in the country at that time). Practically the entire consumption of fuel oil used for generation of steam and medium temperature processes was located in the Central Valley, a relatively small region and therefore quite convenient for allowing the reinforcement of electric distribution lines which would be required if a national programme of substitution of petroleum by electricity were carried out [26].

Brazil is over 8.5 million km^2 in area and has a population of 130 million. Its hydro electric potential is the largest of all the Latin American countries, more than 213,000 MW. By the end of 1984 the installed electric generation capacity was 41,000 MW, 85 % of this being in hydro electric plants [160]. It has been reported that 92 % of the electrical energy demand was supplied from these plants [41], a more recent report estimates this figure as 97 % [96]. Petrol reserves are small, the national production covers only a fraction of the consumption. In 1940 9 % of the energy used in the country came from petrol and 75 % from biomass. Hydro electricity and coal accounted for the rest. In 1981 petrol accounted for 41 %, biomass for 29 % and hydro electricity for 28 % of the total (see [95]). This change is shown in table A.2, the resulting importance of imported oil on the trade balance is shown in table A.3.

Energy Product	1941	1971	1981
Coal & Natural Gas	7.0 %	4.0 %	5.0 %
Biomass	76.8	36.8	25.7
Hydroelectricity	7.0	19.0	28.8
Petroleum	9.2	40.2	40.5

Table A.2 Energy Consumption in Brazil [95].

Economic Variable	1970	1976	1981
Increase in GNP (%)	8.8	9.7	-1.9
Exports (US$ thousand million)	2.7	10.1	23.3
Imports (US$ t.m.)	2.5	12.4	22.1
Petroleum Imports (US$ t.m.)	0.3	3.8	11.3

Table A.3 Impact of Petrol on the External Trade of Brazil [95].

As far as the use of petrol for thermal processes is concerned, fuel oil is again the major component in Brazilian industry [22]. Half of this is used for steam generation, of which a major part is employed in drying processes (see for example [95]). In terms of coffee and cereal grain drying, it has been reported by CESP (Energy Company of the State of Sao Paulo) that, in the early 80's, diesel was no longer used for process heating, 75 % of the fuel oil was used for steam generation and the rest, together with the whole consumption of firewood, in direct heating processes, i.e. generation of hot air.

When the price of petrol increases, industrial consumption tends to concentrate on the heavier oil products which are usually cheaper than the more refined oils. This tendency is justified on the grounds that, in most cases, the change from light to heavy oil products only involves the replacement of burners and auxiliary equipment. Even when the modifications are more complex the substitution is usually economically justifiable, therefore fuel-oil is the real reference against which any substitution of petroleum products by indigenous fuels should be compared.

There has been a noticeable substitution of imported oil in

Brazil, this is motivated by the dependence of the country on imported fuels as shown in tables A.2 and A.3 and also due to internal political and economical factors and a temporary surplus of hydroenergy. In the transport sector the production of alcohol from biomass has resulted in a situation where more than 80 % of all new automobiles are produced to burn this fuel rather than petrol. In industry the substitution of a considerable amount of oil by biomass and electroheat was carried out during 1980-1985. However, the adoption of electroheat techniques occurred due to reduced electric tariffs and not to the promotion of more efficient systems which might have led to a cost-effective technological innovation in industry.

During 1980-1986 new tariffs were designed to increase the consumption of electricity as a substitute for petroleum. These tariffs offered substantial reductions in energy and maximum demand charges, the latter was actually eliminated in some cases. The supply of cheap electricity was usually guaranteed for a limited period of time although some contracts offered no such guarantee, i.e. the utility could interrupt the service at any moment (the customer then needed to maintain the original equipment as a stand-by). All of this certainly promoted investment in low cost equipment with a short pay-back period. Lenza has called this the "resistancialisation de l'electrothermie" in Brazil [95]. It did not lead to any improvement being made in the industrial process itself. A considerable substitution occurred and the Government was able to sell most of the surplus hydroelectricity. However, it may well be that the opportunity presented by the so-called energy crisis in Brazil was largely misused since, with the level of Goverment intervention at that time, it would have been relatively easy to promote the research and application of more advanced electrotechnologies in industry. In other words, a short sighted solution was adopted for what appears to be a chronic cause of problems. Infrared and high frequency heating techniques experienced no significant increase and it is estimated that 70 % of the replacements were in the form of electrical boilers. Lenza reports that the normal price of electricity for industrial customers was between 2.6 and 3.3 cents per kWh whereas the price charged for each kWh used in electroheat plants was 0.6 cents or less.

Most Costa Rican coffee and cereal grain plants use hot air directly produced from combustion ovens and burners. Although a large amount of cereal grain (i.e. rice and maize) is still dried by diesel powered burners it has been reported that the residues from such plants are enough to dry the whole production of the country [47]. The energy potential of rice husks has been discussed elsewhere (see a review presented by Mao & LePori [102]. Coffee plants using wood were retrofitted to diesel oil in the last decade and then from the latter to fuel oil as a consequence of the continuing increase in petrol prices. In the early 80's a further substitution, this time a reversion to wood, was observed. The conversion of oil-fired heating equipment to electricity was not encouraged in industry. This coincided with a fuel oil subsidy due to political and economical conditions. It was noted that the local petroleum refinery was producing a considerable excess of fuel oil which needed to be mostly absorbed by the internal market. The country was able to produce more electricity than it required, the Government solved this problem by selling the surplus to neighbouring Central American countries. The price charged for each kWh of electricity used in electroheat plants was as shown in figure 3.4 where it is noted that the minimum price which an average agro-industrial plant with 0.3 load factor (e.g. coffee drying plants [27] would expect to pay was, even under very restricted conditions (off-peak and seasonal operation only), substantially higher than that being offered in Brazil. This difference becomes even greater if one considers that the tariffs quoted by Lenza are based on the official exchange rate for the dollar, which is normally less than the spot price level that was used in the above reports.

The Costa Rican Government did not encourage the electrothermal solution. The trend was towards an increased use of biomass technology which is understandable in view of the country's resources, agricultural structure and economic status. This is so because, although a large hydro and geothermal potential is available, the resources needed for developing it are mainly dependent on external borrowing. The major investment required in electrical equipment is not in the industrial sector, i.e. in the transformation of secondary energy (e.g. electricity) into useful work (e.g. process heating) since this is seen as relatively small per unit of installed kW as far as conventional electroheat techniques are concerned. Biomass technology may allow for a more uniform development and share of the benefits obtainable from a national program of oil substitution in this particular Country in which agro-industrial co-operatives have been succesful over the past few years. The Government of the Country has financed studies which recommend that these rural co-operatives extend their involvement into forest development projects. It should be noted however that a great deal of planning of production, distribution, storage and handling of biomass products will be required. This is in contrast to with the already well developed electricity utility industry [26].

APPENDIX II

A.2 Economic Analysis of High Frequency Drying

A.2.1 Introduction

Below the feasibility of the process presented in Chapters 6 and 8 is examined based on the case of the commercial drying of crops. The latter has been used in the present study as a vehicle for developing the analysis and apparatus. It should be noted that the experimental drying results were obtained at a frequency of around 40 MHz although the dielectric properties of the materials examined showed little variation in the wider 13-40 MHz RF band. Other applications involving similar granular materials may be analysed following the same methodology used in this Report. The factors which will produce a successful application of dielectric drying are not only related to the change in energy source from the original fuel to electricity although, in fact, such changes enhance the technological level and increase the reliability and productivity of the plant. The energy consumption is not particularly low in dielectric installations as shown in table A.4 where the requirements of different drying methods are compared. Additional benefits such as the roasting and sterilizing of food products may be important and can be taken into account by the user interested in this feature (see Appendix III).

Source	Product	Type of Dryer	M_i, M_f (% w.b.)	Energy Required MJ/kg
Bakker-Arkema et al 1979	Cereal	Standard crossflow	25, 16	7.2
Bakker-Arkema et al 1979	Cereal	Crossflow & air recycling	25, 15	5.1
Laferriere et al 1986	Cereal	Prototype mixed flow	26, 16	3.3
Butler & Gardner 1982	Cereal	Prototype microwave vacuum	22, 14	4.2
Experiments, 1987 (Ch.8)		Experimental RF:		
	Cereal		25, 14	6.3
	Coffee		56, 39	3.2

Table A.4 Energy requirements for various drying methods (1 kWh = 3.6 MJ).

Although each application has to be considered individually, it is possible to analyse the effect which the many quantifiable variables have on the economics of the substitution. The technological parameters include the dimensions of the drying zones in the dielectric and convective plants, the strength of the field to be applied in the material, the initial and final moisture contents of the product and the convective drying mechanism in the conventional plant. Economic factors may also have an effect, e.g. the investment costs and the useful lives of the conventional and dielectric units, the energy costs in both systems and the level of interest rate obtainable. In any event, there should be a major advantage in moving from an external to an internally produced heating effect. It has been noted in this Report that this variation in the energy transfer method may increase the speed of the drying operation which will increase the throughput. However, the response to the internally generated heating effect changes with the characteristics of the material. Hence it will be required to check each individual application under consideration as shown in Chapters 6 and 8.

The question remains as to whether the throughput increase will offset the large capital and running costs associated with a high frequency plant. In so far as the type of materials referred to above is concerned, this is a problem which can be properly addressed with the help of the experimental procedures discussed in Chapter 8 together with the data for a conventional drying plant.

The criteria must be applied carefully since, as mentioned above, an internal heating technique will probably yield an increased throughput. It is customary when considering a plant replacement or extension to compare the alternatives in equal output terms considering the input required or, in this case, the costs required to produce a given product. This means, in strict terms, that the type of analysis in which two components, energy and throughput, of the conventional system are compared with the dielectric option might give misleading results. In doing this we may not be comparing two alternative projects on equal economic terms, i.e. we might be overlooking the changes which might be made in the conventional technology. Thus, in order to be consistent, given a throughput increase obtained by the dielectric method, it is necessary to determine the changes required to equalize the two systems. In many cases this procedure will be difficult, given the impact of the innovation involved, but, nevertheless, every effort should be made to compare the two alternatives on an equal basis. A more detailed discussion of this aspect can be found in engineering economics textbooks such as [137] and [159].

A.2.2 Methodology

Here the two alternatives, i.e. the convective (crossflow) and dielectric technique are compared on an equal throughput basis by considering a given drying zone volume in the dielectric plant and then estimating how large the corresponding volume would need to be in the crossflow case to give the same level of production.

The following methodology can be used:

a. Given the dimensions of the column in a typical crossflow dryer, then it is necessary to determine the volume of the drying zone in a similarly sized RF system. The latter is assumed to be the same as that in the columns of the crossflow unit. In Chapter 8 the dielectric drying of a relatively thin layer of material was considered primarily in order to obtain as uniform drying conditions as possible in the product. The major problem in using thicker layers may well be the deep bed drying effect discussed in Chapter 2. However, since the convective phase of the operation will be present in both the dielectric and the crossflow alternatives, the above assumption is considered to be reasonable. In the dielectric process studied in this report convection has only a limited function, i.e. the carrying away of the surface water coming from the inside of the particles when an electric field is applied. In the crossflow system, however, convection is the major drying element.

b. Select the maximum field strength in the material Ep in accordance with its quality and breakdown characteristics (see Chapter 8). For a given reduction in moisture content, i.e. (M_f-M_i) the drying time t_d (mins) can be found using the methods described in the Report.

c. The velocity of the material passing through the applicator is the ratio of the length of travel through the field and the drying time estimated above. The throughput, with no recirculation, is the product of the velocity and the total cross sectional area between the electrodes;

$$\mathcal{T} = (V/t_d)\times 60 \qquad m^3/h$$

d. Estimate the drying column capacity (in volume terms) required to equalize $\mathcal{T}$ as above. The additional floor space and associated costs involved are small as compared with the drying capacity investment in most agro-industrial applications. A convenient way to express the capacity expansion is in terms of the column height in the cereal drying simulation (e.g. [136]). For other products actual data need to be obtained (e.g. [25], see a summary of this in point f below). Once the required height is found the additional column capacity is;

$$\Delta Cap = Height \times Thickness \times Total\ Length$$

e. Evaluate the ratio of the annual running and capital costs of the dielectric and crossflow systems, the result must be less than unity for the retrofitting to be acceptable.

$$\{HRP_{die}C_{die}+Inv_{die}P_{die}i/[1-(1+i)^{-n}]\}/\{HRP_{c}C_{c}+Inv_{c}\Delta Capi/[1-(1+i)^{-n}]\}$$

P_c and P_{die} are the installed heating capacities in the conventional (crossflow) and dielectric plant, C_c and C_{die} are the unit energy costs in the plants and HR is the hours of operation in a year. Inv_c and Inv_{die} are the unit investment costs in the crossflow and dielectric units, i is the minimum acceptable return on the investment (higher than the interest level in the market) in an annual (per-unit) basis, and n is the anticipated life of the equipment which is assumed equal for both systems.

Various possible energy cost scenarios can be considered from extremely cheap fuels for the crossflow dryer to fuel costs comparable to those of electricity. The former would be the case when the unit is being fed by the crop residues. Rice drying can be made an energy self-sufficient process if the hulls of the material are used as a fuel (Flores and Zeledon [47], Mao and LePori [102]). In coffee processing part of the energy for combustion needs to be supplied by sources other than the hull residues (Caldas [27]). The other extreme condition occurs when electricity is used to heat the drying air in the crossflow system. For a given drying operation both the latter and the dielectric alternative have similar energy requirements (see table A.4) and it is only necessary for the term $\Delta CapInv_c$ to be greater than $Inv_{die}P_{die}$ for the dielectric plant to become the best of the alternatives.

f. From the assessment carried out by Caldas [25], it can be concluded that a popular cross-flow dryer used in the Costa Rican coffee industry is the unit shown in Chapter 1 although, as noted by the manager of FEDECOP (the national association of all the coffee co-operatives in the Country) only the drying section of the apparatus is employed, i.e. there is no cooling section in the system. The following two models are commonly available;

1) "Small Unit"

- Holds 23 m^3 of wet coffee (51 % w.b.) in its interior.
- Volume of drying columns approximately half of the above, i.e. 12 m^3.
- Height, thickness and length of each drying column as 5.8 m, 0.38 m and 2.8 m respectively.
- Total column frontal area 32.5 m^2, total column cross sectional area 2.1 m^2
- Air flow is 80,000 m^3/h, or 41 m^3/min per m^2 of frontal column area.
- Temperature of drying air in the range 60-65 C.
- Processing from 51 to 40 % w.b. 9.2 m^3/h of wet coffee.
- Investment cost is US$ 50,000.

2) "Large Unit"

- Holds 40 m^3 of wet coffee (51 % w.b.) in its interior.
- Air flow is 153,000 m^3/h.
- Temperature of drying air as above.
- Processing from 51 to 40 % w.b. 16.9 m^3/h

of wet coffee.

- Volume of drying columns approximately 21 m^3.
- Thickness of drying columns as above.
- *Investment cost is US$ 100,000.*

The total investment costs of the crossflow plants show a negligible variation when the thickness of the drying columns is varied from, say, 7 to 38 cm, although the unit investment cost per m^3 of drying column, used in the following calculations (Inv_c) is considerably affected.

A.2.3 Economic Analysis

A.2.3.1 Analysis of Drying and Capacity Expansion

Examining first the drying of maize in the type of plant specified in f.1 and following the steps a-d shows that, for a drying zone volume in the RF plant of 12 m^3 and maximum field strength 26E3 V/m, drying from 27 to 17 % w.b. takes t_d=16 mins, and 37 mins from 27 to 13 % w.b. The corresponding throughput values for these conditions are;

$$T = (12/16)x60 = 45\ m^3/h$$

$$T = (12/37) \times 60 = 19.5 \ m^3/h$$

were the lower values refer to thinner layers of material as shown below.

The data given below is then entered in a crossflow dryer simulation program (e.g. [136]):

Product initial moisture content; 27 % w.b.

Product initial temperature; 19 C (as dielectric drying run)

Product density; 755 kg/m^3 (ibid)

Ambient temperature; 19.5 C (ibid)

Air absolute humidity; 0.008 (ibid)

Drying air temperature; 80 C (cereals drying practice)

Air flow; 41 m^3/min per m^2 of frontal column area,

together with the following conditions for each individual simulation:

Sim. 1: Drying from 27 to 17 % w.b. and column thickness 0.38 m, hence flow of wet product is 16 tonnes/h per m^2 of drying zone cross sectional area.

Sim. 2: Drying from 27 to 13 % w.b. and column thickness 0.38 m, hence flow of wet product is 7 tonnes/h per m^2 of drying zone cross sectional area.

Sim. 3: Drying from 27 to 17 % w.b. and column thickness 0.14 m, hence flow of wet product is as in Sim. 1.

Sim. 4: Drying from 27 to 13 % w.b. and column thickness 0.14 m, hence flow of wet product is as in Sim. 2.

Sim. 5: Drying from 27 to 17 % w.b. and column thickness 0.07 m, hence flow of wet product is as in Sim. 1.

Sim. 6: Drying from 27 to 13 % w.b. and column thickness 0.07 m, hence flow of wet product is as in Sim. 2.

The following results are obtained where the terms in parentheses refer to the number of equivalent sized crossflow units which the dielectric plant is replacing in each of the cases. As the column thickness is reduced the crossflow system becomes more effective but even when very thin layers are used the dielectric system can process at least 4 times as much as its convective equivalent.

Sim. 1: h=38m; ΔCap=38x0.38x2x2.8=80m^3 (6.6)

Sim. 2: h=28m, ΔCap=28x0.38x2x2.8=60m^3 (5.0)

Sim. 3: h=30m, ΔCap=30x0.14x2x2.8=24m^3 (5.4)

Sim. 4: h=24m, ΔCap=24x0.14x2x2.8=20m^3 (4.5)

Sim. 5: h=28m, ΔCap=28x0.07x2x2.8=11m^3 (5.0)

Sim. 6: h=22m, ΔCap=22x0.07x2x2.8= 9m^3 (4.1)

A crossflow drying model for coffee is not yet available, therefore, the specifications given in f are used instead. The results are that the maximum field strength would be 24E3 V/m and from the experimentsal results it is found that drying coffee from 51 to 40 % w.b. requires nearly 15 minutes which gives a throughput of 48 m^3/h for a dielectric system with the same drying zone volume as the crossflow in f.1. Comparing this throughput level with that of f.1 indicates that the dielectric unit would replace five such conventional plants.

Turning now to the important case of rice, as shown in Chapter 8 this material is extremely resistant to internal heat dissipation and, for a given field strength, dries much faster than the other products examined. It was not possible to obtain a reliable crossflow simulation program for rice. The program for maize [136] has been used extensively for design purposes in the agro-industries in Brazil and has also been found appropriate for modelling the crossflow drying of wheat when the appropriate data are inserted. Attempts to do the same with rice data have not yielded good results (ibid). Of the three cereals considered in this report, rice is the only one which is covered by a hard hull, this makes convective drying process more difficult and, no doubt, slower. However, as a first approximation the crossflow drying estimates obtained above for maize have been used to evaluate the technical and economic feasibility of the process for rice.

Although rice would probably stand higher field strengths, in the experiments described above it was not possible to exceed the 33 kV/m level with the equipment available. With this field it was possible to dry from 27 to 17 % w.b. in 3 mins and from 27 to 13 % in 5 mins. The corresponding throughputs for a dielectric plant with a drying zone similar to that in f.1 would be:

From 27 to 17 % w.b.: $T = (12/3) \times 60 = 240\ m^3/h$

From 27 to 13 % w.b.: $T = (12/5) \times 60 = 144\ m^3/h$.

where the lower throughput cases are included in the following simulations.

Sim. 1: Drying from 27 to 17% w.b. and column thickness 0.38m, hence flow of wet product is 86 tonnes/h per m^2 of drying zone cross sectional area.

Sim. 2: Drying from 27 to 13% w.b. and column thickness

0.38m, hence flow of wet product is 52 tonnes/h per m^2 of drying zone cross sectional area.

Sim. 3: Drying from 27 to 17 % w.b. and column thickness 0.14 m hence flow of wet product is as in Sim. 1.

Sim.4 : Drying from 27 to 13% w.b. and column thickness 0.14m hence flow of wet product is as in Sim. 2.

Sim. 5: Drying from 27 to 17 % w.b. and column thickness 0.07 m hence flow of wet product is as in Sim. 1.

Sim. 6: Drying from 27 to 13 % w.b. and column thickness 0.07 m hence flow of wet product is as in Sim. 2.

The following results are obtained; as before the terms in parentheses refer to the number of equivalent sized crossflow units the dielectric plant is replacing.

Sim. 1: h=195m; ΔCap=195x0.38x2x2.8=415m^3 (35)

Sim. 2: h=200m, ΔCap=200x0.38x2x2.8=426m^3 (36)

Sim. 3: h=150m, ΔCap=150x0.14x2x2.8=118m^3 (10)

Sim. 4: h=175m, ΔCap=175x0.14x2x2.8=137m^3 (11)

Sim. 5: h=140m, ΔCap=148x0.07x2x2.8= 58m^3 (5)

Sim. 6: h=160m, ΔCap=160x0.07x2x2.8= 63m^3 (5)

A.2.3.2 Discussion on Economic Feasibility

Although the figures quoted for rice are only approximate (believed to be conservative), it is evident that the much greater response of this material to the high frequency field will have a dramatic effect on the feasibility of a dielectric drying process. The results of applying the final item (e) of the evaluation procedure can now be considered, the analysis was carried out with the aid of a computer spreadsheet which was thought to be the most practical way of analysing the effects of several input variables on the final economics. The values of all the parameters were varied, bearing in mind the following points:

i) The energy efficiency of the dielectric drying plant (η_d) will be in the range 0.4-0.6 (see Chapter 8).

ii) The hours of operation in a year of a typical single-crop drying plant will be around HR=2,500.

iii) The unit energy costs of the dielectric plant, C_{die} are those for commercial electricity, e.g. approximately US$ 0.05/kWh for a hydroelectric based system.

iv) The minimum return on investment is considered to be i=0.20 which is a typical industrial figure. In this type of application it is unlikely that a lifetime greater than n=5 years would be considered (see for example [86]).

v) The unit investment costs of an industrial dielectric drying unit are well above US$ 1,000/kW, the latter level will be used here as a reference value only.

At present, the high frequency drying of maize and coffee would not be economically sound, although it is technically feasible. It would cost as much as 30-40 times more to process maize with dielectric than in conventional crossflow drying installations with 130-180 the corresponding ratio for coffee. Even considering an increase of 50% in the crossflow system costs, it would cost at least 20 times more for maize and approximately 80 for coffee. Although many crossflow units are required to match the production of a similarly sized dielectric unit, the investment required for the latter is still too high. Considering similar energy costs in the crossflow and dielectric units for maize it would be necessary to increase η_d to 0.7 and reduce the costs of the dielectric dryer down to the levels presently found in the domestic microwave section of the market (US$200/kW). In the latter case, large volume sales and competition have brought the costs of the heating unit down to much lower levels than in the industrial situation in which custom built plants are likely to be the common rule, unless a very high level of Government intervention in this field were to exist. The thickness of the layer of maize also has a critical effect. Even in the above very favourable circumnstances, the dielectric unit would only be a feasible investment if the unit energy costs of both systems is the same and if the column thickness in the conventional dryer is small (under 10 cm). Typical cereal column thicknesses may be much greater (see [20] for example). The major factors affecting the economics are η_d (this is not likely to exceed 0.7, see Chapter 8), Inv_c and Inv_{die}, which at similar unit energy costs and present Inv_c levels would have to be as low as US$ 50/kW to replace a 0.38 column thick dryer, therefore the maize high frequency drying application is not likely to be adopted in the foreseeable future. For coffee the prospects are even worse. Due to the high moisture content levels during pre-drying much greater installed powers are needed which, coupled with the inherent slowliness of the RF drying in this material (see Chapter 8) would require the investment levels of the dielectric unit to be reduced to US$ 10/kW at η_d=0.7 and C_c=C_{die} in order for the above application to be feasible. It, therefore, appears that such operations as the pre-drying of coffee should not be attempted on a commercial basis using dielectric methods.

It appears that rice is a more appropriate material for the technology considered here, although at present the costs are 6-9 times higher than the existing system. Carrying out a similar analysis to that above and assuming an increase in η_d to 0.7 it is seen that, as for maize, Inv_{die} would need to be reduced to at least US$ 200/kW with similar unit energy costs but in this case crossflow units with column thicknesses as large as 0.38 m could be economically retrofitted to produce a much more compact high frequency installation.

An economic sensitivity analysis of the present situation is presented in table A.5 below. These results were obtained by varying between +50% and -50% the value of each of the input variables around the more likely values given in i-v above and noting the corresponding effect on the cost ratio. The annual hours of operation, the cost of energy, the interest rate and the lifetime of the equipment do not significantly affect the situation, the major factors are the energy efficiency and the investment costs of the two types of plant.

Variables (X)	Cost Ratio Variation for ΔX=+50%,-50% (%) (1)	(2)
η_d	-33, + 100	-33, +100
HR	n.a.	+12, -12
C_{die}	n.a.	+12, -12
Inv_{die}	+50, -50	+34, -34
Inv_c	-33, + 100	-33, +100
i	n.a.	- 4, + 8
n	n.a.	+ 7, -10

Table A.5 Economic sensitivity analysis for the retrofitting of a crossflow plant by a high frequency drying unit. The figures are based on cereal processing from 27 to 13% w.b. (1): C_c=C_{die}; (2) C_c=0.

The economics of drying using high frequency techniques are not directly related to fuel costs or to the inherent value of the product but to its drying characteristics and the investment costs and performance of the plant. This demonstrates the importance of carrying out proper analysis and design procedures during the pre-prototype stage of equipment development program in order to avoid wastage of resources.

APPENDIX III

A.3 Beneficial Side Effects of High Frequency Heating

A.3.1 Pest Control of Agricultural Products

Dielectric heating techniques can be applied for pest control of agricultural products in order to enhance the quality of the material without the need for chemical treatment. The advantage of dielectric over other thermal techniques is the ability to respond to different dielectric properties of the material and therefore, if the insects contained in the product are more receptive to the radiation, they experience more heating than the host material.

As far as agricultural materials are concerned, the insects may infest the crops when the latter are still in the field, usually by means of laying eggs on the surface of the plants from which the larvae penetrate into the nutrient parts of the material. After harvest and during storage the infested material presents a considerable threat to the rest of product since the pest is protected from natural harm and can develop almost uncontrolled. In general the risk of pests is reduced by using chemical treatment before and after harvest and also by drying the product, although in the latter case the product must be exposed to thermal drying methods, i.e. it must experience relatively high temperatures to be effective.

Dielectric heating techniques have been proposed for pest control of many products, for example insects at all stages of development in tobacco shreds were exposed to microwave radiation [76], 100% mortality was achieved if the temperature of the product was raised from 20 to 53 C, if the initial temperature was higher, e.g. 50 C, the maximum temperature to guarantee complete extermination was 57 C. Thomas [161] concludes that temperatures of the order of 60 C are fatal to most biological organisms if they are heated for only a few minutes. At 50 C the exposure time needed may however range from a few seconds to hours although insects which attack agricultural products can be exterminated when their temperature is mantained at 60 C for half a minute. This author reports early studies carried out by Leao in Brazil with pests in cereal, beans and coffee products in which the insects were exterminated within 10 secs of exposure to dielectric heating techniques.

Many reasons for this pest destruction have been suggested, although so far no proof of other than damages produced by thermal effects has been shown. It is well known, for example, that adult insects are less resistant to dielectric heating than larvae but Thomas argues that this phenomenon can be explained by the fact that adult organisms have a more developed central nervous system. Other mechanisms such as radiation shielding, preferential electrocution and so on have been advanced as possible causes by many workers in this field. If the thermal effect is the main cause of the phenomenon then the characteristics of the field and the properties of the material and pest must be such as to guarantee that the latter experiences the maximum heat possible.

Consider an elipsoid body whose dielectric constant is e_i', the body being immersed in a medium with dielectric constant e' and subjected to an effective field strength E as shown in figure A.1. Thomas states that in this case the internal field experienced by the body is:

$$E_i = \{e'/[e'+(e_i'-e')F']\}E \qquad \text{(A.1a)}$$

which is equivalent to

$$E_i = \{e'/[e'(1-F')+e_i'F']\}E \qquad \text{(A.1b)}$$

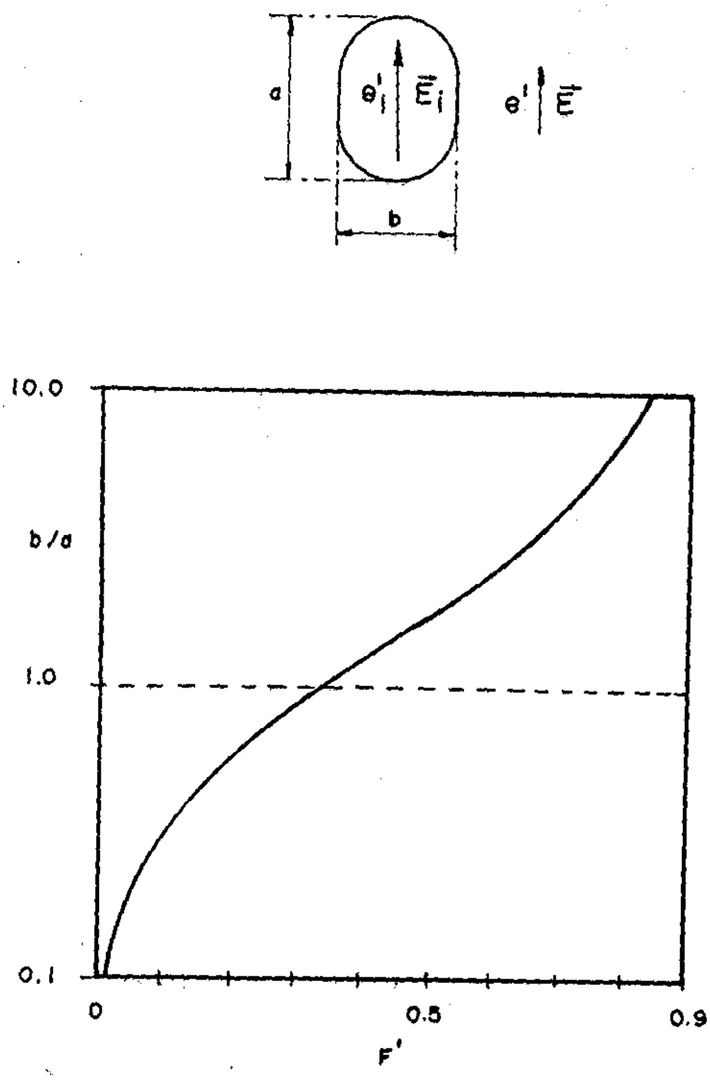

Figure A.1 Simplified model of an insect with dielectric constant e'_i immersed in a material which dielectric constant is e'[161].

where F' is a parameter which is governed by the ratio between the axes of the body as shown in figure A.1 which is a simple model of an insect immersed in a bulk of material where the ellipsoid represents the insect together with an associated surrounding void and therefore the dielectric constant e_1' is the bulk value, as is the case with the corresponding parameter for the product, i.e. e'.

Eq (A.1b) shows that the highest value of E_1 for a given value of E and F' is achieved when e_1' is small as compared to e'. When eqs (A.1) are applied to a sphere, i.e. $b/a=1$ then $F'=1/3$, in which case the above equations revert to eq (6.13a) for $e'=1$, as expected.

Thomas, and subsequently Nelson, defined a "differential heating factor" as a function of the ratio between the dielectric power in the pest to that in the product. These authors do not consider other characteristics of the organisms apart from their dielectric properties, and the insect is assumed to be a sphere. It is considered however that both the specific heat and the bulk density of the materials, in addition to the effect of different F' factors, should be considered as follows. Neglecting the internal temperature gradients in the insects and kernels, the heat conduction from the insect to the bulk of material, and considering the evaporation effect as negligible (or similar in both cases) eq (2.33) shows that the ratio between the rate of temperature rise in the pest to that in the product is given by the following expression

$$R_{heating} = [f(\vec{E}_i)/\rho_i Cp_i]/[f(\vec{E})/\rho\, Cp] \qquad (A.2a)$$

where ρ_i and Cp_i are respectively, the density and specific heat of the insect. The heat transfer relationship has been applied to a small section of material. If the terms in $f(\vec{E})$, the dielectric power densities, are approximated to q_d as in eq (6.4), it follows, when eqs (6.4) and (A.1) are substituted in (A.2) that:

$$R_{heating} = \{e'/[e'+(e_i'-e')F']\}^2(e_i''/e'')(\rho Cp/\rho_i Cp_i) \qquad (A.2b)$$

This heating ratio is not affected by the magnitude of the applied field but depends only on the properties of the pest and product. Three ratios can be distinguished, the first two refer to the dielectric properties of the organisms and the latter refers to the thermal and physical characteristics of both. In order to maximise $R_{heating}$ then each of the above ratios must be a maximum. First, in the moisture range of interest the dielectric constant of the product should be high as compared with that of the insect. Also, the loss factor of the insect should be higher than that of the product in the moisture range involved. Ideally the specific heat and the bulk density of the product should be higher than those of the insect. In addition to this, in theory, organisms with oval forms, e.g. larvae, will experience reduced heating if the F′ factor is increased, i.e. if the organism moves in such a way to place its major axis perpendicular to the direction of the applied field This effect will be less important if the particles in which the insect is enclosed have a relative motion with respect to the field. Nevertheless, in a static condition and if the organism is thin enough, it may benefit from this effect.

An important consequence of the variation of the dielectric properties of the product and pest with field frequency is that increased differential heating may be obtained at certain frequencies. Consider, for example, the case of wheat. Nelson & Charity [126] report on the dielectric properties of dry wheat and rice weevil, considering the range between 1 and 1,000 MHz it is possible to estimate in which region $R_{heating}$ is the highest. Substituting the thermal, physical and dielectric properties in eqs (A.2b) for $F'=1/3$ (spherical insect) the following is obtained:

$R_{heating}$ = 1.4 at 1 MHz

$R_{heating}$ = 2.2 at 10 MHz

$R_{heating}$ = 2.9 at 100 MHz

$R_{heating}$ = 1.0 at 1,000 MHz

and, for F′=0.2 (ellipsoid in which b/a = 0.5):

$R_{heating}$ = 1.9 at 1 MHz

$R_{heating}$ = 2.9 at 10 MHz

$R_{heating}$ = 3.4 at 100 MHz

$R_{heating}$ = 1.1 at 1,000 MHz.

Consider now that the oval insect rotates through 90 with the field maintained in the same direction, then F′=0.5 (b/a=2.0), i.e.

$R_{heating}$ = 1.0 at 1 MHz

$R_{heating}$ = 1.7 at 10 MHz

$R_{heating}$ = 2.4 at 100 MHz

$R_{heating}$ = 0.9 at 1000 MHz.

Thus, although the insect would benefit from rotation, the effect will always be highest in the radiofrequency band.

If it is assumed that the product and pest are at 50 C when admitted to the dielectric heating phase and that it is necessary to increase the temperature of the insect to 65 C to achieve sterilization in one minute then, we obtain, for the insect:

$$\partial T_i/\partial t = 15 \text{ C}/(1/60 \text{ hour}) = 900 \text{ C/h}$$

Taking 2.6 (based on the above results) as an average $R_{heating}$ value in the range 10 - 100 MHz we have, for the product:

$$\partial T/\partial t = 900/2.6 = 346 \text{ C/h},$$

i.e. over one minute, it can be estimated that whilst the pest is heated up to 65 C the bulk of product only reaches 56 C.

The required field strength for sterilization can be calculated from the characteristics of the host material, i.e. from eqs (2.33) and (6.4). Considering the dielectric power density for the RF case we have,

$$E = [(\rho\, Cp/0.556E\text{-}10fe'')(\partial T\ /\partial t)]^{1/2}$$

Substituting the values of ρ and Cp for wheat given in table 6.1, and taking the operating frequency as 27.12 MHz with e"=0.3 (average between 25 and 12 % w.b.), then a field strength of 14 kV/m would be needed to give the required rate of temperature rise in the insect. For a separation between electrodes of 10 cm a cross flow vertical system with a minimum electrode voltage of 1.4 kV would be needed. Table 6.25 indicates that a dielectric power density of 250 kW/m^3 applied between 30 and 12 % w.b. would satisfy this requirement.

The surface of the product could be force cooled but the pest will heat up to the required fatal temperature, and even exceed this level, if the heat dissipated in the insects is not conducted to the surface of the kernels. The product stays much longer in the dielectric drying zone, which implies that when the material leaves, it has certainly received the required sterilization. After long storage periods the product might be easily disinfested if it is passed through the dielectric heating equipment for a short period of time. This could be arranged, for example, in the cross flow vertical system, by loading the material in the unit and adjusting the flow of product in such a way that each particle stays between the electrodes for no longer than, say, a few minutes.

A.3.2 Dielectric Roasting

Products such as coffee and peanuts are usually roasted after drying, this normally takes place in a separate plant. Some of the dielectric drying systems discussed in this Report may offer the opportunity of roasting the product in the same agro-industrial plant, no additional investment being required for this purpose. Here the objective is to raise the temperature of the product to approximately 200 C which must then be mantained for a given period of time. In this case the coupled mass and heat transfer system of equations simplify to the temperature equation alone, since the moisture contained in the material is quickly evaporated in the process, i.e. eq (2.33) reduces to :

$$\partial T/\partial t = f(\vec{E})/(\rho Cp)+k/(\rho Cp)(\partial^2T/\partial r^2+2/r\partial T/\partial r)$$

which shows that the temperature increase of the product is entirely dependent on the dielectric power applied and on the properties of the material. The effect of convection is minimised since only a limited amount of ventilation is required to disperse the toxic fumes produced. However, increased breakdown problems might be expected in this application as can be concluded from the experimental results in Chapter 8.

APPENDIX IV

A.4 Supplement to Experimental Work

A.4.1 Regression Models for the Dielectric Constant and Loss Factor (Moisture Content and Temperature Effect)

Frequency (MHz)	Parameter	a	b	c	d	S_e	r^2
13.5	e"	-0.44	21.35	-204.2	598.8	0.14	0.992
13.5	e´	1.91	9.99	15.5	-21.7	0.15	0.999
27.0	e"	-0.16	9.76	-86.9	251.4	0.07	0.991
27.0	e´	0.88	24.49	-160.8	376.9	0.27	0.993
40.0	e"	-0.10	7.88	-69.0	196.5	0.05	0.991
40.0	e´	1.43	16.45	-55.7	147.3	0.18	0.998

Table A.6 Regression coefficients for the variation in the dielectric constant (e´) and loss factor (e") of rice with moisture content. Moisture range: 4-29 % w.b. Temperature range: 18-22 C.

Frequency (MHz)	Parameter	a	b	c	d	S_e	r^2
13.5	e´ Rice	2.43	2.7E-3	1.3E-4	-8.8E-7	0.08	0.984
13.5	e" Rice	0.13	1.3E-3	-6.5E-6	-5.4E-8	0.01	0.919
27.0	e´ Rice	2.17	-5.3E-3	2.2E-4	-1.1E-6	0.07	0.967
27.0	e" Rice	0.12	1.9E-4	0	0	0.01	0.067
40.0	e´ Rice	2.15	-1.1E-2	3.0E-4	-1.5E-6	0.05	0.989
40.0	e" Rice	0.074	8.1E-4	1.2E-5	-1.3E-7	0.01	0.982
40.0	e´ Wheat	1.73	4.3E-3	-4.0E-3	2.4E-7	0.13	0.502
40.0	e" Wheat	0.042	1.1E-3	-7.3E-6	5.0E-9	0.01	0.827

Table A.7 Regression coefficients for the variation in the dielectric constant (e´) and loss factor (e") of rice and wheat with temperature. Moisture range: 0-1 % w.b. Temperature range: 20-115 C.

Frequency (MHz)	Parameter		a	b	c	d	S_e	r^2
13.5		e′	1.44	33.13	-102.1	153.1	0.47	0.998
13.5	(1)	e"	0.013	4.81	-30.5	84.5	0.17	0.997
13.5	(2)	e"	-87.61	347.61	-410.2	271.9	0.94	0.989
27.0		e′	1.24	18.17	-36.8	60.9	0.40	0.998
27.0	(1)	e"	0.041	1.06	-1.0	16.7	0.10	0.995
27.0	(2)	e"	-434.12	34.03E2	-8.92E3	7.84E3	0.31	0.996
40.0		e′	1.09	24.74	-53.9	65.0	0.41	0.998
40.0	(1)	e"	0.033	2.46	-11.8	31.0	0.05	0.998
40.0	(2)	e"	-106.87	891.38	-2.50E3	2.37E3	0.25	0.996

Table A.8 Regression coefficients for the variation in the dielectric constant (e′) and loss factor (e") of wheat with moisture content. Moisture ranges: 2-44 % w.b. for the dielectric constants, (1) 2-39 % w.b. and (2) 39-44 % w.b. for the loss factors. Temperature range: 20-24 C.

Frequency (MHz)	Parameter		a	b	c	d	S_e	r^2
13.5	(1)	e"	0.54	-8.40	58.0	-70.7	0.04	0.999
13.5	(2)	e"	-82.72	981.67	-3.86E3	5.1E3	0.28	0.999
13.5	(1)	e′	3.38	-20.81	252.2	-515.4	0.27	0.997
13.5	(2)	e′	14.99	-1.05E2	351.3	-317.8	0.34	0.961
27.0	(1)	e"	0.12	0.19	4.8	12.6	0.04	0.995
27.0	(2)	e"	-23.33	277.63	-1.09E3	1.46E3	0.08	0.999
27.0	(1)	e′	2.24	-4.61	126.9	-288.7	0.25	0.991
27.0	(2)	e′	2.20	2.26	54.2	-96.4	0.43	0.702
40.0	(1)	e"	0.23	-1.86	14.9	-7.6	0.03	0.998
40.0	(2)	e"	-21.79	261.67	-1.03E3	1.38E3	0.09	0.999
40.0	(1)	e′	2.70	-15.34	216.6	-481.5	0.22	0.997
40.0	(2)	e′	6.82	-28.07	102.8	-84.1	0.28	0.876

Table A.9 Regression coefficients for the variation in the dielectric constant (e′) and loss factor (e") of maize with moisture content. Moisture ranges: (1) 7-24% w.b. and (2) 24-34% w.b. Temperature range: 18-22 C.

Frequency (MHz)	Parameter	a	b	c	d	S_e	r^2
13.5	e´ Maize	1.97	2.24E-2	-2.91E-4	1.5E-6	0.06	0.967
13.5	e" Maize	0.13	1.33E-4	-1.1E-6	-2.9E-8	0.01	0.921
13.5	e" Coffee	0.059	8.49E-5	0	0	0.01	0.045
13.5	e´Coffee	1.82	6.20E-3	-6.22E-5	3.7E-7	0.09	0.817
27.0	e´ Maize	1.32	2.67E-2	-3.89E-4	2.2E-6	0.08	0.935
27.0	e" Maize	0.10	-2.59E-6	0	0	0.005	1E-4
27.0	e" Coffee	0.058	7.02E-6	0	0	0.007	0.001
27.0	e´Coffee	1.62	1.78E-3	2.04E-5	1.6E-8	0.130	0.854
40.0	e´ Maize	1.83	6.56E-3	-4.87E-5	2.0E-7	0.06	0.843
40.0	e" Maize	0.068	1.55E-3	-1.3E-5	-2.2E-9	0.007	0.820
40.0	e" Coffee	0.051	4.54E-5	0	0	0.003	0.060
40.0	e´Coffee	1.70	2.24E-3	0	0	0.10	0.175

<u>Table A.10</u> Regression coefficients for the variation in the dielectric constant (e´) and loss factor (e") of maize and coffee with temperature. Moisture range: 0-2 % w.b. Temperature range: 20-100 C.

Frequency (MHz)	Parameter		a	b	c	d	S_e	r^2
13.5		e´	0.99	13.67	13.86	-19.55	0.33	0.999
13.5	(1)	e"	2.72	-44.02	248.5	-390.98	0.15	0.984
13.5	(2)	e"	-7.07	75.62	-236.57	260.39	0.50	0.689
27.0		e´	2.77	-10.12	77.49	-81.85	0.43	0.988
27.0	(1)	e"	1.43	-22.55	130.6	-201.30	0.08	0.993
27.0	(2)	e"	10.98	-99.96	314.3	-307.52	0.31	0.767
40.0		e´	2.97	-15.51	110.2	-130.35	0.39	0.994
40.0	(1)	e"	1.32	-19.11	101.7	-140.10	0.08	0.994
40.0	(2)	e"	-0.90	9.86	-20.62	27.65	0.28	0.832

<u>Table A.11</u> Regression coefficients for the variation in the dielectric constant (e´) and loss factor (e") of coffee with moisture content. Moisture ranges: 12-44 % w.b. for the dielectric constants, (1) 12-30 % w.b. and (2) 30-44 % w.b. for the loss factors. Temperature range: 18-22 C.

Frequency (MHz)	Parameter	a	b	c	d	S_e	r^2
13.5	e"	-0.12	2.52	12.75	-8.65	0.28	0.986
13.5	e´	1.04	21.31	-42.42	95.53	0.47	0.998
27.0	e"	-0.087	2.53	5.21	-0.068	0.26	0.983
27.0	e´	1.35	5.19	32.06	-34.57	0.46	0.997
40.0	e"	-0.092	2.51	0.42	11.81	0.26	0.986
40.0	e´	1.59	3.56	42.36	-55.85	0.37	0.998

Table A.12 Regression coefficients for the variation in the dielectric constant (e´) and loss factor (e") of soya with moisture content. Moisture range: 4-40 % w.b. Temperature range: 18-22 C.

Frequency (MHz)	Parameter	a	b	c	d	S_e	r^2
13.5	e´	2.16	1.3E-3	0	0	0.11	0.055
13.5	e"	0.062	-2.5E-5	0	0	0.004	0.019
27.0	e´	1.72	8.7E-3	-1.3E-4	7.1E-7	0.05	0.800
27.0	e"	0.032	3.6E-5	0	0	0.005	0.034
40.0	e´	1.83	-2.7E-3	1.1E-4	-8.1E-7	0.035	0.870
40.0	e"	2.39	6.1E-4	-9.9E-6	5.6E-8	0.003	0.712

Table A.13 Regression coefficients for the variation in the dielectric constant (e´) and loss factor (e") of soya with temperature. Moisture range: 0-2 % w.b. Temperature range: 20-100 C.

The variation of the dielectric constant and loss factor with moisture content at 40 MHz is shown in the following curves.

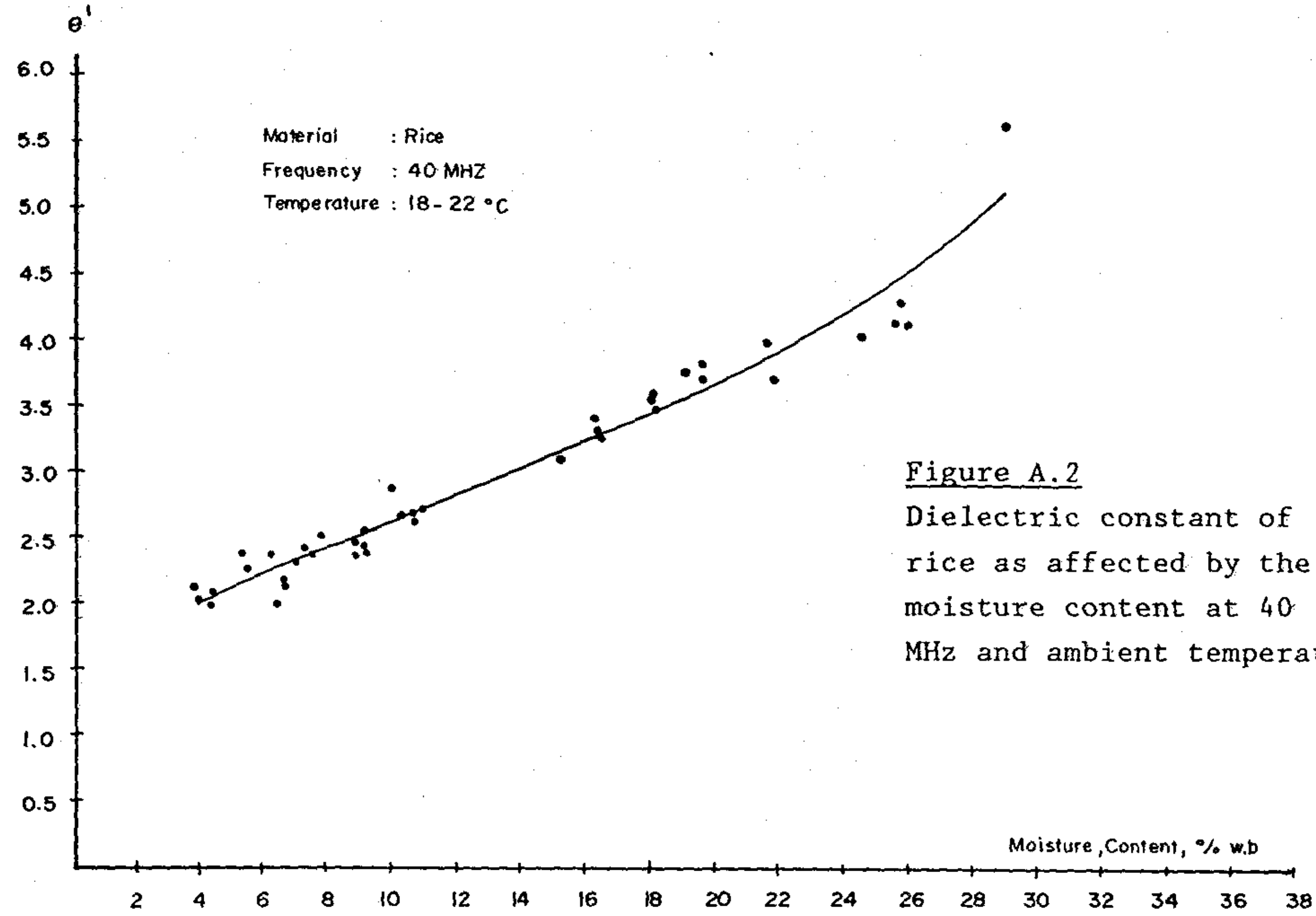

<u>Figure A.2</u>
Dielectric constant of rice as affected by the moisture content at 40 MHz and ambient temperature

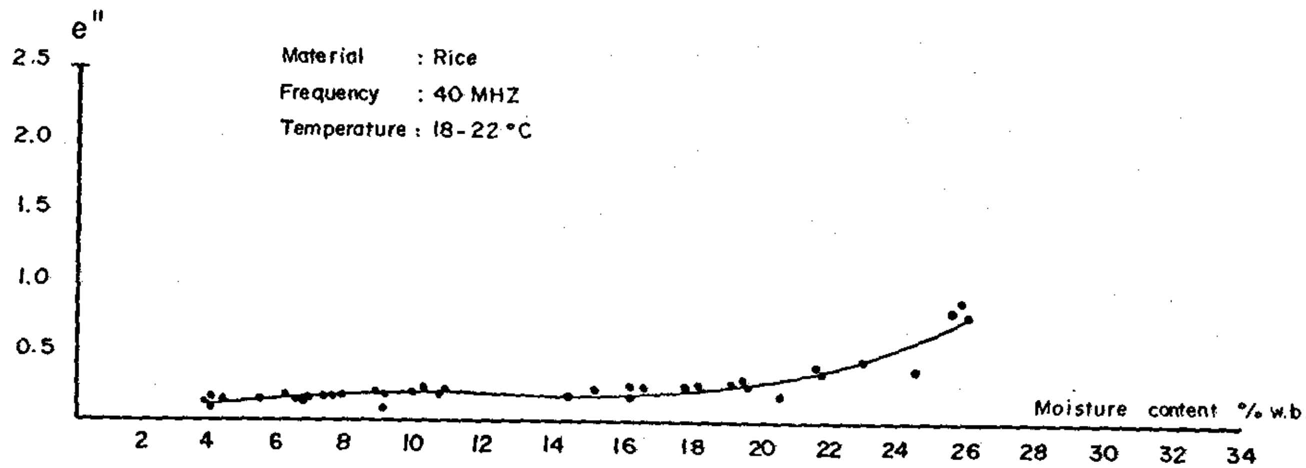

Figure A.3 Loss factor of rice as affected by the moisture content at 40 MHz and ambient temperature.

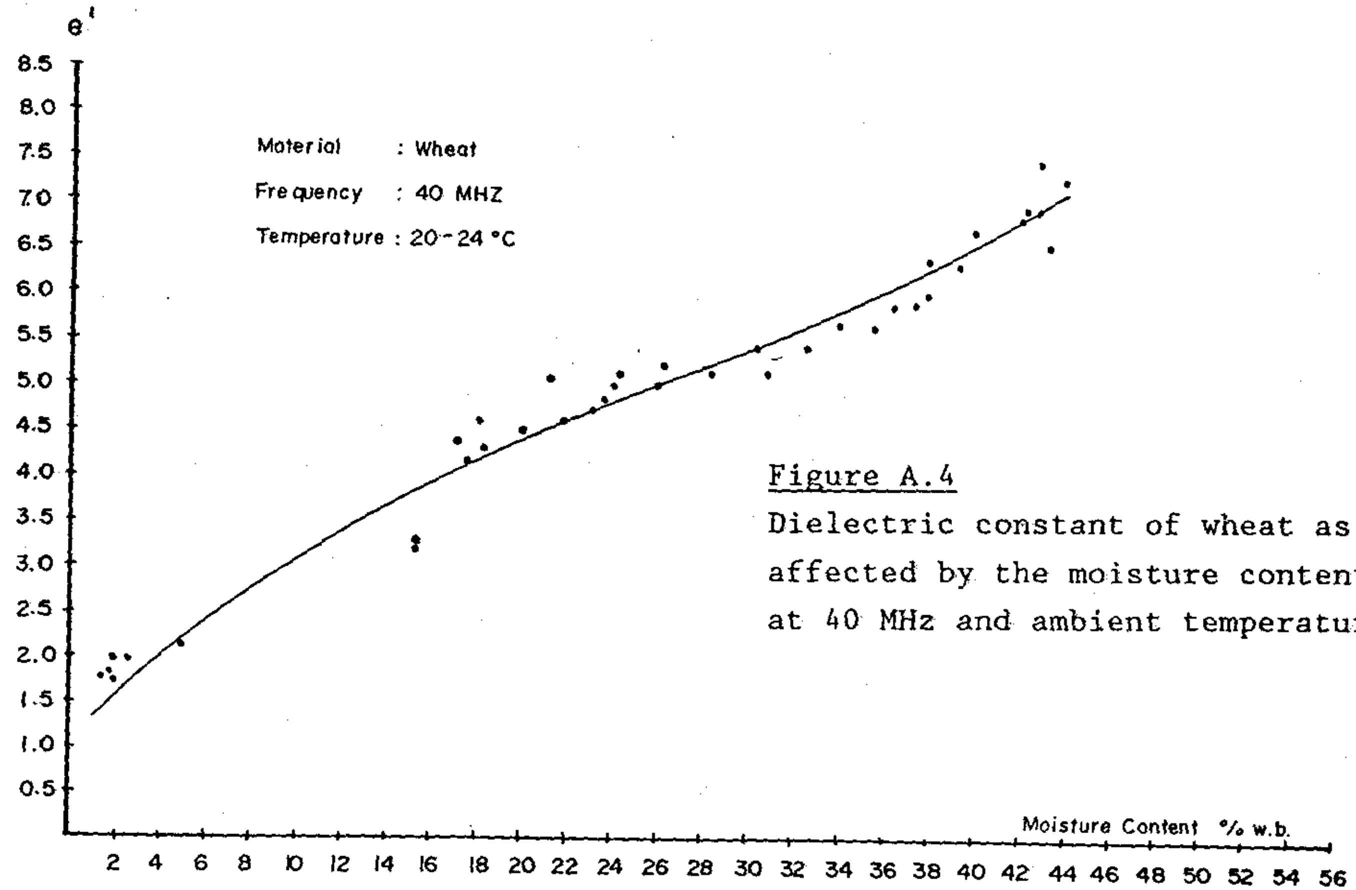

<u>Figure A.4</u>
Dielectric constant of wheat as affected by the moisture content at 40 MHz and ambient temperature.

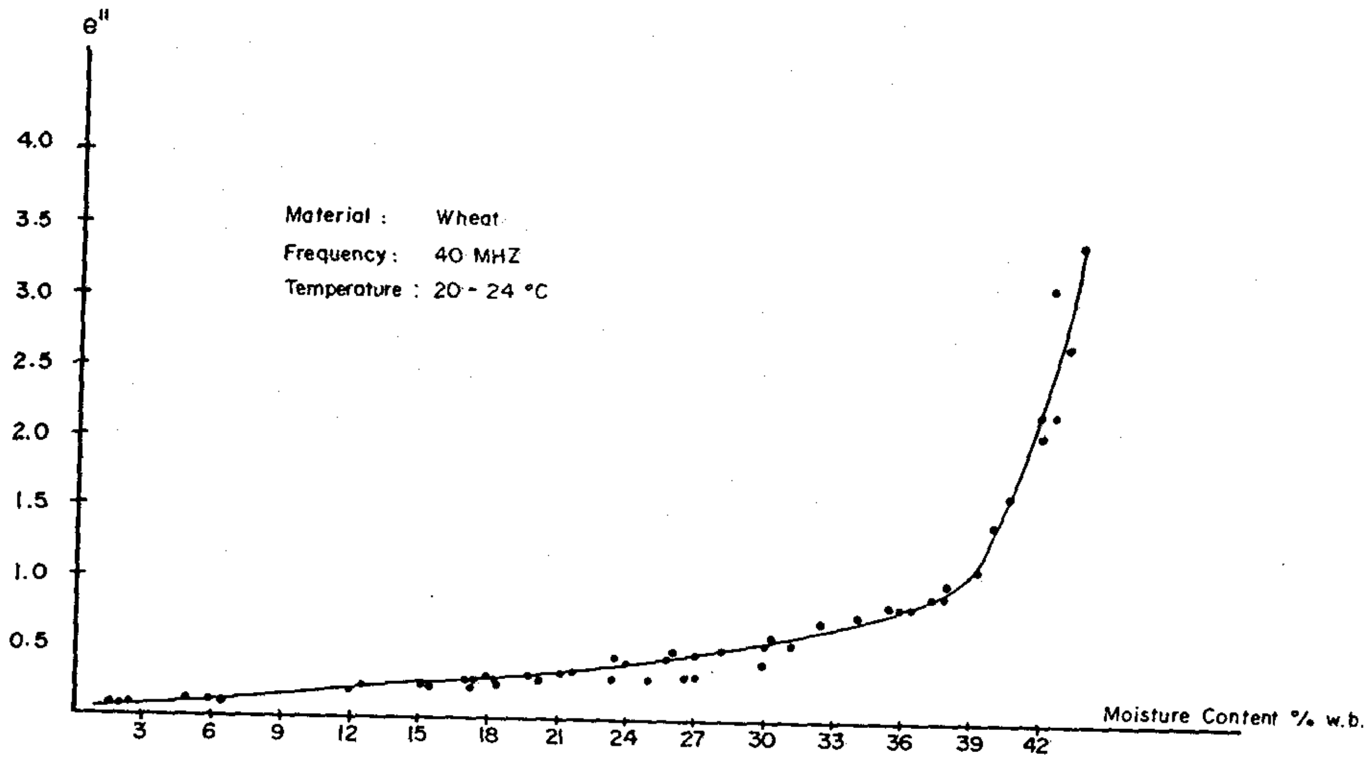

Figure A.5 Loss factor of wheat as affected by the moisture content at 40 MHz and ambient temperature.

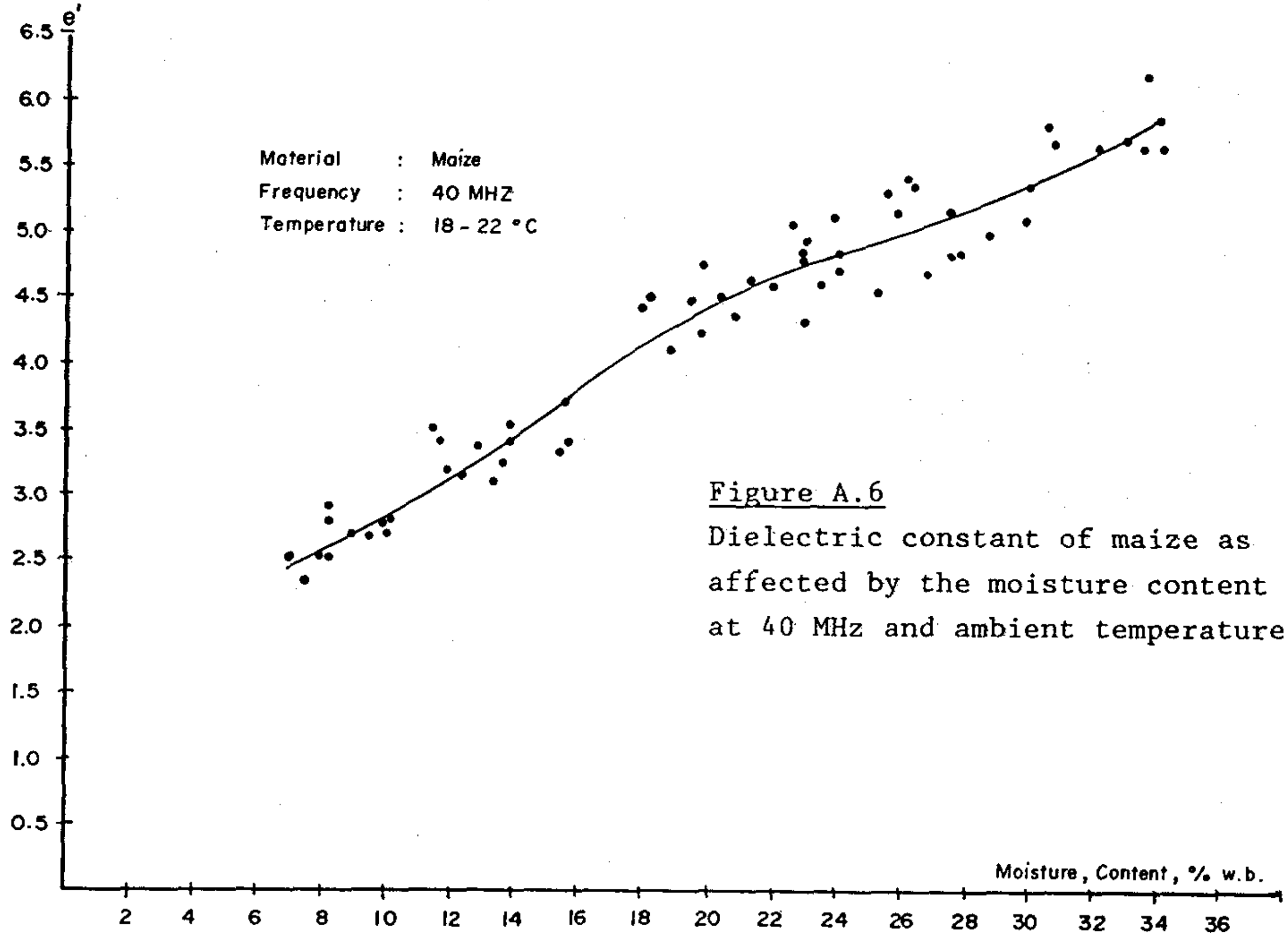

Figure A.6

Dielectric constant of maize as affected by the moisture content at 40 MHz and ambient temperature.

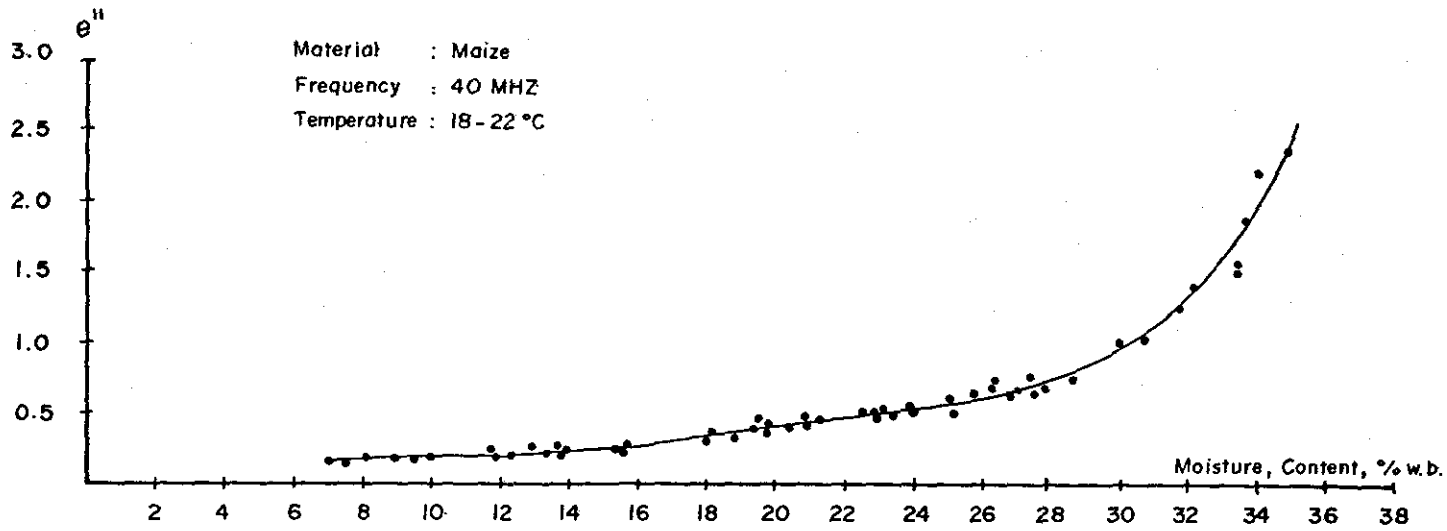

<u>Figure A.7</u> Loss factor of maize as affected by moisture content at 40 MHz and ambient temperature.

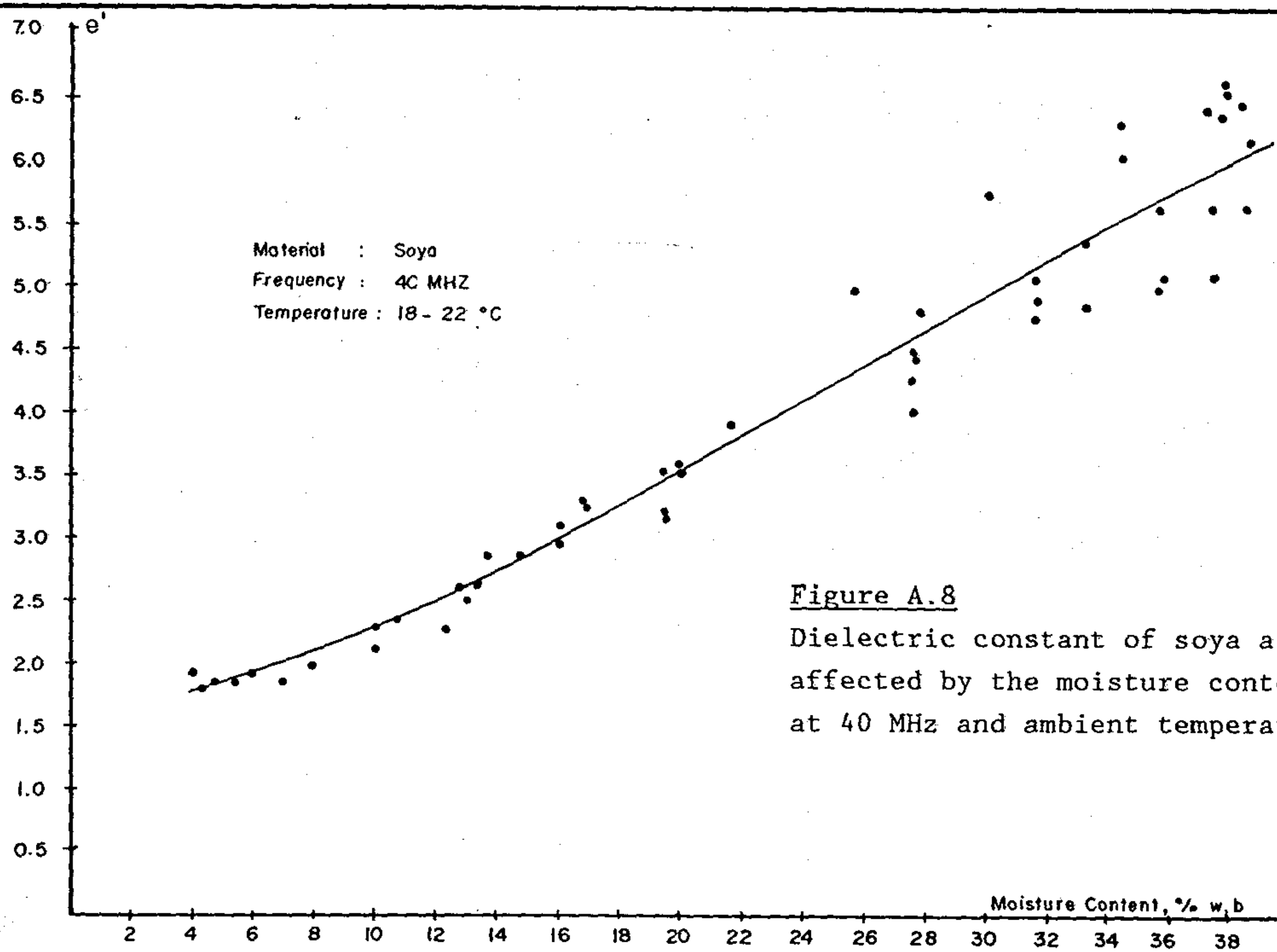

Figure A.8
Dielectric constant of soya as affected by the moisture content at 40 MHz and ambient temperature.

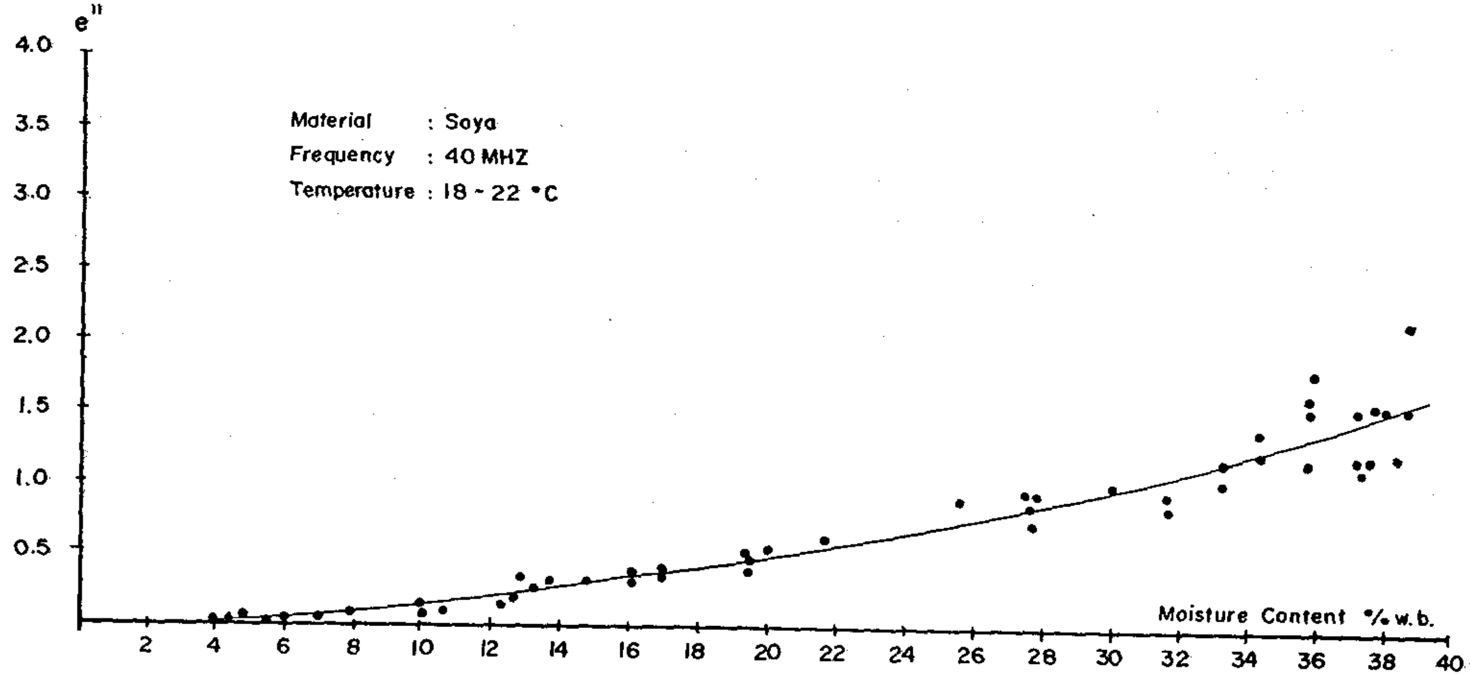

<u>Figure A.9</u> Loss factor of soya as affected by the moisture content at 40 MHz and ambient temperature.

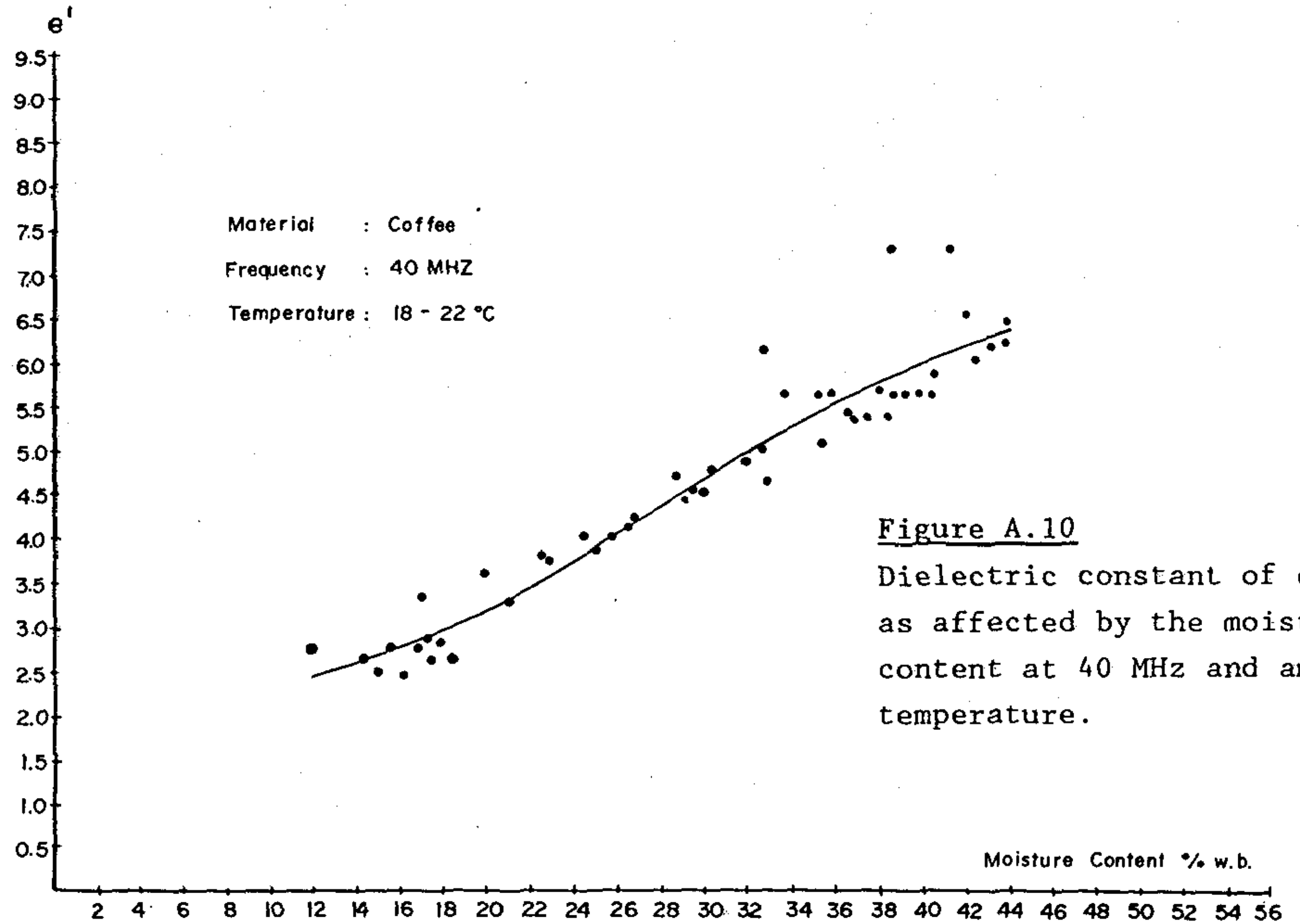

Figure A.10

Dielectric constant of coffee as affected by the moisture content at 40 MHz and ambient temperature.

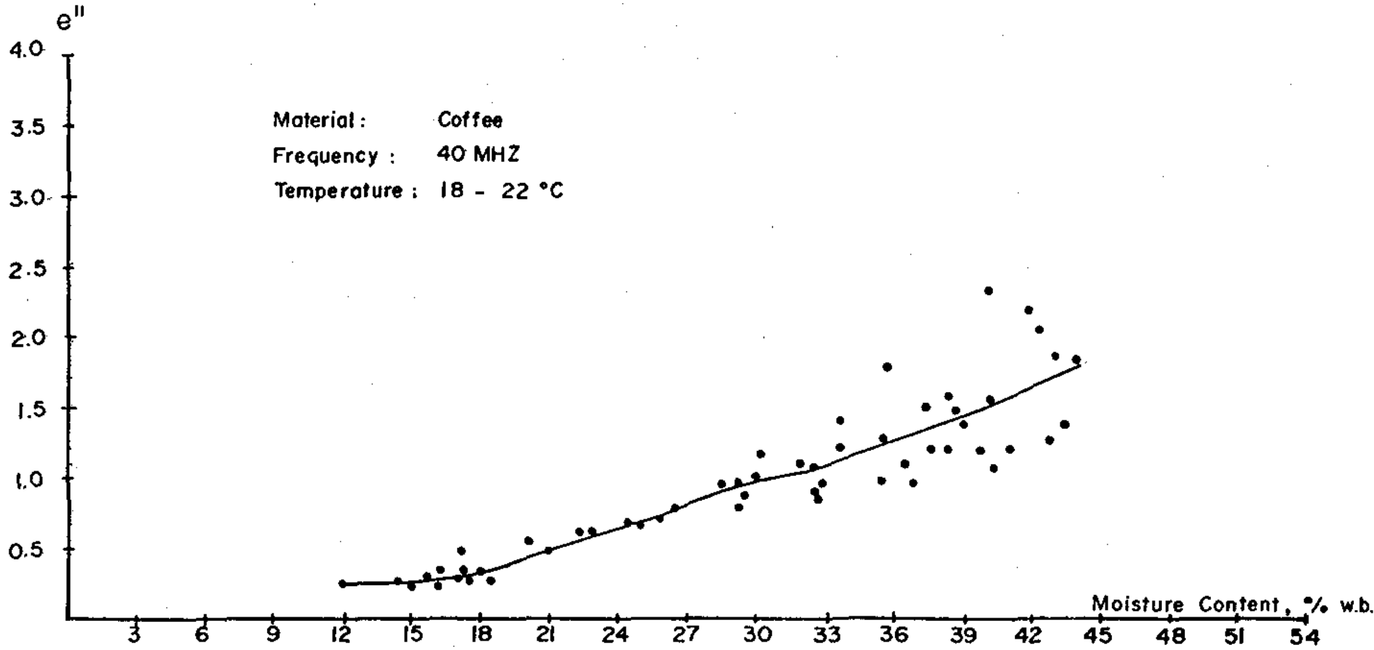

Figure A.11 Loss factor of coffee as affected by the moisture content at 40 MHz and ambient temperature.

A.4.2 Sample of Spreadsheet for Dielectric Properties Experiments (Moisture Effect)

A	B	C	D	E	F	G	H	I
DISH	8		WHEAT			DISH	WEIGHT	
							72.5	
40	MHZ	MOIST	CONTENT	(W.B.)				DRYWEIG
42.1348	36.2624	30.0272	25.4703	19.4053	16.2602	1.90476		124
	WEIGHTS	OF	GRAIN	AND	DISH	(GRAMS)		
161.5	153.3	146.1	141.6	136.4	134	125		
	VOLUMES	OF	GRAIN	SAMPLES	(ML)			
80	80	80	80	80	80	80		
PICOFAR	CAPACIT	OF	LOADED	SAMPLE	HOLDER	(LSH)	USH(C1)	NSH(CO)
49	54.5	54.8	55.7	56.7	56.5	58	58.4	65.7
	QFACTOR	OF	LOADED	SAMPLE	HOLDER	(LSH)		NSH(QO)
15	55	65	80	96	98	110		155.1
MICROHE	INDUCTA	OF	COIL	USED:	0.2			
		DIELEC		CONST				
6.9278	3.8808	3.7146	3.216	2.662	2.7728	1.9418		
		LOSS		FACTOR				
2.20922	0.44448	0.34267	0.23767	0.16184	0.15411	0.11359		

A.4.3 <u>Sample of Spreadsheet for Dielectric Drying Experiment</u>

A	B	C	D	E	F	G	H	I
FinalF	InitiaF		Frequen	of	Field=	3.85E7	VARIAC=	72.8
3.85E7	3.85E7	DIELECT	DRYING/	RICE		Vplate=	1537.7	volts
Kammin	Kammax	Tair	(C)	Velair	(m/sec)	Vprmin	Vprmax	
0.59	0.69	19		0.7,0.9		2.2	3.6	
kWhi	KWhf	Mi(%)	Mf(%)	GrsHold	GrsDRY	GrsInst	Vi(v)	
257.395	257.735	33.1316	11.5	1795	884	385	300	
		NOTES	ON THE	DRYING	PROCESS			
Velair	Final=	0.8,1.0	m/sec	OSCILAT	STOPPED	WORKING	AFTER	10 MINS
				VERY	GOOD	PRODUCT	QUALITY	/VISUAL
		DRYING	TIMES	(mins)				
0	3	6	8	10				
	WEIGHTS	OF	GRAIN,	HOLDER	AND	INSTRUM	(grs)	
3502	3385	3289	3232	3180				
		TEMPERA	OF	PRODUCT	(C)			
13	56	84	94	98				
	METRE	READING	INPUT	POWER	(Watts)			
	127.5	122.5	125	125				
		HEIGHT	OF	PRODUCT	IN	THE	HOLDER	(m)
0.185	0.165	0.15	0.137	0.13				
		VOLUME	OF	PRODUCT	IN	THE	HOLDER	(cumet)
1.85E-3	1.65E-3	1.5E-3	1.37E-3	1.3E-3				

22			VOLUME	OF	PRODUCT	(p.u.)		
23	1	0.89189	0.81081	0.74054	0.7027			
24			BULK	DENSITY	OF	PRODUCT	(Kg/cu	metre)
25	714.595	730.303	739.333	767.883	769.231			
26			GROSS	POWER	DENSITY	(Watts/	cubic	metre)
27	0	3709091	3920000	4379562	4615385			
28			GROSS	POWER	(Watts)			
29	0	6120	5880	6000	6000			
30		NOMINAL	POWER	USE	FACTOR			
31	0	0.51	0.49	0.5	0.5			
32			NET	POWER	DENSITY	(Watts/	cubic	metre)
33	0	337277	116526	66311.8	58074.9			
34			NET	POWER	(Watts)			
35	0	556.506	174.789	90.8471	75.4974			
36			LOAD	RESISTA	(Ohms)			
37	308.965	883.166	2651.25	4368.04	4759.77			
38			LOAD	CAPACIT	(Farad)			
39	9.2E-12	8.2E-12	7.4E-12	6.8E-12	6.5E-12			
40			LOAD	IMPEDAN	(ohms)			
41	254.808	438.497	543.86	602.589	635.427			
42		EQUIVAL	RMS	OSCILLA	VOLTAGE	V(volt)		
43		757.866	735.899	680.981	648.031			
44		MAX AMP	OSCILLA	CURRENT	(amps)			
45		1.74112	0.57999	0.35203	0.32306			

```
                   MOISTUR CONTENT (%w.b.)
 33.1316  26.639 20.2885 15.9696    11.6
                   MOISTUR CONTENT RATIOS    MR     (p.u.)
        1 0.69986 0.40628 0.20662 4.62E-3
                   LOAD    QFACTOR
 0.68575 1.74828  4.7712 7.17947 7.42361
          AMPLITU MODULAT FACTOR  (Ka.m.)
             0.69    0.67    0.62    0.59
                   ENERGY  EFFICIE  (p.u.)
          9.09E-2 2.97E-2 1.51E-2 1.26E-2
                   THRPUT  (Mj-Mf)     (cu  metre/ hour)
  7.8E-3 1.11E-2 1.95E-2  3.9E-2
                   DRYING  EFFICIE (Mi-Mf) (p.u.)= 0.29708 ======= 0.3030
```

REFERENCES

1. A.S.H.R.A.E., 1985, "ASHRAE Handbook", Part F, Ashrae, USA.
2. Agencia para Aplicacao de Energia, 1985, Personal Communication, Brazil.
3. Alam, A., Shove, G.C., 1973, "Higroscopicity and Thermal Properties of Soybeans", Trans ASAE, 16 (4), 707-709, USA.
4. Albuquerque, C.A., 1983, "The Agroenergy Program: Energy for the Development of Rural Areas in Brazil", Resource Management and Optimization, 3 (1), 23-45.
5. Allen, J.R., 1960, "Application of Grain Drying Theory to the Drying of Maize and Rice", J. Agric. Engng. Res., 5, 363-385, UK.
6. Ang, T.K. et al, 1977, "Microwave Freeze Drying: An Experimental Investigation", Chemical Engineering Science, 32, 1477-1489.
7. Angladette, A., 1969, "Rice" (In Spanish), Blume, Spain.
8. Atwater, H.A., 1962, "Introduction to Microwave Theory", Mc Graw-Hill.
9. Baden Fuller, A.J., 1979, "Microwaves", Pergamon Press.
10. Bakker-Arkema, F.W. et al, 1979, "Testing of Commercial Crossflow Grain Dryers", ASAE Paper, 79-3521, USA.
11. Bakshi, A.S. et al, 1978, "Energy Costs of a Conventional

and Air Recycling Crossflow Rice Dryer", ASAE Paper, 78-3011, USA.

12. Bal, S. et al, 1970, "An Analytical and Experimental Study of Radiant Heating of Rice", Trans ASAE, 13 (5), USA.
13. Bandle, A.M., 1986, "Safety in the Use of RF Dielectric Heating Equipment", Conference Heating and Processing 1-300 MHz, Cambridge, UK.
14. Barber, H., 1983, "Electroheat", Granada, UK.
15. Barber, H., Harry, J.E., 1979, "Electroheat: Electric Power for Industrial Heating Processes", Proc. IEE, 126 (11), 1126-1148, UK.
16. Becker, H.A., Sallans, H.R., 1955, "A Study of Internal Moisture Movement in the Drying of the Wheat Kernel", Cereal Chem, 32, 212-226.
17. Bienville Co, 1982, "Estimated Cost and Efficiency in Using Several Fuels for Drying Coffee", Contract MAG/Bienville 32-81, MAG, Costa Rica.
18. Bleaney, B.I., Bleaney, B., 1976, "Electricity and Magnetism", Oxford University Press, UK.
19. Bories, S., Pourhiet, A., 1980, "Analysis of the Role of a Microwave Energy Contribution in Drying Porous Media", Proc. 2nd. Symposium on Drying, Montreal, Canada.
20. Brooker, Bakker-Arkema, F.W., Hall, C.W., 1974, "Drying of Cereal Grain", Avi Publishing Co., USA.

21. Brown, G.H. et al, 1947, "Theory and Application of Radio Frequency Heating", D. Van Nostrand, USA.

22. Busse, A.G. et al, 1983, "Fuel Oil Substitution by Electricity" (In Portuguese), Technical Note 20, Market Department/Eletrobras, Brazil.

23. Butler, J.L, Gardner, D.R., 1982, "Preparing Crops for Storage with a Microwave Drying System", Drying' 82, 248-251.

24. Buxo, D., Felipes, L.G., 1958, "The Development of an All-Electric Cacao and Coffee Drier", World Power Conference, Paper 24G/13, Montreal, Canada.

25. Caldas, F.C.R., 1987, Interviews with Mr R Cleves (Coffee Institute) and Mr F Rodriguez (Fedecoop): Technical Data on Crossflow Dryers Used in Coffee Industry, Costa Rica.

26. Caldas, F.P., 1982, "Energy Use and Alternatives for Costa Rican Industry and Agro-industry (In Spanish)", Energy Directorate, Costa Rica.

27. Caldas, F.P., 1983, "Impact on the National Electrical System by the Electrical Drying of Coffee" (In Spanish), ICE, Costa Rica.

28. CESP, 1981, "Electricity Penetration, Evaluation in CESP Area" (In Portuguese), CESP, Brazil.

29. Chapman, A.J., 1974, "Heat Transfer".

30. Chilton, C.H., Perry, R.H., 1973, "Chemical Engineering

Handbook", Mc Graw-Hill Co, USA.

31. Chromalox, 1981, "Radiant Heaters", Manuals PG-108, CRAD-65-6, USA.
32. Chugh, R.K., Stuchly, S.S., Rzepecka, M.A., 1973, "Dielectric Properties of Wheat at Microwave Frequencies", Trans ASAE, 16 (5), USA.
33. Chung et al, 1976, "Summarizing and Reporting Equilibrium Moisture Data for Grains", ASAE Paper, 76-3520, USA.
34. Cliff, M.J., 1986, "Drying of Highly Active Pharmaceutical Products Using Microwaves", Conference Heating and Processing 1-3,000 MHz, Cambridge, UK.
35. Collier et al, 1985, "The Cambridge Encyclopedia of Latin America and the Caribbean", Cambridge University Press, UK.
36. Cranfield Institute of Technology, 1984, "Conduction Heat Transfer", M.Sc. Course in Energy Conservation and the Environment, Cranfield, UK.
37. Cranfield Institute of Technology, 1984, "Fuels and Combustion", M.Sc. Course in Energy Conservation and the Environment, Cranfield, UK.
38. Cranfield Institute of Technology, 1984, "Radiation Heat Transfer", M.Sc. Course in Energy Conservation and the Environment, Cranfield, UK.
39. Crank, J., 1956, "The Mathematics of Diffusion", Oxford University Press, UK.

40. Dagerskog, M., Osterstrom, L., 1979, "Infrared Radiation for Food Processing", Lebensm-Wiss U. Technol., 12, 237-242.

41. De Franco, N., 1985, "The Superelectrification of Brazil", IEEE Spectrum, 19 (5), 57-62, USA.

42. Desrosier, N.W., Sivetz, M., 1979, "Coffee Technology", Avi Publishing Co., USA.

43. Dittrich, H.F., 1977, "Tubes for RF Heating", Philips, Eindhoven.

44. Dryden, I.G.C., 1975, "Efficient Use of Energy", IPC Science & Technology Press, UK.

45. Durosset, P., Le Corre, F., 1987, "Potential and Present Agro-food Applications of Infrared" (In French), EDF/Adria/Noveletec, France.

46. Fanslow, G.E., Saul, R.A., 1971, "Drying Field Corn with Microwave Power and Unheated Air", J. Microwave Power, 6 (3), Canada.

47. Flores, R., Zeledon, R., 1982, "Evaluation of the Energy Potential of Rice Hulls and Maize Cobs" (In Spanish), Congress Copimera, Costa Rica.

48. Foord, A., 1986, "Process Economics", M.Sc. Course, Loughborough University of Technology.

49. Forth, M.W., Jenkins, C.W., 1965, "Infrared Drying of Shelled Corn", Trans ASAE, 8 (4), 457-459, USA.

50. Forwalter, J., 1978, "Microwave/ Vacuum Dryer Cuts Drying Time by 1/3 at 100 F", Food Processing, 176-177, USA.

51. Garber, H., Tiller, F.M., 1942, "Infrared Radiant Heating", Industrial and Engineering Chemistry, 34 (7).

52. Garber, H., Tiller, F.M., 1950, "Infrared Radiant Heating", Industrial and Engineering Chemistry, 42 (3).

53. Gillet, J.E., 1982, Proc. International Drying Symposium, 397-406, Birmingham, UK.

54. Ginzburg, A.S., 1969, "Application of Infrared Radiation in Food Processing", Leonnard Hill Books, London, UK.

55. Goodger, E.M., 1977, "Combustion Calculations", Mac Millan Press, UK.

56. Grant, E.H., 1986, "Biological Effects of Radiowaves and Microwaves", Conference Heating and Processing 1-3,000 MHz, Cambridge, UK.

57. Gray, W.A., Muller, R., 1974, "Engineering Calculations in Radiative Heat Transfer", Pergamon Press.

58. Grunewald, C.E., 1984, "Research and Development of a Total Electric Commercial Grain Dryer", ASAE Paper, 84-3544.

59. Gupta, K.C., 1976, "Cylindrical Waveguide Applicators with Uniform Power Flow Distribution", J. Microwave Power, 11 (4), Canada.

60. Gupta, K.C., 1979, "Microwaves", Wiley Eastern Limited.

61. Gupta, K.C., Bahl, I.J., 1978, "RF Applicators Find Jobs on

Farms, In Factories", Microwaves, 17 (6), 52-64.

62. Hall, C.W., Headley, V.E., 1963, "Drying of Shelled Corn Vibrated in an Infrared Energy Source", Trans ASAE, 1 (2).

63. Hall, C.W., 1962, "Theory of Infrared Drying", Trans ASAE, 14-16.

64. Hall, C.W., 1979, "Dictionary of Drying", Marcel Dekker, USA.

65. Hamblyn, S.M., 1986, "The Capenhurst Rotary Induction Kiln", Colloqium on Electricity in Clay and Ceramics, Stoke-on-Trent, UK.

66. Hamid, M.A.K. et al, 1968, "Control of Grain Insects by Microwave Power", J. Microwave Power, 3 (3), Canada.

67. Hamid, M.A.K. et al, 1969, "A New Method for the Control of Moisture and Insect Infestation of Grain", J. Microwave Power, 4 (1), 11-18.

68. Hamid, M.A.K. et al, 1969, J. Microwave Power, 4 (3), 194-208.

69. Hamid, M.A.K., Mostowy, N.J., Bhartia, P., 1975, "Microwave Bean Roasters", J. Microwave Power, 10 (1).

70. Hammond, L.H., 1967, "Economic Evaluation of UHF Dielectric vrs Radiant Heating for Freeze Drying", Food Processing, 21.

71. Hardiman, R.G., 1974, "Infrared Heating", M.Sc. Course, Loughborough University of Technology, UK.

72. Harry, J.E., 1979, "Heat Transfer, Temperature Measurement and Control", Loughborough University of Technology, UK.

73. Hasatani, M. et al, 1986, "Hybrid Drying of Coals by Combined Radiative and Convective Heating", Drying' 86, 227-231.

74. Henderson, S.M., Pabis, S., 1962, "Grain Drying Theory", J. Agric. Engng. Research, 7, 85-89.

75. Henderson, S.M., Pabis, S., 1961, "Grain Drying Theory", J. Agric. Engng Research, 6, 167-174.

76. Hirose et al, 1975, "The Use of Microwave Heating to Control Insects in Cigarette Manufacture", J. Microwave Power, 10 (2), Canada.

77. Hobson, L., 1985, "Principles of RF Heating", Loughborough University of Technology, UK.

78. Hoover, M.W. et al, 1966, Food Technology, 20.

79. Hoover, M.W. et al, 1966, Food Technology, 24.

80. Howatson, A.M. et al, 1972, "Engineering Tables and Data", Chapman and Hall.

81. Husain, A. et al, 1973, "Simultaneous Heat and Mass Diffusion in Biological Materials", J.Agric.Engng. Research, 18, UK.

82. Husain, A. et al, 1972, "Mathematical Simulation of Mass and Heat Transfer in High Moisture Foods", Trans ASAE, 15, USA.

83. Hustrulid, A., Chu, S., 1968, "Numerical Solution of Diffusion Equations", Trans ASAE, 11, 705-708, USA.

84. Hustrulid, A., Flikke, A.M., 1959, "Theoretical Drying Curve for Shelled Corn", Trans ASAE, 2, 112-114, USA.

85. Hutchinson, F.W., 1952, "Industrial Heat Transfer".

86. IDB/Inter-American Development Bank, 1982, "Hydro and Geothermal Electricity as an Alternative for Industrial Petroleum Consumption in Costa Rica", Washington, USA.

87. INDEECO/ Industrial Engineering and Equipment Co, 1980, "Finned Tubular Electric Duct Heaters", Catalogue C20-1, USA.

88. IPT/ Instituto de Pesquisas Tecnologicas do Estado de Sao Paulo, 1983, "Study of Electrothermal Alternatives for Petroleum Consumption in Industry" (In Portuguese), Report 17.519 and Project 2109.01.7, Sao Paulo, Brazil.

89. Jones, R.N., Bussey, H.E., Little, W.E., Metzku, R.F., 1978, "Electrical Characteristics of Corn, Soya and Wheat in the 1-200 MHz Range", NBSIR 78-897, National Bureau of Standards, US Department of Commerce, USA.

90. Junge, D.C., 1982, "Design and Operation of Industrial Boilers Fired with Wood and Bark Residues", SERI Midwest Research Institute, USA.

91. Kashyap, S.C., Wyslouzil, W., 1977, "Methods for Improving Heating Uniformity of Microwave Ovens", J. Microwave Power, 12 (3), Canada.

92. La Toison, M., 1964, "Infrared and its Thermal Applications", Philips Technical Library.

93. Laferriere et al, 1986, "Energy Recovery from Exhausted Air of Grain Dryers", ASAE Paper, 86-3001, USA.

94. Lefeuvre, S., Paresi, A., Mangin, B., Rezuan, Y., 1978, "Industrial Material Drying by Microwave and Hot Air", Proc. IMPI Conference, 65-67, Ottawa, Canada.

95. Lenza, A., 1984, "The Electrothermal Potential for Brazil" (In French), 10th UIE Congress.

96. Lepecki, J., Kelman, J., 1985, "Brazilian Hydroelectric System", Water International, 10, 156-161.

97. Lewis, W.K., 1921, "The Rate of Drying of Solid Materials", The Journal of Industrial and Engineering Chemistry, 13 (5), 427-432.

98. Liang et al, 1983, "Semicontinuous Macadamia Nut Curing Device", ASAE Paper, 83-3048, USA.

99. London, A., 1972, "Electric Resistance Heating Elements", Industrial Process Heating, 12 (12), 26-29.

100. Luikov, A.V., 1966, "Heat and Mass Transfer in Capillary Porous Bodies", Pergamon Press, USA.

101. Luikov, A.V., 1975, "Systems of Differential Equations of Heat and Mass Transfer in Capillary Porous Bodies", Int. J. Heat and Mass Transfer, 18, 1-14.

102. Mao, Le Pori, 1984, "Rice Drying with no Foreign Energy Source", ASAE Paper, 84-3079, USA.

103. Marcuvitz, N., 1951, "Waveguide Handbook", Mc Graw-Hill.

104. Marin, E.T. et al, 1985, "Study of the Processing Costs of Coffee (Harvest 1982/83)" (In Spanish), Agricultural Economy Department, University of Costa Rica, Costa Rica.

105. Massie, D.R., Norris, K.H., 1965, "Spectral Reflectance and Transmittence of Grain in the Visible and Near Infrared", Trans ASAE, 8 (4), 588-600, USA.

106. Meredith, R.J., 1986, "Recent Advances in Industrial Microwave Processing in the 896/915 MHz Band", Conference Heating and Processing 1-3,000 MHz, Cambridge, UK.

107. Metaxas, A.C., 1981, "The Future of Electrical Techniques in the Production of Printed Tufted Carpets", J. Microwave Power, 16 (1), Canada.

108. Metaxas, A.C., 1974, "Design of TM010 Resonant Cavity as a Heating Device at 2.45 GHz", J. Microwave Power, 9, Canada.

109. Metaxas, A.C., 1976, "Rapid Heating of Liquid Foodstuffs at 896 MHz", J. Microwave Power, 11 (2), Canada.

110. Metaxas, A.C., Meredith, R.J., 1983, "Industrial Microwave Heating", Peter Peregrins Ltd, UK.

111. Mohsenin, N.N., 1970, "Physical Properties of Plant and Animal Materials", Gordon & Breach Science Publishers.

112. Mohsenin, N.N., 1980, "Thermal Properties of Foods and Agricultural Materials", Gordon & Breach Publishers.

113. Muckle, T.B., Stirling, H.G., 1971, "Review of the Drying

of Cereals and Legumes in the Tropics", Tropical Stored Products, 22, 11-30.

114. Mullard Ltd, 1981, "Valves and Tubes/ Tubes for RF Heating", Mullard Technical Handbook, Book 2 Part AA, UK.

115. Mc Cabe, W.L., 1956, "Unit Operations of Chemical Engineering", Mc Graw-Hill Co.

116. Mc Donald, C.R., Freire, E.S., 1982, "Investigation of the Characteristics of a Traditional Natural Convection Cocoa Dryer", Trop. Agric., 59 (1), 25-32, Trinidad.

117. Mc Kenzie-Low, L., 1986, "Drier Advances Microwave Technology", Electrical Engineer, August, 70-72, Australia.

118. Nelson, S.O., 1979, "Microwave Dielectric Properties of Fresh Fruits, ASAE Paper, 79-3546, USA.

119. Nelson, S.O., 1983, "Observations on the Density Dependenca of Dielectric Properties of Materials", J. Microwave Power, 18 (2), 143-152, Canada.

120. Nelson, S.O., 1985, "A Mathematical Model for Estimating the Dielectric Constant of Wheat", Trans ASAE, 28 (1), 234-238, USA.

121. Nelson, S.O., 1985, "A Model for Estimating the Dielectric Constant of Soybeans", Trans ASAE, 28 (6), 2047-2050, USA.

122. Nelson, S.O., 1982, "Factors Affecting the Dielectric Properties of Grain", Trans ASAE, USA.

123. Nelson, S.O., 1984, "Moisture, Frequency and Density Dependence of the Dielectric Constant of Maize", Trans ASAE, 27 (5), USA.

124. Nelson, S.O., 1965, "Dielectric Properties of Grain and Seed in the 1 to 50 MHz Range", Trans ASAE, 8 (1), 38-48, USA.

125. Nelson, S.O., 1979, "RF and Microwave Dielectric Properties of Shelled, Yellow-Dent Field Corn", Trans ASAE, 22 (6), 1451-1457, USA.

126. Nelson, S.O., Charity, L.F., 1972, "Frequency Dependence of Energy Absorption by Insects and Grain", Trans ASAE, 15, 1099-1102, USA.

127. Nelson, S.O., Stetson, L.E., 1979, "250 Hz to 12 GHz Dielectric Properties of Grain and Seed", Trans ASAE, 18 (4), USA.

128. Newman, A.B., 1931, "The Drying of Porous Solids: Diffusion Calculations", American Inst. Chem. Eng., 27, 310-333.

129. Pabis, S., 1967, "Grain Drying in Thin Layers", Proceedings Agric. Engng. Symposium, Institute of Agricultural Engineers, Silsoe, UK.

130. Parry, J.L., 1983, Ph.D. Thesis, Cranfield Institute of Technology, UK.

131. Parry, J.L., 1985, J. Agric. Engng. Research, 32, 1-29, UK.

132. Perkin, R.M., 1983, "The Drying of Porous Materials with Electromagnetic Energy Generated at Radio and Microwave Frequencies", Progress in Filtration and Separation, UK.

133. Perkin, R.M., 1979, "Prospects of Drying with Radio Frequency and Microwave Electromagnetic Fields", Journal of Separation Process Technology, 1 (2).

134. Perkin, R.M., 1980, "The Heat and Mass Transfer Characteristics of Boiling Point Drying Using RF and Microwave Fields", Int. Journal of Heat and Mass Transfer, 23.

135. Puschner, H., 1966, "Heating with Microwaves", Philips Technical Library.

136. Queiroz, D.M., Pereira, J.A.M., 1984, "Simulation of Maize Drying in a Crossflow Dryer Using Thompson Model" (In Portuguese), Centreinar, Brazil.

137. Riggs, J.L., 1982, "Engineering Economics", Mc Graw-Hill, USA.

138. Rojas, E., 1986, "Costs of Processing/ Harvest 1984-85" (In Spanish), Coffee Institute, Costa Rica.

139. Rojas, E., Moya, J., 1986, "Study on Costs of Processing/ Harvest 1983-84" (In Spanish), Coffee Institute, Costa Rica.

140. Sanchez, S., Cervantez, J., 1986, "Infrared Thermal Radiation Drying of Coffee Beans", Drying' 86, 537-541.

141. Schroeder, H.W., Rosberg, D.W., 1964, "Effect of Infrared

Intensity on Drying Rexoro Rough Rice", Rice Journal, 67 (3), 28-29, USA.

142. Senise, J.T., 1985, "Utilization of RF and Microwaves in the Industrial Electronics" (In Portuguese), Revista Brasileira de Engenharia Quimica, 8 (1), 51-61, Brazil.

143. Sharaf-Eldeen et al, 1979, "Mathematical Simulation of Drying Fully Exposed Ear Corn and Its Components", ASAE Paper 79-6523, USA.

144. Sherwood, T.K., 1936, "The Air Drying of Solids", Trans American Institute of Chemical Engineers, USA.

145. Shupe, W.L., Delwiche, S.R., 1984, "Drying Shelled Peanuts in a Microwave Vacuum Dryer: Current Status", ASAE Paper, USA.

146. Simmonds et al, 1953, "The Drying of Wheat Grain, Part I: The Mechanism of Drying", Trans Inst. Chem. Engng., 31, 265-278, UK.

147. Singh, Wang, 1978, "A Single Layer Drying Equation for Rice", ASAE Paper, 78-3001, USA.

148. Singh, R.P., Chandra, P.K., 1982, "Computer Aided Simulation of an Industrial Scale Crossflow Rice Dryer", Drying' 82, Birmingham, UK.

149. Singh, R.P., Bakshi, A.S., 1980, "Drying Characteristics of Parboiled Rice", Drying' 80, Hemisphere Publ. Co.

150. Singh, R.P., Agrawal, Y.C., 1977, "Thin Layer Drying Studies on Short Grain Rough Rice", ASAE Paper, 77-3531, USA.

151. Smythe, W., 1968, "Satic and Dynamic Electricity", Mc Graw-Hill Co.

152. Sokhansanj, S., Bruce, D., 1986, "Heat Transfer Coefficient in Drying Granular Materials", Drying' 86, 862-867.

153. Sokhansanj, S., Gustavson, R.J., 1980, "Prediction of Heat and Mass Transfer within a Grain Kernel - A Finite Element Application", Drying' 80, 229-232, Hemisphere Publ. Co.

154. Steffe, J.F., Singh, R.P., 1982, "Diffusion Coefficients for Predicting Rice Drying Behaviour", J. Agric. Engng. Research, 27, 489-493, UK.

155. Stuchly, M.A., Stuchly, S.S., 1983, "Industrial, Scientific, Medical and Domestic Applications of Microwaves", IEE Proc, 130 A (8), 467-503, UK.

156. Suarez, C., Viollaz, P., 1980, "Kinetics of Soybean Drying", Drying' 80, 251-255.

157. Sunderland, J.E., 1982, "An Economic Study of Microwave Freeze Drying", J. Food Technology, 36 (2), 50-56.

158. Syarief et al, 1984, "Moisture Diffusion Coefficients for Yellow-Dent Corn Components", ASAE Paper 84-3551, USA.

159. Taylor, G., 1980, "Managerial and Engineering Economy", D. Van Nostrand, USA.

160. Terry, L.A., et al, 1986, "Within the Energy Network" (In Portuguese), Ciencia Hoje, 4 (23), 40-46, Brazil.

161. Thomas, A.M., 1952, "Pest Control by High Frequency Electric Fields", Technical Report W/T23, The British Electrical Association, UK.

162. Ulku, S., Uckan, G., 1986, "Corn Drying in Fluidized Beds", Drying' 86, 531-536.

163. UNIDO-United Nations Industrial Development Organization, 1986, "Agro-food Industrial Development in Latin America", UNIDO IS.623.

164. UNIDO-United Nations Industrial Development Organization, 1986, "Capital Goods in Oilseeds Processing and Grain Milling Industries", UNIDO IS.630.

165. Von Hippel, A.R., 1954, "Dielectric Materials and Applications", MIT Press, Massachussets, USA.

166. Wear, F.C., 1977, "Microwave Vacuum Drying System", Report TID 27933, US Energy Department, USA.

167. Whitaker, S., 1977, "Simultaneous Heat, Mass and Momentum Transfer in Porous Media", Advanced Heat Transfer, 13, 119-203.

168. White, G.M. et al, 1981, "Thin Layer Drying Model for Soybeans", Trans ASAE, 1643-1646, USA.

169. Whitney, J.D., Porterfield, J.G., 1968, "Moisture Movement in a Porous, Hygroscopic Solid", Trans ASAE, 11 (5),

716-719, 723, USA.

170. Williams-Gardner, A., 1971, "Industrial Drying", Leonard Hill, London, UK.

171. Wong, H.Y., 1977, "Heat Transfer for Engineers", Longman.

172. Woodroof, J.G., 1983, "Peanuts: Production, Processing, Products", Avi Publishing Co, USA.

173. World Crops, 1975, "Tropical Crop Processing, Drying and Storage Equipment", World Crops, Sep/October, 207-216, London, UK.

174. Wratten, F.T. et al, 1985, "Effects of Drying Air Parameters on Rice Drying Models", Trans ASAE, 28 (1), 296-301, USA.

175. Wratten, F.T., 1950, "The Application of Dielectric Heating to the Processing of Rice", M.Sc. Thesis, Lousiana State University, USA.

176. Young, J.M., 1982, "Brazil: Emerging World Power", Robert Krieger Publ Co., USA.

177. Young, I.H., 1969, "Simultaneous Heat and Mass Transfer in a Porous, Hygroscopic Solid", Trans ASAE, 12 (5), 720-725, USA.